The Subcellular Localisation of HAX1 Isoforms and Their Roles in Cancer Cell Migration, Autophagy and Apoptosis

Chia-Yu Chen

Submitted to the University of London for the Degree of Doctor of Philosophy
February 2013

Centre for Tumour Biology
Barts Cancer Institute- a Cancer Research UK Centre of Excellence
Barts and The London School of Medicine and Dentistry
Queen Mary, University of London
John Vane Science Centre
Charterhouse Square
London EC1M 6BQ

DECLARATION

The work described in this thesis was carried out by the author, Chia-Yu Chen, in the Centre for Tumour Biology, Barts Cancer Institute - a Cancer Research UK Centre of Excellence, Queen Mary, University of London.

I hereby declare that this thesis entitled "**The Subcellular Localisation of HAX1 Isoforms and Their Roles in Cancer Cell Migration, Autophagy and Apoptosis**" has not been submitted for the award of any degree, or its equivalent to any other university.

(Chia-Yu Chen), February 2013

DEDICATION

This thesis is dedicated to my beloved grandparents and parents,

and to the memory of my grandmother

ACKNOWLEDGEMENTS

First and foremost I want to thank my supervisor, Dr. **John Marshall,** who is always patient and encouraging. It has been an honour to work with him and I appreciate all his contributions of time and ideas to make my Ph.D. experience productive and stimulating.

I wish to express my gratitude to Dr**. Delphine Lees**. I have learned a lot, both scientific knowledge and attitude, form her and this work would not have been possible without her support and encouragement.

I am also indebted to my guide, Prof. **Ian Harts**, for providing guidance and resources to allow me to accomplish my research work.

I would like to acknowledge the technical support from Dr. **Guliemo Rosignoli** and Dr. **Linda Hammond**. I am also thankful to the members of my group: **Sab, Kate, Stella, Adrian** and **Mike** for all their scientific advice and support. I would like to thank my lovely colleagues: **Ludovic, Kayi, Ling, Cheng, Maria, Silvia, Bernardo, Tony, Margot, Abasi, Rachel, Marianne, Tanguy, Muge, Nuria**, **Estefania, Isabelle, Debbie, George, James, Eiman, Mo, Katie and Pam**; and my friends in Taiwan: **Momo, Mary, Hui-Yi and Yumiko** for making my PhD full of so much fun and joy.

To my family, **my grandparents, my parents and my sisters**, I cannot do this without them. To my partner **Bob**,whose love makes everything possible.

ABSTRACT

It has been reported that HAX1 is a multi-functional protein which protects cells from apoptosis, modulates autophagy, regulates membrane protein trafficking and promotes cell migration. Many studies have shown it has many different intra-cellular binding partners (including integrin β6 subunit) and exists in multiple cellular locations, including the nucleus, mitochondria and cytoplasm. This behaviour seemed unlikely for a single protein. My lab discovered that there are at least eight different HAX1 isoforms in humans and this might explain why multiple roles and sub-cellular locations are described for HAX1. In this study, I sought not only to confirm the role of HAX1 in cell behaviour, but also to examine specifically the role of HAX1 isoforms in different biological functions. I screened a panel of cancer cell lines for αvβ6-dependent migration, including breast (MCF10.CA1a), pancreatic (CFPac1 and Panc04.03), and αvβ1-dependent migration in cervical cancer (HeLa); siRNA designed to knockdown all HAX1 isoforms significantly decreased cell migration indicating HAX1 is required for cell migration in cells from multiple tissues, regulating both αvβ6 and αvβ1-dependent cell migration in various cancer types. In order to establish the functions attributable to individual isoforms, I re-introduced individual HAX1 isoforms into HAX1-null (siRNA knockdown) cells and then studied their subcellular localisation and whether they modulate migration, apoptosis and autophagy. The immunofluorescent staining revealed the predominantly mitochondrial localisation of HAX1.1, HAX1.4, HAX1.5 whereas HAX1.2 showed a very unique pattern of location in the cytoplasm. Overexpression of HAX1.2 decreased cell motility on αv-dependent ligand latency associated peptide (LAP) and knockdown of HAX1.2 increased cell migration. Furthermore,

HAX1.2 protected cells from cell death induced by various cytotoxic drugs. Moreover, HAX1.1, HAX1.2 and HAX1.5 increased autophagy by elevating the levels of Beclin-1 and LC3b-II.

However, it also is clear that much further study is needed to thoroughly understand the biology of each isoform. These are the first experimental data that demonstrate different HAX1 isoforms have different biological activities in human cancer cells, helping to explain the conflicting literature describing HAX1.

TABLE OF CONTENTS

LIST OF FIGURES

LIST OF TABLES

LIST OF ABBREVIATIONS

3'UTR: 3' untranslated region
5-FU: 5-fluorouracil
a.a.: Amino acid
Ab: Antibody
AIDS: Acquired immunodeficiency syndrome
AIF: Apoptosis-inducing factor
AK2: Adenylate kinase-2
Akt/PKB: Protein kinase B
ANT2: Adenine nucleotide translocator 2
AP-2: Adaptor protein-2
APAF1: Apoptotic protease activating factor 1
Arp2/3: Actin-related protein 2/3
Atg: Autophagy-related gene
BCR: B cell receptor
BSEP: Bile salt export protein
CaMKII: Ca^{2+}–calmodulin-dependent protein kinase II
CARD: Caspase recruitment domain
CQ: Chloroquine
DED: Death effector domain
DISC: Death-inducing signalling complex
EBNA-LP: Epstein-Barr virus Nuclear Antigen leader, also designated as EBNA5
EBV: Epstein-Barr virus
ECM: Extracellular matrix
EGF: Epidermal growth factor
EIF3G: Eukaryotic translation initiation factor 3, subunit G
ELA2: Elastase 2
EMP: Empty vector
Eps-15: EGFR-pathway substrate
ER: Endoplasmic reticulum
ETO: Etoposide
FADD: Fas-associated death domain protein
FAK: Focal adhesion kinase
FMDV: Foot-and-mouth-disease virus
G6PC1: Glucose-6-phosphate
GDP: Guanosine diphosphate
GFP: Green fluorescent protein
Grb7: Growth factor receptor bound protein-7
GST: Glutathione S-transferase
GTP: Guanosine triphosphate
HAX1: HS1-associated protein-X 1
HCV: Hepatitis C Virus
HGF: Hepatocyte growth factor
HIV: Human Immunodeficiency Virus
HRP: Horse-radish peroxidase
HS1: Haematopoietic cell-specific protein1
HtrA2: High temperature requirement protein A2, also named as Omi
IAP: Inhibitor of apoptosis protein

IL-1α: Interleukin-1 α
kDa: KiloDalton
KSHV: Kaposi's sarcoma-associated herpesvirus
LAP: Latency-associated protein
LC3: Microtubule-associated protein 1 light chain 3
LTBP: Latent TGF-β binding protein
mIgE: Membrane-bound IgE
Mit: Mitochondria
MMPs: Matrix metalloproteinases
MOMP: Mitochondrial membrane membrane permeabilisation
mTOR : Mammalian target of rapamycin
MTS: Mitochondria-targeting sequence
MYPT1: Myosin phosphatase-targeting subunit 1
n.t.: Nucleotide
NTC: Non-targeting control vector
NU: Nuclear
PAI1: Plasminogen activator inhibitor 1
PARL: Presenilin-associated, rhomboid-like
PARP: Poly-ADP-ribose polymerase
PCR: Polymerase chain reaction
PE: phosphatidylethanolamine
PH domain: Pleckstrin homology domain
PHB2: Prohibitin 2
PI3K: class III phosphotidylinositol-3-OH kinase
PKC: Protein kinase C
PKD2: Polycystic kidney disease
PLN: Phospholamban
RA domain: Ras associating domain
RCC: Renal cell carcinoma
RGD: Arginine-glycine-aspartic acid
RhoGEF: Rho guanine-nucleotide exchange factors
ROCK1: Rho-associated, coiled-coil containing protein kinase 1
RRE: Rev response element
RT: Reverse Transcription
SAGE: Serial analysis of gene expression
SCC: Squamous cell carcinoma
SCN: Severe congenital neutropenia
SERCA2: Sarcoplasmic reticulum Ca^{2+} ATPase
SH2: Src homology 2
SMAC/DIABLO: Second mitochondria-derived activator of caspase
SR: Sarcoplasmic reticulum
SRPX: Sushi-repeat containing protein, X-linked
SV40: Simian virus-40
TGF-β: Transforming growth factor β
TNFα: Tumour necrosis factor α
TRADD: TNFR-1-associated death domain protein
ULK1: Unc-51-like kinase1
uPA: Urokinase-type plasminogen activator
uPAR: Urokinase-type plasminogen activator receptor

VDA2: Voltage-dependent anion channel 2
VEGA: Vertebrate genome annotation database
Vpr: Human immunodeficiency virus type 1 viral protein R
WASP: Wiskott-Aldrich syndrome protein
WAVE: WASP family Verprolin-homologous protein
XIAP: X-linked inhibitor of apoptosis protein

CHAPTER 1. INTRODUCTION

1.1 Haematopoietic cell-specific protein-associated protein X-1: HAX1

1.1.1 Background of the study

My laboratory is interested in the role of integrins in cancer. This is particularly true of the role of integrin αvβ6, since its expression is associated with poor survival in many cancers. Attempts to understand the molecular basis of αvβ6-promoted invasion identified HAX1 as an intracellular molecule that binds to the β6 cytoplasmic tail [1]. Further studies showed that HAX1 was required for αvβ6-dependent carcinoma cell invasion. Moreover, studies from the literature reported that HAX1 regulated apoptosis, endocytosis, autophagy and was shown to be localised in cytoplasm, ER (endoplasmic reticulum), mitochondria, and nucleus. It was considered that so many functions and subcellular localisations were unlikely for a single molecule. The beginning of the solution to this confusion was revealed when my lab discovered that HAX1 consisted of at least eight alternative spliced proteins in humans [2]. Thus we hypothesised that different isoforms could be differently located in cells and perform different functions. In this thesis I extend the data on the importance of HAX1 in cancer cell migration and investigate the biology of individual HAX1 isoforms, concentrating on those isoforms (HAX1.1, HAX1.2, HAX1.4 and HAX1.5) that potentially can bind to the β6 cytoplasmic tail. I shall now review the discovery and reported biology of HAX1.

1.1.2 The discovery and the early studies of HAX1

HAX1 (haematopoietic cell-specific protein-associated protein X-1) was discovered as a binding partner of HS1 (haematopoietic cell-specific protein 1) by Suzuki *et al* in 1997 [3]. HS1 is a 75-kDa molecule expressed mainly in haematopoietic cells [3]. HS1 predominantly resides in the cytoplasm and has been shown to translocate to the cytoplasmic membrane after it is activated through tyrosine phosphorylation [4,5]. HS1 is involved in proliferation and apoptosis downstream of B cell and T cell receptor activation [4,6]. Upon the binding to antigen receptor, a number of tyrosine kinases become activated and, in turn, phosphorylate cellular proteins including HS1 [7]. Suzuki and colleagues originally aimed to investigate the mechanism of HS1 in the signal transduction of lymphoid cells [3]. Yeast two-hybrid was performed to gain more knowledge and as the result HAX1 was identified to interact with the amino terminal region of HS1 [3]. Although there was no functional examination in this study, this paper revealed that the expression of the HAX1 gene was widely distributed among human tissues including heart, brain, placenta, lung, liver, skeletal muscle, kidney, pancreas, spleen, thymus, prostate, testis, small intestine, ovary, colon and leukocytes [3]. The authors also reported that the protein was localised mostly to mitochondria with minor staining on the nuclear envelope and endoplasmic reticulum (ER) in human B lymphoma Daudi cells [3].

Two years after the first discovery of HAX1, Gallagher *et al* described the interaction of HAX1 with the PKD2 protein (polycystic kidney disease 2), again using a yeast two-hybrid screen [8]. The PKD2 protein is located in the ER and it is responsible for the second form of autosomal dominant polycystic kidney disease

[9,10]. Co-immunoprecipitation confirmed that exogenous full-length HA-tagged human PKD2 and GST–tagged full-length HAX1 interacted [8]. Moreover, by transfecting GST/HAX1 fusion protein and a plasmid coding for myc-tagged cortactin into COS-1 cells, co-immunoprecipitation and GST pull-down experiments with whole-cell lysates indicated that cortactin, also interacts with HAX1 [8]. Further double-immunofluorescence studies showed HAX1 and PKD2 co-expression in lamellipodia (flat membrane protrusions at the leading edge of migrating cells) in COS-1 cells, implying their possible association with cell motility [8]. The idea that HAX1 was involved in migration also has been suggested in another study. IL-1α (Interleukin-1 α), a cytokine which recently has been indicated to enhance cancer cell migration, was found as a binding partner of HAX1, providing further evidence for a role of HAX1 in cell migration or adhesion [11].

Sharp and colleagues showed HAX1 interacts with the C-terminus of the K15 protein (a viral protein with unknown function) from Kaposi's sarcoma-associated herpes virus (KSHV) and also investigated the role of HAX1 in apoptosis [12]. Bax (a Bcl-2 family member with a strong pro-apoptotic function) was transfected into HeLa cells to induce cell apoptosis. Co-transfection of HAX1 decreased cell death induced by Bax, thus protecting the host cell from apoptosis [12]. This paper was the first study formally to show a functional link between HAX1 and its ability to protect against apoptosis [12].

Severe congenital neutropaenia (SCN), or Kostmann's disease, was the first inborn systemic immune dysfunction disease recognised in 1950 and it is defined by when the absolute neutrophil count is less than 1500 cell/ mm^3 of blood [13,14].

Consequently, patients with SCN are vulnerable to recurrent infections [14]. SCN is caused by the maturation-arrest in neutrophil differentiation during promyelocyte/myelocyte stages in the bone marrow [15]. SCN is caused by mutations in several different genes including ELA2 (elastase 2), AK2 (adenylate kinase-2), WASP (Wiskott-Aldrich syndrome protein) and G6PC1 (glucose-6-phosphate) [16]. Klein and colleagues revealed that HAX1 gene deficiency also causes SCN [16]. Sequencing of genomic DNA identified a homozygous single-nucleotide insertion (position 130-131insA) leading to a premature stop codon (W44X) in SCN patients [16]. To directly assess the role of HAX1 in apoptosis, neutrophils from affected individuals and healthy donors were purified and analysed [16]. The study showed the enhanced neutrophil apoptosis in HAX1-deficient cells induced by H_2O_2, staurosporine and tumour necrosis factor α (TNFα) [16]. Neutrophils isolated from HAX1-deficient individuals also showed a rapid dissipation of mitochondrial inner membrane permeabilisation by staining with JC-1 (JC-1 is a dye which accumulates in mitochondria and forms J-aggregates emitting an orange fluorescence. Upon loss of the mitochondrial membrane potential, the JC-1 dye accumulates in mitochondria, adopts a monomeric conformation and emits green fluorescence) whereas the inner mitochondrial membrane potential in neutrophils from healthy individuals was maintained [16]. This study revealed that HAX1 deficiency causes SCN and suggested the mechanism involved stabilising the mitochondrial membrane potential therefore protecting cells from apoptosis.

Thus these early studies of HAX1 showed a confusing picture of “the” protein HAX1, which was demonstrated to be localised in multiple cellular compartments with different binding partners in different cell types. In addition, these studies

ascribed multiple biological functions to HAX1. Notwithstanding this lack of clarity, these studies have generated much interest in HAX1. In the following sections I will review the current knowledge of HAX1 in detail and discuss why it is important to understand the roles of individual isoforms of HAX1 in disease, including cancer.

1.1.3 Protein domains of HAX1

HAX1 protein contains several notable domains: an "acid box" of 11 consecutive acidic residues (a.a. 30-41, indicated as yellow in Figure 1.1), a putative PEST sequence (a.a. 104-147, indicated as red in Figure 1.1), and an αvβ6 binding site (a.a 271-279, indicated as blue) [2,3] (see Figure 1.1). The acid box is comprised mostly of glutamic acid and aspartic acid residues (amino acids 30–41 of HAX1: DEDDDEEEEEEG) which was also found in fibroblast growth factor receptor and shown to increase retention of this protein at the plasma membrane [2,17]. A PEST sequence (proline, glutamic acid, serine, threonine-rich sequence), usually indicates a protein with a short half-life [18]. At the C-terminus, a.a. 271-279 were identified as the integrin β6 subunit-binding domain which is encoded in the HAX1 isoform 1, 2, 4 and 5 [1,2]. In the study from Yap and colleagues, overexpression of full-length HAX1 (a.a. 1‑279) preferentially concentrated in mitochondria in HEK-293 cells; upon removal of the first 59 amino acids, the truncated HAX1 (HAX1 a.a. 60−279) failed to codistribute with MitoTracker, but instead exhibited a diffuse cytoplasmic distribution, indicating the N-terminus of HAX1 (a.a. 1-59) contains residues required for entry into mitochondria [19]. The same report also demonstrated a region of the C-terminus (a.a. 182-245) as being responsible for ER localisation, through the same approach [19] (see Figure 1.1).

To characterise the HAX1 localisation in cell migration, a study from Cavnar and colleagues generated truncation constructs lacking the C-terminal 166 amino acids; this truncated HAX1 (1–113–GFP mutant) no longer showed leading edge localisation and concentrated in the middle of the cell body of neutrophils [20]. In

contrast, even with deletion of the N-terminal 113 a.a., the remaining residues were sufficient to localise to the leading edge; thus the C-terminal region (a.a. 113-279) contains residues essential for the localisation to the leading edge of the neutrophil [20]. Apart from the subcellular localisation studies, there also are several studies that showed specific HAX1 sequences linked to particular biological functions. A study from Han *et al* showed full length HAX1 protects myocytes from cell death induced by caspase-9 overexpression [21]. Mutants lacking amino acids from 1 to 261 of HAX1 lost anti-apoptotic activity in response to caspase-9 overexpression, indicating the a.a 1-261 of HAX1 are required for full anti-apoptotic effects [21]. Another study showed that the full-length HAX1 and N-terminal 113 amino acids of HAX1, rescued neutrophil adhesion and motility and uropod retraction in PLB-985 cells, indicating this N-terminal region (a.a. 1-113) is responsible for these functions in neutrophils [20]. In Figure 1.1, I have also noted two major functions that often were ascribed to HAX1: anti-apoptosis and regulation of cell migration and the binding partners associated with these activities. Figure 1.1 shows C-terminal sequence of HAX1 contributes to the interaction with other molecules.

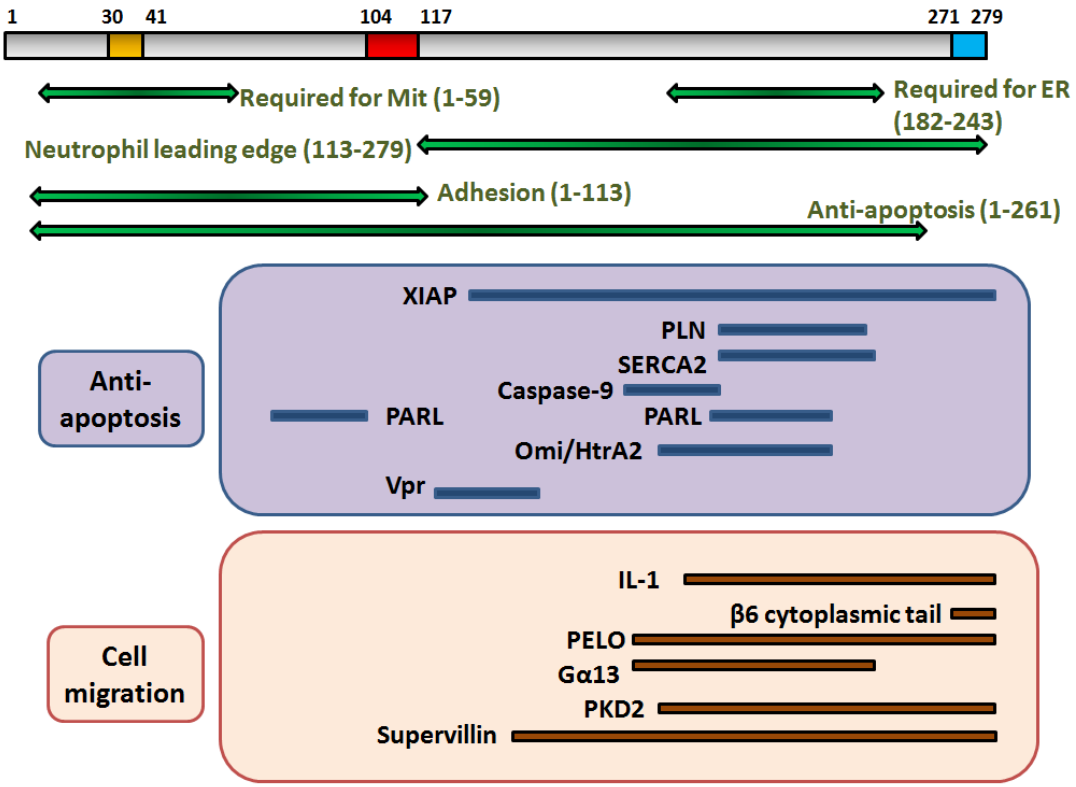

Figure 1.1 HAX1 protein domains.

The full length of human HAX1 contains 279 a.a. An acid box, from a.a. 30-41, is indicated as yellow colour and a putative PEST sequence, which is from a.a. 104 to 147, is shown in red. Integrin β6 binding site exists in the C-terminal end from 271-279 a.a., indicated as blue. The N-terminal of HAX1 (a.a. 1-59) is required for mitochondrial (Mit) localisation [22] whereas C-terminal (a.a 182-243) is required for endoplasmic reticulum (ER) localisation [22]. This figure shows some of the HAX1-binding proteins discovered to date and the regions of HAX1 they were reported to bind to, illustrates that the C-terminal of HAX1 seems to be responsible for most protein interaction identified to date. Proteins are classified into two major groups according to their cellular functions: anti-apoptosis and cell migration.

1.1.3.1HAX1 distribution in human tissues

HAX1 expression in human tissues has been analysed in several different studies. In general, it is expressed ubiquitously in human tissues with the highest expression levels found in metabolically active tissues [3,23,24]. Suzuki *et al* were the first to report the differentially regulated expression of HAX1 mRNA in multiple tissues from humans [3]. In that study, HAX1 expression was assessed by Northern Blot and data showed the highest levels of HAX1 expression in the heart and colon, followed by slightly lower levels in the skeletal muscle, lung, liver, and pancreas [3]. On the other hand, the brain, placenta, kidney, spleen, thymus, intestine, prostate, ovary, and testes exhibited lower levels of expression [3]. Highest expression level of HAX1 mRNA was also found in skeletal and heart muscles by Mirmohammadsadegh *et al* who also reported lower levels in kidney, liver, lung; the placenta contained the least amounts of HAX1 [23]. Carlsson *et al* used quantitative RT-PCR analysis to examine the mRNA expression patterns of different HAX1 isoforms in 20 different human tissues and showed both HAX1.1 and HAX1.4 (discussed later in section 1.1.5) were detected in all tissues analysed [24]. Interestingly, the authors found that the amounts of isoform 1 mRNA were about 20-fold higher than isoform 4 in all tissues analysed [24]. Collectively, the studies suggested HAX1 is expressed ubiquitously throughout human tissues but with the highest expression in human cardiac and skeletal muscles (Table 1.1).

Tissue	Relative expression
Suzuki *et al*, 1997	
Northern Blot/Total HAX1 mRNA	
Heart	++++
Colon	++++
Skeletal muscle	+++
Lung	+++
Liver	+++
Pancreases	+++
Brain	++
Thymus	++
Spleen	++
Intestine	++
Testis	++
Prostate	++
Ovary	++
Placenta	++
Mirmohammadsadegh *et al*, 2003	
Northern Blot	
Skeletal muscle	++++
Heart	+++
Liver	++
Pancreases	++
Brain	+
Kidney	+
Lung	+/-
Placenta	+/-
Carlsson *et al*, 2008	
RT-PCR	
Cumulative levels of HAX1.1 and HAX1.4	
Testis	++++
Skeletal muscle	+++
Heart	++
Brain	+
Liver	+
Relative expression of HAX1.1	
Skeletal muscle	++++
Testis	+++
Heart	++
Brain	+
Liver	+
Relative expression of HAX1.4	
Testis	++++
Skeletal muscle	++
Heart	++
Brain	+
Liver	+

Table 1.1 HAX1 mRNA expression in human tissues.

Table shows the tissue expression pattern of HAX1 by three different studies. It shows that HAX1 is ubiquitously expressed in human tissues. Data adapted from [25].

1.1.3.2Subcellular localisation of HAX1

Since the very first paper to describe HAX1, many studies have attempted to investigate the subcellular distribution of HAX1 for the better understanding of its cellular functions. Exogenous HAX1 expressed from transfected plasmids have largely been employed to observe HAX1 for its localisation; the data from different studies showed HAX1 exists in different subcellular compartments including, predominantly in the cell mitochondria (in HeLa, COS-7, HEK293, DG75, B lymphoma and striated muscle cells [3,12,19,26,27]), in the nucleus (COS-7 and DG75 [3,27]), in the ER (in COS-7, HeLa, HEK293 cells [3,12,28]) and in the cytoplasm (COS-7 and HEK293 cells [21,29]). HAX1 was also shown to be expressed in the plasma membrane and the lamellipodia in COS-7 cells [8]. Cell fractionation studies also revealed the mitochondrial residence of endogeneous HAX1 in HEK cells [30]. Table 1.2 shows the subcellular localisation of HAX1 described from different studies.

Cell type	Subcellular localisation				Co-transfection	Reference
	MT	ER	NU	Others		
Exogenous HAX1						
COS-7	**v**	**v**	**v**		-	[3]
B-lymphoma	**v**	**-**	**-**		-	[3]
COS-7	**-**	**-**	**-**	cytoplasmic	EBNA-LP	[29]
HeLa	**-**	**v**	**-**		-	[8]
HeLa	**-**	**-**	**-**	lamellipodia	PKD2	[8]
COS-7	**-**	**-**	**-**	lamellipodia	Cortactin	[8]
HeLa	**v**	**v**	**-**		-	[12]
MDCK-II	**-**	**-**	**-**	apical cell	BSEP	[31]
HeLa	**v**	**-**	**-**	membrane	-	[26]
HeLa	**-**	**-**	**v**		Vpr	[26]
Cardiocytes	**v**	**-**	**-**		-	[21]
HEK293	**v**	**-**	**-**	cytoplasmic	-	[28]
HEK293	**v**	**v**	**-**		PLN	[28]
HEK293	**v**	**-**	**-**		SERCA	[28]
Endogenous HAX1						
DG75	**v**	**-**	**v**		-	[27]
HEK293	**v**	**-**	**-**		-	[30]
Testis	**v**	**-**	**v**		-	[32]
Striated muscles	**v**	**-**	**-**	sarcoplasmic reticulum	-	[19]

Table 1.2 Summary of studies on the subcellular distribution of HAX1.

Table shows the reported subcellular localisation of HAX1 from different studies; the table is modified from [25]. MT, mitochondria; ER, endoplasmic reticulum; NU, nuclear. The tick "V" indicates positive and "-" indicates negative

1.1.4 HAX1 functions

1.1.4.1HAX1 regulates trafficking of membrane proteins

Endocytosis of adhesion molecules from the cell membrane and exocytosis to the leading edge of migrating cells are crucial steps for cell migration [33] (see section 1.2.3.3). The first study to reveal HAX1 regulates membrane molecule trafficking showed that HAX1 promoted BSEP (bile salt export protein) endocytosis in a clathrin-dependent pathway [31]. In this study, HAX1 was found as a binding partner for BESP; depletion of HAX1 by siRNA in Madin-Darby canine kidney (MDCK) cells suppressed internalisation of BSEP and resulted in a 70% increased surface expression, while BSEP translation, post-translational modification, delivery to the plasma membrane, or half-life were not affected [31]. Oberndorfer *et al* demonstrated the direct interaction of murine HAX1 with the cytoplasmic tail of mIgE (membrane-bound IgE) and this modulated mIgE-mediated antigen internalisation to BCR (B cell receptor) [34]. In order to test for the ability to internalise BCR after BCR stimulation with anti-IgE antibody, the authors used a siRNA to knockdown murine HAX1 expression [34]. The data showed HAX1 depletion reduced the BCR internalisation efficiency after stimulation with anti-IgE Ab in murine B cells [34]. No further biological functions were provided but the existence of an interaction of these two molecules leads to the suggestion that this interaction is important for the efficient antigen-internalisation in mIgE(+) B cells which is crucial for its antigen presentation to T cells during B cell proliferation [34]. In a previous study from my lab, Ramsay *et al* showed HAX1 bound to the integrin β6 subunit and this promoted oral squamous carcinoma cell migration by regulating

αvβ6 endocytosis [1]. Using capture-ELISA assays, oral squamous carcinoma cells transfected with HAX1 siRNA decreased the internalisation rate of integrin αvβ6 (while no effect was apparent on β1 and αvβ5) but had no effect on the recycling rate [1]. This study was the first to reveal that HAX1 may play an important role in cancer progression via regulating integrin endocytosis and cancer cell migration and invasion (further details see 1.1.4.3) [1].

1.1.4.2HAX1 and mRNA regulation

HAX1 has been reported to have a mRNA transcript binding property that interacts with mRNAs encoding for vimentin and rat DNA polymerase β [32,35]. There are common features of these two transcripts for HAX1 to bind to: both interact with HAX1 via their 3' untranslated region (UTR) and both are characterised as having hairpin structures [32,35].

The hairpin structure is reported to stabilise mRNA transcripts by binding to factors that protect them from nuclease cleavage, and it also regulates mRNA transport [32]. HAX1 was shown to associate with the 3'UTR hairpin region of vimentin mRNA in HeLa cells and the authors suggested this interaction facilitated the proper localisation of the transcript to the perinuclear cytoplasm [35]. Perinuclear localisation of certain transcripts, and their subsequent translation at this site, could facilitate efficient nuclear import of newly synthesised proteins [36]. By transporting mRNA transcripts to certain subcellular localisations, there could be benefit from this mechanism [36]. Vimentin is a cytoskeletal protein involved in cell migration of mesenchymal type cells and the vimentin transcript localisation alters cell

morphology and motility [37]. Thus HAX1 was suggested to regulate vimentin mRNA transport/ stability and therefore modulate cell motility [35].

HAX1 was also reported to bind to the hairpin structure of the 3'UTR of rat DNA polymerase β mRNA [32]. The disruption of this hairpin structure generated by site-directed mutagenesis impaired the interaction with HAX1, implying the hairpin structure is important for this RNA-protein binding [32]. The study suggested that the hairpin structure is associated with (i) mRNA degradation, (ii) enhanced mRNA transport and/or enhanced translation [32]. Therefore the role of HAX1 binding to DNA polymerase β is proposed to stabilise its mRNA and/or regulate post-transcriptional expression [32]. Interestingly, vimentin and DNA polymerase β are not functionally related to each other and also not involved in the same pathway. The U-rich single-stranded regions (vimentin: AGUUUU in the terminal loop, DNA polymerase β: AGUUAU in the internal loop) represents the only similarity between the two structures [32]. The lack of similarities has suggested that the HAX1-binding mechanism might be different for these two structures [32].

Apart from directly interacting with hairpin structures of mRNAs from mammalian cells, HAX1 is also reported to mediate viral RNA transcription via binding to the viral protein Rev [38]. The HIV-1 Rev protein facilitates the nuclear export of viral mRNAs containing the Rev response element (RRE) [39]. A study demonstrated that HAX1 mediates the RRE regulation by interacting with Rev [38]. By using immunofluorescence studies, co-transfection of HAX1 and Rev revealed that full-length HAX1 altered the original localisation of Rev from the nucleus to the

cytoplasm in COS-1 cells [38]. By changing the localisation of Rev, it was suggested that HAX1 could therefore interfere with the stability/export of RRE-containing mRNAs and thus inhibit RRE-mediated gene expression [38]. The authors implied that by generating small molecules that mimic HAX1, to specifically interfere with the viral protein pathway, such an approach could become useful in the treatment of HIV-1-infected AIDS (acquired immunodeficiency syndrome) patients [38].

1.1.4.3HAX1 regulates cell migration

1.1.4.3.1 Cytoskeleton dynamics in cell migration

Cell migration is mediated by coordinated actions between the cytoskeleton and integrin-mediated adhesion. The integrin–mediated migration is discussed in section 1.2.3.2. In this section I will review the cell migration regulated by other cytoskeletal molecules as this will set the scene for other HAX1 binding partners.

During cell movement, cells rearrange the cytoskeleton to form actin stress fibres that attach to ECM (extracellular matrix) surface at the front, followed by retraction and destabilisation of adhesions at the rear of the cell [40]. Stress fibres are actin filaments that are organised into thick bundles which are essential for cell motility [40]. The actin cytoskeleton is critical for the process of cell migration, including polarisation, leading edge protrusion and contraction [40]. The first step for the cell movement is polarisation and extending the protrusions which are driven by the polymerisation of actin filaments [41]. The protrusion structures, including lamellipodia and filopodia, are modulated by signalling pathways stimulating actin

cytoskeleton arrangement [42]. Within these two structures, actin filaments exhibit specific patterns of assembly-disassembly and translocation dynamics that are directed by the actin regulatory proteins [42]. The actin filaments' protrusion formation is mediated by actin-related protein 2/3 (Arp 2/3) complex that is regulated by the small GTPases RhoA, Rac and Cdc42 [42]. Rac and Cdc42 are activated at the leading edge whereas RhoA is more prominently activated at the cell rear [43]. Rac and Cdc42 induce protrusions by activating the WASP (Wiskott–Aldrich syndrome protein) homologue domain containing proteins, neural-WASP (NWASP) and WAVE (WASP family Verprolin-homologous protein), which in turn induce actin polymerisation by activating the Arp2/3 complex [41]. Arp 2/3 complex initiates the actin branches and nucleates new actin filament branches in the sides of pre-existing filaments which drives lamellipodia protrusion [44]. In the rear of the cell, RhoA activates ROCK1 (Rho-associated, coiled-coil containing protein kinase 1) and ROCK2, which act as inhibitors of myosin phosphatases (myosin phosphatase-targeting subunit 1 [MYPT1]), and thus sustain myosin II phosphorylation and therefore promotes cell contraction [43]. Myosin II mediates the contraction of actin stress fibres and moves antiparallel actin filaments past each other providing the force to rearrange the actin cytoskeleton [45]. RhoA also activates the formin mDia1 to promote actin polymerisation [40]. These pathways contribute to actin polymerisation, bundling and adhesion formation [45].

1.1.4.3.2 HAX1 regulates cell migration via cytoskeleton-associated proteins

Cortactin is a cytoskeletal protein which promotes actin assembly and is also associated with tumour invasiveness and metastasis [46]. Cortactin interacts with the

Arp2/3 complex, promoting actin polymerisation during actin network reconstruction in motile cells [46]. Guanine nucleotide-binding proteins (G proteins) are signalling transduction molecules that bind to the intracellular side of membrane bound G protein coupled receptors and regulate cell migration [47]. G proteins are unified by a common activation mechanism involving exchange of bound GDP (Guanosine diphosphate; inactive form) with GTP (Guanosine triphosphate: active form), resulting in a conformational change in the protein [48]. Gα13, a subfamily of G proteins, interacts with Rho guanine-nucleotide exchange factors (RhoGEF) and thus activates RhoA facilitating changes in the actin cytoskeleton, and promoting cell adhesion [48]. In the study from Radhika *et al*, HAX1 was identified as the binding partner of Gα13 from human HeLa cell cDNA library and the interaction was confirmed by co-immunoprecipitation and confocal imaging studies [49]. Decrease of stress fibre formation and increase in actin-rich structures at the leading edges is a characteristic feature of cell migration [49]. Transfection of full-length HAX1 caused a reduction of Gα13-induced stress fibre formation and less cell spreading as well as increased cell migration in NIH3T3 cells [49,50]. In reverse, HAX1 silencing reduced cell migration [49]. These data indicated HAX1 is an important regulator for Gα13-mediated cell migration [49]. According to the immunoprecipitation studies and the observations that Gα13 stimulates the activation of Rac, which is potentiated by HAX1, the authors suggested a model whereby HAX1 forms a complex with Gα13, cortactin and Rac, therefore bringing these molecules closer to Gα13 which allows cortactin to be stimulated by Gα13-activated Rac1, resulting in actin polymerisation and cell migration [49]. This was the first report to reveal the pro-motility function of HAX1 (Figure 1.2).

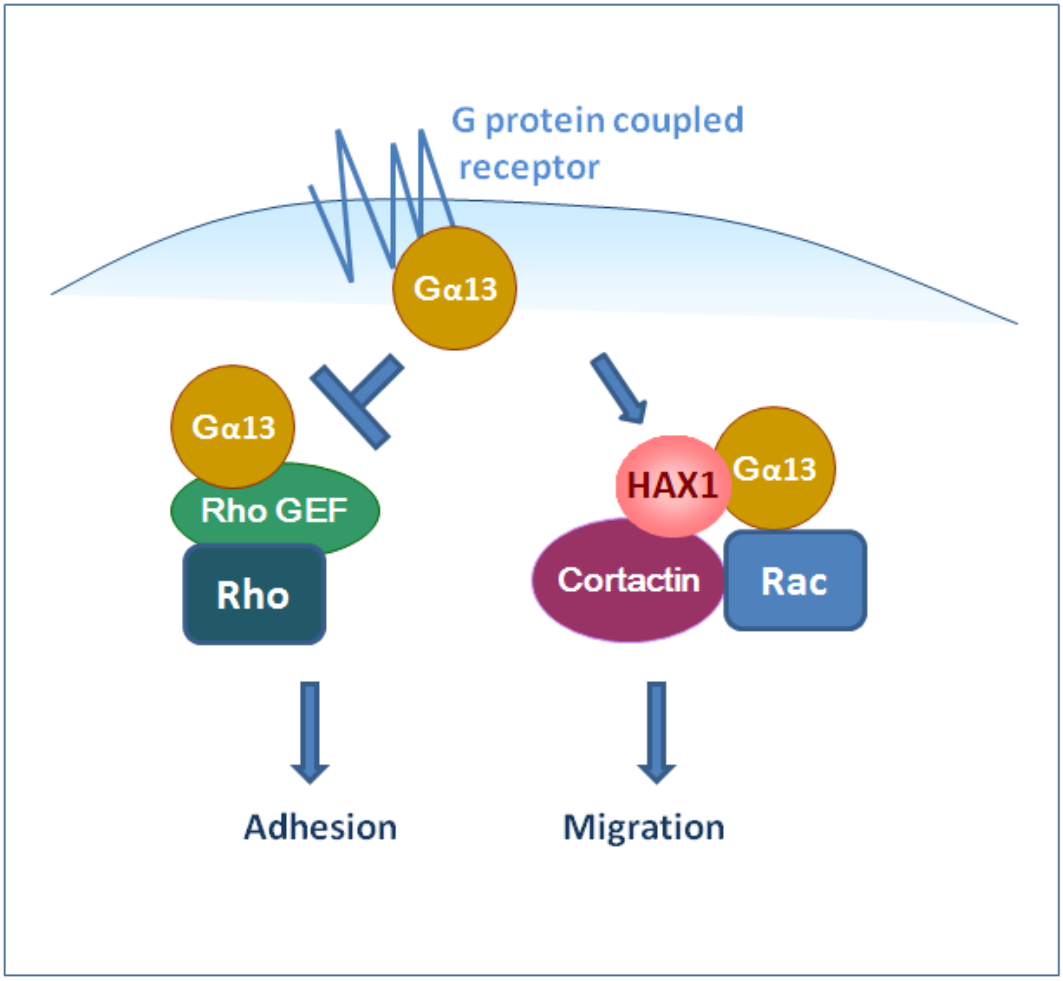

Figure 1.2 Model for how HAX1 promotes cell migration and adhesion by forming a complex with Gα13, cortactin and Rac.

The interaction of HAX1 and Gα13 negatively regulates the Gα13-mediated activation of Rho while it increases Gα13-mediated activation of Rac. By forming a complex with Gα13, cortactin and Rac, HAX1 brings Gα13 closer to cortactin which, in turn, can be stimulated by Gα13-activated Rac, to initiate actin polymerisation, cell protrusion, and subsequent cell movement. It is likely that the group of Gα13, Rac, HAX1, and cortactin stimulates cell migration by countering Gα13- Rho-mediated cell adhesion [49].

Growth factor receptor bound protein-7 (Grb7) was identified originally as an SH2 (Src homology 2) domain-containing adaptor protein bound to the activated EGF (epidermal growth factor) receptor and also has been reported to regulate cancer cell migration [51,52]. Grb7 mediates cell migration through an interaction with focal adhesion kinase (FAK) via the Grb7-SH2 domain [52]. By yeast two-hybrid analysis, HAX1 was demonstrated to interact with the RA (Ras associating) and PH (Pleckstrin homology) domains of Grb7. This HAX1-Grb7 association was confirmed by co-transfecting full-length HAX1 and full-length Grb7 in HeLa cells followed by co-immunoprecipitation [53]. Although there were no further experiments to determine the biological impact of this interaction, it was proposed that HAX1 may participate in Grb7 mediated cell migration signalling [53].

PELO is a cytoplasmic protein which is important for germline stem cell self-renewal by repressing the Bam-independent differentiation pathway and it was recently found to be responsible for degrading aberrant mRNAs [54,55]. A recent study showed the interaction between PELO, HAX1 , eukaryotic initiation factor EIF3G (eukaryotic translation initiation factor 3, subunit G) and apoptosis-inducing tumour suppressor SRPX (sushi-repeat containing protein, X-linked) [56]. EIF3G represents a subunit of the eukaryotic translation initiation factor 3 (eIF3) [56] and it has been reported to associate with AIF (apoptosis-inducing factor) that induces apoptosis through inhibition of protein synthesis [57]. SRPX, was originally isolated as a suppressor of v-src transformation [58]. Subsequent reports found that SRPX induced apoptosis through an ER-dependent pathway and suggested that this pathway might contribute to the suppression of tumour formation [59]. The interaction of HAX1 and PELO was then confirmed by GST-pull down and co-

immunoprecipitation studies [56]. This study also employed bimolecular fluorescence complementation assays (BiFC assay) to show the interactions between PELO and HAX1, EIF3G or SRPX and these were mainly localised to cytoskeletal filaments in HeLa cells [56]. This approach is based on the complementation between two non-fluorescent fragments of EGFP, which are brought together by interaction of two proteins fused to each EGFP fragment, resulting in visualisation of the restored fluorescence in living cells [60]. Cells transfected with either both empty vector or with either PELO-GFPC (full length PELO cDNA in-frame to the C-terminal half of EGFP) or HAX1-GFPN (N-terminal half of EGFP fused with 178-279 a.a of HAX1) alone did not show any fluorescence [56]. In contrast, cells co-transfected with PELO-GFPC and HAX1-GFPN displayed fluorescence, which was accumulated mainly at the cytoskeletal filaments [56]. Moreover, overexpression of PELO showed disassembly of actin stress fibres and reduction in cell spreading (measurement of spreading velocity was done according to the distinct differences in surface area and morphology of adherent cells) in Hep2G cells, reminiscent of the Gα13 study described above (a phenomenon caused by HAX1 overexpression) [49,56].

In a separate study, HAX1 (and another 11 molecules) was identified as a binding partner for supervillin [61]. Supervillin is a cytoskeletal protein that regulates cell motility and the authors showed transfection of a.a. 144–279 of HAX1 (supervillin-binding sequence of HAX1) decreased HeLa cell spreading on fibronectin [61]. Interestingly, supervillin also physically associated with one of the binding partners of HAX1: cortactin [62]. The interaction of these molecules may play a role in cell

motility regulation and further investigation is needed to develop a detailed mechanism.

The urokinase-type plasminogen activator receptor (uPAR) is an important regulator of ECM proteolysis [63]. The interaction with its ligand, the serine protease urokinase-type plasminogen activator (uPA; also known as urokinase), regulates the cleavage of plasminogen and this leads to ECM degradation and facilitates cell penetration of tissue boundaries [63] (see1.2.3.2). HAX1 has been identified as a binding partner for uPAR by yeast two-hybrid screening of a breast cancer cDNA library and this was confirmed by GST-pull down, co-immunoprecipitation assays and confocal microscopy [64]. Additional studies from the same lab showed that the endogenous HAX1 is localised in the cytoplasm (however the possibility for HAX1 to be localised in mitochondria or ER was not demonstrated) in human embryonic kidney, HEK293, cells and human breast cancer, MDA-MB-231 cells, [65]. Upon the stimulation to activate uPAR with EGF (epidermal growth factor), uPA, or uPA-ATF (amino-terminal fragment of uPA), HAX1 redistributed and colocalised with uPAR in the cell membrane, suggesting a physiological role for HAX1 in the regulation of uPAR signal transduction [65]. Overexpression of HAX1 in HEK293 and MDA-MB-231 cells increased the cell migration upon uPA and EGF stimulation [65].

1.1.4.3.3 HAX1 regulates cell migration by mediating endocytosis of integrin αvβ6

The integrin αvβ6 expression is low or absent on resting epithelial cells and the enhanced expression of this integrin is linked to various cancers and also indicates more aggressive invasive carcinoma cell behaviour and poorer clinical prognosis [66-70]. By using the yeast two-hybrid assay, HAX1 (a.a 270-279, the sequence in the C-terminal end which is encoded in the HAX1 isoform 1, 2, 4 and 5) was identified as a binding partner for the β6 cytoplasmic tail (a.a 731-758, which incorporates the juxtamembrane region and cytodomain 1) from a human keratinocyte cDNA library [1]. This binding was confirmed by co-immunoprecipitation [1]. By using a siRNA targeting to HAX1 in oral squamous carcinoma cell lines, VB6 and H400, migration on the αvβ6-specific ligand latency associated peptide (LAP) was significantly decreased whereas migration toward laminin, type 1 collagen, and vitronectin, mediated by non-αvβ6 integrins was unaffected by HAX1 depletion [1]. During cell migration, integrins internalise continually from the plasma membrane into endosomal compartments, and recycle back to the cell surface [33]. To investigate the mechanism of HAX1 in αvβ6 regulation, the membrane permeant peptide Tat (from HIV-1) was synthesised as a conjugate with the β6-binding site of HAX1 (HAX1 peptide) [1]. This HAX1 peptide was shown to disrupt completely the intracellular interaction of HAX1 and β6 by co-immunoprecipitation [1]. With the HAX1 peptide treatment, Clathrin-dependent internalisation of αvβ6 was significantly decreased, and there was decreased cell migration and invasion [1]. These data imply that the interaction of

HAX1 and αvβ6 is crucial for cancer cell migration and invasion; this study was the first to reveal that HAX1 possibly plays an important role in cancer progression [1].

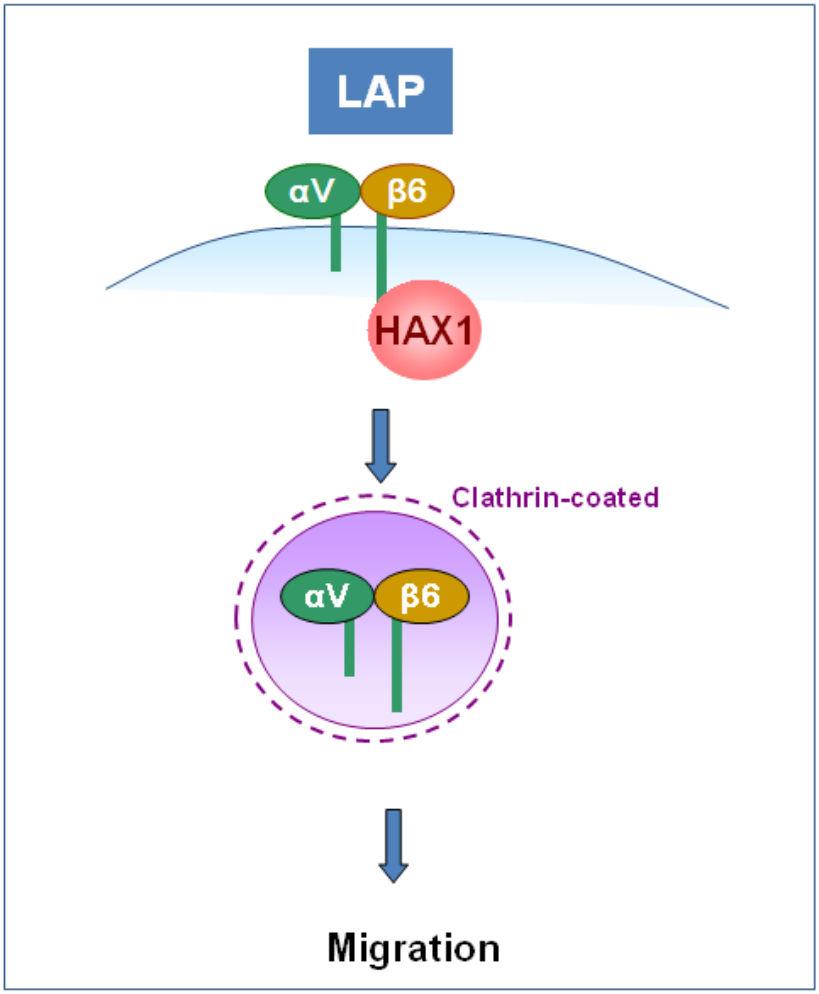

Figure 1.3 Schematic model of how HAX1 regulates integrin αvβ6-mediated cell migration and invasion.

1.1.4.3.4 HAX1 regulates cell migration via RhoA

Severe congenital neutropaenia (SCN or Kostmann's disease) is an inherited disorder due to nonsense HAX1 mutations and premature stop codons [16,71]. The SCN patients are vulnerable to recurrent infections caused by lack of mature neutrophils in peripheral blood (absolute neutrophil count is less than 1500 cell/ mm^3) [71]. A recent study showed HAX1 regulates motility of neutrophils by modulating the localised polarity of F-actin dynamics [20]. HAX1-deficient neutrophils revealed less F-actin at the uropod compared with the control cells, implying that HAX1 regulates the polarity of F-actin dynamics and rear detachment [20]. The same study also observed these HAX1-deficient cells displayed impaired motility and an elongated uropod during chemotaxis on fibrinogen [20]. The abnormal uropod morphology and detachment phenotype are similar to that which has been reported previously with Rho inhibition [72], suggesting that HAX1 may modulate rear retraction by regulating Rho GTPase signalling. Pull-down assays demonstrated that RhoA activation was significantly decreased in HAX1-deficient neutrophils stimulated with N-formyl-l-methionyl-l-leucyl-l-phenylalanine (fMLP, a strong chemoattractant for neutrophils) [20]. In contrast, Rac activation was increased in HAX1 knockdown cells [20]. Moreover, depletion of RhoA increased neutrophil adhesion and impaired migration, and constitutively active RhoA rescued adhesion and partially rescued motility of HAX1-deficient neutrophils suggesting that HAX1 regulates neutrophil adhesion and chemotaxis through RhoA [20].

1.1.4.3.5 HAX1 regulates cell migration via CXCR4

HAX1 was recently shown to regulate the expression of CXCR4, a chemokine receptor tightly linked to lymphocyte homeostasis and cancer [73]. CXCR4-expressing cells migrate towards its receptor CXCL12, which is expressed by bone marrow stromal cells and this is crucial for B cell maturation [73]. In a study investigating lymphocyte development, HAX1-knockdown B cells from HAX1-deficient mice showed a significantly reduced expression of CXCR4 [73]. This decreased expression of CXCR4 has been suggested to cause the impaired migratory behaviour of B-cell precursors resulting in a failure to be retained in the bone marrow [73]. It will be interesting to further investigate the relationship of HAX1 and CXCR4 in a cancer environment.

In summary, HAX1 is reported to mediate cell migration by binding to multiple cytoskeleton associated molecules, including Gα13, Cortactin, PKD2, PELO, which contribute to actin dynamics. HAX1 also mediates endocytosis for the integrin αvβ6 and this process is crucial for cell migration. Table 1.3 shows a brief review of how HAX1 regulates cell migration by different pathways.

Pathway	Cell lines	Mechanism
uPAR	HEK, MDA-231	Endogenous HAX1 is showed to localise with uPAR upon stimulation, and the exogenous HAX1 is shown to increase cell migration in scratch wound healing assays [65].
Grb-7	HeLa	It is proposed that HAX1 regulates migration via interaction with protein Grb-7 [53].
Supervillin	HeLa, COS7-2	Supervillin and its interaction partners coordinate actin and microtubule motors and therefore facilitate cell movement [61].
PELO	HeLa	Interactions between PELO and HAX1 are mainly localised to cytoskeletal filaments [56]
RhoA	PLB-985	HAX1 knockdown in neutrophils showed decreased RhoA-GTP level and this is associated with changes in neutrophil uropod detachment and directed migration. Constitutively active RhoA rescues adhesion and partially rescues motility of HAX1-deficient neutrophils suggesting that HAX1 regulates neutrophil adhesion and chemotaxis through RhoA [20].
Gα13	COS-7, NIH3T3	HAX1 binds to Gα13 and exogenous HAX1 overexpression showed reduction of the formation of actin stress fibres and focal adhesion complexes and increased cell migration in Gα13-expressing cells [49].
CXCR4	mouse splenic B lymphocytes	Real-time PCR showed a reduced CXCR4 expression of HAX1-deficient B cells. The authors suggested this caused the observation of defects in B-cell development owing to the failure of B cell migration [73].
αvβ6	VB6 and H400	HAX1 regulates oral cancer cell migration via clathrin-mediated integrin αvβ6 endocytosis [1].

Table 1.3 HAX1 regulates cell migration via different pathways.

1.1.4.4HAX1 and autophagy

1.1.4.4.1 Autophagy

Autophagy is a cellular mechanism that has been described as a “self-eating” process [74]. In normal cellular homeostasis, autophagy is a cellular function that contributes to the removal of damaged organelles and misfolded proteins by directing them to lysosomal degradation [75]. In stress situations, autophagy also is activated to degrade intracellular materials to provide a source of energy, thereby enabling cells to survive during harsh conditions, such as nutrient deprivation or the treatment to induce inhibition of mammalian target of rapamycin (mTOR) [75]. Autophagic flux is a term which refers to the complete process of autophagy which begins with the formation of the phagophore and ends with end stage autophagosomes [76-78]. The general process of autophagy involves sequestration of cytosol contents into a double-membrane vesicle, termed the autophagosome, which will then fuse with lysosomes to become an autolysosome where the cargo is degraded by acidic lysosomal enzyme [79]. The kinase mTOR is a critical regulator of autophagy induction, with activated mTOR (via Akt and MAPK signalling) suppressing autophagy, and negative regulation of mTOR (via AMPK and p53 signalling) promoting it [80]. Once mTOR kinase is inhibited, the Unc-51-like kinase1 (ULK1) is activated and forms a large complex with the autophagy-related gene13 (Atg13) and the scaffold protein FIP200 [80]. This complex leads to the recruitment of the downstream mammalian homologue of yeast Atg6 (Beclin-1) complex which includes class III phosphatidylinositol-3-OH kinase (PI3K), Atg14 and the mammalian homologue of yeast Vps15 (P150) [75,81]. The Beclin-1 complex then

induces the sequestration process which requires a group of Atg proteins for the formation of the autophagosome [82]. The initial sequestering compartment is called the phagophore and it is controlled by two conjugation systems: Atg12 system and the microtubule-associated protein 1 light chain 3 (LC3b or Atg8) system [82]. Atg12-conjugation is essential for the formation of the phagophore whereas LC3-modification is essential for the formation of autophagosomes [83]. Atg12 is activated by Atg7 and Atg10 and then conjugates to Atg5 and subsequently interacts with Atg16 to form a large complex to initiate the early stage of the phagophore [82]. After translation, LC3/Atg8 is cleaved at its C terminus by Atg4 protease to generate the cytosolic LC3-I [80]. LC3-I is activated by Atg7, transferred to Atg3, and conjugated to phosphatidylethanolamine (PE) as the lapidated form LC3-II [84]. LC3-II is then attached to the autophagosome membrane and often is used as an autophagosomal marker [85]. Sequestosome-1 (p62), a ubiquitin-binding protein, binds LC3 and ubiquitylated proteins and might contribute as a cargo receptor for autophagic degradation, so that the autophagosome contains only its cargo and excludes other cytosolic components [84].

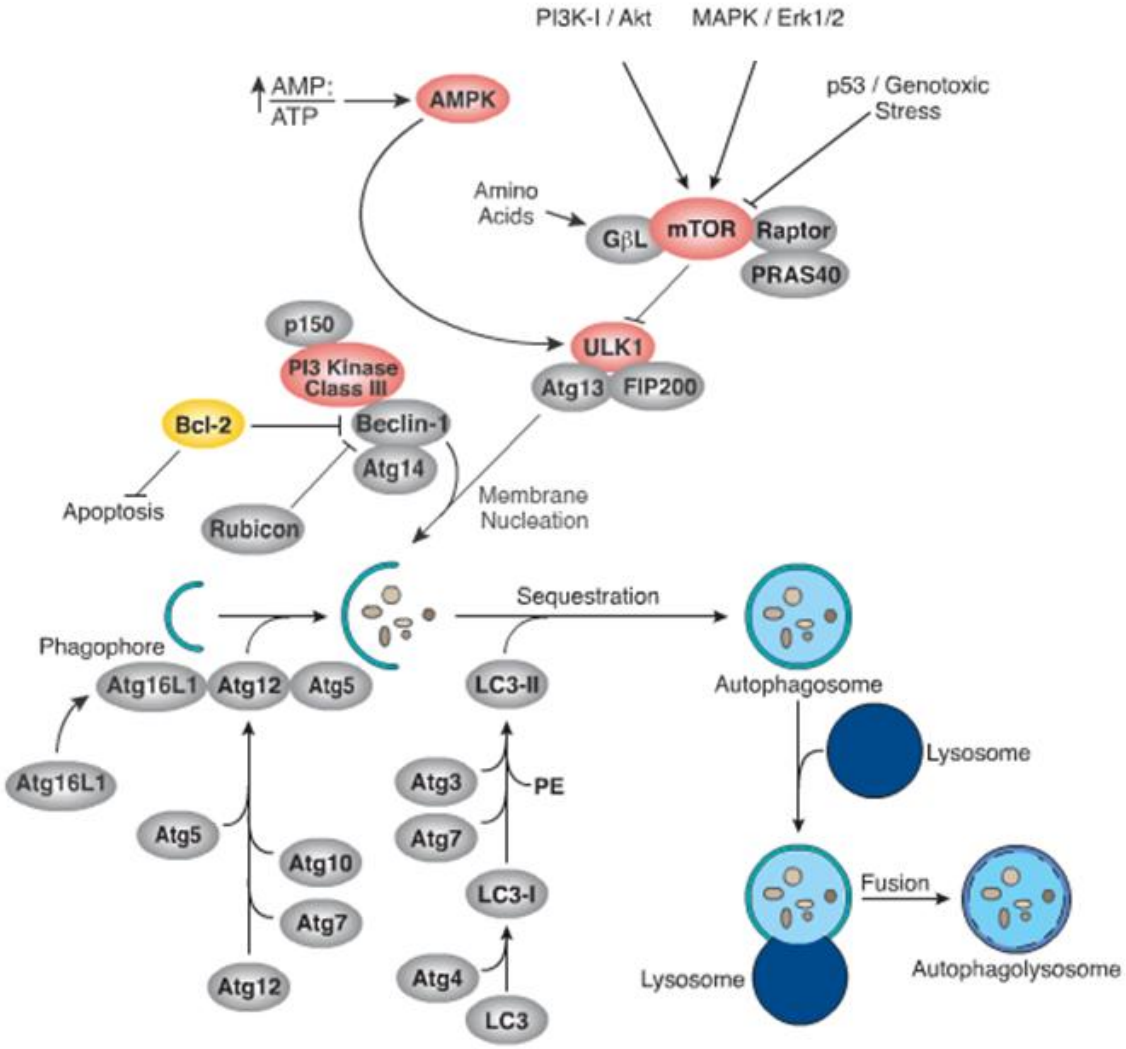

Figure 1.4 A schematic model illustrating the autophagy pathway.

Picture adapted from [86].

1.1.4.4.2 The role of HAX1 in autophagy

A recent study reported the direct linkage of HAX1 to autophagy. Li *et al* aimed to understand the role of Omi/HtrA2 in neuron degenerative disease [87]. Omi/HtrA2 is an homotrimeric serine protease that localises to the mitochondria and promotes apoptosis by both caspase-dependent and caspase-independent pathways [88,89]. The involvement in autophagic-mediated cell death pathway was therefore investigated. As HAX1 was previously reported as a specific substrate of Omi, the role of HAX1 was also investigated in this study [30]. Overexpression of Omi/HtrA2 decreased the level of endogenous HAX1 in HeLa cells, therefore these authors investigated whether HAX1 regulates autophagy through interaction/regulation of Beclin-1 which is similar to other Bcl-2 family proteins [87]. Overexpression of HAX1 attenuated Omi/HtrA2-induced autophagy and also decreased LC3b-II level, and this inhibition is rescued by overexpression of Beclin-1 [87]. By immunoprecipitation and GST pull-down, HAX1 has been found to bind to Beclin-1 and to repress autophagy [87]. Moreover, a HAX1 mutant that was designed to delete the Omi/HtrA2 binding sequence, demonstrated the enhanced inhibition of Omi/HtrA2-induced autophagy, suggesting Omi/HtrA2 activates autophagy by binding and cleaving HAX1, therefore abolishing its ability to inhibit Beclin-1 [87]. The authors suggested further that HAX1 can be digested by Omi/HtrA2 to elicit autophagy in response to autophagic stimuli or to stimulate apoptosis when cells ultimately are sentenced to die [87] (Figure 1.5).

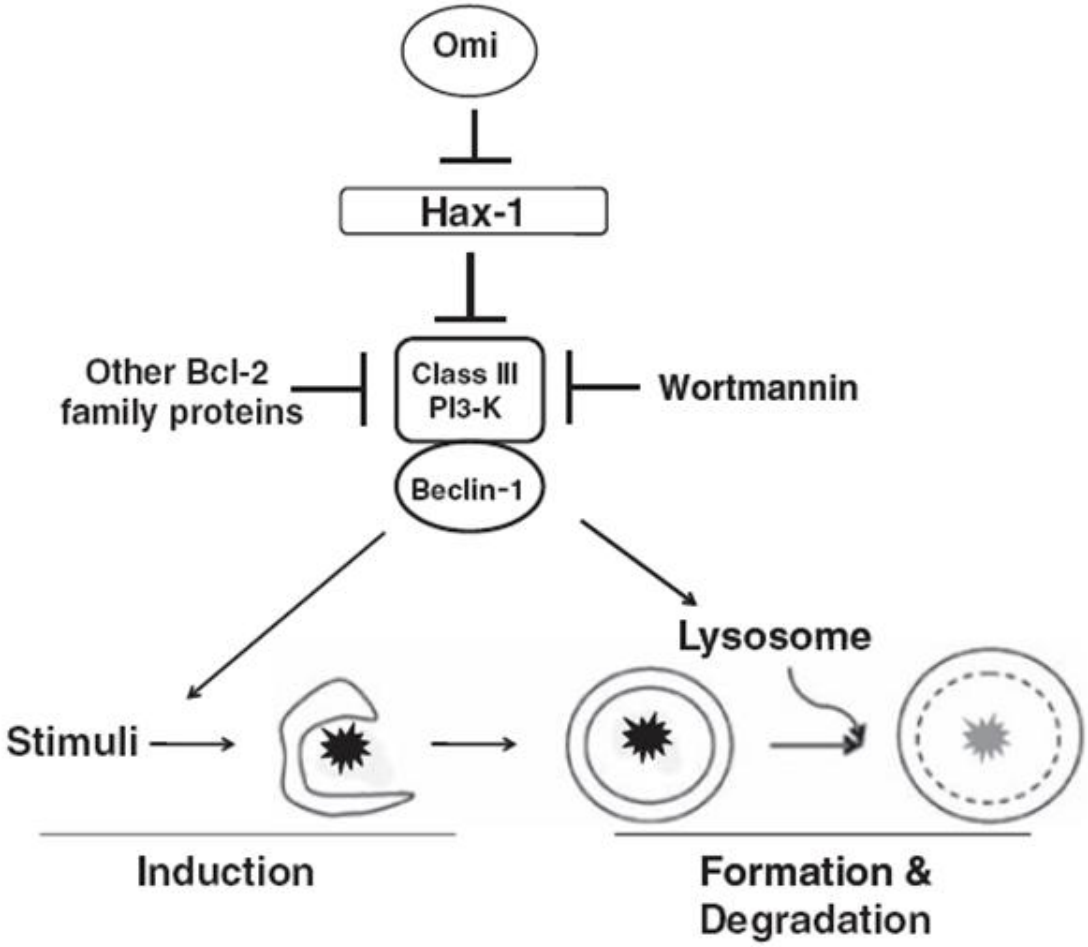

Figure 1.5 A schematic model illustrating the role of Omi and HAX1 in the regulation of autophagy through the Beclin-1 pathway.

Picture modified and adapted from [87].

1.1.4.5 HAX1 and apoptosis

In the original study from Suzuki *et al*, it was suggested that HAX1 contained sequences homologous to the anti-apoptotic protein Bcl-2 and therefore a proapoptotic function was proposed for HAX1 [3]. Although a later study showed, by sequence analysis and secondary structure prediction, that HAX1 is extremely unlikely to be a Bcl-2-family-related protein because it lacks Bcl-2 homology modules [90], after more than a decade since the discovery of HAX1 its anti-apoptosis function has become the most well-established biological role assigned to HAX1. Many studies have discovered various different anti-apoptotic mechanisms of HAX1 to protect cells from cell death, these include inhibiting caspases; maintaining mitochondria membrane integrity and modulating calcium homeostasis in the sarcoplasmic reticulum. It is also reported that many viral proteins interact with HAX1 to hijack the anti-apoptosis function in order to replicate in the surviving host cells. In the following sections I will discuss the molecular mechanisms of apoptosis and then review the antiapoptosis functions ascribed to HAX1.

1.1.4.5.1 Cell apoptosis

Cell apoptosis is a type of programmed cell death that plays a fundamental role in development and tissue homeostasis (such as in development, wound healing and intestinal cell turnover) by eliminating excess cells [91,92]. Apoptosis typically is induced via two pathways: the intrinsic and the extrinsic pathways. Both mechanisms result in similar morphological changes, including cell rounding, pseudopod retraction, reduction of cellular volume, chromatin condensation, nuclear

fragmentation (karyorrhexis), plasma membrane blebbing, but little or no ultrastructural modifications of the cytoplasmic organelles [93,94]. The apoptosis process is executed by a cascade of caspase (cysteinyl, aspartate-specific proteases) family members which cleave and activate their own substrates at short tetrapeptide recognition motifs terminating in an aspartate residue (X-X-X-Asp) [95]. The caspases are divided into two groups: initiators (caspase-2, 8, 9) and effectors (caspase-3, 6, 7) and they are synthesised as inactive zymogens containing several domains: an N-terminal prodomain (for initiator caspases), a large subunit (p20) and a small subunit (p10) (Figure 1.6) [95,96]. The prodomains of initiator caspases contain further distinct motifs: the death effector domain (DED) and the caspase recruitment domain (CARD) (Figure 1.6) [97]. These domains interact between procaspases and their adapters and consequently lead to caspase activation [97]. The large and small subunits are then cleaved and this induces proximity of two caspase monomers which promote and lead to the formation of an active caspase tetramer that contains two small and two large subunits [95,98]. Initiator caspase activation induces the activation of the downstream executioner caspases which can cleave various death substrates to induce apoptosis [97].

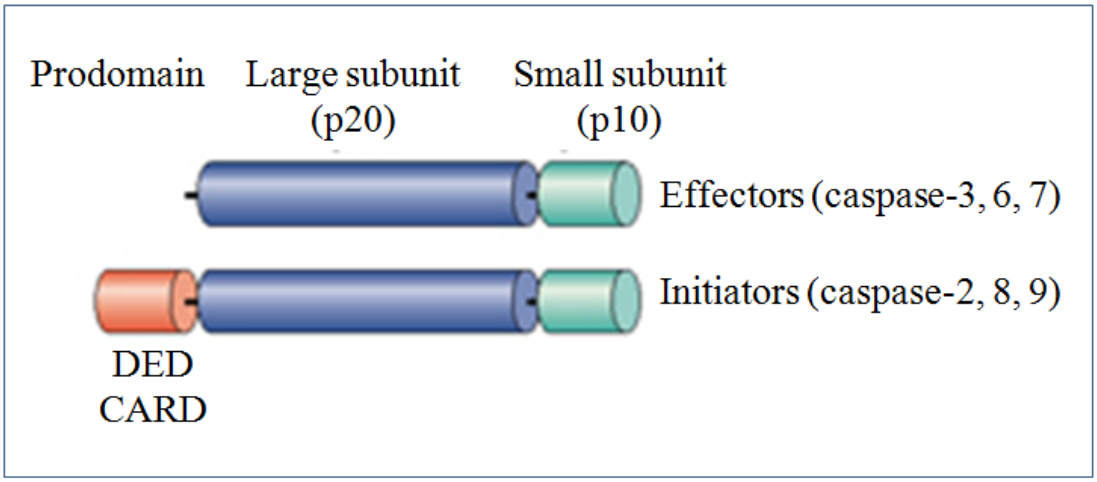

Figure 1.6 Schematic of the structure of caspases.

Caspases contain three main domains: a prodomain and large (p20) and small (p10) catalytic subunits. The large domain contains the active site Cys residue. Activation of caspases involves the proteolytic cleavage of zymogens, the removal of the prodomain and separation of the p20 and p10 subunits, or allosteric conformational changes. The prodomains of activator and inflammatory caspases contain protein–protein-interaction domains (such as the caspase-recruitment domain (CARD) and the death-effector domain (DED) that link them to apoptosis signalling molecules [96].

Apoptosis can be induced by various factors and, as mentioned, this is divided into two major pathways: intrinsic and extrinsic [99]. The intrinsic pathways, also known as the mitochondrial pathway or stress pathway, are activated by a range of stress stimuli including DNA damage, cytoskeletal damage, endoplasmic reticulum stress, growth-factor deprivation and oncogenic factors [100]. These intrinsic activations trigger translocation of proapoptotic Bcl-2 family members (e.g. Bid or Bax) to the mitochondrial cytosol. In particular, Bid is cleaved by caspases or other proapoptotic proteases to form truncated Bid (tBid), which then localises to the mitochondria [101]. Here, tBid interacts with other proapoptotic Bcl-2 member proteins such as Bax and/or Bak, resulting in pore formation and permeabilisation of the outer mitochondrial membrane permeabilisation (MOMP) [100,101]. MOMP is the 'point of no return' during apoptosis as it results in the release proapoptotic molecules into the cytosol from the mitochondria intermembrane space including cytochrome c, a second mitochondria-derived activator of caspase (SMAC; also known as DIABLO), and HtrA2/Omi [94,100]. After release from mitochondria, cytochrome c binds to the apoptotic protease activating factor 1 (APAF1) forming a structure termed the apoptosome [102]. The apoptosome recruits, and activates, the initiator caspase-9, which then cleaves and activates its effector caspases-3 and -7 [94]. Moreover, along with other molecules released from mitochondria, cytochrome c, DIABLO and HtrA2/Omi also can bind directly to X-linked inhibitor of apoptosis protein (XIAP) which antagonises its ability to inhibit caspases [88,103,104] (Figure 1.7).

The extrinsic pathway involves the stimulation of various cell-surface transmembrane death receptors such as Fas (CD95), tumour necrosis factor-α (TNF-α) or the granzyme/perforin system [105-107]. Death receptor stimulation results in

the formation of death-inducing signalling complex (DISC) by the adaptor proteins Fas-associated death domain protein (FADD) and TNFR-1-associated death domain protein (TRADD) and these act as platforms for the activation of pro caspase-8 [108]. This further activates the downstream caspase-3 and caspase-7 and also activates intrinsic signalling through the cleavage of Bid (Figure 1.7).

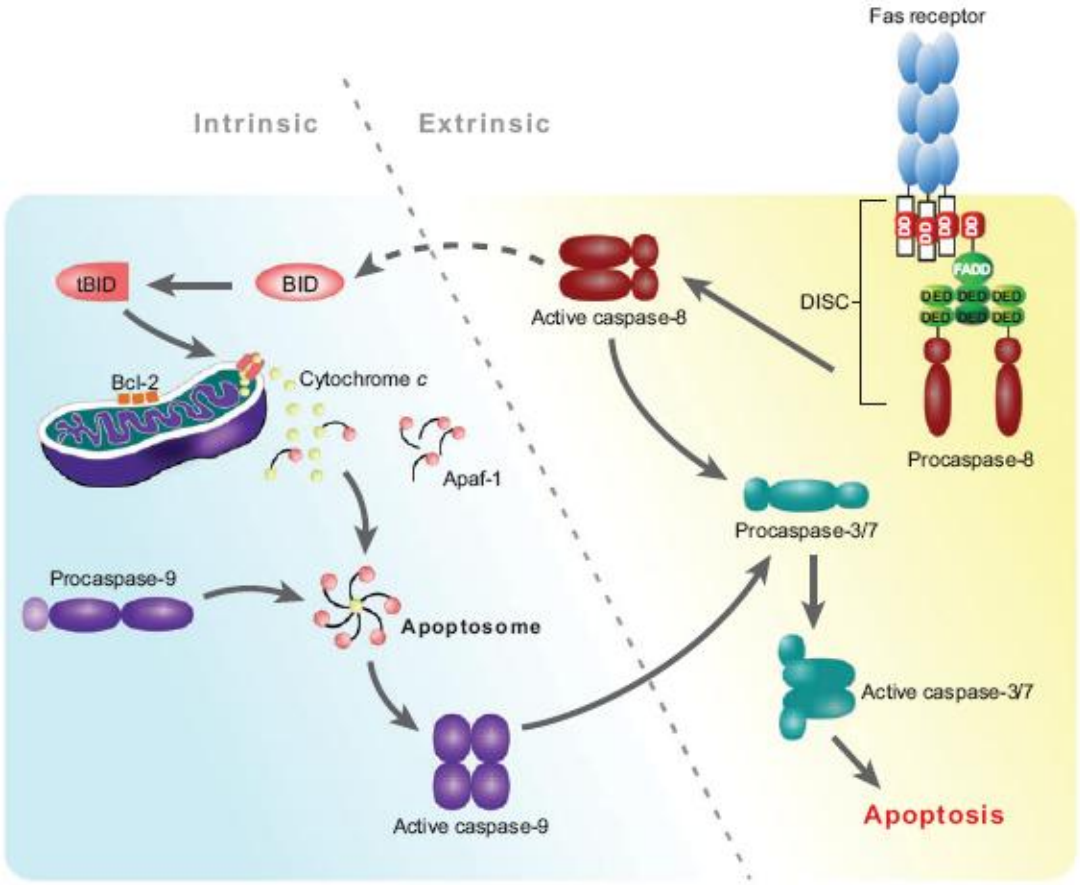

Figure 1.7 The caspase cascade in cell apoptosis.

Both the intrinsic and extrinsic pathways use related principles in sensing an apoptotic signal and executing apoptosis. In the intrinsic pathway, an apoptotic stimulus in the cell leads to the assembly of the apoptosome, which activates caspase-9. An extrinsic apoptotic signal, by contrast, is mediated by binding of an extracellular ligand to a transmembrane receptor, leading to the formation of the death-inducing signalling complex (DISC), which is capable of activating the initiator caspase-8. Once activated, either caspase-9 or caspase-8 cleaves executioner caspase-3 and caspase-7 and leads to apoptosis. Picture adapted from [101].

1.1.4.5.2 HAX1 and associated viral proteins in apoptosis

HAX1 has been reported to interact with a number of viral proteins including: Epstein-Barr virus nuclear antigen 5 (EBNA5, also designated as Epstein-Barr virus Nuclear Antigen leader protein, EBNA-LP) from Epstein-Barr virus (EBV) [27,29], K15 from Kaposi's sarcoma-associated herpes virus (KSHV) [12], Vpr and Rev protein from Human Immunodeficiency Virus (HIV) [38] [26], HCV core protein from Hepatitis C Virus (HCV) [109] and N^{pro} from classical swine fever virus (CSFV)[110]. Viruses have developed multiple strategies to regulate host cell apoptosis for their own benefit. Many viral proteins are capable of binding to apoptosis-associated molecules in order to suppress apoptosis in infected cells. For example, the Epstein–Barr nuclear antigens (EBNA) 3A and 3C (EBNA3A and EBNA3C) protected Burkitt's lymphoma cells from various cytotoxic drugs by downregulating the proapoptotic Bcl-2-family member Bcl-2-interacting mediator of cell death (Bim), and hence reduce the propensity of host cells to undergo apoptosis [111,112]. Potentially, HAX1 binds and destabilises viral proteins by altering their distribution and therefore affect cell apoptosis. In this section, I will overview the current understanding of, and the impact of, the interaction between HAX1 and different viral proteins.

It has been demonstrated that EBNA5 physically associates with HAX1 in the cytoplasm in COS-7 cells and predominantly in mitochondria in the DG75 Burkitt's lymphoma cell line [27,29]. EBNA5 is one of the proteins produced in EBV-infected cells and it is responsible for the immortalisation of those infected cells [112]. Although there was no further information on the interaction, it was suggested that

the possible role of HAX1 was in preventing cell death of EBV-infected cells [27,29].

In contrast to these findings, another study showed that the role of HAX1-viral protein interaction was to destabilise the viral RNA. HAX1 interacts with two HIV (Human Immunodeficiency Virus) proteins: Rev and Vpr [26,38]. Rev protein recognises and exports viral RNA which carries the RRE (Rev-response element) sequence, shuttling between the nucleus and the cytoplasm in a complex with RRE-containing RNA [38]; this is crucial for the expression of unspliced, or singly spliced, viral mRNA that encodes the structural (Gag, Pol, and Env) and accessory (Vif, Vpr, Vpu) proteins [113]. HAX1 binds to and inhibits Rev from binding to its target RRE RNA, consequently causing destabilisation and degradation of viral RNA in the host cell nucleus; thus suggesting that HAX1 provides protection against virally infected cells [38]. Another study showed HAX1 interacts with Vpr (Human immunodeficiency virus type 1 viral protein R) and caused a protein redistribution [26]. Vpr is required for viral pathogenesis and has been implicated in T-cell apoptosis through its destabilisation of mitochondrial membrane potential and subsequently activation of caspase-3 and caspase-9 [26]. Overexpression of Vpr causes the egress of HAX1 from the mitochondria into the cytoplasm and this resulted in mitochondrial instability and cell death [26]. Conversely, overexpression of HAX1 suppressed the pro-apoptotic activity of Vpr [26]. Together, these studies support the notion that Rev and Vpr share some common steps that interface with the nuclear import/export pathways modulated by HAX1. Furthermore small peptides that mimic HAX1, and specifically interfere with the pathway(s) shared by Rev and Vpr, could provide a valuable therapeutic approach against AIDS [26].

Although the majority of studies demonstrated the anti-apoptosis function of HAX1, there is a study which has reported a converse function of this molecule. Banerjee *et al* reported that decreased HAX1 levels promoted cell apoptosis in the presence of HCV (Hepatitis C Virus) core protein after treatment with 5-fluorouracil (5-FU) [109]. 5-FU is a drug which is known to modulate p53 and is used widely for cancer treatment, such as against gastrointestinal, pancreatic, breast, bladder and prostatic cancers [114]. 5-FU belongs to the antimetabolite class of chemotherapy agents and interrupts the cell cycle by interfering with DNA synthesis through the inhibition of the enzyme thymidylate synthase in cancer cells, ultimately causing cell death [114]. Previous studies have shown that 5-FU treatment results in activation of p53 [115]. HCV core protein is a viral protein that enhances HCV infected cells to become immortalised, resulting in chronic infection and hepatocellular carcinoma [109]. In this study, the authors reported that HepG2 cells expressing HCV-core protein were more susceptible to 5-FU-induced growth inhibition than control cells, whereas cell survival was enhanced after suppression of HAX1 by small interfering RNA [109]. Depletion of HAX1 by siRNA did not significantly alter the status of p53 after 5-FU treatment in HepG2 cells [109]. Interestingly, the reduction of HAX1 in core-expressing cells by siRNA prior to 5-FU treatment led to the loss of p53 enhancement in response to treatment, indicating that HAX1 itself cannot potentiate the accumulation of p53 [109]. The same study also showed suppression of HAX1 by siRNA did not significantly increase procaspase-9 cleavage in core-expressing hepatocytes after 5-FU treatment compared to cells treated with unrelated siRNA as a negative control [109]. Thus the HCV core protein can potentiate the activity of 5-FU through the induction of p53, and subsequent cell death, via a mechanism that relies upon the expression of HAX1 [109].

1.1.4.5.3 HAX1 regulates apoptosis by regulating caspase activity

Apoptosis requires the activity of a group of cysteine-dependent proteinases known as caspases. Apoptosis, or programmed cell death, results in the permeabilisation of mitochondria and release of the apoptotic-activating protein cytochrome c into the cytosol, which then results in activation of caspase-9 and caspase-3 that drives apoptosis [116] (see section 1.1.4.5.1).

A study from Li and colleagues, using flow cytometry, showed that HAX1 siRNA treatment increased the sub-G1 fractions (often apoptotic cells) in melanoma cells and this observed cell death was blocked by a broad-spectrum caspase inhibitor, Z-VAD-fmk, indicating that HAX1 protects cells from apoptosis by inhibiting caspases [117]. Although there were no further experiments from this study, to investigate which specific caspase was involved in those cells, the data indicated caspase-dependent apoptosis is induced by the absence of HAX1 [117].

In other studies, HAX1 has been found to interact with caspase-3 and caspase-9 and subsequently blocks their activation, and thus, the cell apoptosis pathway, protecting cells from programmed cell death [21,28,118,119]. In cardiac research, HAX1 is a survival factor for cardiac cells exposed to hypoxia and protects cells from apoptosis by inhibiting activated caspase-3 and -9 [28]. In the first study that reported the physical interaction between HAX1 and a caspase, Han *et al* found caspase-9 was expressed to a significantly higher level in normal adult cardiac tissue (specifically cardiac myocytes) compared with other tissues (brain, liver, kidney, lung, skeletal muscles, spleen), but these cells were, strangely, resistant to caspase-induced cell

apoptosis [21]. In order to investigate this, wild type procaspase-9 was used as bait in a yeast-two-hybrid study and HAX1 was identified as a binding partner of this molecule [21]. Full length HAX1 also was pulled-down with caspase-9-GST [21]. In addition, a co-immunoprecipitation assay, using human anti-caspase-9 and anti-HAX1 antibodies, further confirmed the interaction of caspase-9 and HAX1 [21]. To define the effect of the interaction, HAX1 function was examined in a cell-free caspase activation system [21]. In this system, the addition of *in vitro* translated caspase to a mixture of cytochrome c/dATP and S100 fraction results in caspase processing [21,120,121]. The result showed HAX1 not only inhibited the activation of caspase-9 but also caspase-3 and the overexpression of HAX1 revealed its protection of cardiac myocytes from H_2O_2-induced apoptosis through blocking caspase-9 activation [21]. This was the first paper describing HAX1 protection of cell death by directly interacting with and inhibiting caspases-9 and -3 [21]. Thus HAX1 negatively regulates caspase family members and thereby exerts an anti-apoptosis effect in cardiac myocytes (Figure 1.8) [21].

X-linked inhibitor of apoptosis protein (XIAP) is a member of the IAP (inhibitor of apoptosis protein) family and it is known to prevent apoptosis by inhibiting caspase-3, -7 and -9 [122]. XIAP interacts with caspase-9 in the cytosol by binding to the active caspase-9-Apaf-1 holoenzyme complex through the amino terminus of the linker peptide on the small subunit of caspase-9, exposed after proteolytic processing at Asp315 [122]. During apoptosis, the protein level of XIAP is regulated by ubiquitination [123]. To investigate whether HAX1 may affect the ubiquitination of XIAP, Kang *et al* performed *in vitro* ubiquitination assays [123]. GST-XIAP was expressed in HEK 293T cells with or without FLAG-HAX1 and HA-ubiquitin, and

GST-XIAP was then isolated by incubation with glutathione agarose beads [123]. In the absence of FLAG-HAX1, polyubiquitinated XIAP was identified as a ladder of protein bands [123]. In contrast, the addition of FLAG-HAX1 significantly suppressed the level of ubiquitinated XIAP, indicating that the interaction between HAX1 and XIAP blocked the polyubiquitination of XIAP [123]. The cell viability was also measured by CCK-8 assay and the data showed that HAX1-XIAP interaction inhibited cell death triggered by Etoposide in HEK293 cells (data did not show HAX1 alone) [123]. Taken together, it was suggested that the association of HAX1 and XIAP provided protection to XIAP from degradation via poly-ubiquitination, thereby inhibiting cell apoptosis [123].

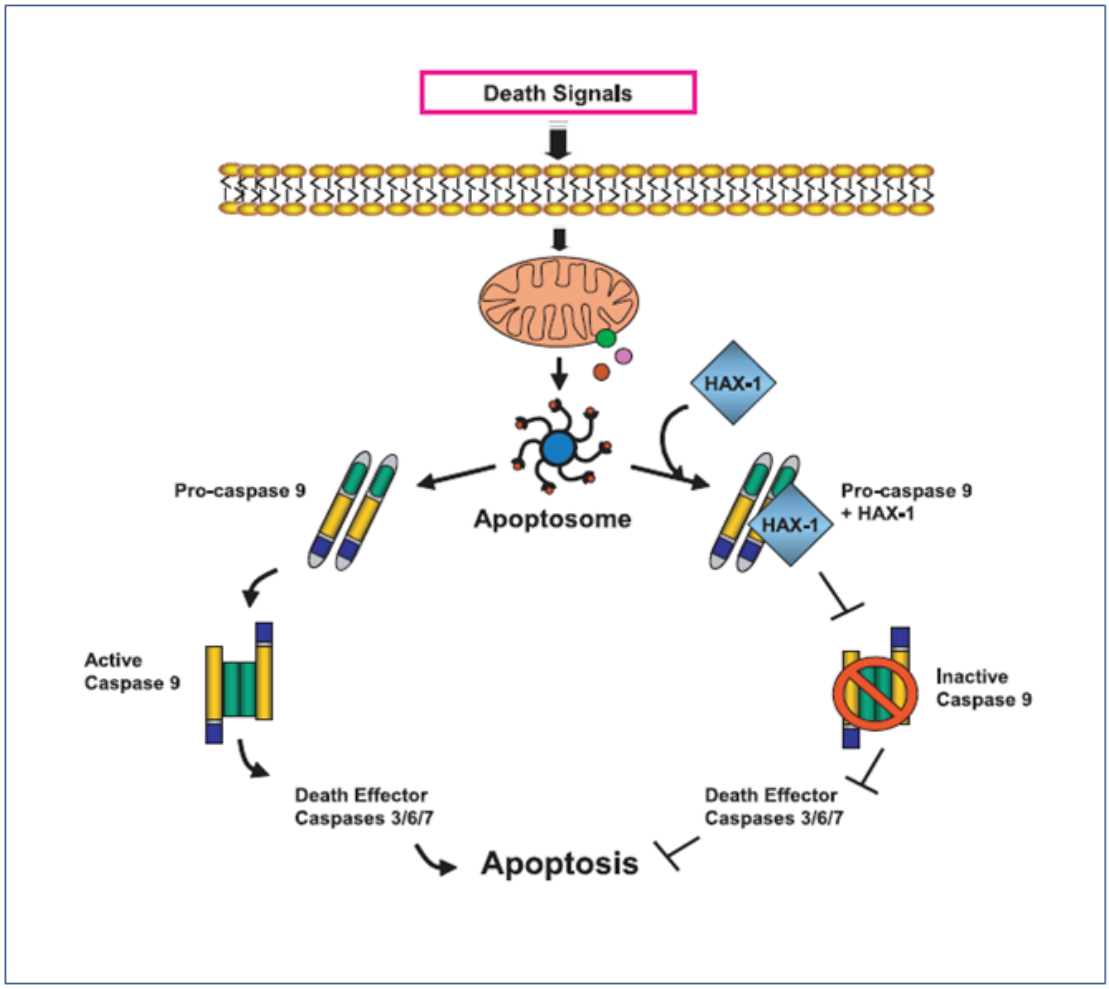

Figure 1.8 Apoptosis pathways in cardiac myocytes.

Death signal (stress-inducing stimuli) activate apoptosis by depolarising mitochondria and opening permeability transition pores. Pro-apoptotic factors, such as cytochrome c, Smac (second mitochondrial activator of caspases), AIF (apoptosis-inducing factor), Omi/HtrA2, are then released into the cytoplasm. Cytochrome c and pro-caspase-9 from the apoptosome trigger the activation of downstream caspase-3, -6, -7 to execute cell apoptosis. In the presence of HAX1, caspase-9 is blocked thereby blocking downstream death factors. Figure adapted from [119].

1.1.4.5.4 HAX1 modulates calcium homeostasis in the sarcoplasmic reticulum (SR)

Cardiac function is tightly controlled by calcium regulation. When the demand arises, the heart can respond to the stress and increase blood flow to peripheral tissues immediately [124]. Adrenaline is the hormone that, when released into blood by demand, initiates an important signal-transduction pathway in the heart by binding to β-adrenergic receptors in the cardiac myocyte cell membrane [124]. The activated adrenaline receptor can phosphorylate the downstream molecules and subsequently increases cell contraction by elevating the cytosolic calcium concentration [125]. The sarcoplasmic reticulum (SR) is the calcium storage site in cardiac cells, and the Ca^{2+} can be transported to the cytoplasm by phospholamban (PLN) and its substrate, also a Ca^{2+} pump, SR calcium ATPase (SERCA) [126]. PLN is a small integral membrane protein (52 residues) localised in the SR membrane, and it mediates downstream signals for the adrenaline-signalling pathway upon stimulation [125]. PLN can be reversibly phosphorylated and its phoshorylation status regulates the calcium flow [127]. Unphosphorylated PLN binds to and inhibits SERCA, the enzyme which is a calcium pump, that is responsible for calcium re-uptake into the SR lumen from the cytosol, by reducing its affinity for calcium [126]. The inhibition of SERCA results in an elevated cytosolic Ca^{2+} level and initiation of the heart muscle contraction [126]. To allow muscle relaxation between the heart muscle contractions, cytosolic Ca^{2+} needs to be decreased rapidly. Upon adrenergic stimulation, protein kinase A phosphorylates PLN and this releases the inhibition to SERCA and therefore restores SERCA activity, as a result cytosolic Ca^{2+} is decreased as Ca^{2+} is transported back to the SR, and causes muscle relaxation [125].

These events are responsible for normal heart functioning and if disrupted may lead to heart failure [128].

In order to investigate further the mechanism of the regulation of PLN/SERCA, Vafiadaki *et al* used the yeast two-hybrid approach to identify additional proteins that may interact with PLN [28]. In this study, HAX1 was identified to interact with PLN from an adult human cardiac cDNA library and this was confirmed by GST-pull down in human and mouse cardiac cells [28]. The binding region of HAX1 for PLN was in the C-terminal fragment (a.a. 203–245), whereas the PLN binding region contained residues 16–22, a region that includes both the Ser16 and Thr17 phosphorylation sites [28]. It has been shown that PLN can be phosphorylated at three distinct sites: Ser16 by cAMP and cGMP dependent protein kinases (PKA and PKG, respectively), Thr17 by Ca^{2+}–calmodulin-dependent protein kinase II (CaMKII), and Ser10 by protein kinase C (PKC) [127,129]. These data imply HAX1 may play an important role in regulating the activation of PLN. The study also showed phosphorylation of PLN, or elevation of the concentration of Ca^{2+}, led to dissociation of exogenous HAX1 from PLN [28]. Phosphorylation of PLN by cAMP dependent protein kinase reduced binding to HAX1, while increasing concentrations of Ca^{2+} diminished the PLN/HAX1 interaction in a dose dependent manner , and this is similar to the findings on the PLN/SERCA2a interaction, implicating the physiological/pathophysiological significance of PLN/HAX1 association in cardiac muscle [28]. The same study also showed the presence of PLN enhanced the HAX1 protective effects from hypoxia/reoxygenation induced HEK293 cell death measured by the MTT assay [28]. These findings imply a possible link between the Ca^{2+}

handling by the sarcoplasmic reticulum and cell survival mediated by the PLN/HAX1 interaction [28].

Interestingly, HAX1 is in fact a binding partner for both PLN and its substrate SERCA2 with almost an identical binding domain (a.a. 203-225 for PLN, and aa. 203-245 for both PLN and SERCA2) reported by the same group in a subsequent study [28,130]. PLN can exist as an oligomer, in which form it is unable to bind to SERCA2 [130]. The study showed that HAX1 overexpression enhanced formation of PLN monomers which are active for binding with SERCA2, and promoted the inhibition to SERCA2 [130]. The authors also showed that both elevated calcium level and phosphorylated PLN can reduce the PLN/SERCA2 and PLN/HAX1 interaction [28,130]. PLN also played a role of modulating HAX1 expression as decreased HAX1 mRNA and protein were found in PLN knockdown cells whereas PLN was not affected by HAX1 levels, indicating the PLN may be an upstream regulator of HAX1 [28]. The HAX1 expressing cells exhibited increased viability and cotransfection with PLN resulted in a further increase in cellular survival in the treatments of H_2O_2 and thapsigargin, a selective inhibitor of SERCA2, that induces apoptosis through ER stress after perturbation of Ca^{2+} levels [130]. On the contrary, co-transfection with SERCA2 caused a reduction in cell viability in HAX1 or in PLN/ HAX1 co-transfected HEK293 cells [130]. All together, these findings suggest that PLN enhances the protective role of HAX1 against cell death, but SERCA2 promotes the opposite phenomenon, suppressing the antiapoptotic capacity of HAX1 [28,130].

Interestingly, studies showed other antiapoptotic proteins such as Bcl-2, BAX and BAK influence cell survival through regulation of ER Ca^{2+} homeostasis by decreasing ER and mitochondrial Ca^{2+} levels [131-133]. These molecules also prevent sustained Ca^{2+} increase in the cytoplasm and mitochondria that would trigger activation of cell death signalling cascades [131,132]. HAX1 presents a similar anti-apoptotic role through the same pathway as these apoptotic proteins. Overall, the evidence indicates that HAX1 regulates SR/ER Ca^{2+} homeostasis and this represents a critical determinant of cellular sensitivity to apoptotic stimuli in cardiac muscle [28,130].

1.1.4.5.5 HAX1 regulates mitochondrial permeability by binding to Omi/HtrA2 and PARL

High temperature requirement protein A (HtrA2 also named as Omi) is a mitochondrial serine protease that belongs to the HtrA family of proteases [89]. The mammalian HtrA2 protease, Omi, is much better known than other HtrA family members for its proapoptotic activity [134]. Omi/HTRA2 resides in the mitochondrial intermembrane space and translocates to the cytoplasm where it binds to, and cleaves, its downstream substrates, inhibitor of apoptosis proteins (IAPs) and therefore facilitates caspase-dependent and caspase-independent apoptosis [88,89,134].

To investigate the mechanism of Omi-induced apoptosis, Cilenti *et al* set out to isolate novel substrates that are cleaved by this protease and HAX1 was found to be a substrate of Omi/HtrA2 [30]. By overexpression of HtrA2/Omi, it was

demonstrated that HtrA2/Omi-mediated degradation of endogenous HAX1 correlated with extensive cell death induced by Etoposide, cisplatin and H_2O_2 in HK-2 cells [30]. In contrast to Omi /HtrA2, endogenous HAX1 protein levels were significantly reduced but remained associated with mitochondria of cisplatin- and H_2O_2-treated HEK293 cells [30] Overexpression of HAX1 significantly increased resistance to cisplatin-induced apoptosis compared with cells transfected with the empty vector [30].

In a separate study, a different role for HAX1 and Omi/Htra2 was suggested. Chao *et al* reported that HAX1 is a mediator which presents inactive Omi/HtrA2 to another mitochondrial protease PARL (presenilin-associated, rhomboid-like) [135]. Omi/HtrA2 contains a MTS (mitochondria-targeting sequence) which is cleaved in the active form [136]. Omi/HtrA2 binds to HAX1/PARL complex in the mitochondrial inner membrane and this interaction allows PARL to cleave the MTS (mitochondrial-targeting sequence) of Omi/HtrA2 and turns it into the processed form [135]. The cleaved Omi/HtrA2 is subsequently released to the mitochondrial inter-membrane space and removes pro-apoptosis proteins, such as active Bax, therefore promoting cell survival [135].

1.1.4.5.6 HAX1 modulates cell apoptosis by interaction with a mitochondrial protein, PHB2 (Prohibitin 2)

Prohibitin (PHB) comprises two subunits, PHB1 and PHB2, and they are ubiquitous proteins that are mainly localised in mitochondria [137]. These two proteins assemble into a ring-like macromolecular structure at the inner mitochondrial membrane and protrude into the intermembrane space [138]. The first mammalian prohibitin (PHB1) was identified as a potential tumour suppressor with anti-proliferative activity and hence was named prohibitin [139]. PHB2 was identified to repress nuclear estrogen receptor activity by interacting with and inhibiting the transcriptional activity of the estrogen receptor [140]. To study the regulatory mechanism of PHB2 in mammalian cells, Kasashima *et al* identified HAX1, ANT2 (adenine nucleotide translocator 2) and VDAC2 (voltage-dependent anion channel 2) as binding partners for PHB2 using mass spectrometric analysis [141]. In PHB2 knockdown HeLa cells, the endogenous HAX1 was down-regulated with associated cell apoptosis increased (by measuring cell count and staining with rhodamine123, which indicates decrease of mitochondrial membrane potential, and also cytochrome *c*); this evoked cell death was suppressed by caspase inhibitor Z-VAD-FMK, indicating apoptosis was caused by a caspase-dependent pathway [141]. In contrast, PHB2 protein levels were unchanged after HAX1 knockdown, suggesting PHB2 might be an upstream regulator of HAX1 and thus PHB2 may prevent cell apoptosis through maintaining HAX1 levels [140].

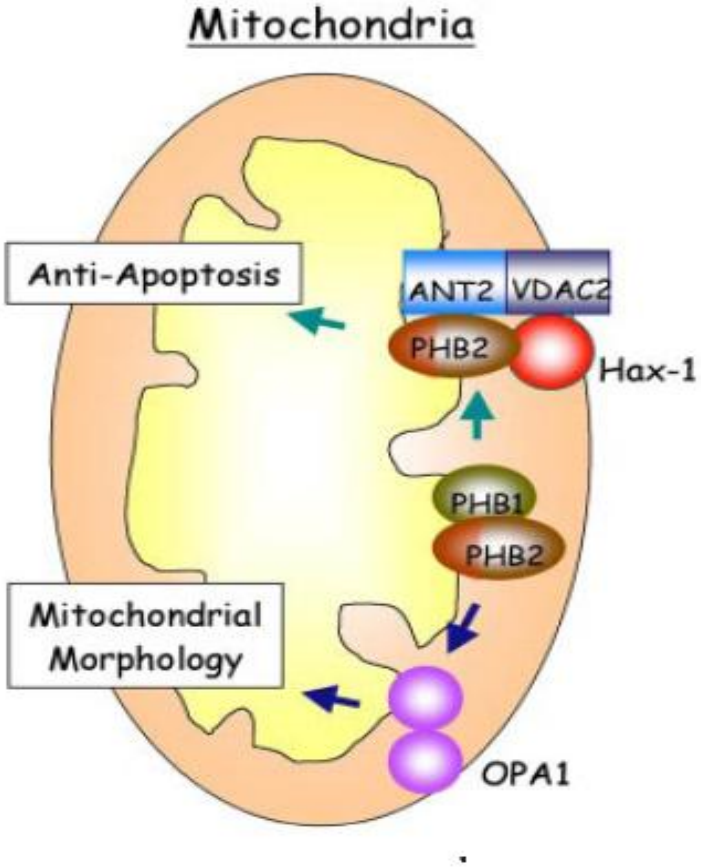

Figure 1.9 HAX1 forms a complex with PHB2 in mitochondria.

HAX1, ANT2 (adenine nucleotide translocator 2), VDA2 (voltage-dependent anion channel 2), and PHB2 comprise a mitochondrial complex in the intermembrane space. PHB2 protects cell from apoptosis by interacting with HAX1 and maintains the mitochondrial morphology via OPA1 (optic atrophy 1). Figure adapted from [140].

In conflict with these reports, a study from Jeyaraju and colleagues pointed out that HAX1 does not possess a C-terminal α-helix by sequence analysis, which is required for the transmembrane domain that anchors in mitochondrial membrane [90]. Also, HAX1 does not contain cysteine residues required for mitochondrial intermembrane space protein import through the MIA (mitochondrial intermembrane space assembly) pathway or any predictable mitochondrial import peptide [90,142]. The cell fractionation data showed that heavy membranes contain HAX1, but that the protein is absent in highly purified, intact mouse liver mitochondria preparations [90]. Thus the activity of HAX1 cannot be mechanistically coupled to PARL because the two proteins are confined in distinct cellular compartments *in vivo*, suggesting their interaction *in vitro* is an artefact [90]. The authors concluded that HAX1 is not imported inside the mitochondria, although it might be peripherally associated with the organelle [90].

1.1.4.5.7 HAX1 regulates cell apoptosis in neutrophils

In a recent paper demonstrating that HAX1 regulates neutrophil functions, it was shown that, a mild increase in the H_2O_2 induced apoptosis of HAX1-deficient cells compared with control cells by annexin V staining, suggesting that HAX1 modulates the sensitivity of pro-apoptotic stimuli in the neutrophil-like PLB-985 cells [20].

1.1.4.6 Summary of HAX1 functions

Thus the HAX1 protein has been implicated in various cellular functions with different binding partners: these functions include mediating endocytosis of membrane protein; promoting cell migration and invasion; possibly having a role in stabilising mRNA; autophagy regulation and anti-apoptosis. The HAX1 binding proteins and functions are summarised in Table 1.4

Proteins	Interaction in HAX1 (isoform 1)	Cell line studied	Functions
Membrane proteins			
mIgE	50-279	J558L myeloma cells	HAX1 protein levels influence Ag-internalisation efficiency [34]
αvβ6	271-279	VB6 and H400 oral cancer cell lines	The interaction promotes β6 internalisation and is required for cancer cell invasion [1]
BSEP	-	HEK293, MDCK, liver cells	HAX1 and cortactin promote BSEP internalisation [31]
Cytoplasmic proteins			
HS1	114-279	COS-7 cells	Suggestion of regulating B cell signalling [3]
PKD2	179-279	HeLa cells	HAX1 links PKD2 to cell-matrix contacts [8]
Gα13	176-247	COS-7, NIH3T3 cells	HAX1 promotes Gα13-mediated cell migration [49]
IL-1	187-279	Skin fibroblast,HEK293 cells	The link between IL-1α and HAX1 suggest effects on cell motility/adhesion [11]
PELO	176-279	HeLa cells	Suggestion of mediating cell migration or degradation of No-Go mRNAs [50]
Supervillin	144-279	HeLa, COS7-2 cells	Promotion of cell motility [61]
XIAP	128-279	HEK293 cells	Stabilises XIAP which inhibits apoptosis [143]
PrP	38-129	293T	Protect cells to resist the challenge of H_2O_2
Grb7	-	HeLa cells	Possible role in cell migration [53]

Mitochondrial proteins			
PHB2	-	HeLa cells	Stabilises mitochondrial morphology, anti-apoptosis [140]
Caspase-9	175-206	Adult rat cardiomyocytes	Inhibits caspape-mediated apoptosis [21,119]
Caspase-3	-	HeLa cells	Caspase-3 cleaves HAX1 at the Asp^{127}, overexpression of HAX1 protects cell from apoptosis [118]
Omi/HtrA2	187-235	HEK293, HK-2 cells	Omi/HtrA2 cleaves and degrades HAX1, activating apoptosis [30]
PARL	79-100,187-235	COS-7 cells	Processes Omi/HtrA2 and protects cell from cell death [135]
ER protein			
PLN	203-225	Cardiac muscle, HEK293 cells	Regulate ER/SR Ca2+ homeostasis and promote cell survival [28]
SERCA2	203-245	HEK239 cells	HAX1 promotes cell survival by binding and inhibiting SERCA2 [130]
Nuclear proteins			
DNA polymerase β mRNA	129-279	Rat hepatoma FTO-2B cells	Post-translational regulation (stabilises) mRNA[32]
Vimentin	-	HeLa cells	Suggestion of helping mRNA translocation [35]
Viral proteins			
EBNA-LP	-	COS-7 cells	Suggestion of the anti-apoptosis function in EBV-infected cells [27,29]

K15	109-279	HeLa cells	Suggestion of viral-associates anti-apoptosis and invasion [12]
Vpr	117-143	HeLa cells	HAX1 inhibits apoptosis by suppressing Vpr [26]
Rev	176-261	HEK293, COS-1 cells	HAX1 binds to Rev and inhibits its function to transport viral RRE-containing mRNA [38]
HCV core protein	-	HepG2, Huh7, Hep3B cells	Promote the growth inhibition in 5-FU-mediated apoptosis [109]
N^{pro}	-	Max cells	Regulate subcellular localisation N^{pro} [110]

Table 1.4 HAX1-interacting proteins.

This table illustrates the HAX1 binding proteins described to date and catalogues them according to their subcellular localisations. The HAX1 binding regions for each are shown as the amino acid residue numbers (a.a.). The biological functions of the interactions between HAX1 and each protein are briefly explained in the Table.

1.1.5 HAX1: a family of splice variants

The human HAX1 gene is located on chromosome 1 (location 1q21.3, GenBank gene ID10456) and it has a processed pseudogene located on chromosome X (Xq28) [2]. To date, there are at least eight HAX1 variants identified in human tissue, which are generated by alternative splicing, encoding separate isoforms ranging in size from 15kDa to 32 kDa [2] (Figure 1.10 and Figure 1.11). Sequence comparison of the GenBank and VEGA (Vertebrate Genome Annotation Database) HAX1 entries revealed that the GenBank variant 1 is identical with VEGA HAX1-001 and that the GenBank variant 2 corresponds to the full-length version of VEGA HAX1-004. In my study, I follow the HAX1-001-to-HAX1-008 VEGA annotation referring to the isoforms as HAX1.1 to HAX1.8 (Figure 1.10).

From previous work in my lab, the specific primers for HAX1 isoforms1-8 were designed based on the sequences published in GenBank and Ensembl and were used to screen a panel of 19 human cell lines as well as primary fibroblasts, primary oral keratinocytes and peripheral blood mononuclear cells [2]. All the cells expressed the HAX1 isoforms 1, 3, 5, 6, and 8 whereas the isoforms 2, 4 and 7 were absent in some of the cells [2]. All cells tested expressed six to eight HAX1 isoforms [2].

As shown in Figure 1.10 and Figure 1.11, the full length HAX1 isoform 1 (HAX1.1) contains seven exons and encodes a 279 a.a. protein (molecular mass = 31.62 kDa) [2]. HAX1.2 lacks the first exon, and uses an alternative start codon 27 bases inside exon 2 (of HAX1.1) and it is in-frame with the original stop codon, producing a protein that lacks the first 26 a.a., starting just 3 a.a. before the acid box (molecular

mass = 28.64 kDa) [2]. HAX1.3 has intron retention between exon 2-3 and ends 11 nucleotides before the original end of exon 3, resulting in a putative protein that is identical with isoform 1 for the first 105 a.a. and is followed by an unique and truncated C-terminus ending at a stop codon 56 nucleotides into intron 3 (molecular mass = 14.23 kDa) [2]. Isoform 4 uses an internal splicing site in exon 2, skipping the first 144 nucleotides of this exon [2]. This results in an internal deletion of 48 a.a. and produces a protein that lacks the acid box but retains an identical 3' end to HAX1.1 (molecular mass = 26.09 kDa) [2]. HAX1.5 contains an internal splice site at the end of intron 2 which introduces 24 nucleotides in-frame, resulting in an 8 a.a. insertion into the PEST sequence (positions 106–113) (molecular mass = 32.41 kDa) [2]. HAX1.6 uses an alternative splice site in exon 2, creating a 64 nucleotide deletion in the end of exon 2 and this introduces a frameshift with a unique C-terminal end from a.a. 84 in the isoform (molecular mass = 21.80 kDa) [2]. HAX1.7 and HAX1.8 both start in exon 3; HAX1.7 has a retention in intron 4-5, and intron 5-6 retained in isoform 8 [2]. This encodes a putative HAX1.7 protein of 90 aa with the first 38 aa identical with HAX1.6 (a.a. 127–164) and a new C-terminal sequence for HAX1.7 (molecular mass = 10.02 kDa) [2]. The putative protein of HAX1.8 is 65 aa long (molecular mass = 7.48 kDa) and is 100% identical with the last 65 a.a. of HAX1.6 [2]. Even the intron 5–6 is retained at the mRNA level in HAX1.8, this has no impact on the protein produced as it terminates 26 bases before this intron sequence [2]. The predicted protein sequences encoded by the mRNA and protein are depicted in Figure 1.10 and Figure 1.11.

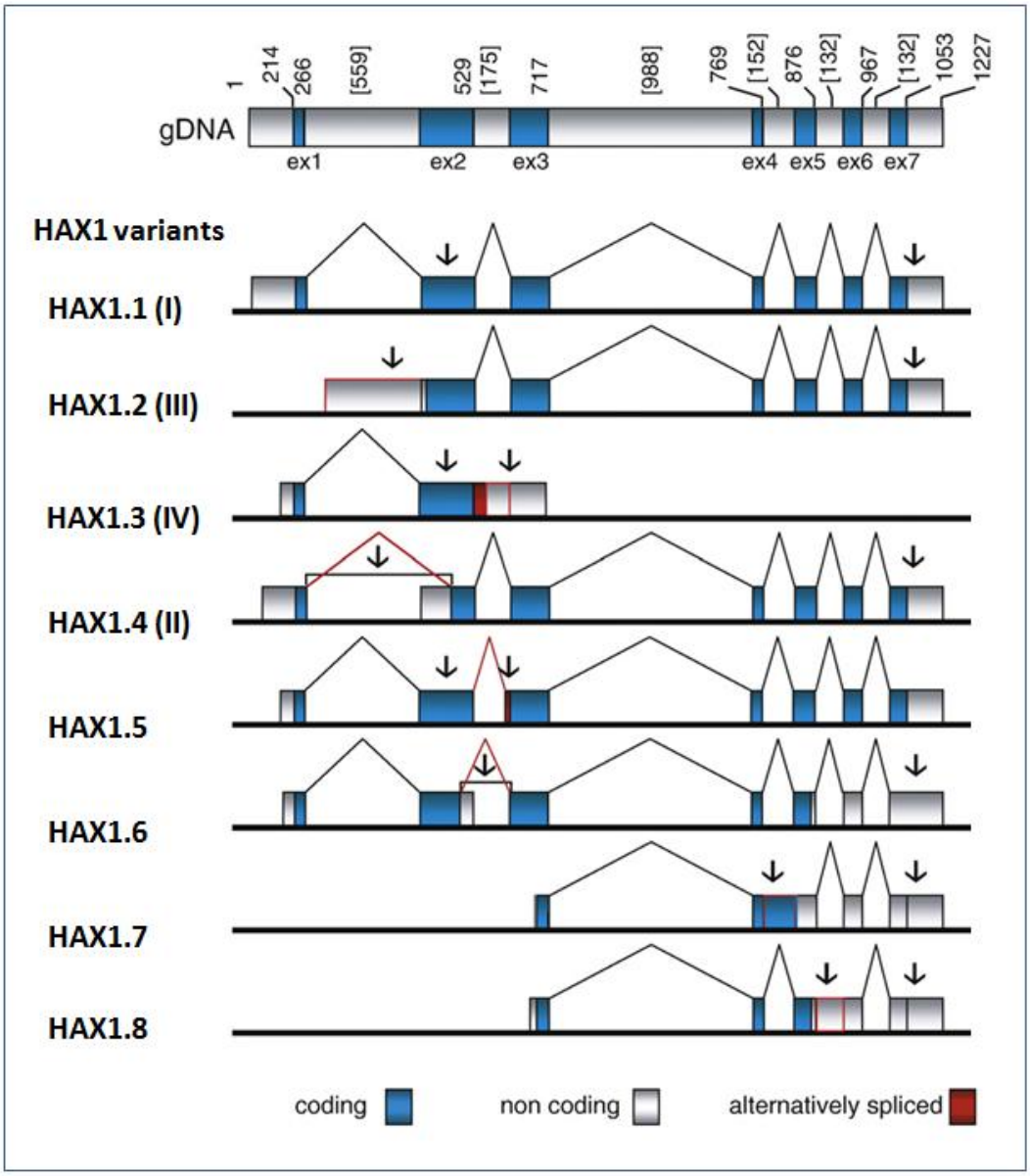

Figure 1.10 Genomic structures of human HAX1 gene and mRNA splice variants.

HAX1 genomic organisation: exons are shown in blue, introns are shown in gray and the alternatively spliced sequences are in red. The arrows indicate the positions of the specific primers used for RT-PCR. Splice variants depicted here are named according to VEGA with the GenBank nomenclature in brackets. Figure adapted from [2].

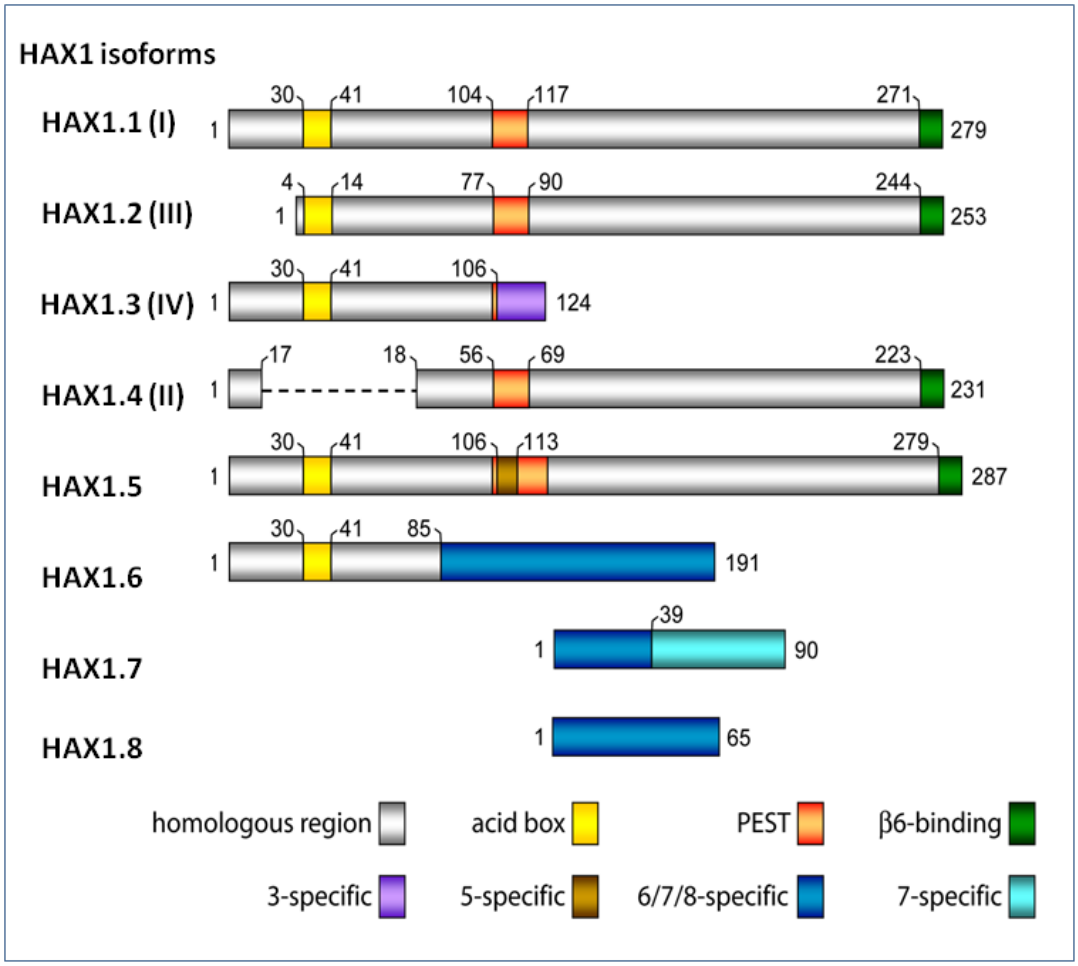

Figure 1.11 HAX1 protein isoforms translated from the eight variants:

Different domains are indicated in different colours. An acid box exists in isoform 1, 2, 3, 5, 6 (yellow) and a β6-interacting domain is possessed by isoforms 1,2,4,5. The HAX1 isoforms depicted here are named according to VEGA with the GenBank nomenclature in brackets. Figure adapted from [2].

1.1.6 Association of HAX1 with disease

1.1.6.1 HAX1 deficiency in severe congenital neutropaenia (SCN; Kostmann's disease)

HAX1 deficiency in mice was described in the study from Chao *et al* [59]. The heterozygous HAX1 deleted mice were found to be viable and fertile whereas homozygous-null mice died within 14 weeks due to loss of motor coordination and activity resulting in a failure to eat [135]. Histological analysis of these null animals identified that there was an extensive apoptosis of neurons in the striatum and the cerebellum [135]. Deletion of HAX1 also resulted in the loss of lymphocytes, with age, in the spleen, bone marrow and thymus and this was associated with increased cell apoptosis [135]. Nevertheless, in bone marrow there was a preferential loss of progenitor-B cell and pre-B cell populations and an associated increase in apoptotic cells [135].

In humans, loss of HAX1, due to nonsense mutations and premature stop codons, has been linked to severe congenital neutropaenia (SCN) or Kostmann's disease. This was the first inborn systemic immune dysfunction disease recognised in 1950 [13]. Patients have severe neutropaenia which is defined as the absolute neutrophil count is less than 1500 cell/ mm^3 blood [14]. Consequently, patients with SCN are vulnerable to recurrent infections [14]. SCN is caused by the maturation-arrest in neutrophil differentiation during promyelocyte/myelocyte stages in the bone marrow due to the mutations in several different genes including ELA2 (elastase 2), AK2 (adenylate kinase-2), WASP (Wiskott-Aldrich syndrome protein), G6PC1 (glucose-

6-phosphate); HAX1 deficiency is found in approximately one third of SCN patients [13].

In general, two human splice variants were reported and changes in these developed different phenotypes of SCN: loss of isoform 1 and the additional loss of isoform 4 [24,144]. Isoform 4 is characterised by a splice event removing part of exon 2 and is preferentially expressed in neuronal cells (see 1.1.5) [2,144]. Mutations affecting only isoform 1 (mutations in 3' terminal of exon 2) gave rise to a phenotype restricted to congenital neutropenia, while mutations affecting both isoform 1 and isoform 4 were associated with a phenotype of congenital neutropenia plus variable degrees of neurological impairment [24,144].

Many HAX1 mutations have now been discovered, most of which are located in exon 2 and 3 and these translational frame-shift mutations result in premature stop codons and missense mutations, resulting in loss of the functional full-length protein [16,24,144] (Figure 1.12). Klein and colleagues were the first to report HAX1 is associated with Kostmann's disease and sequencing data revealed all affected patients had a premature stop codon (Trp44X) in exon 2, which was induced by homozygous single nucleotide insertion (a.a. 130-131), affecting only isoform 1 but not isoform 4, showing the neutropenia phenotype without neurological impairment [16]. Later studies confirmed the striking correlation between the genotype and phenotype: mutations affecting only isoform 1 were associated with neutropenia (Ala25Val, Glu31LysfsX54, Ser43LeufsX11, Trp44X, Glu59X, Glu60Asp), whereas mutations affecting both transcript variants 1 and 4 caused neutropenia and neurologic symptoms, including epilepsy and neurodevelopmental delay

(Leu130Arg, Arg86X in exon 2; Gln123LeufsX4, Arg126fsX128, Gln137X, Val144GlyfsX5, Gln155ProfsX14 in exon 3; Val172Ile in exon 4 and Gln190X in exon 5) (Figure 1.12) [16,24,144-148]. It was suggested that different mutations could have different impacts on the expression of the HAX1 variants in different tissues, regardless of the specific HAX1 mutations, all SCN patients display a HAX1 isoform 1 deficiency in the bone marrow, whereas SCN patients harbouring the mutation affecting isoform 4 may also be deficient for HAX1 protein expression in the brain/neurons [24]. This speculation was confirmed by PCR which showed the tissue expression pattern of isoform 1 and 4 [24]. The overall pattern of expression was similar for both transcripts; isoform 4 was less abundant in the bone marrow, whilst clearly detectable in the brain [24]. So, in theory, when the mutations are only affecting isoform 1 (e.g. Trp44X), isoform 4 could still be expressed normally in the brain of SCN patients, whilst isoform 1 should not be expressed in the bone marrow of the same individuals with the Trp44X mutation [24]. Thus two different types of HAX1 mutations, the first affecting both splice variants 1 and 4, and second affecting splice variant 1 only could result in divergent outcomes in terms of protein expression, and explain the resulting differences in clinical manifestations. The known HAX1 mutations and their locations are shown in Figure 1.12.

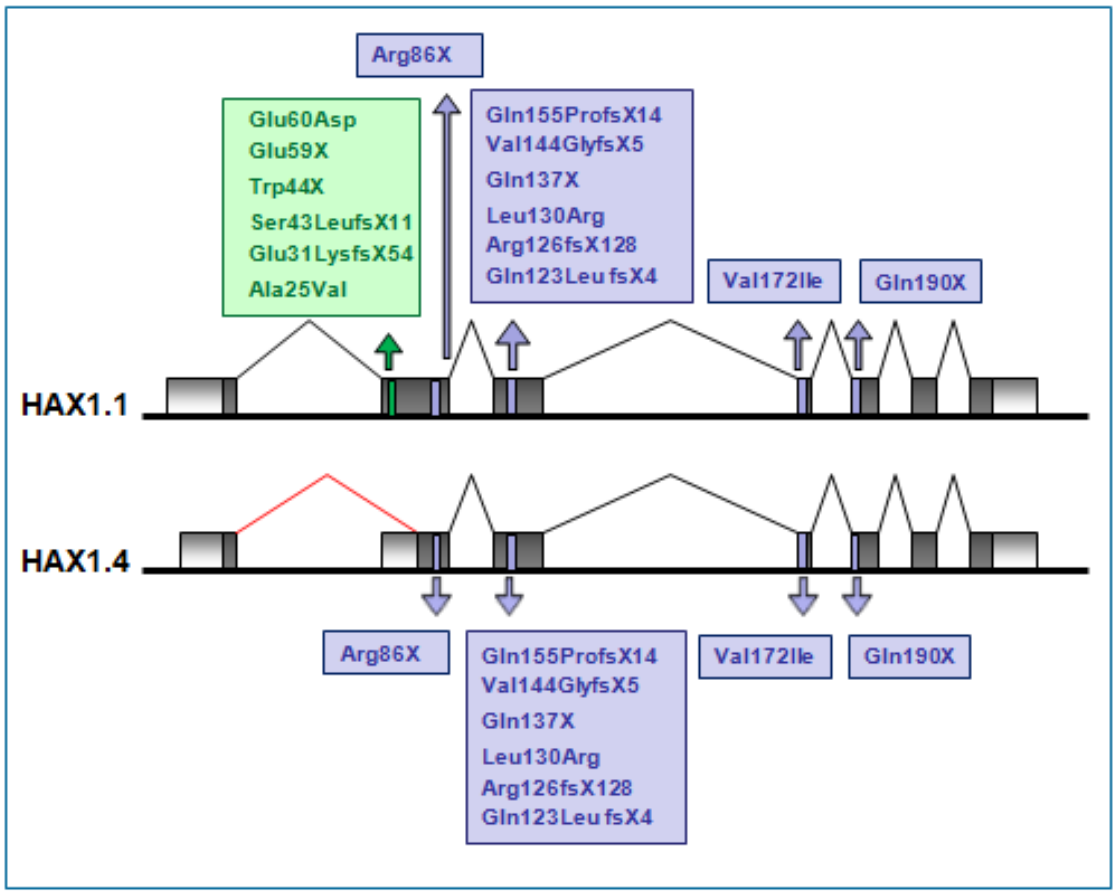

Figure 1.12 HAX1 human mutations and their locations.

A number of HAX1 mutations have been reported. The mutations in the blue box affect both HAX1.1 and HAX1.4 whereas mutations in the green box only affect isoform 1. The amino acid residue number for each mutation is indicated as well as the replaced amino acid. Introns are shown in light gray, exons are shown in dark gray and the alternatively spliced sequences are in red.

1.1.6.2HAX1 overexpression in psoriasis

Overexpression of HAX1 is reported both in psoriasis and in many types of malignancy [1,23,65,117,149]. Interestingly, both cancer and psoriatic cells share the common feature of diminished susceptibility to apoptosis. Since HAX1 is implicated strongly as an anti-apoptosis protein, and it is shown that the association of abnormally high levels of HAX1 in cancer and psoriasis, this finding perhaps is not inexplicable.

Overexpression of HAX1 has been observed in lesional psoriasis, a chronic inflammatory disease characterised by increased proliferation and diminished apoptosis [23]. By using mRNA differential display to search for disease-associated genes, Mirmohammadsadegh *et al* demonstrated the overexpression of HAX1 in lesional psoriatic skin by Northern Blot, Western blot, *in situ* hybridisation and immunohistochemistry. [23]. This confirmed the relatively weaker HAX1 expression in healthy and non-lesional skin compared with hyperproliferative psoriatic lesions [23]. In the same study, the authors also showed caspase-3 activity was increased after HAX1 depletion by HAX1 siRNA after UVB treatment of the HaCat karatinocyte cell line, suggesting an antiapoptotic role for HAX1 [23]. Thus it was suggested that, in psoriasis, the epidermal differentiation could be disturbed due to the increased expression of HAX1 and hence there was a prolonged resistance to terminal differentiation [23].

1.1.6.3HAX1 overexpression in cancer

There are many functions attributable to HAX1 that could lead it to contribute to promoting the progress of cancer: thus the ability of HAX1 to inhibit members of the caspase family [21,117,118]; maintaining mitochondrial membrane integrity and regulating calcium homeostasis which are crucial for cell survival [28,30,130,135,140]; promoting cell migration by regulating cell cytoskeleton arrangement and modulating activity of signalling molecules (Gα protein and RhoA) that regulate motility [20,49]. Collectively, the involvement of HAX1 in inhibition of cell apoptosis and promotion of cell migration suggest HAX1 could be associated with carcinogenesis. Indeed, several studies have linked HAX1 to malignancy. The previous work from my group, by Ramsay *et al* reported that up-regulated HAX1 expression is observed in oral cancer tissues by immunostaining [1]. Expression of HAX1 occasionally occurred at a low level in normal epithelial tissue, but it was up-regulated in SCC (squamous cell carcinoma), with moderate to strong expression in 90% of tumours [1]. HAX1 was also demonstrated to be expressed in melanoma cells and it was associated with cancer cell survival [117]. According to Oncomine, a cancer microarray database, HAX1 is overexpressed in hepatoma, lung cancer, lymphoma, melanoma, leukaemia and myeloma [150]. In a gene expression profiling study utilising serial analysis of gene expression (SAGE), HAX1 overexpression was demonstrated to be induced specifically by hypoxia in renal cell carcinoma (RCC) cells [151]. A recent study also reported HAX1 overexpression in breast cancer and lung cancer and melanoma by using a cDNA array panel [149]. Further RT-PCR analysis from the same study showed HAX1.2 was detected in breast cancer cases (8 out of 15 cases) but not in the matching normal tissues [149].

This suggests that upregulation of isoform 2 may be related to breast cancer development and also suggests there may be different regulation for different HAX1 isoforms and that this may associate with the various stages/types of cancers. The fact that different HAX1 isoforms associate with various functions also gave us the confidence to hypothesise that different isoforms may well perform different functions and that this might be related to specific subcellular localisation. Thus, elucidating the particular roles of each isoform may provide novel therapeutic opportunities for targeting diseases associated with HAX1. More evidence is needed to explain the contributions of each isoform, and this is the goal of my study. In the next section I will introduce the connection of HAX1 and integrins focusing specifically on integrin αvβ6 since my lab already has shown it interacts with HAX1.

1.2 Integrins

1.2.1 Integrin Structure and Function

Integrins are a group of cell-surface adhesion molecules which mediate extracellular binding to extracellular matrix (ECM) glycoproteins and, in some cases, proteins expressed on other cells (e.g. β2 integrins binding immunoglobulin superfamily proteins such as ICAM1) [152-154]. Thus integrins act as a bridge between cells and the ECM across which information can pass in both directions [152]. They are transmembrane αβ heterodimers, comprising 24 distinct integrins in humans constituted by 18 α-subunits and 8 β-subunits (Figure 1.13) [153]. Integrins have an extracellular domain which is exposed on the cell surface and interacts with its ligands; a transmembrame domain anchored in the cell membrane and a relatively

shorter cytoplasmic domain [155]. Physically they appear (at electron microscopy levels) as a globular (ligand-binding) head on two thin stalks that traverse the membrane [156]. Not all cells express all integrins as some integrins are tissue-specific (e.g. αIIbβ3 on platelets and α6β4 on epithelial cells) whereas some are more widely expressed (e.g. α5β1 is on many epithelial and mesenchymal derived cells) [152,157].

The ECM is a glycoprotein scaffold to support tissues and organs and it is produced jointly by epithelial, endothelial, and stromal cells [158]. It is composed of a mixture of different molecules including structural proteins, such as fibronectin, collagens, laminins, proteoglycans, in which are embedded growth factors [159]. Some ECM proteins are recognised by many different integrins. For example, laminins are recognised by α1β1, α2β1, α3β1, α6β1, α6β4, α7β1 whereas collagen is recognised by α1β1, α2β1, α10β1, α11β1, αvβ3 [153]. The reasons why there are so many different integrins for some ligands are not always clear but may relate to the different intracellular signals generated by the different integrins [158]

Integrins bind to discrete amino-acid motifs in their ligands and individual integrins are specific for particular proteins. The most common motif recognised by integrins is RGD (arginine-glycine-aspartic acid) which occurs in many ECM proteins (such as fibronectin, vitronectin and TGFβ latency-associated peptide [LAP]) [153,160,161]. There are eight integrins that bind to RGD as part of their recognition site (αvβ1, αvβ3, αvβ5, αvβ6, αvβ8, αIIbβ3, α8β1 and α5β1) [162]. In my thesis, I shall concentrate on the expression and regulation of one integrin, αvβ6, and its cytoplasmic binding partner HAX1.

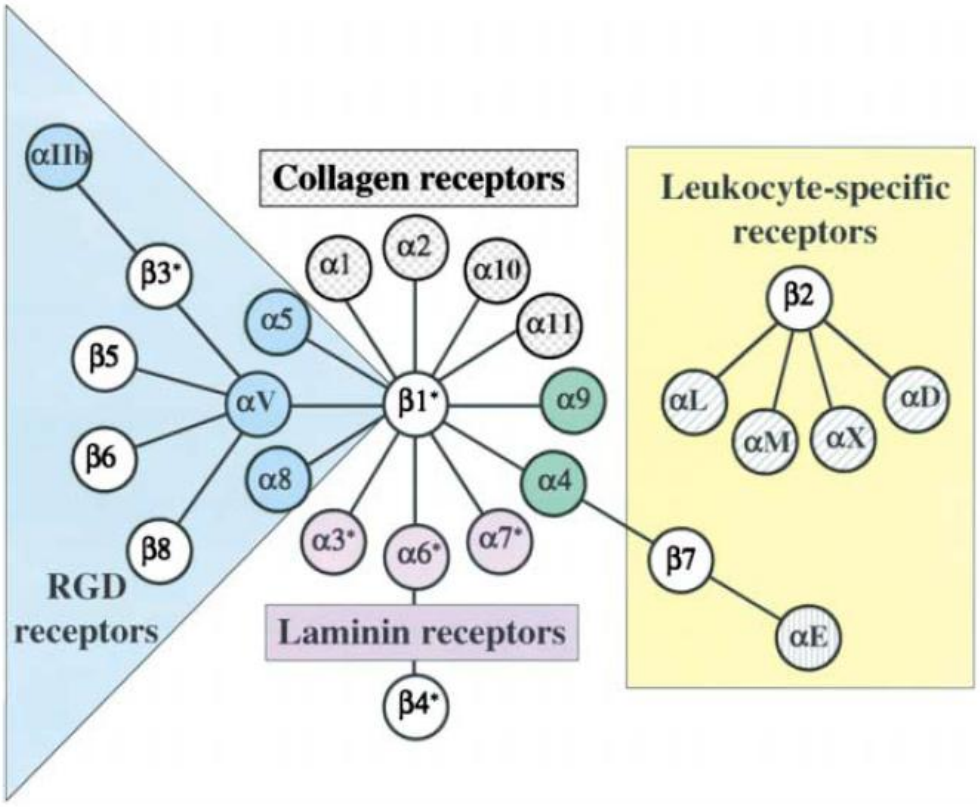

Figure 1.13 The integrin family.

Integrins are heterodimeric transmembrane receptors comprising alpha and beta subunits. 18α and 8β subunits form 24 distinct human integrin heterodimers [152]. These constitute several subfamilies based on evolutionary relationships (colouring of α subunits), ligand specificity and, in the case of β2 and β7 integrins, restricted expression on white blood cells. α subunits with gray stippling recognise collagen. Such α subunits are restricted to chordates, as are α4 and α9 (green) and subunits β2-β8. Purple indicates the α subunits with specificity for laminins whereas blue is for RGD. Asterisks denote alternatively spliced cytoplasmic domains. Each of the 24 integrins shown appears to have a specific, nonredundant function. Figure adapted from [152].

1.2.2 Regulation of integrin activation and signalling

Integrins act not only as anchors of cells to ECM by linking them to the actin cytoskeleton, but also mediate a great variety of cellular functions via their cytoplasmic tails [152]. Binding to their ligands transmits signals bi-directionally and regulates a vast number of downstream cellular functions such as adhesion, survival, cell proliferation and cell motility [152,153,163] (Figure 1.14). Integrins can exist in different states of activation and this regulation controls the ability of integrins to bind to their ligands; the regulation of the switch for on and off is critical for pathological consequences. Many integrins are not constitutively active, as they can be expressed in an inactive state which cannot bind to ligands and, therefore, cannot signal [152]. The activation of integrin is associated with a major conformational change of the heterodimers by the disruption of the non-covalent binding [152]. Electron microscopy studies show that in inactive integrins the globular head is bent toward the cell membrane whereas in activated integrins the integrin 'flicks' up extending the binding region from the cell membrane [156]. In the inactive state, the α-subunit and β cytoplasmic tails interact with each other through a membrane-proximal salt bridge, and this interaction keeps the integrin in the inactive state [163].

Regulation of integrin activation from within cells is referred to as "inside-out" signalling and this regulates integrin affinity for their extracelluar ligands [152]. Essentially inside-out signalling regulates the dissociation of the intracellular salt-bridge and, as consequence, the integrin becomes activated by exposing the ligand-binding site in the extracellular region [158,163]. This dissociation of heterodimer is

caused by the binding to the cytoplasmic tail of cellular adaptor proteins such as talin, filamin or tensin [155,163,164] and this separation transforms the integrin to a high-affinity ligand binding state [165]. In addition to conformational changes, inside-out signals also control integrin clustering and accumulation at specific regions of the plasma membrane [166]. In leukocytes, these activating signals can be transduced by chemokine and other cell membrane receptors (inflammatory receptors, adhesion molecule receptors) [166]. For example, αIIbβ3 is presented on the circulating platelets as inactive integrin and this inactive status is necessary for preventing the inadvertent occurrence of platelet aggregation [167]. Upon stimulation, triggered by G-protein coupled receptors, by the von Willebrand factor receptor or by collagen-binding integrin receptors, the activated αIIbβ3 binds to fibrinogen and thereby generates a fibrin-platelet clot promoting fibrin deposition; however, since platelet activation is induced by factors released (e.g. thrombin) or exposed (e.g. collagen) at sites of damage, inappropriate fibrin clots that could be lethal are avoided [167].

Apart from "inside-out" signalling, integrins also mediate "outside-in" signalling regulation [152]. Upon ligand binding to the extracellular domain, the integrins activate downstream intracellular signalling [33]. When ligands such as fibronectin, collagen, vitronectin bind to integrins, the integrins cluster leading to the formation of a macro-molecular complexes of integrins with their cytoplasmic tail associated molecules [163]. Although integrins lack intrinsic kinase activity, they are able to transduce signals by recruiting kinases at these macromolecular complexes which become activated when they come into juxtaposition with activators in the complex;

this may be through dimersation (e.g. FAK [focal adhesion kinase]) or via activity of other molecules in the complex (e.g. src, phosphorylates multiple sites on FAK) [168]. A common structure seen when cells adhere to rigid planar surfaces, the focal adhesion, actually is just such a macromolecular complex [159]. Through focal adhesions, integrins can regulate signalling functions as well as interacting with cytoskeleton and therefore mediate a vast number of cellular functions (Figure 1.14) [161]. Through focal adhesions, integrin tails bind and activate intracellular kinases such as FAK, Serine/threonine kinases, lipid kinases (eg PI 3-kinase), phosphorylases (e.g. RPTPα), and these enzymes modulate cellular proteins post-transcriptionally [169]. Also, integrins regulate cell motility by interacting with the actin cytoskeleton directly or indirectly [168]. Many different molecules are recruited to the focal adhesion complex and these regulate different cell signals in response to the various integrin-ECM binding events (Figure 1.14) [159].

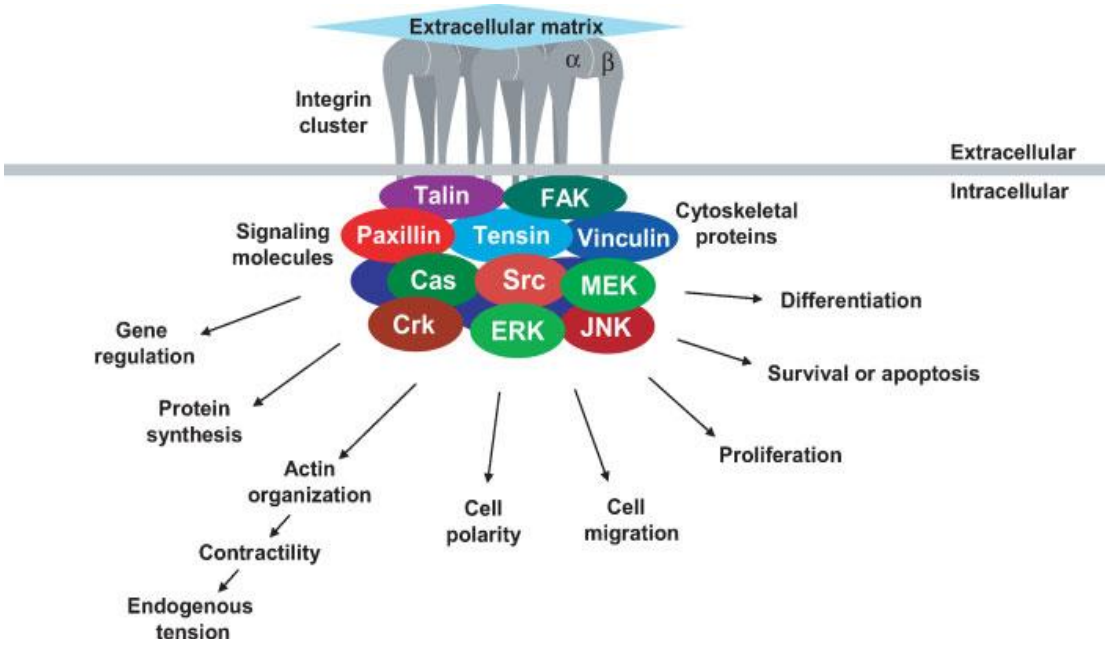

Figure 1.14 Integrins clustered at a focal adhesion.

Integrins bind to ECM proteins and cluster together which recruits structural and signalling molecules. Clustering of integrin receptors, or particularly integrin β cytoplasmic domains, activates non-receptor tyrosine kinases such as focal adhesion kinase (FAK) leading to localised increases in the levels of tyrosine-phosphorylated proteins. Serine/threonine kinases including members of the protein kinase C family, and lipid kinases such as PI3-kinase are also regulated by integrin engagement and clustering. These kinase and phosphatase signalling pathways induce post-translational modifications regulating the protein interactions and/or enzymatic activity of the substrates. They specify protein recruitment to adhesion complexes and thereby selectively link matrix adhesions to various downstream signalling cascades that control cytoskeletal organisation, gene regulation, and diverse cellular processes and functions. Figure adapted from [159].

Thus, integrins transmit signals bi-directionally: inside-out signalling is the separation of integrin subunit cytoplasmic tails by the action of the intracellular molecules and this activates the extracellular domains for ligand binding; outside-in signalling, the binding to the extracellular ligands, may result in clusters of integrin and therefore contribute to intracellular signal transduction by allowing interaction of cytoskeletal proteins and signal transduction molecules. The bi-directional signalling is required for integrins to mediate or promote many cellular behaviours including adhesion, migration, invasion, differentiation, survival and gene expression [152,163,165]. In the following section I will give examples of data describing many of these processes, mostly using the integrin αvβ6 as an example.

1.2.3 Integrin functions

1.2.3.1 Integrins and cell survival

Cell growth and differentiation requires interaction of cells with ECM through integrins, and loss of matrix attachment can lead to anoikis [170]. Anoikis is a term to describe a phenomenon of programmed cell death due to lack of appropriate anchorage to ECM or neighbouring cells [171]. Integrins interact with their ligands in ECM and this relays survival signals whereas unbound integrins can promote cell apoptosis; such adhesions to the ECM are crucial to determine whether the cell is in a correct location within tissues [172]. For example, unoccupied αvβ3 integrins activate apoptosis in cells by recruiting caspase-8 [173]. α6β4 binding to laminin-5 protects breast cancer cells from several death signals (activated by treatment with TNF-α, Fas or Etoposide) [174]. Also, successful keratinocyte growth in three-dimentional methylcellulose requires the interaction between α5β1 and its ligand, fibronectin [175]. Moreover, melanoma cells required interaction of the integrin αvβ3 to sustain viability and growth in three-dimensional collagen [176]. However, many cancer cells develop mechanisms to resist anoikis and grow in an anchorage-independent way in order to survive beyond the basement membrane [172,177]. FAK is a nonreceptor tyrosine kinase predominantly localised in focal adhesions of adherent cells [168,178]. FAK activation and phosphorylation by integrin-mediated cell adhesion provided anchorage-independent growth of cancer cells by signalling through phosphatidylinositol 3-kinase (PI3K) to the Akt/protein kinase B (PKB) [179]. Janes and Watt (2004) found that up-regulation of αvβ6 protects squamous carcinoma cells from anoikis by activating Akt survival signals, a downstream target

of FAK and PI3K signalling [68]. They also reported that this involved a switch from αvβ5 to αvβ6 integrin expression, to the advantage of the αvβ6-expressing cells enabling them to grow in an anchorage independent fashion [68]. This anchorage-independent growth is proposed to allow the invasive tumour cells to survive beyond the confines of the basement membrane [172].

1.2.3.2Integrins and cell migration and invasion

The cytoskeleton, the intracellular scaffolding of each individual cell, provides the strength of cell structure. The cytoskeletal network integrates with various intracellular signalling molecules and organelles, generating coordinated force for cells to change their shape during cell migration [180]. The main elements of cytoskeleton include actin filaments, microtubules, and intermediate filaments, and their polymerisation and depolymerisation controls cell structure as well as motility [41]. In the leading edge of migrating cells, integrin-ligand interaction triggers actin filament assembly into stress fibres which generate protrusion at the front, whereas actin-myosin filaments produce contraction at the rear [155]. Also, as a result of focal adhesion induced by integrins, the cytoplasmic tails of integrins bind directly to cytoskeleton and signalling molecules such as α-actinin, FAK and vinculin, or through indirect binding to adaptor proteins, such as talin, filamin, and tensin, and these associations promote cell movement [155,164].

Integrin αvβ6 is expressed only by epithelial cells and then usually only when cells are undergoing tissue-remodelling, including development, wound healing, chronic inflammation and cancers [69]. Thomas *et al* showed that αvβ6 on normal and

transformed keratinocytes promoted adhesion to, and migration toward, fibronectin and latency-associated peptide (LAP), the pro-peptide of TGF-β [181]. Adhesion to fibronectin of transformed keratinocytes was also mediated by α5β1 but only αvβ6 mediated the migration on this ligand [182]. Overexpression of αvβ6, by retroviral vector delivery of β6 cDNA, increased migration on fibronectin and also enhanced cell invasion in 3D environments [70].

1.2.3.2.1 Integrins and MMP family

Matrix metalloproteinases (MMPs) are a family of zinc-dependent enzymes that degrade a range of ECM components such as collagens, laminins, vitronectin, and fibronectin [183,184]. MMPs are produced as inactive enzymes (zymogens) which need proteolytic cleavage to be activated, subsequently resulting in ECM degradation which is crucial for cancer cell migration and invasion. The activation of MMPs is activated by proteolytic removal of an autoinhibitory N-terminal domain by different molecules including integrins [158]. Integrins regulate MMPs via different mechanisms, including recruiting the proteases to the cell surface and also regulating matrix degradation [158]. There are 25 MMPs which have been identified and most of them exist as secreted forms, except six membrane-anchored (MT) MMPs (MT1-MMP to MT6-MMP, also named as MMP-14, MMP-15, MMP-16, MMP-17, MMP-24 and MMP-25) [185]. A vast number of studies have shown MMPs (MT1-MMP, and MMP-1, -2, -3, -7, -9, and -13) are upregulated in cancers and associate with tumour metastasis [184-186].

For example, direct binding of MMP2 to αvβ3 is required for presenting activated matrix MMP2 on the cell surface of invasive cells [187,188]. αvβ3 recruits pro-MMP2 to the cell surface where the pro-MMP2 is cleaved and activated, and subsequently can degrade basement membrane [187]. This study demonstrated that the presence of activated MMP2 correlated with expression of αvβ3 in human melanoma cells both *in vitro* and *in vivo*, and the expression of both factors was required for melanoma cell invasion and metastasis formation [187]. Binding of oral SCC (squamous carcinoma cells) to fibronectin or LAP resulted in an increased secretion of pro-MMP2 and pro-MMP9 which promoted invasion through Matrigel [189]. Ramos *et al* also reported that αvβ6 promoted oral SCC invasion by increasing pro-MMP3 secretion [189]. Agrez *et al* showed that the C-terminal 11 amino-acid of the β6 subunit is required for promoting proliferation of colon cancer cells [190] whereas Morgan *et al* showed these same 11 a.a. sequence were required for αvβ6-dependent invasion and also were sufficient to transfer a pro-invasive ability to αvβ3 when expressed *de novo* in epithelial cells; this increased invasive ability correlated with an increase in release of pro-MMP2 [191].

1.2.3.2.2 Integrins and the uPAR activation system

Urokinase-type plasminogen activator receptor (uPAR) is an important regulator of ECM proteolysis. uPAR binds to the serine protease urokinase-type plasminogen activator (uPA; also known as urokinase) and its zymogen form, pro-uPA and regulates the activity of the plasminogen activation system [63]. uPA is one of the plasminogen activators that converts the extracellular plasminogen into plasmin and this, in turn, promotes an extracellular proteolytic cascade which degrades ECM

components including fibrinogen, fibronectin and vitronectin but also activates MMPs [63,192]. The plasmin also cleaves and activates pro-uPA as a positive feedback loop [63]. The plasminogen activation system is negatively regulated by plasminogen activator inhibitor 1 (PAI1; also known as SERPINE1) and PAI2 (also known as SERPINB2) [193] (Figure 1.15). "Cleaved" PAI-1 is unable to interact with its target plasminogen activators uPA and tissue-type PA (tPA) to inhibit plasmin-based proteolysis but retains its ability to bind the low-density lipoprotein receptor-related protein- 1 (LRP1) and this enhances cell migration, through a uPA/tPA complex-independent interaction [194] (Figure 1.15).

Several integrins are associated with uPA which provides an additional proteolysis function and enhances cancer cell migration and invasion [195]. αvβ3 is a marker of progression in malignant melanoma, and it was reported that αvβ3 expression is correlated with uPA [196]. αvβ6 is also correlated with expression levels of uPA and its receptor uPAR [66]. Another example, in oral keratinocytes, has indicated αvβ6 plays an important role in modulating cell-surface uPA proteolytic activity by decreasing uPAR expression through the β6 cytoplasmic domain [197]. In contrast, PAI-1 can inhibit integrin binding to the extracellular ligands and therefore alter the cell functions. For example, PAI-1 inhibits cell migration by inhibiting integrins' binding to their ligands. Vitronectin promotes cell migration via RGD-dependent interactions with integrins αvβ3 and also by binding with uPAR [198,199]. PAI-1 competes with uPAR for the binding to vitronectin (to the same domain) and as a result alters the ability of these receptors to engage vitronectin [198,199]. The uPAR activation system is illustrated in Figure 1.15.

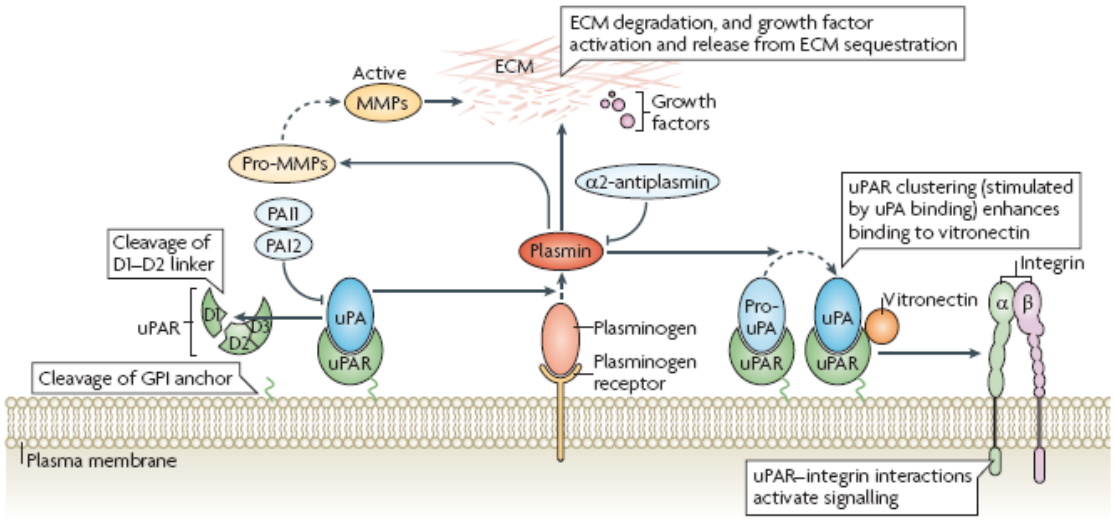

Figure 1.15 Function and regulation of uPAR in the plasminogen activation system.

Urokinase-type plasminogen activator receptor (uPAR) binds the protease urokinase-type plasminogen activator (uPA) in its active and zymogen (pro-uPA) forms. uPA cleaves plasminogen, generating the active protease plasmin. Plasmin activates pro-uPA as positive feedback. Increased cell surface concentration of uPA or pro-uPA (by binding to uPAR) and plasmin or plasminogen (via multiple receptors) accelerates their mutual activation. Plasmin cleaves and activates matrix metalloproteases (MMPs). Both plasmin and MMPs degrade many ECM components and activate growth factors or liberate them from ECM sequestration. The proteolytic activities of uPA and plasmin are antagonised by the serine protease inhibitors (serpins) plasminogen activator inhibitor 1 (PAI-1; also known as SERPINE1) and PAI-2 (also known as SERPINB2) and α2-antiplasmin. uPA–uPAR binding promotes clustering of uPAR in the plasma membrane, and increases its ability to bind the ECM protein vitronectin. uPA also cleaves uPAR in the linker between its first and second domains (D1 and D2), generating a soluble D1 fragment and a membrane-associated D2–D3 fragment. uPAR cleavage abrogates uPA binding, thereby inactivating the function of uPAR in proteolysis, and also inactivates or modifies the signalling functions of uPAR. Picture adapted from [63]

1.2.3.2.3 Integrins and oncogenes

It also has been reported that integrins can cooperate with oncogenes to promote cancer cell invasion. For example, integrin α6β4 is vital for tumour formation in breast cancer as it cooperates with EGFR, the receptor for epidermal growth factor (EGF), with ERBB2, and with c-Met and this promotes spontaneous mammary tumour formation and tumour cell invasion [200]. Also, Trusolino *et al* reported that complex formation between c-MET and integrin α6β4 enhances hepatocyte growth factor (HGF)-induced signals, including tumour cell invasion [201]. This effect may be due to the potentiation of HGF-induced Ras and PI3K signalling by α6β4-mediated recruitment of proteins such as Shc1 and PI3K [201].

1.2.3.3Integrins and endocytosis

Endocytosis of integrins influences their biological functions (such as cell migration) by recycling the adhesion molecules to the front where cells need the adhesion molecules to interact with ligands in ECM [202]. There is more than one endocytosis pathway involved in integrin trafficking. In general, they are divided into two main groups: clathrin-dependent and clathrin-independent pathways [33]. In the clathrin-dependent pathway, clathrin assembles into a lattice-like structure around the vesicles forming a clathrin coat [203]. The clathrin coat needs certain intracellular molecules, called adaptor proteins, to bind to specific cargoes [203]. Common adaptor proteins include AP-2 (adaptor protein-2), Numb, Eps-15 (EGFR-pathway substrate) and cortactin [204]. Once the clathrin-coated vesicle forms, this integrin-packaged vesicle travels to early endosomes and then to sorting-endosomes where

the fate of the cargo is determined, recycling back to the cell surface or sent to late endosomes and lysosomes for degradation; in both routes different members of the Rab GTPase family are required [33]. In addition to the classical clathrin-dependent mechanism of endocytosis, several pathways do not use a clathrin coat. These other vesicular uptake processes (clathrin-independent pathways) can be associated with, for instance, RhoA, Rac, Cdc42, Arf6, caveolae and macropinocytosis [205]. It is reported that some integrins use both ways for endocytosis (e.g. α5β1, αvβ3 and α2β1) [43]. The integrin αvβ6 was shown to be endocytosed by the clathrin-mediated mechanism but non-clathrin pathways were not investigated [1]. In the previous work from my lab, HAX1 was investigated as an adaptor protein for this integrin [1]. HAX1 binds directly to the β6 cytoplasmic tail of integrin αvβ6 [1]. The internalisation rate of αvβ6 was reduced to similar levels by either siRNA to HAX1 or clathrin, suggesting both were part of the same endocytotic pathway [1]. Also, the endocytosis of αvβ6 was reduced significantly by treating cells with a membrane-permeant peptide corresponding to the β6 binding site of HAX1 [1]. This peptide inhibited the direct interaction between HAX1 and β6, reducing endocytosis of αvβ6 but also blocking the migration and invasion ability of oral squamous carcinoma cells [1]. These data suggests the internalisation of integrin αvβ6 is crucial for biological functions such as migration and invasion, and that HAX1 plays the role of an adaptor protein to regulate this process [1].

1.2.3.4 αvβ6 and cancer

αvβ6 is an epithelial-specific integrin and its expression is limited to development [206], wound healing [69], chronic inflammation [67] and cancer [1,69,189,207-

209], all processes that involve tissue remodelling; in contrast, it is absent/low in healthy adult tissue [210,211]. Expression of αvβ6 is linked to poor survival in certain cancers. Yang *et al* have shown patients who were αvβ6-positive had higher liver metastasis rates [212]. In colon cancer, high αvβ6 expression was associated with a reduction in median survival time from 16 to 5 years compared with αvβ6-negative or αvβ6-low cancers [207]. In line with this observation, another study showed that gastric carcinoma patients who were αvβ6 negative had much longer survival times than those who were αvβ6 positive and its value as a prognostic marker is significant for early stage tumours [213]. This integrin also has been reported in ovarian cancer, where the expression of αvβ6 is much more significant in Grade III tumours than low Grade tumours [66]. In cervical squamous cell carcinoma, strong expression of αvβ6 in tumour cells correlated with different clinical-pathological parameters and with worse overall and disease-free survival [214]. Furthermore, αvβ6 expression correlated positively with TGF-β1 mRNA expression as well as with fibronectin expression in cervical cancer, suggesting αvβ6 is a prognostic factor for decreased survival for cervical squamous cell carcinoma [214]. In a separate report, the expression of αvβ6 was detected by tissue microarray in early-stage, non-small cell lung carcinoma (NSCLC) [215]. Log-rank test and Cox regression analyses showed that expression of this integrin was significantly associated with poor patient outcome, indicating that αvβ6 is a prognostic biomarker for NSCLC and may serve as a receptor for targeted therapies [215]. Since *in vitro* and *in vivo* data show αvβ6 promotes a variety of processes that appear to promote cancer, including migration, invasion, MMP secretion and survival (discussed above), these clinical observations are possibly explained by these biological

activities of αvβ6. Thus, since αvβ6 is implicated strongly in carcinogenesis, the molecular mechanisms that regulate this molecule and how this integrin promotes cancer progression are questions which need to be answered. The mechanism by which αvβ6 promotes cancer is not completely known but is likely to be a combination of its direct functions including promoting secretion of MMPs, invasion, survival and its direct functions via the activation of TGF-β.

Aa mentioned, a major function of αvβ6, which is very likely to contribute to its role in cancer progression, is the ability to activate transforming growth factor β (TGF-β). TGF-β is a cytokine family (TGF-β1, TGF-β2 and TGF-β3) which modulates multiple cellular functions such as cell proliferation, inflammation, matrix synthesis, and angiogenesis [69,216]. TGF-β is secreted as a biologically inactive (latent) protein complex consisting of the TGF-β homodimer (25 kDa) bound to the latency associated protein (LAP) (75 kDa). LAP is further associated with latent TGF-β binding protein (LTBP) (190 kDa) glycoprotein via a disulphide bond (Figure 1.16) [216,217]. In most conditions, active TGF-β is generated by dissociation from a large latent protein complex (LLC) that sequesters latent TGF-β in the extracellular matrix (ECM) (Figure 1.16) [217]. When αvβ6 binds to the RGD sequence in LAP (from TGF-β1 or TGF-β3; TGF-β2 LAP does not have an RGD motif), the activation of TGF-β1 is triggered by an αvβ6-dependent physical force, requiring an intact cytoskeleton, that results in a conformational change of the complex [216]. This then exposes active TGF-β1 and allows it bind to its receptor, probably on adjacent cells, thus initiating downstream pathways [181]. Thus the TGF-β-αvβ6 interaction is important for cancer progression, not only for the independent activity

of the TGF-β1 but also as it has been shown to promote cell migration and MMP-9 expression in carcinoma [69,181].

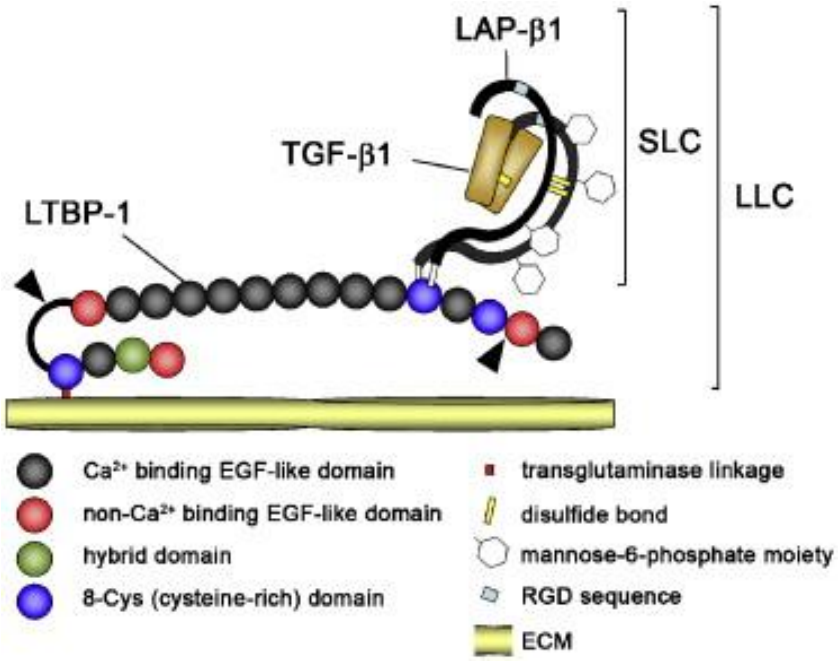

Figure 1.16 Schematic of the structure of TGF-β1.

TGF-β is secreted as a biologically inactive complex as the large latent complex (LLC) consists of TGF-β1, LAP and the fibrillin-superfamily member LTBP-1. Together, TGF-β1 and LAP form the small latent complex (SLC) which is intracellularly formed as a homodimer linked by disulphide bonds. TGF-β1 contains four mannose-6-phosphate moieties that are required to associate with LAP. LAP-β1 and LAP-β3 contain the amino acid sequence motif RGD serving as recognition site for various integrins. LTBP-1 contains three cysteine-rich domains, and the second cysteine-rich domain binds the SLC via disulphide bonds whereas the third cysteine-rich domain at the N-terminus of LTBP-1 links the protein complex to the ECM via transglutamination. The flexible hinge region, separating the central hybrid domain and the third cysteine-rich domain, is sensitive to proteolytic digestion (arrowhead). Another protease-sensitive site is present close to the C-terminus of LTBP-1 (arrowhead). Picture adapted from [217].

1.3 Summary of HAX1 biology to date and the goals of this study

The previous section has discussed multiple functions implicating HAX1 in many different biological processes. Most of these studies did not consider that HAX1 was a family of proteins and therefore which isoforms were principally responsible for the observed results was not addressed. Only in a few genetic studies ([147,148]) were researchers able to point out the differences of the isoforms and only recently are studies ([19,149]) attempting to characterise which isoforms are critical. In this study, I have attempted to address this problem by combining genetic and immunological methods. Thus the hypothesis is:

The multiple functions and subcellular localisation attributed to HAX1 are due to the presence of multiple isoforms whose individual functions and subcellular localisation may differ from each other.

In our lab, we want to investigate the role of individual isoforms of HAX1 in cancer, in particular, their variations in subcellular localisation, proliferation, migration, apoptosis and autophagy. Since my lab has an interest in the integrin αvβ6, I have chosen to focus on HAX1.1, HAX1.2, HAX1.4 and HAX1.5 as these isoforms possess the β6 binding site. Specifically, the main aims of my PhD are:

1) To investigate the role of HAX1 in cell migration in a range of cancer cell lines from different tissues, and establish the role of individual isoforms in migration.

2) To generate oral carcinoma cell lines that stably have HAX1 knocked down. These lines will be analysed at the protein and RNA level for expression of HAX1 isoforms and also the protein level of αvβ6.

3) To characterise the cellular functions of these cells in terms of growth, migration, and susceptibility to apoptosis and autophagy.

4) To re-introduce singly the various HAX1 isoforms into HAX1-null cells and study the subcellular localisation and biological functions dependent upon this re-introduction.

CHAPTER 2. MATERIALS AND METHODS

2.1 Cell lines and tissue culture

2.1.1 Cell lines, media and cell maintenance

VB6 and H400 are human oral squamous cell carcinoma lines. H400 expresses integrin αvβ6 endogenously [1] whereas VB6 was engineered, by retroviral vector transduction, to express high αvβ6 levels [70]. Both cell lines are cultured in KGM (keratinocyte growth medium: α-MEM supplemented with 0.18mM adenine (Sigma-Aldrich), 0.4µg/ml hydrocortisone (Sigma-Aldrich), 10ng/ml EGF (Sigma-Aldrich), 5µg/ml insulin (Sigma), 220mM glutamine (PAA Labs), $0.1x10^{-7}$mM cholera toxin and 10% foetal bovine serum (FBS; PAA Labs). 1.25 µg/ml of puromycin (Sigma-Aldrich, #p9620) was employed to select pGIPZ lentivirus-infected VB6 and H400 cell lines. HEK 293T cells are human embryonic kidney cells, used for lentivirus packaging. The culture media used for HEK239 cells is DMEM (Dulbecco's modification of Eagle's medium) supplemented with 10% FBS. CFPAC1 and Pac04.03 are pancreatic adenocacinoma cell lines and grow in RPMI media (Sigma-Aldrich), supplemented with 10% FBS. MCF10CA1a is a breast malignant epithelial cell line and is cultured in DMEM/F-12 (1:1) medium (Sigma-Aldrich) supplemented with 5% horse serum. HaCat is an immortalised normal human keratinocyte line and the culture medium consists of 10% FBS in DMEM (Sigma-Aldrich). HeLa cell is a malignant cervical epithelial cell line and growth occurs in DMEM (Sigma-Aldrich) with 10% FBS. All the cell lines were cultured as adherent

monolayer in sterile tissue culture flasks in an humidified atmosphere at 37°C, 8% CO_2.

2.1.2 Trypsin detachment of cells

Cells were detached from plastic using a solution of trypsin/EDTA (0.5%(w/v)/5mM) (PAA Laboratories, #L11-003). Trypsin cleaves peptide bonds at lysine and arginine residues and hydrolyses intracellular junctions whereas EDTA binds to divalent cations, such as calcium and magnesium, which are essential for functioning of integrins and E-cadherin adhesion molecules. Briefly, old media was removed and sufficient trypsin/EDTA added to cover the cells (eg 1.5ml/75cm^2 flask) for 5 minutes incubation at 37°C to detach the cells from the surface. The cells were resuspended with suitable growth media (with serum) to inactive trypsin and passaged into new flasks.

2.1.3 Freezing and thawing cells

Log-phase growing cells were trypsinised, as described in the above section, and were collected by centrifugation at 250 x g, 3 minutes. The supernatant was aspirated off and cells were resuspended with 1ml freezing fluid (70% DMEM, 20% FCS, 10% DMSO). Cells were then frozen overnight at -1°C per minute to -80°C, and then transferred to liquid nitrogen. In the thawing procedure, cells were recovered to 37°C as quickly as possible to prevent ice crystal formation and induced cell death. The Cryovials were placed into a waterbath and the cells allowed to thaw out. The cell suspensions were then transferred to a tube containing 10ml pre-warmed media. The

DMSO was removed by centrifugation at 250 x g for 3 minutes and resuspending the cell pellets with growth media.

2.2 Small interfering RNA (siRNA) oligos

siRNA oligos were used to transiently knockdown endogenous HAX1 expression. Si192 targets to 3'UTR of HAX1 recognising isoforms1-9. Si1-6 targets to exon2 and knocksdown isoforms 1-6. Si86 targets to the beginning of exon3, recognising isoforms1-6. The sequences of siRNA are shown in Table 2.1

si RNA	Sequences	HAX1 isoform							
		1	2	3	4	5	6	7	8
si192	CCC TCA GAG GCC TTC AAG T	v	v	v	v	v	v	v	v
si1-6	CTT CGG CTT TGA TGA CCT A	v	v	v	v	v	v	-	-
si86	GGG ACT CAA TGC TTA AGT A	v	v	v	v	v	v	-	-
siNTC	ACT ACC GTT GTT ATA GGT G	-	-	-	-	-	-	-	-

Table 2.1 Sequences of siRNA oligos.

This table shows the siRNA and their sequences, the targeted HAX1 isoforms are indicated as "V".

2.3 Lentiviral vectors

Lentiviral vectors were used for stable HAX1-knockdowns. Four pGIPZ plasmids (p86, p87, p89, p90) were obtained from Open Biosytems, each encoding a different short-hairpin RNA (shRNA) to HAX1. The sequences of the hairpins of shRNAs are comprised of a 19nt loop and 22nt of dsRNA. Table 2.2 shows the sequences and also the isoforms targeted. The detailed information on the vectors is discussed in the Results section.

sh RNA	Sequences	HAX1 isoform							
		1	2	3	4	5	6	7	8
86 shRNA	GGG ACT CAA TGC TTA AGT A	v	v	v	v	v	v	-	-
87 shRNA	GAC CTA GTA CGA GAT TTC A	v	v	v	v	v	-	-	-
89 shRNA	CAG CCC AAA TCC TAT TTC A	v	v	-	v	v	v	v	v
90 shRNA	GCT CCC AGA GGC CAT TTC A	v	v	-	v	v	v	v	v

Table 2.2 pGIPZ vectors and targeted HAX1 isoforms.

This table shows four different shRNAs to HAX1 and their sequences, the targeted HAX1 isoforms are indicated as “V”.

2.4 Mutant HAX1 isoforms

Mutated HAX1 isoforms were generated to resist siRNA degradation (by Dr. Delphine Lees). Mutants were created by site-directed mutagenesis: C249T, A252G, A255G, T390C, G393A, T396C. These mutated bases are designed to protect from a specific siRNA (si86) which targets to exon 3 of HAX1. Mutated isoforms 1,2,4,5 were generated with a pFLAG-CMV2 vector (Sigma) with a FLAG-tag inserted on the N-terminal of the isoform sequences. The mutations and the sizes of each mutant isoform are shown in the Table 2.3. The detailed vector map is shown in Appendix II.

Vectors	Insert size (bp)	Mutated Sequence
HAX1.1	840	C249T_A252G_A255G T390C_G393A_T396C
HAX1.2	762	
HAX1. 4	696	
HAX1.5	864	

Table 2.3 Mutated sequence of HAX1 isoforms.

HAX1 isoforms with sequence mutated: C249T, A252G, A255G, T390C, G393A, T396C were created by site-directed mutagenesis and inserted into pFLAG-CMV2 vector.

2.5 Antibodies

Table 2.4 shows the antibodies used for this study.

Antibody	Species	Source	Dilution (WB)	Dilution (IF/ flowcytometry)
HSC70	Mouse	Santa Cruz, #sc-7298	1:10000	N.A.
Tubulin	Mouse	Abcam, #ab325935	1:1000	N.A.
Actin	Mouse	Abcam, #ab8224	1:1000	N.A.
β6	Goat	Santa Cruz, #sc-6632	1:1000	N.A.
10D5:αvβ6	Mouse	Chemicon, #MAB2077Z	N.A.	10 μg/ml
23C6: αvβ3	Mouse	Chemicon, #CBL544	N.A.	10 μg/ml
P1F6: αvβ5	Mouse	Chemicon, #GEM1961	N.A.	10 μg/ml
4F1: αvβ8	Mouse	prepared in house	N.A.	10 μg/ml
L230: αv	Mouse	prepared in house	N.A.	10 μg/ml
P4C10: β1	Mouse	Chemicon, #MAB1987	N.A.	10 μg/ml
FLAG	Rabbit	Sigma-Aldrich, #F7425	1:1000	1:7000
Lamin	Mouse	Cell Signalling, #4777	1:1000	N.A.
Caspase-3	Mouse	Abcam, #ab13585	1:1000	1:100
PARP	Rabbit	Cell Signalling, #5625	1:1000	N.A.
LC3b	Rabbit	Cell Signalling, #2775	1:1000	1:400
Beclin-1	Mouse	BD Bioscience, #1612112	1:1000	N.A.
HAX1, BD	Mouse	BD Bioscience, #610825	1:500	1:75(1:200 for RS.)
HAX1, RD	Goat	R&D Systems, #AF5458	1:1000	1:75 (1:200 for RS.)
HAX1, N-17	Goat	Santa Cruz, #sc-16636	1:250	1:50
HAX1, E-20	Goat	Santa Cruz, #sc-34237	1:250	1:50
HAX1, P-20	Goat	Santa Cruz, #sc-16637	1:250	1:50
Anti-mouse HRP	Rabbit	Dako, #E0432	1:2000	N.A.
Anti-rabbit HRP	Goat	Dako, #E0432	1:2000	N.A.
Anti-goat HRP	Rabbit	Dako, #E0466	1:2000	N.A.
Anti-mouse-488	Goat	Invitrogen, #A11001	N.A.	1:250
Anti-rabbit-488	Goat	Invitrogen, #A11008	N.A.	1:500
Anti-goat-488	Donkey	Invitrogen, #A11055	N.A.	1:250
Anti-rabbit-555	Donkey	Invitrogen, #A31572	N.A.	1:500
Anti-rabbit-647	Donkey	Invitrogen, #A31573	N.A.	1:500
Anti-mouse-647	Donkey	Invitrogen, #A31571	N.A.	1:500

Table 2.4 Summary of antibodies used in this study.

WB, Western blotting; IF, immunofluorescent staining

2.6 Plasmid amplification and purification

shRNA plasmids were supplied as bacterial stabs. The bacteria were streaked on to agar plates with appropriate antibiotics (100µg/ml of ampicillin; Sigma-Aldrich) and incubated at 37 °C overnight. Single colonies were picked and used to incubate a starter culture of 5 ml LB (Luria Broth; Sigma-Aldrich) medium containing 100µg/ml of ampicillin at 37°C for 8 hours with vigorous shaking (300 rpm). The starter culture was then diluted 1/500 in 250ml of the selective LB medium, and incubated at 37°C overnight with vigorous shaking (300 rpm). Bacterial cells were harvested by centrifugation at 6000xg for 15 minutes at 4°C. Maxiprep kits (Qiagen, #12163) were used to purify plasmid DNA according to the manufacturer's protocol. The procedure is based on the alkaline lysis of bacterial cells followed by adsorption of DNA onto the Maxiprep membrane in high-salt buffer and its elution in low-salt buffer.

2.7 Agarose gel electrophoresis

Vectors were analysed by agarose gel electrophoresis to examine the purity. 1% agarose gels were prepared by dissolving agarose in TBE buffer (Fisher Bioreagents, #BP2430-20) by boiling in a microwave oven with regular stirring. Once cooled, 0.5ug/ml ethidium bromide (Invitrogen; #15585-011) was added to the gel to facilitate visualisation of DNA fragments under UV light. The warm solution was poured into a gel cassette containing combs to form wells. 5 µl of each sample was loaded in to the wells alongside Hyper Ladder I DNA ladder (Bioline, #BIO-30025), and the gel was run for 40 minutes at 100V to separate the DNA fragments. Samples

were visualised on a UV transilluminator (UVP Products), and digital images captured on Labworks software.

2.8 Transfections

2.8.1 Oligofectamine transfection-for siRNA

Oligofectamine Transfection Reagent (Invitogen, #12252-011) forms stable complexes with oligomers, permitting efficient transfection into eukaryotic cells. Cells were grown in a well of a 6-well plate to about 50% confluency at the time of transfection. The transfection mixture was generated by mixing siRNA dilution (2µl of 100nM siRNA with 348 µl Opti-MEM [Invitrogen]) and Oligofectamine dilution (10 µl of oligofectamine with 40 µl Opti-MEM). The trasfection mixture was then incubated for 10 minutes at room temperature. Cells were rinsed with Opti-MEM, fed with 800 µl Opti-MEM before adding the transfection mixture.

2.8.2 pGIPZ-lentiviral transfection for stable knockdown

To generate lentiviruses required a triple transfection of three plasmids into HEK 293T cells; the 3 plasmids were the shRNA encoding pGIPZ, p8.91vector (encoding gag and pol) and the pMDG.2 vector (encoding VSV-G) which contain viral structural and envelope encoding genes, respectively. The plasmids were obtained from Open Biosytems and an illustration of the process is demonstrated in Figure 2.1.

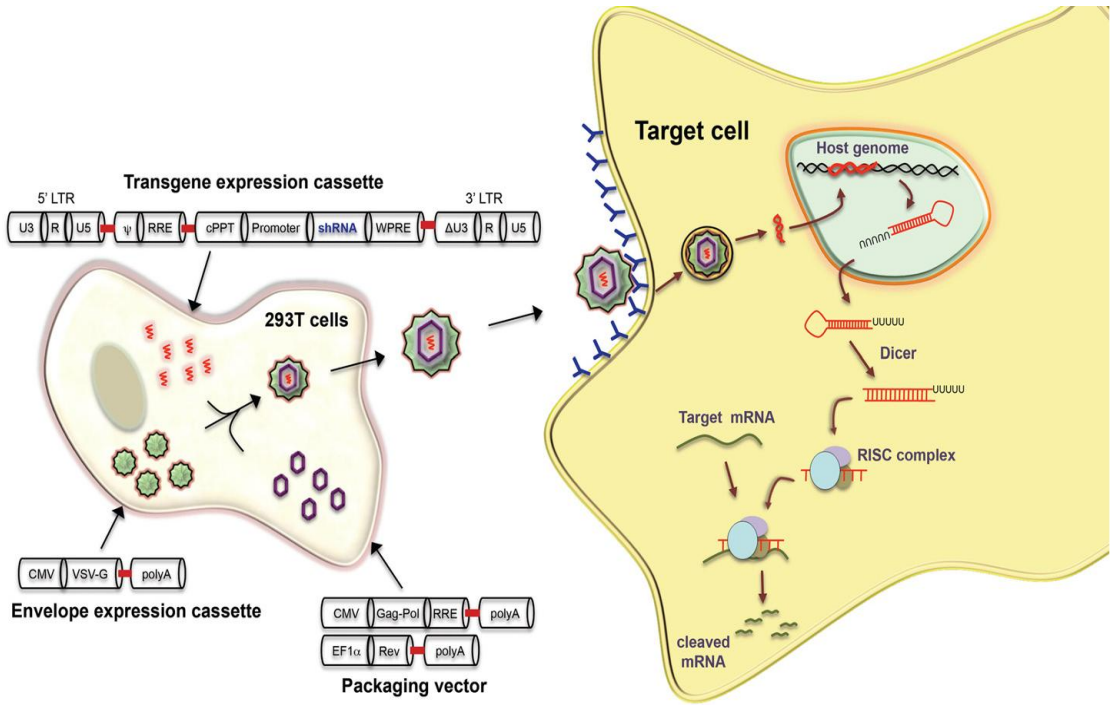

Figure 2.1 Lentiviral vectors for shRNA expression.

In the RNA interference processes after lentiviral infection of the target cell, shRNA is produced by the sequence that became integrated into the host genome. The pre-miRNA, which is a long primary double-stand RNA, is produced in the nucleus, and then cleaved by the endoribonuclease, Drosha, into shorter pre-miRNA with approximately 70 nucleotides. These are exported out into the cytoplasm by Exportin-5 and then cut by the enzyme Dicer into functional miRNA of about 22 nucleotides. Subsequently, the anti-sense strand of the miRNA will be introduced into the RNA-induced silencing complex (RISC) and the RISC functions to recognise its mRNA target for gene silencing. Figure adapted from [218].

2.8.2.1Lentivirus packaging

The packaging cell line, HEK293T cells, was seeded in 75cm^2 flasks to achieve sub-confluence (approximately 70%) the next day. Plasmid transfection was performed using Fugene 6 method (Roche, # 11815091001) with 1 µg of packaging plasmids (pMDG and p8.91) and 1.5 µg of pGIPZ vectors (15 µl total volume). The plasmid mixture was added to the Fugene 6 mixture (10 µl Fugene reagent with 200µl Opti-Mem), and incubated for 15 minutes at room temperature. The culture media was replaced with 8 ml fresh growth media before the plasmid mixtures were added to the cells and then incubated at 37 °C overnight. The next day, media was then replaced with 8ml of fresh media and the cells were placed back at 37°C. 24 hours later, the media containing virus particles was collected and filtered through a 0.45µm filter, and the samples stored at -80°C until used. Media (8 ml) was similarly collected for each of the next two days. Six days after transfection, HEK293T cells were trypsinised and analysed for GFP expression to determine transfection efficiency by flow cytometry.

2.8.2.2Lentiviral Infection

Target cells were seeded in 25cm^2 flasks to reach sub-confluence and the media was replaced with 2 ml of virus-containing media described in the previous section and supplemented with polybrene (1:2000, Millipore, #TR-1003-G). Polybrene is a polycation which is a positively charged molecule that is able to help negatively charged proteins to bind to negatively charged cell membranes, thus promoting transfection. Cells were incubated at 37°C for four hours and then 2 ml of growth

media was added to the cells which were incubated at 37°C overnight. 24 hours after viral infection, puromycin selection was performed by replacing fresh media containing 1.25µg/ml puromycin to the cells. Flow cytometry was used to observe the efficiency of infection (by detecting turbo-GFP).

2.8.3 Fugene6 transfection- for isoform plasmid restoration

Fugene 6 transfection reagent (Roche, # 11815091001) utilises cationic polymers for transduction of DNA. The negatively charged DNA binds to the polycation (eg. lipid) present in the reagent, and the complex is taken into cells via endocytosis. The optimal ratio of transfection complex is 1 µg plasmid: 6 µl Fugene Reagent in 100 µl Opti-MEM according to the manufacturer's instructions. Thus 6µl Fugene 6 Transfection Reagent was added to 100 µl of Opti-MEM and incubated for 5 minutes at room temperature. 1µg of plasmid DNA was added to the mixture and incubated for 15 minutes at room temperature. The DNA mixture was added to the cells in 12 well-plates. Cells were harvested and the protein lysates were examined by Western blotting 48 hours after transfection.

2.9 Western blotting

2.9.1 Cell lysate preparation

Confluent cells were washed with cold PBS and lysed with NP40 lysis buffer (50mM Tris [pH 7.4], 250mM NaCl, 5mM EDTA, 50mM NaF, 1mM Na_3VO_4, 1% Nonidet p40 [NP40], 0.02% NaN_3) supplemented with 1mM dithiothreitol (DTT;

Invitrogen, #D-1532) and protease inhibitor cocktail (Calbiochem, #539134).The lysates were collected using cell scrapers and sonicated at 4 °C to form homogenous cell lysates. Protein concentrations were quantified with the DC Protein assay kit (Bio-Rad Laboratories) according to manufacturer's instructions using a bovine serum albumin (BSA) standard curve. Samples containing equal amounts of protein were added to 2x loading buffer (Fermentas) and heated for 10 minutes at 70°C.

2.9.2 Western blot analysis

Samples were loaded onto SDS-PAGE pre-cast gels (12% acrylamide; Invitrogen system). 10ul of Prestained protein ladder (Fermentas, #SM0671) was loaded in one well of each gel to confirm molecular weights. Gels were electrophoresed for 100 minutes at 125 volts or until the dye front had reached the bottom of the gel. Separated proteins were electro-transferred to a nitrocellulose membrane (GE Healthcare Life Sciences) for 1 hour at 30V (Invitrogen system). The membrane was then stained with Ponceau Red solution (Fluka Chemicals, #09276-6X1EA-F) to visualise the quality of the protein transfer. The Blot was incubated for 30 minutes at room temperature with blocking buffer (TBS with 0.1% Tween 20 and 5% (w/v) non-fat milk protein [Marvel]) which was used to reduce non-specific protein binding. The Blots were placed in 50ml centrifuge tubes and indicated primary antibodies (see section 2.5) diluted in 4 ml blocking buffer added overnight at 4°C under continuous rotation (Jencons-PLC, UK) . The membrane was washed with wash buffer (TBS/ 0.1% Tween 20) four times for 20 minutes. Appropriate horseradish peroxidase (HRP)-conjugated secondary antibody (see section 2.5) was incubated with the membrane in blocking buffer for 30 minutes at room

temperatures. After washing, bound antibodies were detected with enhanced chemiluminescence (ECL) reagents (GE Amersham).

2.9.3 Densitometry analysis

Digital images of autoradiographs were collected and densitometric analysis of specific bands was done using Image J software. Detection of endogenous HSC70 was used as a loading control. For the autophagy experiments, LC3b-II was normalised with LC3b-I.

2.10 RNA analysis

2.10.1 RNA extraction

RNA extraction was performed with Absolutely RNA Miniprep Kit from Stratagene (#400800). Following the manufacturer's protocol, cells were placed in a 6-well plate till confluent and were lysed with lysis buffer (2.5 µl β-Mercaptoethanol with 350 µl lysis buffer [Absolutely RNA Miniprep Kit, Stratagene] per well). Cell lysates were mixed by pipetting and transferred to a microcentrifuge tube. Cell lysates were then vortexed to homogeneity. The manufacturer's instructions were followed and total RNA was eluted from the RNA binding tube with Elution Buffer provided.

All samples were quality assessed by agarose gel electrophoresis (Bio-Rad system) and quantified by measuring the optical density (OD) at 260 nm with Nanodrop

Spectrophotometry (Thermo) (as nucleic acids absorb ultraviolet light at 260nm). RNA samples were stored at -80 °C.

2.10.2 Reverse Transcription (RT)

Reverse transcription (RT) was performed using Reverse Transcription Kit from Promega (#A3500). 1µg total RNA was used to generate cDNA. The reactions were prepared on ice as follows (1mM dNTP [deoxynucleoside triphosphates] mix, 5µM $MgCl_2$, 1x Transcription Buffer, 0.5 µg Random primers/ oligo dT primers, 1u/ µl Recombinant Ribonuclease Inhibitor, 15u/ µg AMV [Avian Myeloblastosis Virus] and Reverse transcriptase and Nuclease–free water to a final 20 µl total reaction volume). The reaction programme for random primer RT was: 22°C/ 10 min, 48°C/30 min, 95°C/ 5 min, 4°C. For oligo dT primer RT, the programme was: 48°C/ 30 mins, 95°C/ 5 min, 4°C. After the RT reaction, 1µg of total RNA generated a corresponding 1µg of cDNA.

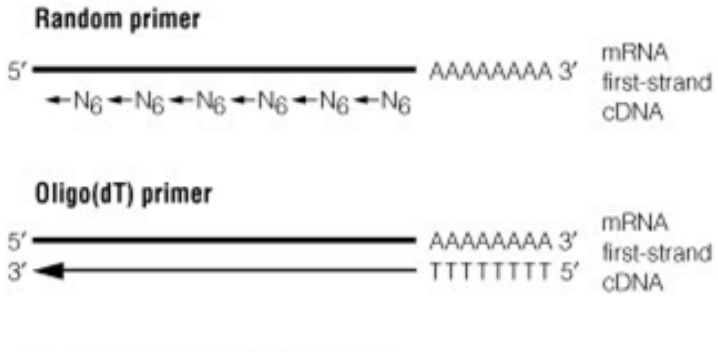

Figure 2.2 Alternative types of PCR primer.

Random primers start reverse transcription at multiple points along the transcripts, normally useful for long mRNA. Oligo dT primers are comprised of oligomers of dT sequence, which can recognise and bind to the poly A tail of mRNA, and an adaptor sequence at the 5' end; it is generally used for amplification if the target sequence is adjacent to the poly adenylation region. Figure adapted from Promega.

2.10.3Polymerase chain reaction (PCR)

All PCR products (25 µl) were loaded in to a well in 1% agarose gel, alongside the DNA ladder IV (Bioline, #BIO-33029). Image J software was used to quantify PCR products by densitometry and all the data were generated relative to GAPDH. Triplicate samples from at least three independent biological replicates were analysed to generate standard deviations. Different PCR reaction conditions used for different HAX1 isoforms are listed in Table 2.5.

Targets	Name of Primer	Sequence of Primer	PCR Reaction Condition	Product Size (base pairs)
HAX1.1	sF389	AGGAATTTGGCTTCGGCTTC	94 ˚C , 30sec/ 55˚C, 30 sec/ 72˚C, 30sec/25 cycle	151
	eh1eR	CTGGAAGTTCAGGAGGATGG		
HAX1.2	sh2F1	GAGCTGAGG TCTGACTTTGA	94 ˚C , 30sec/ 55˚C, 30 sec/ 72˚C, 30sec/35 cycle	1009
	shSTPOR	TGAGGGTTA ACAAGGCTACC		
HAX1.3	sF389	AGGAATTTGGCTTCGGCTTC	94 ˚C , 30sec/ 55˚C, 30 sec/ 72˚C, 30sec/33 cycle	316
	sh5R	TGCAGAAAGGTG GCAGGTGTT		
HAX1.4	V2	ACCTCGGAGCTTCAGCCCAGGA	94 ˚C , 30sec/ 55˚C, 30 sec/ 72˚C, 45sec/30 cycle	667
	shSTPOR	GAGGGTTA ACAAGGCTACC		
HAX1.5	sF389	AGGAATTTGGCTTCGGCTTC	94 ˚C , 30sec/ 55˚C, 30 sec/ 72˚C, 30sec/33 cycle	165
	sh5R	TGCAGAAAGGTGGCAGGTGTT		
HAX1.6	h6F	GATGACCTAAACTTCCAG GTC	94 ˚C , 30sec/ 55˚C, 30 sec/ 72˚C, 45sec/35 cycle	548
	shSTPOR	TGAGGGTTA ACAAGGCTACC		
GAPDH	GAPDHF1	CATTGCCCTCAACGACCACT	94 ˚C , 30sec /55˚C, 30 sec/ 72˚C, 30sec/25 cycle	232
	GAPDHR1	TACATGGCAACTGTGAGGAGG		

Table 2.5 PCR primers and conditions for each reaction.

2.11 Fluorescence Activated Cell Sorting (FACS)

Cells infected with Turbo-GFP tagged shRNA were harvested by trypsinisation and, to maintain sterility, antibiotic (1.25 µg/ml of puromycin) was added. Cells were sorted on a FACS machine (Aria II: Beclon-Dickinson) by Dr. G. Rosignoli in the Cell Imaging and Analysis Lab, Barts Cancer Institute. 100,000 cells from the top 10% GFP-positive cells were sorted and re-cultured in a well of a 24 well plate, incubated at 37 °C. Cells were expanded and re-analysed for GFP and HAX1 expression.

2.12 Flow Cytometry

Confluent cells were trypsinised and washed with E4/0.1/0.1 buffer (DMEM/ 0.1% (w/v) BSA [Bovine Serum Albumin, Invitrogen]/ 0.1% (w/v) sodium azide) three times. The cells were mixed well by pipetting to generate single cell suspensions and were labelled with appropriate antibodies (10μg/ml 10D5: against αvβ6 integrin, Chemicon, #MAB2077Z; 23C6: against αvβ3 integrin, Chemicon, #CBL544; P1F6: against αvβ5 integrin, Chemicon, #GEM1961; 4F1: against αvβ8 integrin, Chemicon; L230: against αv integrin subunit, Chemicon; P4C10: against β1 integrin, Chemicon, #MAB1987;) or mouse IgG isotype control (10μg/ml, BD) on ice for 45 minutes. After three washes, cells were labelled with appropriate secondary antibodies: Alexafluor 488 conjugated goat-anti-mouse antibody (Invitrogen, #A11001) or Alexafluor 647 conjugated donkey-anti-mouse antibody (Invitrogen, #A31571) for GFP-expressing cells and incubated on ice for 30 minutes. Cells were analysed on a FACScalibur (Becton Dickinson) flow cytometer using Cellquest Pro software and data were generated from analysing 10,000 cells.

2.13 Immunofluorescence Staining and Confocal microscopy

Cells were seeded and grown on glass slides before 50nM of MitoTracker Orange CMTMRos was added to the cells in growth medium for 30 minutes at 37°C to stain mitochondria (Invitrogen, #M7510). MitoTracker Orange CMTMRos is an orange-fluorescent dye that stains mitochondria in live cells and its accumulation is

dependent upon membrane potential. The dye is well-retained after aldehyde fixation. The cells were then fixed with actin fixer (0.5M MES, Sigma-Aldrich, #M5287; 1M KCl, Fisher Scientific, #p/4280/53; 1M $MgCl_2$, Sigma-Aldrich, #M8266; 0.5M EGTA, Sigma-Aldrich, #E2478) for 10 minutes at room temperature and permeabilised in 0.1% Triton X-100 for 5 minutes before being blocked with blocking solution E4/0.1/0.1 buffer (DMEM/ 0.1% (w/v) BSA/ 0.1% (w/v) sodium azide) for 30 minutes. Cells were then incubated with the desired primary antibody for 1 hour at room temperature followed by appropriate secondary antibodies for 30 minute (see 2.5). The coverslips were then mounted with 5µl Prolong Gold reagent with 4',6-diamidino-2-phenylindole (DAPI, Invitrogen, #P36931). Confocal images were generated on a Zeiss LSM510 and LSM710 laser scanning microscope and quantification analysis was generated by using Zen software.

2.14 Cell density dependent –HAX1 expression experiments

VB6 and H400 oral carcinoma cells were seeded with different cell numbers (2.5 x 10^4, 5 x 10^4, 10 x 10^4, 20 x 10^4, 40 x 10^4) in a 12-well plate, after indicated time points of culture (24, 48 and 72 hours), cells were harvested at the different confluences. Protein concentrations were determined and equivalent amounts of protein were added to 12 % gels for Western blot analysis.

2.15 MTT colorimetric assay

100 µl of MTT solution (0.2mg/ml) (3-(4,5-dimethylthiazol-2-yl)-2,5-diphenyltetrazolium , Sigma Chemicals, #5655) diluted in serum-free medium was

added to the cells after removal the culture medium, and incubated at 37◦C for an additional 45 minutes. The reaction was terminated and formazan crystals were dissolved with dimethylsulphoxide (DMSO, 100 µl per well). Absorbance values were determined at 550nm by using a spectrophotometer. Data are expressed as mean percentage of survival. Experiments were repeated at least three times in quadruplicate wells.

2.16 Cell fractionation

2.16.1 Cell harvest

Confluent cells cultured in a 10cm dish were washed in cold PBS once and washed in cold hypotonic buffer (10mM HEPES pH 6.9, 10mM KCl). The cells were then lysed and scraped in 500 µl hypotonic buffer with protease inhibitor cocktail (1:100, Calbiochem). The cell lysate was then incubated on ice for approximately 25 minutes (cells were observed to lose cell membrane potential by microscopy) and then I separated the supernatant and pellet by centrifugation at 1000 x g for 3 minutes at 4°C. The resulting supernatant comprised the cytoskeletal fraction (process to 2.16.2) while the pellet contained the cytosolic and heavy membrane fractions (process to 2.16.3).

2.16.2 Nuclear fraction isolation

The resulting pellet was subsequently washed with 150µl NTENT lysis buffer (10mM Tris-HCl pH 7.2, 10mM NaCl, 1mM EDTA, 1% Triton X-100, 1:100

protease inhibitor cocktail). The resulting pellet was resuspended in 100µl NTENT buffer and centrifuged at 14000 x g for 3 minute at 4°C. The pellet represented the nuclear fraction.

2.16.3 Cytosolic fraction isolation

The pellet contained the cytosolic and heavy membrane fractions (from 2.16.1) were centrifuged at 14,000 x g for 30 min at 4°C. The resulting supernatant contained the cytosolic fractionation. The pellet was then processed to isolate the heavy membrane fraction (to 2.16.4).

2.16.4 Heavy membrane fraction isolation

The pellet was suspended in 150µl NTENT buffer before being centrifuged at 14,000 x g for 30 min at 4°C. The resulting supernatant contained the heavy membrane fraction.

Western blotting was employed to examine the proteins in each fraction. Markers for the protein fractionation are used to validate the purity of the fractions: β6 for heavy membrane (β6 was found in heavy membrane in the previous study from my lab), actin for the cytoplasm and lamin for the cell nucleus. The fractionation protocol is adapted from [219].

2.17 Functional assays

2.17.1 Clonogenic assay

100 cells were plated in triplicate wells of 6-well plates. Cells were cultured for 10 days with media changed every three days. The cells were then stained with 0.1% crystal violet in methanol for 1 hour at room temperature. The excess stain was removed with running water and the plates were left to dry. Image J software was used to measure the number of colonies from triplicate wells.

2.17.2 Proliferation assay

Cells were seeded at 5000 cells per well in 96-well plates and grown in growth media at 37°C and harvested at predetermined time points (1, 2, 4, 6, 8 days). Proliferation was measured by Picogreen-based fluorescence assay. PicoGreen is a fluorescence-generating dye, which binds to DNA, and the relative fluorescence can be detected quantitatively by a fluorimeter. 200 µl TE buffer (10 mM Tris-HCl, 1 mM EDTA, pH 7.5) was added to the cells and mixed with PicoGreen fluorescent dye (Invitrogen, #P7581) and incubated for 5 minutes at room temperature, protected from light, following manufacturer's guideliness. After incubation, the sample fluorescence was measured by using a fluorescence microplate reader at 480nm/520nm. To ensure that the sample readings remain in the detection range of the fluorimeter, the gain was set so that the sample containing the highest DNA concentration yields fluorescence intensity near to, but below, the fluorimeter's maximum. To minimise photobleaching effects, the time for fluorescence

measurement was constant for all samples. The data represent triplicate samples from one of two independent experiments showing similar results.

2.17.3 Migration assay

Cell migration assays were performed with Transwell inserts (Corning, #3422) with 8µm polycarbonate pores. Before use, the underside of the membranes were pre-coated with 70µl of 0.5% BSA or extracellular matrix substrate (0.5µg/ml LAP, Sigma-Aldrich, #L3408; 10µg/ml laminin, Sigma-Aldrich, #L2020; 10µg/ml collagen, Sigma-Aldrich, #C7774; 10µg/ml fibronectin, Sigma-Aldrich, #F2006) for 30 minutes at room temperature. Cells were trypsinised, washed in serum-free media. 100 µl of cells (5×10^4) were plated into the top chamber of the Transwell filters with the lower chamber containing 480µl of migration buffer (1g of BSA and 5ml glutamine in 200ml serum-free media). Cells were allowed to migrate for 16 hours at 37°C. The cells were then trypsinised to detach separately from both the top and bottom chambers and counted on a CASY-1 cell counter (Scharfe System GmbH). Percentage migration was determined by the number of cells in the lower chamber relative to the total number of cells in the well. Data are expressed as mean percentage of cells migrating. Experiments were repeated at least three times in quadruplicate wells.

2.17.4 Scratch-wound healing assay

1 x 10^5 cells were plated in 24-well plates with coverslips and allowed to grow to a confluent monolayer. Experimental wounds were made by dragging a plastic blue

pipette tip across the cell culture. Cultures were then rinsed with PBS three times to remove non-adherent cells and replaced with fresh culture media and cells were allowed to migrate overnight. Cells were then incubated with 300µl of 50nM mitotracker (Invitrogen, #M7510) for 30 minutes at 37°C and fixed with actin fixer for 10 minutes at room temperature. Permeabilisation was done with 0.1% Triton X in PBS for 5 minutes before blocking with blocking buffer for 30 minutes. The procedure for staining is outlined in section 2.13.

2.17.5 Invadopodia formation-ECM degradation assay

2.17.5.1 Preparation of fluorescent Rhodamine-gelatin

50ml buffer solution was made with 61 mg NaCl (Sigma-Aldrich, #21346) and 50mM sodium borogydrate (Sigma-Aldrich, #21346). 100mg of gelatin (Sigma-Aldrich, #120240) was dissolved in the buffer solution at 37°C for 1 hour. 1.8mg of Rhodamine (Sigma-Aldrich, Rhodamine123) was then added, mixed and covered in the dark for 2 hours at room temperature. The solution was placed in a Slide-a-Lyzer (Thermo Fisher) and dialysed in PBS for 48 hours at 4°C. Two litres of PBS were changed three times each day. 136 x g spin for 30 seconds was applied to remove insoluble material before adding 1g sucrose. The homogenous Rhodamine-gelatin solution was aliquoted and stored at 4°C till use.

2.17.5.2 Coating coverslips with Rhodamine-gelatin

Rhodamine-gelatin was warmed in a waterbath and quickly centrifuged to remove the insoluble materials before use. Coverslips were inverted on a 40µl drop of gelatin

and incubated for 15 minutes in dark. The coverslips were then transferred to 20µl of 0.5% glutaraldehyde (Sigma-Aldrich, #G5882) for 5 minutes, and gently washed three times with PBS in a well of a 24-well plate. Coverslips were incubated with 200 µl of NaBH4 (Aldrich Chemicals) at 37°C for 3 minutes. After washing three times with PBS, 70% ethanol was then added to the coverslips for 5 minutes. Ethanol was washed away by PBS and the coverslips were incubated with growth media for 1 hour at 37°C. The coverslips were then ready to use.

2.17.5.3 Invadopodia assay

1.5 x 10^5 of cells were seeded on the Rhodamine-getatin coated coverslips in a well of a 12-well plate and incubated for 1, 2, 3, and 4 hours. PBS was used to rise off unattached cells and 300 µl of actin fixer (0.5M MES, Sigma-Aldrich, #M5287; 1M KCl, Fisher Scientific, #p/4280/53; 1M $MgCl_2$, Sigma-Aldrich, #M8266; 0.5M EGTA, Sigma-Aldrich, #E2478) was applied to the coverslips for 20 minute to fix the cells. After washing with PBS, cells were then incubated with 500µl of 50mM NH_4Cl for 10 minutes. To detect actin, 200µl of 10 µg/mL of FITC-labelled phalloidin (Sigma-Aldrich, #P5282) was added and incubated for 20 minutes. The final wash was then performed with PBS for three times and followed by distilled water for three times. The coverslips were then mounted with 5µl Prolong Gold reagent with DAPI (Invitrogen, #P36931). The samples were examined on an Axioplan upright fluorescence microscope (Zeiss, UK) using x40 and x63 objective oil-immersion objective lens. The image analysis was done by using Image J software.

2.17.6 Invasion assay

Invasion assays were performed using Transwell plates (8μm pore, 6.5mm diameter, Corning, #3422) which allow any invasive cell to go through. Matrigel (BD Bioscience, #354234), which is a mixture of basement membrane-like proteins, including laminin, collagen IV, heparan sulphate proteoglycans, entactin/nidogen and growth factors such as TGF-beta, epidermal growth factor, insulin-like growth factor, fibroblast growth factor, tissue plasminogen activator, was added to the upper chamber (70 μl Matrigel [1:2 dilution in α-MEM]) and incubated at 37 °C for an hour to allow gelling. Cells ($5x\ 10^4$) in 200 μl serum-free α-MEM were then placed into the upper chamber and 500 μl of KGM was added in the lower chamber as a chemoatractant. After 72 hours incubation, invaded cells were harvested by trypsin/EDTA to detach cells in the lower chamber and on the undersurface of the filter. Cell numbers were counted on a CASY1 Cell counter (Scharfe Systems, Germany). Transwell invasion assay experiments were repeated three times, with sextuplicate wells for each treatment. Invasion analysis showed the number of cells invaded through to the lower chamber.

2.17.7 Organotypic invasion assay

The organotypic gels were composed of a 1:1 mixture of Matrigel and type 1 collagen (Upstate, Millipore) containing $5\ x10^5$ human fibroblasts. Once set in a well of a 24 well plate $5\ x\ 10^5$ carcinoma cells were added. The mixtures were plated into wells of a 24-well plate and the growth media was changed every 2 days for 14 days incubation. The gels were then fixed in 10% formal saline, bisected, and embedded

to paraffin. Bright field images of H&E staining were taken at ×630 magnification. All cell counts and analyses were done in six random fields per gel from at least three independent gels. Image J software was employed to analyse the images. The invasion index was calculated using the product of the average depth of invasion, the number of invading particles, and the area of the invading particles. Method adapted from [220].

2.17.8 Autophagy assay

2.17.8.1 Blockage of autophagosome-lysosome fusion by chloroquine

Cells were grown to sub-confluence and the growth media was replaced with normal growth media with or without 50μM chloroquine (CQ, Sigma-Aldrich, #C6628) for 24 hours before fxation for the confocal microscopy examination. For Western blot, the cells were rinsed twice with HBSS (Invitrogen, #14025-076) before adding HBSS containing 50μM CQ for starvation with CQ treatment, or normal growth media with CQ. The cells were returned to the incubator for designated time courses. Method adapted from [221].

2.17.8.2 Starvation-induced autophagy

Cells were grown to sub-confluence and the growth media was replaced with HBSS for “starvation” (two rinses in HBSS before being placed in HBSS). The cells were then incubated in HBSS for various time points.

2.17.8.3 Rapamycin-induced autophagy

The cells were grown to about sub-confluence and the 1, 10 or 20 μM rapamycin (Sigma-Aldrich, #R0395) was added and incubated for designated time points.

2.17.8.4 Confocal microscopy

Confocal images of LC3b signals were generated on a Zeiss LSM510 and LSM710 laser scanning microscope. The detailed procedure is referred to in section 2.13.

2.17.9 Cytotoxic assay

Cells were seeded at 5000 per well in 96-well plates and grown in media overnight. Induction of cell death was performed by incubation with various concentrations of cytotoxic drugs (5-FU; Etoposide; Taxol; Cisplatin) for 72 hours. After treatment, cell viability was determined using MTT colorimetric assay (see section 2.15.). Experiments were repeated at least three times in quadruplicate wells.

2.18 Statistical analysis

Statistical differences between experimental groups were evaluated by Student's t test (two tailed). The Mann-Whitney U test was advised to evaluate the significance of the changes in the cytotoxic assay by statistician Mr. Adam Brentnall (Barts Cancer Institute). The statistical calculations were conducted by using Prism software.

CHAPTER 3. CHARACTERISATION OF HAX1 ANTIBODIES

3.1 Introduction

There is a broad range of commercially available HAX1 antibodies and the variation between each antibody may give different results for HAX1 expression, functions or subcellular localisations. Thus it is very important to characterise the HAX1 antibodies and choose the optimal antibody for each application.

I tested a panel of five different antibodies to HAX1: E20 from Santa Cruz, sc-34273; P20 from Santa Cruz, sc-16637; N17 from Santa Cruz sc-16636; BD from BD Transduction Laboratories, 610825; RD from R&D Systems, AF5458. Among these, the BD antibody had been used most widely in various studies [1,20,26,30-32,110,140,144,149,222].

I examined the different HAX1 antibodies for their ability to Western blot and also for their ability to immunostain since there are various subcellular localisations which have been reported for HAX1: predominantly in the cell mitochondria (in HeLa, COS-7, HEK293, DG75, B lymphoma and striated muscle cells [3,12,19,26,27]), also found in the nucleus (COS-7 and DG75 [3,27]), ER (in COS-7, HeLa, HEK293 cells [3,12,28]), cytoplasm (COS-7 and HEK293 cells [21,29]) and in the plasma membrane and the lamellipodia in COS-7 cells [8].

3.2 Results

3.2.1 siRNA oligos target to HAX1

To verify that the antibodies used in this study recognised HAX1, I tested siRNAs to HAX1 that could knockdown all HAX1 isoforms. Two different siRNA duplexes were designed by Dr. Delphine Lees and produced by Dharmacon RNAi Technologies. The sequences were validated by using BLAST (Basic Local Alignment Search Tool). Table 3.1 shows the sequences and the targeting HAX1 isoforms: si192 targets to the 3'UTR of HAX1 recognising isoforms1-8; si1-6 targets to exon2 and knocksdown HAX1 isoforms 1-6.

(a)

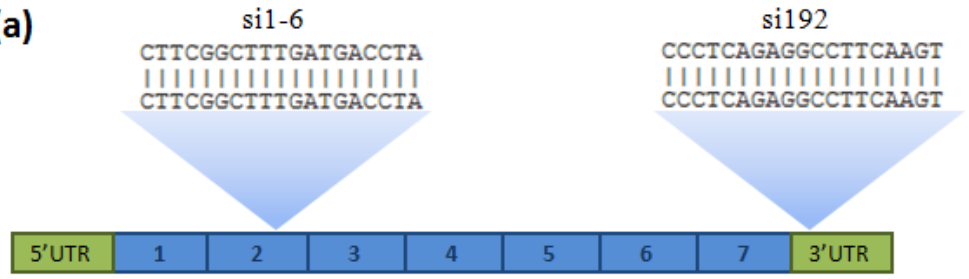

(b)

si RNA	Sequences	Targeting regions to HAX1	HAX1 isoform targeted							
			1	2	3	4	5	6	7	8
si192	CCC TCA GAG GCC TTC AAG T	3'UTR	V	V	V	V	V	V	V	V
si1-6	CTT CGG CTT TGA TGA CCT A	Exon 2	V	V	V	V	V	V	-	-
siNTC	ACT ACC GTT GTT ATA GGT G	Non	-	-	-	-	-	-	-	-

Table 3.1 Sequences of siRNA oligos and the sequences targeted.

siRNA oligos which target to different regions of HAX1 are shown in (a). si1-6 recognises exon 2 of HAX1 whereas si192 targets 3'UTR of HAX1. (b) shows targeted HAX1 isoforms by siRNAs and the isoforms are indicated as "V".

3.2.2 Testing HAX1 antibodies by Western blotting

I firstly characterised the different HAX1 antibodies by Western blot. Oral squamous carcinoma cells VB6 were treated with control siRNA (siNTC) or HAX1 siRNA (si1-6) to transiently knockdown the endogenous HAX1. The lysates were prepared 48 hours after transfection and equal amounts (30μg) of protein were loaded onto a 12% SDS-PAGE gel. Western blots probed with different anti-HAX1 antibodies (E20 from Santa Cruz, sc-34273; P20 from Santa Cruz, sc-16637; N17 from Santa Cruz sc-16636; BD from BD Transduction Laboratories, 610825; RD from R&D Systems, AF5458, Table 3.2) and suitable secondary antibodies (see Methods section). Table 3.2 also shows the epitopes for the antibodies, the antibodies from BD and RD recognise the HAX1 sequence from amino acid 10-148 and 2-261, respectively, whereas the antibodies from Santa Cruz (P20, E20, P17) were not characterised in full detail. Results show that BD and RD antibodies successfully detected endogenous HAX1 as around a 34 kDa band whereas other antibodies (E20, P20 and N17) were not sufficient for detecting HAX1 by Western blotting (Figure 3.1). This band of the endogenous HAX1 is confirmed by the absence of a similar band following by siRNA (si1-6) treatment (Figure 3.1).

HAX1 antibodies	*Species*	*Source*	*Immunogen*
P20	Goat	Santa Cruz, sc-16637	Internal region of HAX1
E20	Goat	Santa Cruz, sc-34273	Internal region of HAX1
N17	Goat	Santa Cruz sc-16636	Internal region of HAX1
BD	Mouse	BD Transduction Laboratories, 610825	Human HAX1 a.a. 10-148
RD	Goat	R&D Systems, AF5458	Human HAX1 a.a. 2-261

Table 3.2 Souces of antibodies to HAX1.

Different antibodies to HAX1 are listed in the Table. The antibodies from BD and RD recognise the HAX1 sequence from amino acid 10-148 and 2-261, respectively, whereas the antibodies from Santa cruz (P20, E20, P17) did not give the full detail of the immunogen used.

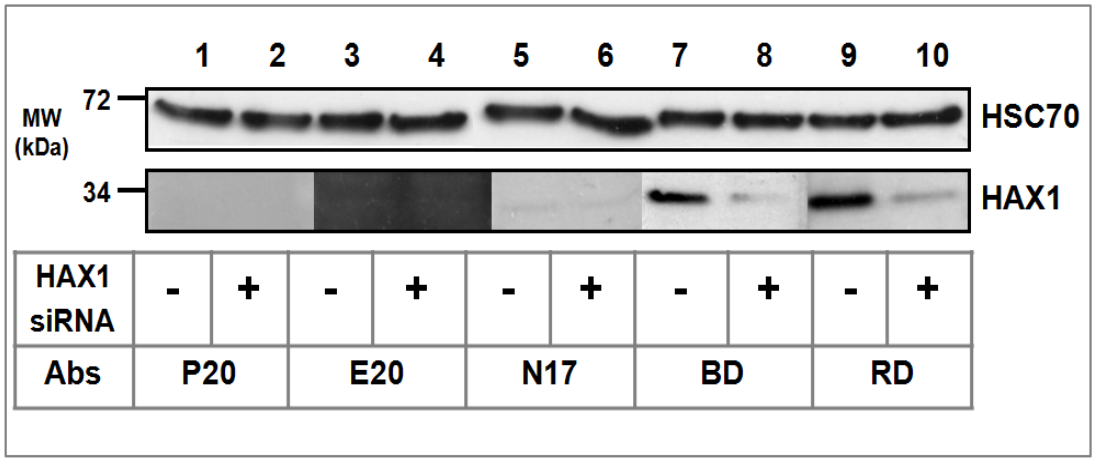

Figure 3.1 Testing different HAX1 antibodies by Western blot.

VB6 were treated with HAX1 siRNA (si1-6) or control siNTC [shown as (-)] and the cell lysates were prepared 48 hours after transfection. Equal amounts of protein were loaded onto 12% SDS-PAGE gels. After Blotting, Ponceau Red was used to stain the Blot which was then cut into five separate strips which were then probed with different anti-HAX1 antibodies. HSC70 served as loading control. Results show that BD and RD antibodies successfully detected endogenous HAX1 whereas the other antibodies (E20, P20 and N17) did not. Please note, even though this experiment was repeated the E20 antibody always generated a non-specific Blotting (lane 3 and 4) which resulted a black background after Chemiluminescence-HRP detection.

3.2.3 Antibodies from BD and RD showed endogenous HAX1 localised in mitochondria

In order to examine the subcellular distribution of endogenous HAX1 in VB6 cells, different HAX1 antibodies were tested for immunofluorecence and analysed by confocal microscopy. The endogenous HAX1 was knocked-down by HAX1 siRNA (si1-6) and the control cells were treated with control siRNA (siNTC). Cells were incubated with the mitochondrial dye, Mitotracker (MitoTracker is a fluorescent dye that passively diffuses across the plasma membrane and accumulates in active mitochondria), before staining with the different HAX1 antibodies and DAPI. Thus, labelling control siRNA treated cells showed that BD and RD antibodies gave a similar pattern of staining (green, Figure 3.3 and Figure 3.4) which colocalised with the Mitotracker labelling (red). The data suggest that the dominant localisation of endogenous HAX1 is either on or in mitochondria in VB6 cells. To confirm this, the HAX1 siRNA (si1-6) was used to knockdown HAX1 and the repeated immunostaining results showed that the mitochondrial labelling was absent in the HAX1 siRNA treated cells (Figure 3.3 and Figure 3.4). Of note, sometimes nuclear staining of HAX1 was observed, (BD and RD, Figure 3.3 and Figure 3.4) consistant with previous reports [3,12,28]. Other antibodies (E20, P20 and P17) did not show detectable staining for endogenous HAX1 (Figure 3.2 and Figure 3.3).

In order to confirm the subcellular localisation of HAX1, cell fractionation was also performed followed by Western blotting with the RD antibody. To confirm the purity of each fraction, blotting for β6, actin, and lamin was used as the markers for heavy membrane, cytoplasm, and nuclear fractions respectively (Figure 3.5).

Endogenous HAX1 was detected at approximately 34 kDa (Figure 3.5); the identity of the band was confirmed by the reduction in the band intensity after HAX1 siRNA treatment [shown as (+)] (Figure 3.5, lane 2, 4 and 6). Data show that the endogenous HAX1 was located in the heavy membrane fraction (lane 5 and 6) and also in nuclear fraction (lane 3 and 4). Cytosolic HAX1 was at very low levels (lane 1 and 2, Figure 3.5).

Together, antibodies from BD Transduction Laboratories (610825) and R&D Systems (AF5458) successfully detected endogenous HAX1 by Western blot and immunofluorecence staining. Table 3.3 summarises the suitable applications for commercially available HAX1 antibodies.

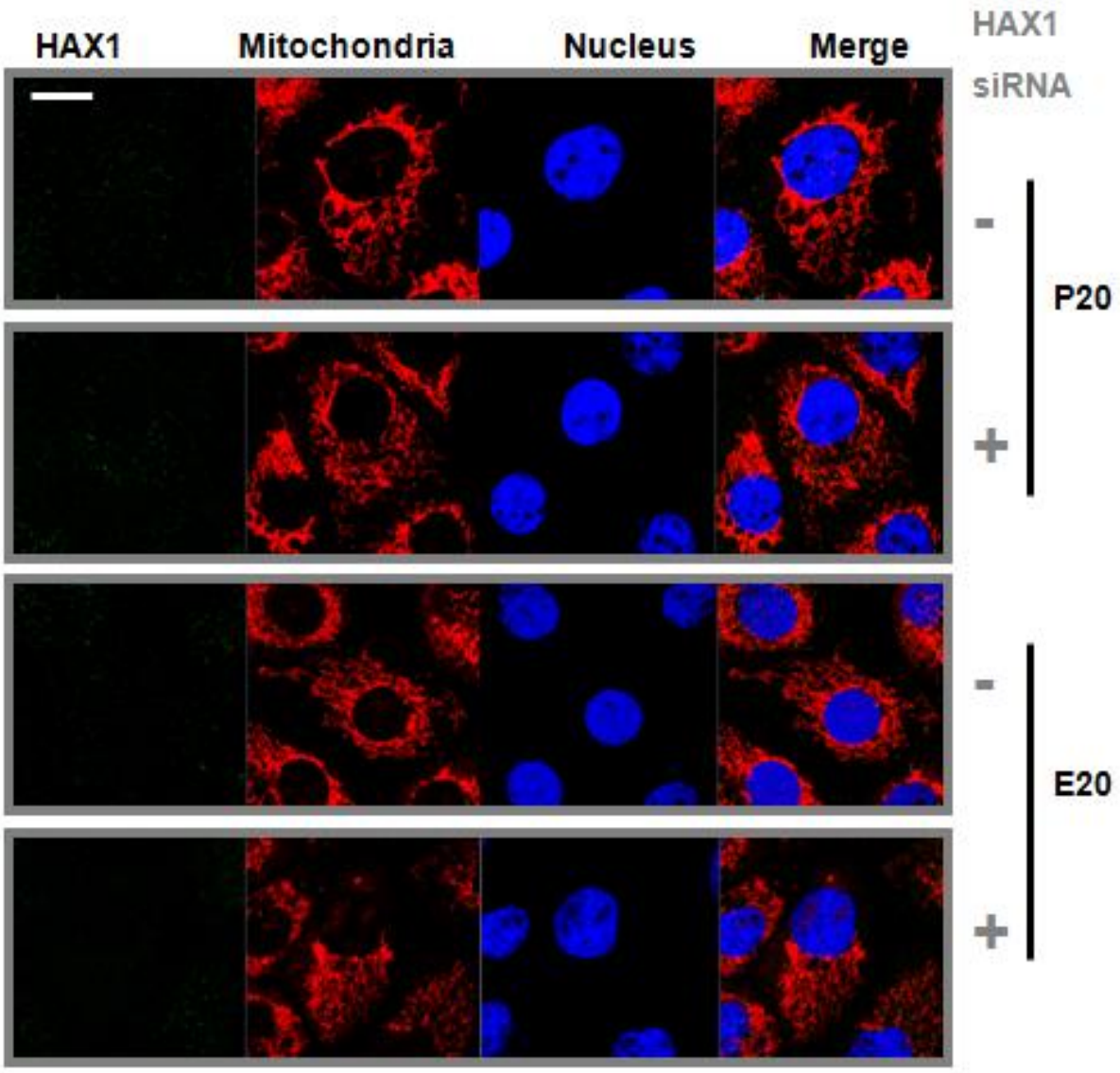

Figure 3.2 Testing the anti-HAX1 antibodies P20 and E20 by immunofluorescence.

VB6 cells treated with control siRNA or HAX1 siRNA (si1-6) were incubated on the coverslips for 48 hours. Mitotracker was employed to stain the mitochondria (red) before fixation and permeabilisation. Cells subsequently were stained with anti-HAX1 antibodies (BD and E20) and DAPI (blue). FITC-labelled donkey-anti-goat or goat-anti-mouse antibodies were used as corresponding secondary antibodies to visualise HAX1 expression (green). Confocal images showed P20 and E20 antibody did not detect endogenous HAX1. Scale bar, 10 μm.

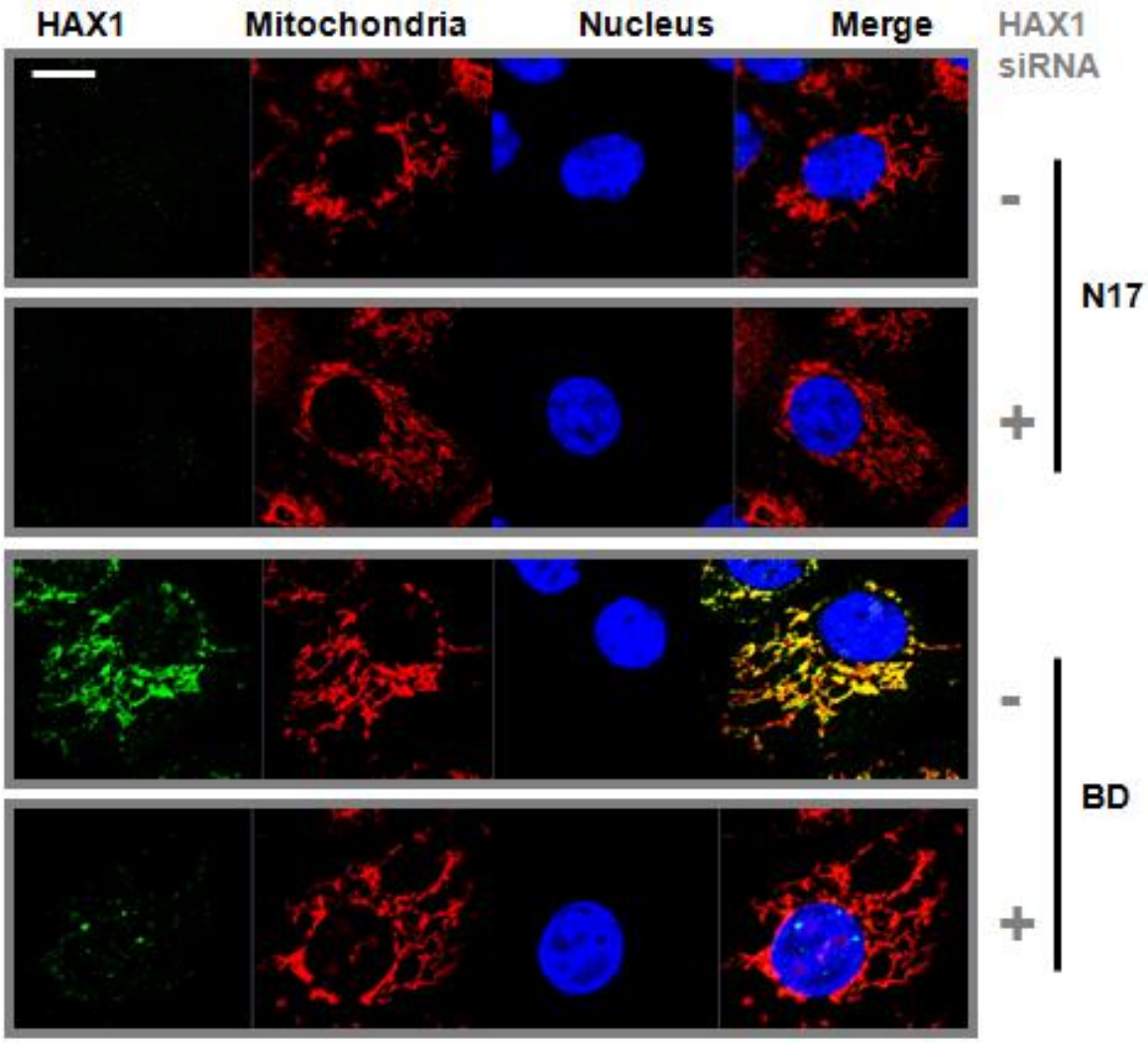

Figure 3.3 Testing the anti-HAX1 antibodies N17 and BD by immunofluorescence.

VB6 cells treated with control siRNA or HAX1 siRNA (si1-6) were incubated on the coverslips for 48 hours. Mitotracker was employed to stain the mitochondria (red) before fixation and permeabilisation. Cells subsequently were stained with anti-HAX1 antibodies (N17 and BD) and DAPI (blue). FITC-labelled donkey-anti-goat or goat-anti-mouse antibodies were used as corresponding secondary antibodies to visualise HAX1 expression (green). Confocal images showed N17 antibody was not able to detect endogenous HAX1 whereas BD antibody successfully stained for endogenous HAX1 which was concentrated in the mitochondria as shown by colocalisation with Mitotracker (indicated as yellow from red and green). Note there is also the nuclear staining with BD antibody. Scale bar, 10 μm.

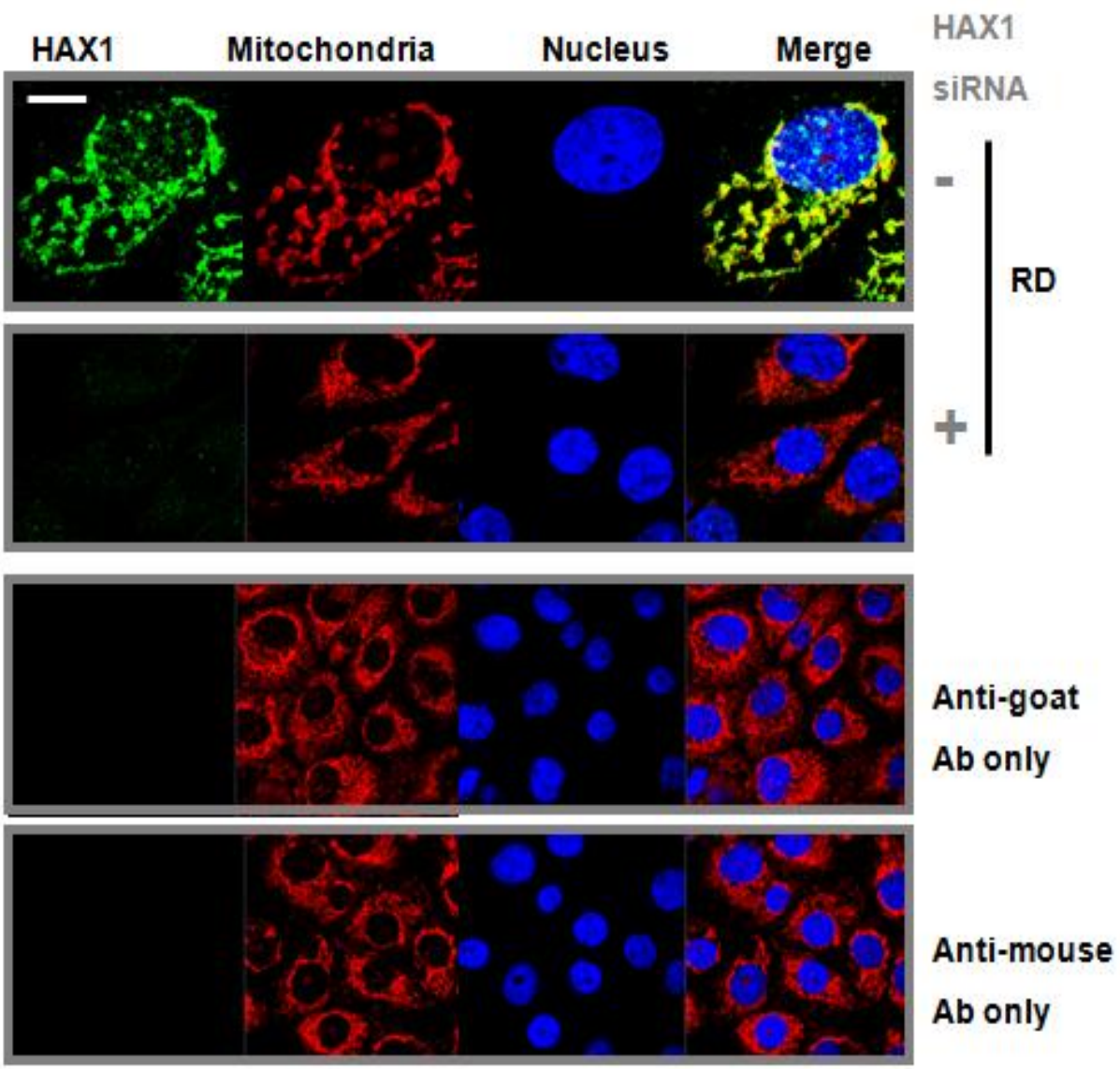

Figure 3.4 Testing the anti-HAX1 antibody RD by immunofluorescence.

VB6 cells treated with control siRNA or HAX1 siRNA (si1-6) were incubated on the coverslipes for 48 hours. Mitotracker was employed to stain the mitochondria (red) before fixation and permeabilisation. Cells were subsequently stained with anti-HAX1 antibodies (RD) and DAPI (blue). FITC-labelled donkey-anti-goat or goat-anti-mouse antibodies were used as corresponding secondary antibodies to visualise HAX1 expression (green). Confocal images showed RD antibody successfully detected endogenous HAX1, and that it was concentrated in the mitochondria as shown by colocalisation with Mitotracker (indicated as yellow from red and green) and also showed the expression in the nucleus. Scale bar, 10 μm.

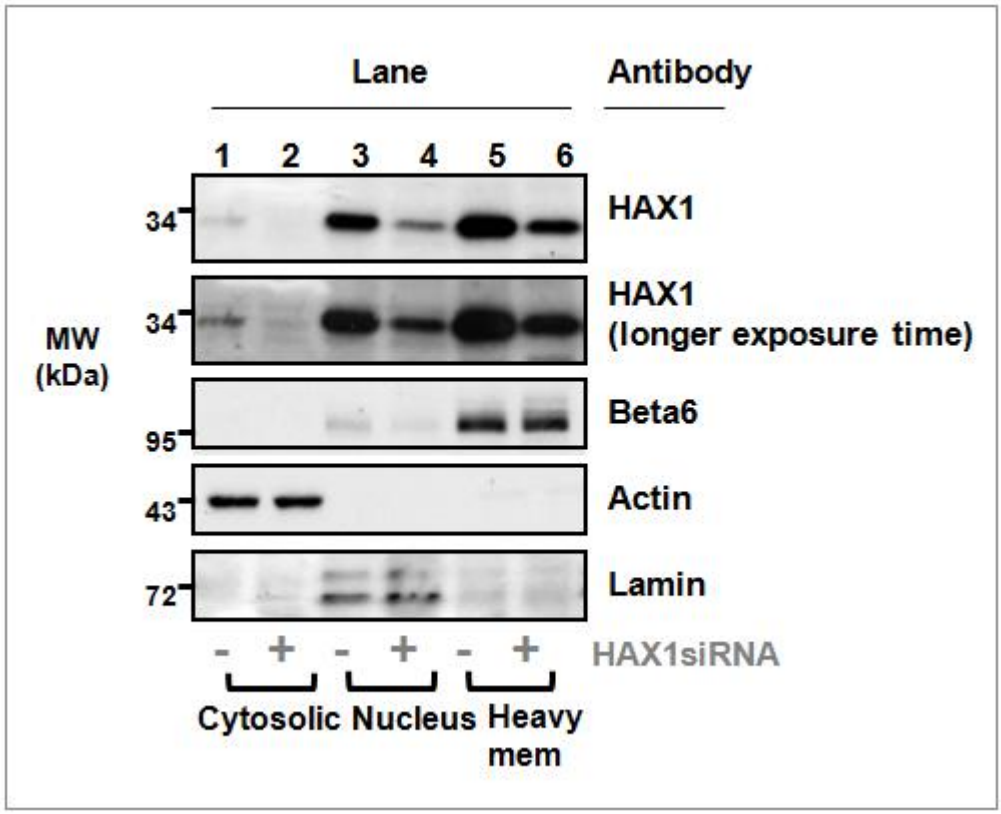

Figure 3.5 HAX1 subcellular distribution.

VB6 cells were treated with an siRNA which targets to exon 2 of HAX1 (si1-6; indicated as [+]) or control siRNA (indicated as [-]), and protein fractionation was performed to determine the band(s) for the endogenous HAX1. The equal amounts of protein were loaded for each fraction and the endogenous HAX1 was detected around 34 kDa (by RD antibody). Western blot shows the expression of HAX1 is located in the nuclear fraction (lane 3 and 4) and the heavy membrane fraction (lane 5 and 6) whereas the HAX1 level is only a trace in the cytosolic compartment (lane 1 and 2). The markers for the protein fractionation are β6 (110kDa, for heavy membrane), actin (42kDa, for cytoplasm) and lamin (lamin A/C, 74 and 65 kDa, for cell nucleus).

HAX1 antibodies	*Western blot*	*Immunofluorescence staining*
P20	**x**	**x**
E20	**x**	**x**
N17	**x**	**x**
BD	**v**	**v**
RD	**v**	**v**

Table 3.3 Characterisation of HAX1 antibodies.

HAX1 antibodies from different sources were used to examine the suitable applications. Results from Figure 3.1, Figure 3.2, Figure 3.3 and Figure 3.4 show the antibodies from BD Transduction Laboratories (610825) and R&D Systems (AF5458) successfully detected endogenous HAX1 by Western blot and immunofluorescence staining. Santa Cruz antibodies (P20, E20, N17) were ineffective. x= poor or ineffective, v= good/ effective.

3.2.4 HAX1 expression is cell density-dependent

3.2.4.1HAX1 protein is expressed at levels which depend on cell density

Integrin αvβ6 expression has been shown to be dependent on cell density [223] I therefore investigated if cell density also affected the expression of the αvβ6 binding partner HAX1. To examine whether HAX1 expression is affected by different cell densities, VB6 and H400 oral carcinoma cells were seeded into 12-well plates at different cell densities (2.5, 5, 10, 20, and 40 x 10^4 cells, Figure 3.6, a and b), and cells were harvested after 24 hours incubation. Protein concentrations were determined and equivalent amounts of protein were added to 12% SDS-PAGE gels. The results of Western blotting show that the expression of HAX1 varied significantly depending on the cell density (Figure 3.6, a and b) in both H400 and VB6 oral cancer cell lines. Thus Figure 3.6 (c and d) shows the densitometry from three independent experiments indicating that when either VB6 or H400 oral cancer cell lines cells were grown in low density (e.g. plated at 2.5 x 10^4) they expressed very little HAX1 protein whereas when the cells were plated at high density they expressed significant amounts of HAX1. The experiment, which was repeatable with similar results (data not shown), also showed that HSC70 was not an accurate loading control for this experiment (24 hours time point) since it also seems to be expressed at reduced levels in low density cells (Figure 3.6.).

As both HAX1 and the loading control HSC70 were affected by cell density 24 hours after seeding, it was considered that maybe 24 hours after cell seeding was too short to be an accurate time point to assess stable protein expression. Thus Western

blot analysis was repeated with cells cultured and harvested at longer time points (48 and 72 hours after plating). Data demonstrated that all control loading proteins examined (HSC70, actin, tubulin) and HAX1 showed cell density-dependent expression at all time points (Figure 3.7, a, b and c). However, while HAX1 expression was still much more varied with cell density at 48 h and 72 h (Figure 3.7, b and c), the expression of the control proteins (HSC70, actin and tubulin) were more consistent (especially HSC70). These data revealed that HAX1 protein expression correlates with cell density. Hence all the subsequent analyses of HAX1 expression were performed on confluent cells that had been plated for at least 48 hours and I chose HSC70 as a loading control.

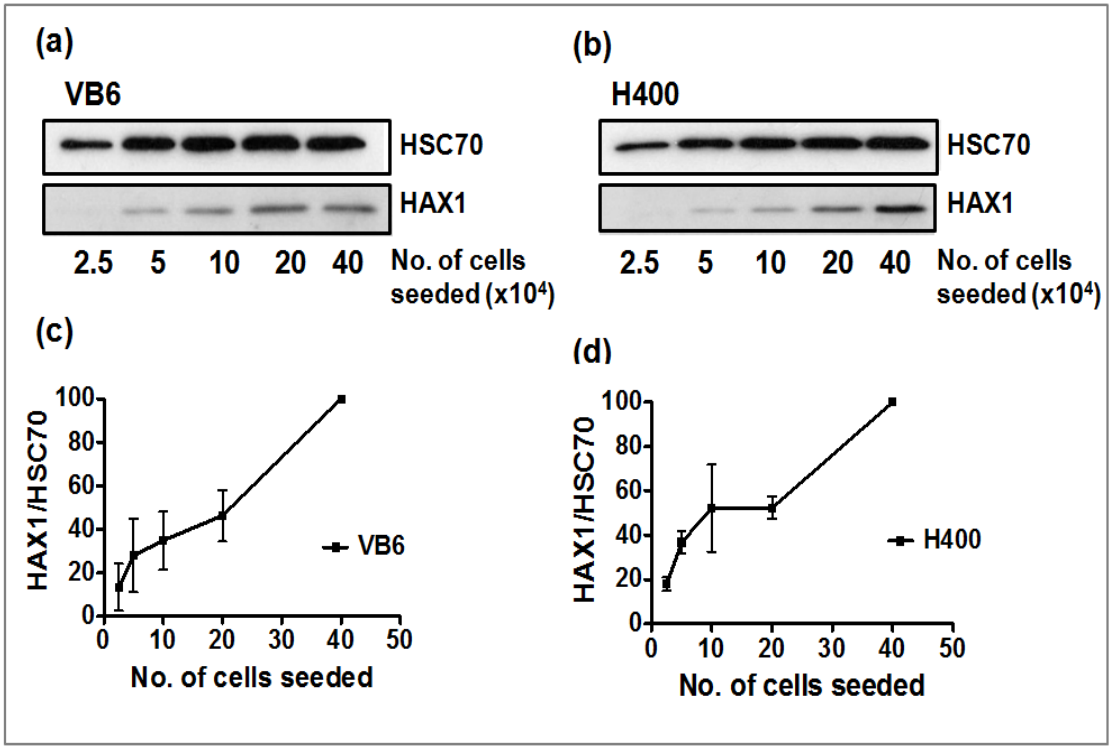

Figure 3.6 Density-dependent expression of HAX1 protein.

VB6 and H400 cells were seeded at different cell numbers and were harvested after 24 hours. Equal amounts of protein were loaded onto 12% SDS-PAGE gels and Western blots were probed with anti-HAX1 antibody (BD). The bands were analysed by densitometry and HAX1 expression was plotted with the loading control HSC70. Data show that the expression of HAX1 varies significantly depending on cell density (a, b). In both VB6 and H400 oral cancer cell lines, cells grown at low density have very little HAX1 whereas cells at high density have significant amounts of HAX1 (c, d). Note that at low density, the expression of HSC70 also is reduced. Experiments were repeated at least three times and the figures (a and b) show one of the experiments. Data show mean +/- one standard deviation of at least three experiments.

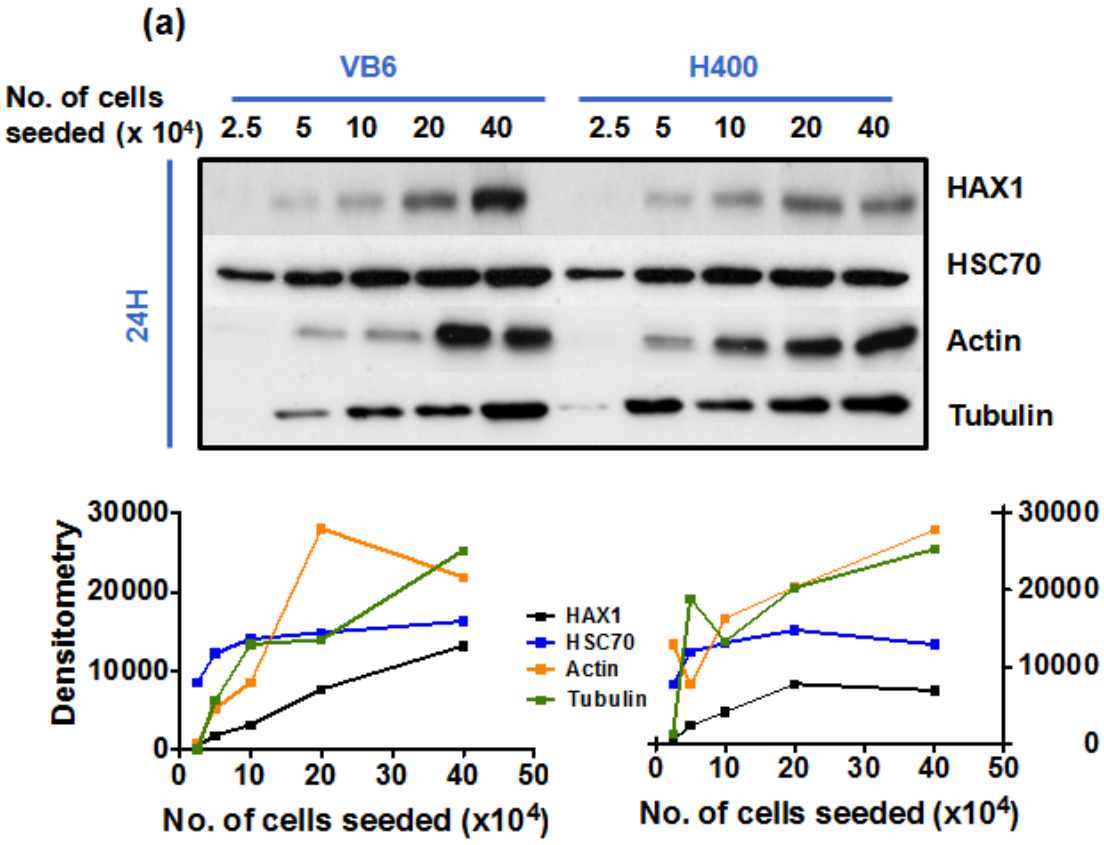
(a)
VB6
H400
No. of cells seeded (x 10⁴)
2.5 5 10 20 40
2.5 5 10 20 40
24H
HAX1
HSC70
Actin
Tubulin
Densitometry
30000
20000
10000
0
0 10 20 30 40 50
No. of cells seeded (x10⁴)
HAX1
HSC70
Actin
Tubulin

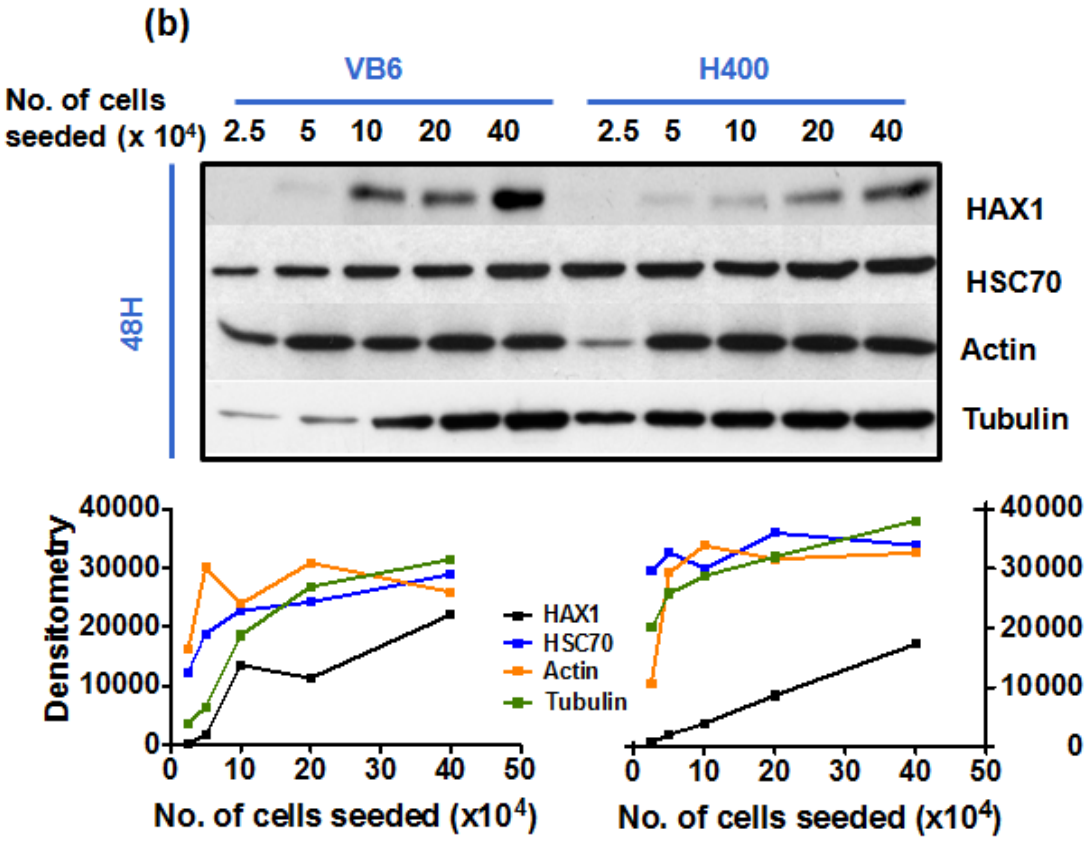
(b)
VB6
H400
No. of cells seeded (x 10⁴)
2.5 5 10 20 40
2.5 5 10 20 40
48H
HAX1
HSC70
Actin
Tubulin
Densitometry
40000
30000
20000
10000
0
0 10 20 30 40 50
No. of cells seeded (x10⁴)
HAX1
HSC70
Actin
Tubulin

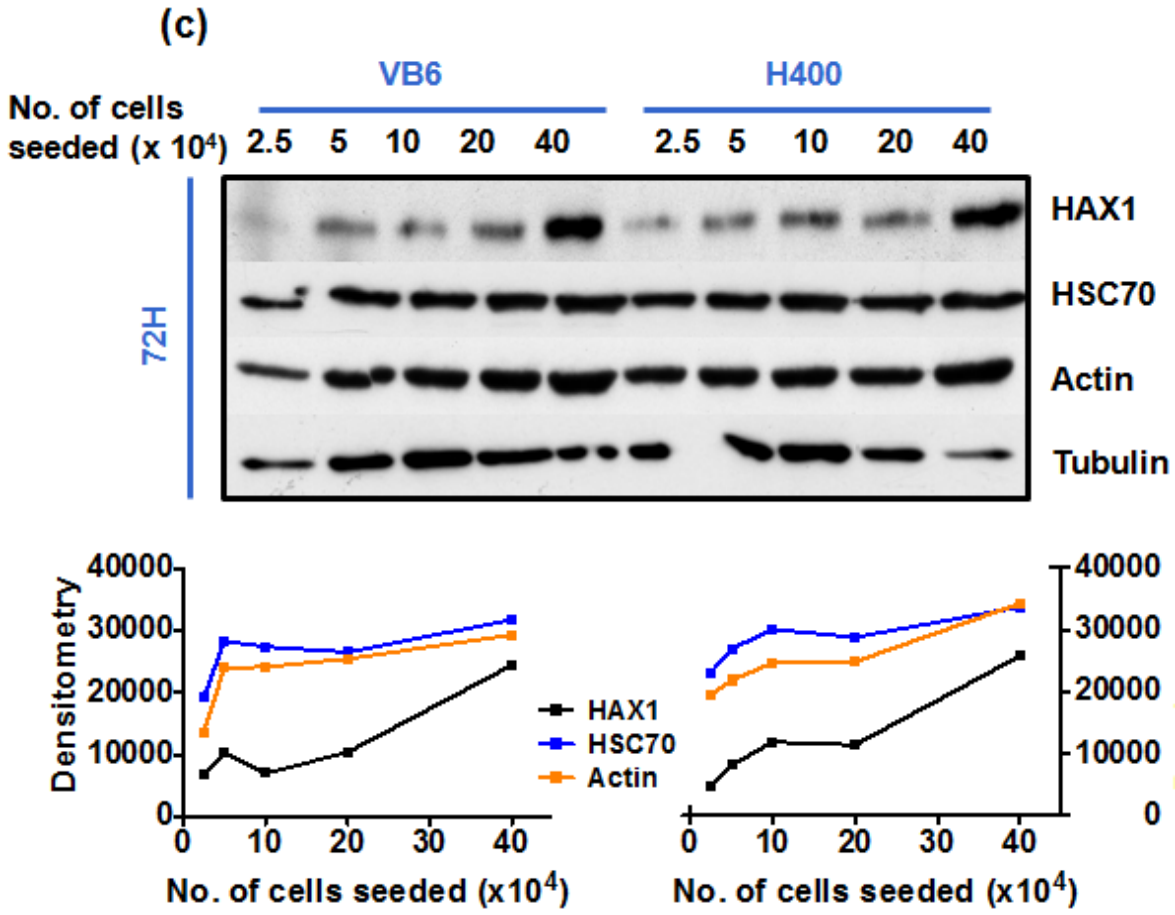

Figure 3.7 Analysis of HAX1 protein expression at different cell densities.

VB6 and H400 cells were seeded at 2.5, 5, 10, 20 and 40 x10^4 into wells of 12-well plates. Cells were harvested at 24 (a), 48 (b) and 72 (c) hours, protein concentrations were determined and equal amount of protein was loaded onto 12% SDS-PAGE gels. The membranes were probed for HAX1 (BD), HSC70, actin and α-tubulin. The bands were quantified by densitometry and expression of proteins was plotted against cell density.

3.2.4.2HAX1 changes its subcellular localisation in different density cultures

In order to investigate further the density-dependent expression of subcellular distribution patterns, immunocytostaining was employed to examine HAX1 localisation under the conditions of sparse culture versus confluent culture. Images from confocal microscopy showed HAX1 is localised predominantly in mitochondria in sparse culture, whereas in confluent monolayers an increased amount of HAX1 was seen also in the cytosol, distinct from the mitochondria (Figure 3.8, a). To quantify these differences, the colocalisation coefficient of HAX1 signal and mitochondrial signal was analysed with Zen software. This analysis showed that in dense culture HAX1 colocalisation in mitochondria was significantly ($p< 0.0001$) reduced compared with cells in sparse culture (Figure 3.8, b) indicating that HAX1 protein can both change localisation as well as modify the level of expression at different cell densities.

To validate the observations from staining, the cell fractionation technique also was employed to separate the cell compartments. To ensure the purity of each fraction, the appropriate markers were also Blotted (actin for cytosolic marker; beta6 for heavy membrane marker; lamin for nucleus marker). Fractionation data also showed the increased HAX1 expression in the cytosolic fraction at high cell density culture (Figure 3.8, (c), cytosolic H) compared with low cell density culture (Figure 3.8, (c), cytosolic L).

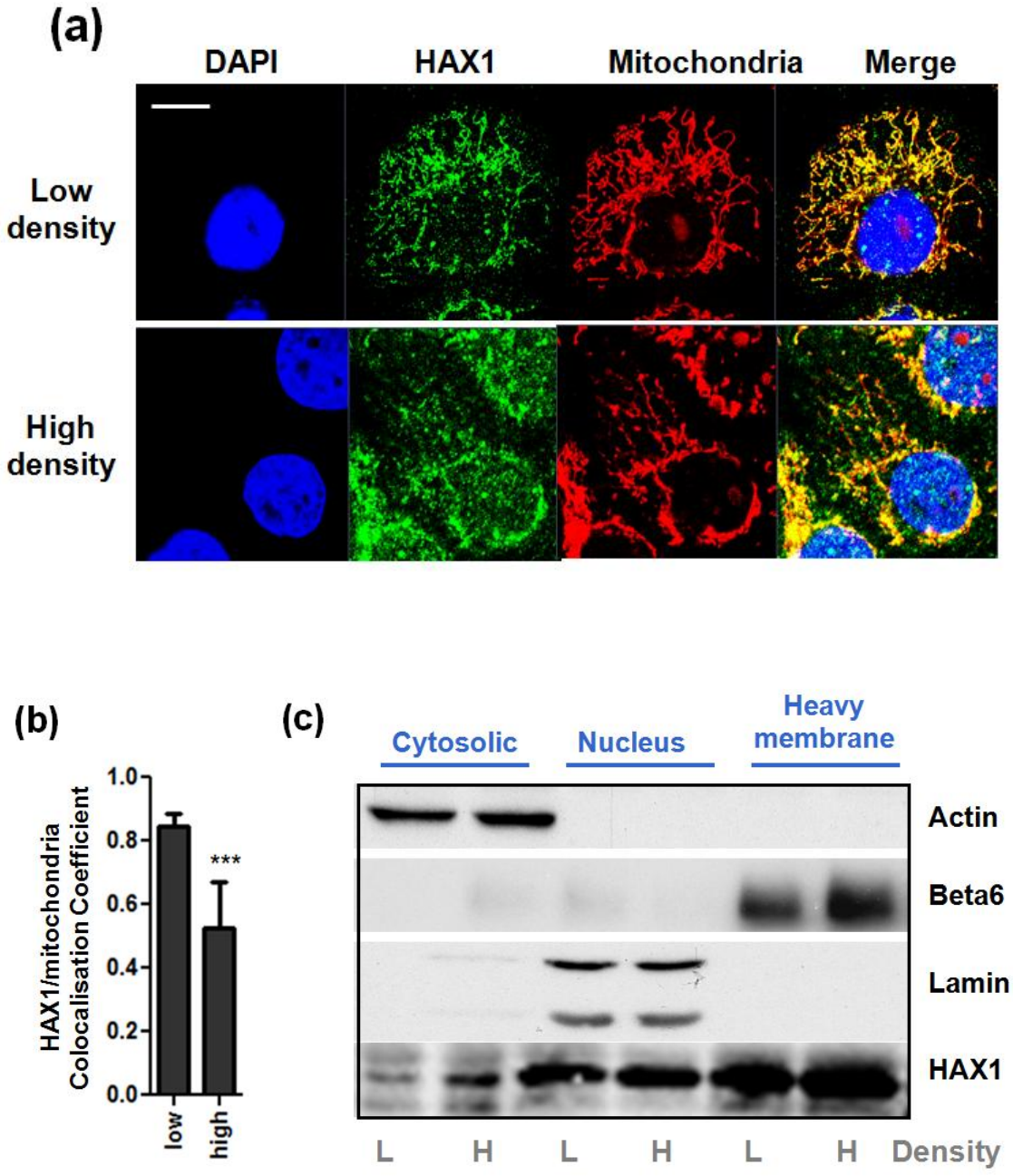
(a)
DAPI
HAX1
Mitochondria
Merge
Low density
High density
(b)
HAX1/mitochondria Colocalisation Coefficient
1.0
0.8
0.6
0.4
0.2
0.0
***
low
high
(c)
Cytosolic
Nucleus
Heavy membrane
Actin
Beta6
Lamin
HAX1
L
H
L
H
L
H
Density

Figure 3.8 Sub-cellular localisation of HAX1 protein varies with cell density.

To determine the sub-cellular distribution of HAX1, VB6 cells were labelled with an antibody which recognises all HAX1 isoforms (RD). The cells were fixed with methanol/acetone and then stained with Mitotracker (red), anti-HAX1 antibody (green) and DAPI for cell nucleus (blue). HAX1 expression was primarily localised in mitochondria in sparse culture (a, top panel), whereas more diffuse staining was observed in confluent cell culture (a, lower panel). Scale bar, 10 μm. Figure (b) shows the HAX1 localisation in mitochondria is significantly less at high cell density compared with low cell density. Quantification was done with Zen software (Zeiss LSM710) with 30 cells from 3 random fields, colocalisation coefficient represents relative number of colocalising pixels as compared with the total number of pixels, (0: no colocalisation, 1: all pixels colocalise). *** = p value < 0.0001. (c) VB6 cells were harvested at confluence or sparse culture and samples fractionated into cytosolic, nuclear and heavy membrane fractions. Purity of fractions was confirmed by Blotting for actin, lamin or β6 as shown. Membrane was blotted with anti-HAX1 antibody (RD). L: low cell density, H: high cell density.

3.2.4.3mRNA of HAX1 isoforms was not altered by different cell densities

In order to analyse the relationship between the cell density and HAX1 isoform expression, semi-quantitative PCR was employed to detect each HAX1 isoform mRNA level by using specific primer pairs. To optimise PCR conditions and determine the amount of template to use, initially, variable amounts of cDNA templates (1, 5, 25, 50, 100 and 200 ng) were used to perform PCR for each isoform, in triplicate. After electrophoretic separation of the PCR products, densitometric digital images were analysed by Image J. Figure 3.9 shows the plots for the PCR products for each isoform. From these data, I chose 50 ng of template for semi-quantitative PCRs for each reaction so that the reactions remained in the exponential amplification range.

In order to examine the cell density and HAX1 isoform expression, semi-quantitative PCR was performed to investigate the mRNA level of individual isoforms at different cell confluence. VB6 cells were seeded into 12-well plates with different cell numbers (2.5, 5, 10, 20, and 40 x 10^4 cells) and total RNA was extracted after 48 hours. 1µg of RNA was reverse-transcribed and 50 ng of cDNA was amplified with specific primer pairs and using the optimal, but different, PCR reactions (see Methods section). Figure 3.10 shows the transcripts for the HAX1 variants were unchanged at the different cell densities. All PCR results were performed at least three times and data were generated relative to GAPDH.

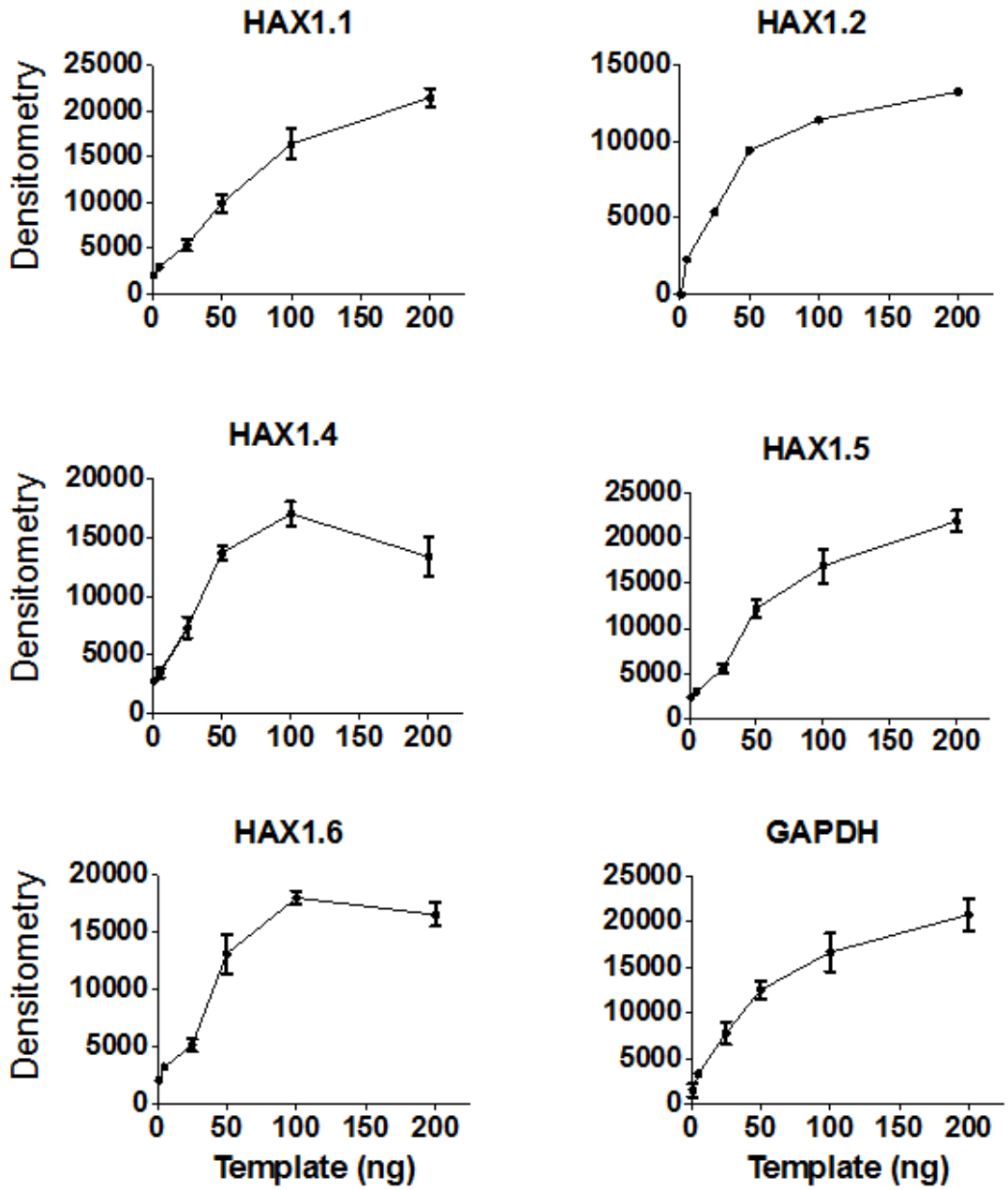

Figure 3.9 Analysis of the variation of HAX1 isoform levels.

Variable amounts of cDNA templates (1, 5, 25, 50, 100 and 200 ng) were used to perform PCR for each isoform. After electrophoretic separation of the PCR products, densitometric digital images were analysed by Image J. GAPDH was used as control. The plots are the mean of three independent experiments.

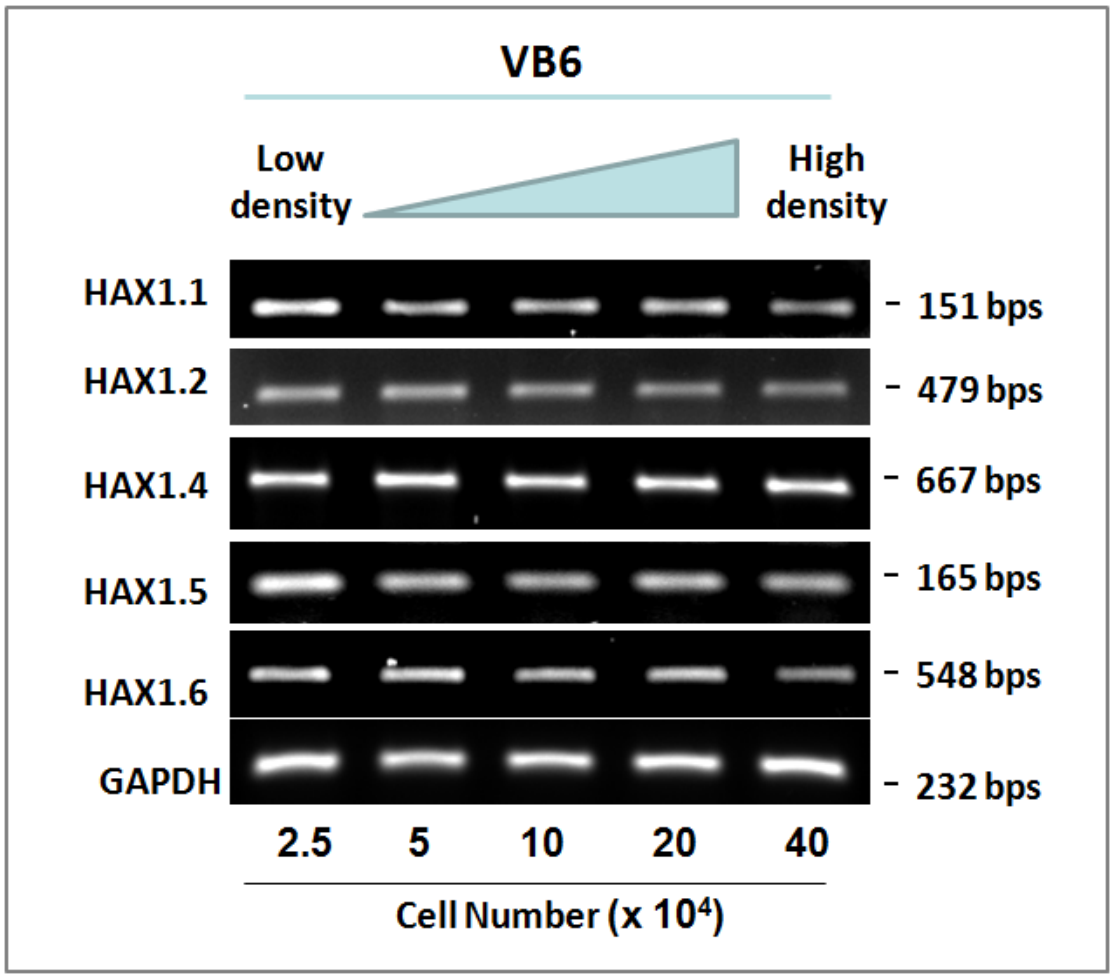

Figure 3.10 HAX1 variant mRNA expression at different cell densities.

Semi-quantitative RT-PCR was employed to analyse the mRNA level of HAX1 isoforms. VB6 cells were seeded into 12-well plates with different cell numbers (2.5, 5, 10, 20 and 40 x10^4) and cells were harvested at different stages of confluence after 48 hours. 1µg of RNA was reverse-transcribed and 50 ng of cDNA was amplified with specific primer pairs using the optimal but different PCR reactions. Data show that equal amounts of mRNA were expressed for all isoforms at the different cell densities. All PCR data were from experiments performed at least three times, GAPDH is employed as loading control.

3.3 Discussion

There are various commercially available antibodies for HAX1 and it was important to characterise the HAX1 antibodies before choosing which antibody was suitable for specific applications in my project. Herein, I tested various HAX1 antibodies by Western blot and immunofluorescence staining. The results showed that HAX1 antibodies (from BD and RD) are efficient for both applications. Another method I could have used to evaluate the antibody specificity is by pre-incubation of antibody with the immunogen prior to its use immunochemically. If the antibody bound to the specific blocking peptide used to generate the antibody, then it would no longer be available to bind to the epitope present in the protein on the western blot or in the cell, resulting an absence of staining. The antigen used for the BD monoclonal antibody to HAX1 was the peptide sequence a.a 10-148. In contrast, the RD goat antibody is to a.a 2-261 of HAX1, almost the whole protein. The antibody from BD antibody demonstrated a weaker signal for Western blotting (it needs higher antibody concentration as well as longer exposure time for the chemiluminescent signals) compared with RD antibodies, probably because the latter is a polyclonal with multiple anti-HAX1 antibodies in the mixture. Thus I primarily use the RD antibody for the following experiments.

HAX1 has been reported to localise in multiple cellular compartments (mitochondria, ER, cell nucleus) [3,19,27]. In VB6 cells, the endogenous HAX1 showed a predominant localisation to the mitochondria and this was confirmed by two different HAX1 antibodies (BD and RD) (unpublished data from my lab). The mitochondrial HAX1 staining was absent following treatment with HAX1 siRNA,

confirming this is genuine HAX1 expression. In line with the immunofluorecence staining results, cell fractionation experiments also demonstrated the abundant expression of HAX1 in heavy membrane compartment (which includes cell membrane and mitochondria) and this is also the major localisation reported for HAX1 [19,27,30-32]. Despite the predominated mitochondrial expression, HAX1 also appeared in cell nucleus using immunofluorescent staining approach, indicating the nuclear localisation. By fractionation, endogenous HAX1 also appeared in the cell nuclear fraction, this observation has also been reported previously [27,32,224]. In addition, minor expression of HAX1 was observed in the cell cytoplasm, in line with other studies [29,38,65].

Contact inhibition is a process by which cells stop proliferating when they reach confluence, despite the availability of extracellular nutrients and growth factors [225,226]. Cancer cells develop mechanisms to escape contact inhibition resulting in unlimited growth [227]. Interestingly, αvβ6 has been reported to be expressed in a density-dependent manner. Niu *et al* showed that high cell density selectively enhanced expression of β6 (with unchanged levels of the αv-subunit) in a protein kinase C (PKC)–dependent manner in colon cancer cells [223], resulting in a marked increase in MMP-9 secretion as cells reached confluence. This may facilitate ECM degradation, which helps overcome cell crowding and restore cell proliferation as well as cell invasion [223]. We investigated whether HAX1 is also influenced by cell density. Results showed that endogenous HAX1 expression, like integrin αvβ6, increased with increasing cell density. Data show the relatively lower expression of the protein in cells grown in the sparse culture while abundant amounts of HAX1 were expressed in confluent culture. Of note, overcrowding and excessive cell death

was observed in the highest cell density (40 x 10^4) after 48 hours culture, indicating this seeding density caused stress by overcrowding the cells. The second dense confluency (20 x 10^4) showed a confluent and healthy cell culture after 48 hours incubation, thus it was chosen as the confluency that I should use for further experiments. These experiments also showed the density dependent expression of all "loading control" proteins tested (HSC70, tubulin and actin) especially at the 24 hours time point post-plating while they seen stabilised at the longer time points. HSC70 performed as the most stable marker among these molecules therefore I used HSC70 as my loading control for all the following experiments. Taken together, these observations are very important for my study of the cellular functions of HAX1 and thus I always ensured experiments were done with confluent cells (20 x 10^4 in a well of a 12-well plate). Interestingly, the RT-PCR showed there was no significant change in the mRNA levels of HAX1 isoforms 1, 2, 4, 5 and 6 at the different cell densities, suggesting the increase in HAX1 protein must be post-translational. It also is possible that HAX1 half-life increases at higher cell densities but I have not evaluated this possibility.

Immunofluorescence staining was performed with different densities of cell cultures to examine subcellular distribution of HAX1. This revealed a striking expression pattern of endogenous HAX1: from a predominantly mitochondrial expression in sparse culture, HAX1 appeared at a markedly higher level in the cytosol in confluent cells. HAX1 has been reported to change its subcellular distribution in order to execute certain cellular functions. For example, exogenous HAX1 was located in mitochondria but when it was co-expressed with either PKD2 in HeLa cells or cortactin in COS-7 cells, it preferentially concentrated into the plasma membrane

and at the tips of cell processes, respectively, where its binding partners were also located [8]. This redistribution of HAX1 was shown in migrating cells, further suggesting that it may be involved in cell motility and migration through its direct binding to cytoskeletal proteins such as PKD2 or cortactin [8].

CHAPTER 4. HAX1 REGULATES MIGRATION IN VARIOUS CANCER CELL LINES

4.1 Introduction

HAX1 has been reported to regulate cell migration via different mechanisms. HAX1 binds to cytoskeleton associated molecules such as Gα13, Cortactin, PKD2, PELO which contribute to actin dynamics and cell movement [8,49,56]; a recent study also showed it interacts with urokinase-type plasminogen activator (uPA) receptor (uPAR) and enhances breast cancer cell migration [65]; the previous work from in my lab, by Ramsay *et al*, showed that HAX1 binds to the cytoplasmic tail of integrin αvβ6, and the interaction is essential for the endocytosis of the integrin and this internalisation of αvβ6 is also crucial for oral squamous carcinoma cell migration and invasion [1].

Integrins act as adhesion receptors by binding cells to extracellular ligands such as collagens, laminins, or fibronectin and vitronectin [158]. The interaction between integrins and their ligands controls cell behaviour by signalling from the extracellular environment [158]. Latency-associated peptide (LAP) is the protective propeptide of latent TGF-β and it is also a ligand for certain integrins [216]. LAP-β1 and LAP-β3 contain the integrin-recognition motif Arg-Gly-Asp site (RGD). Eight integrins recognise the RGD site in their ligands: α5β1, α8β1, αvβ1, αvβ3, αvβ5, αvβ6, αvβ8 and αIIbβ3, of these αvβ6 and αvβ8 are high affinity receptors for LAP-β1 and LAP-β3 [216].

In this section, I will firstly repeat the experiments from Ramsay *et al* [1] to examine whether HAX1 regulates oral cancer cell migration, and then I will test HAX1-regulated migration in other cancer cell lines (breast, pancreas and cervix) in order to see whether this is an oral cancer cell-specific or a general phenomenon for a broad range of cancer cells. Also I will test which integrins HAX1 regulates for cell migration in these cancer cell lines. Finally I shall test the immortalised human keratinocyte line HaCat cells as an example of a non-cancerous keratinocyte for the role of HAX1 in noncancerous cell migration.

4.2 Results

4.2.1 HAX1 regulates oral carcinoma cell migration

As described in the previous section (see 3.2), siRNA1-6 targets isoforms 1-6 of HAX1 and was used to knockdown HAX1 in the oral squamous carcinoma VB6. Western blotting showed the level of HAX1 expression was reduced with siRNA (Figure 4.1, a). Transwell cell migration assays were performed toward LAP where the migration of VB6 cells is modulated solely through αvβ6 [181]. The depletion of HAX1 by HAX1 siRNA significantly decreased migration toward LAP (Figure 4.1, b), in line with previous data reported from my lab [1]. Figure 4.1 (c) shows the growth study over the same period of time and revealed that there was no significant difference in cell number, indicating the change of migration was not due to the change of cell growth.

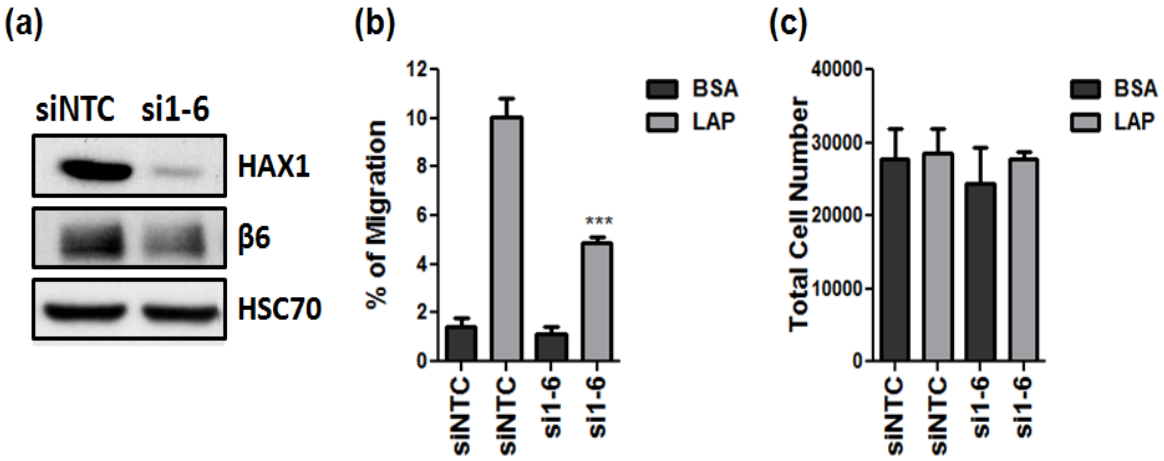

Figure 4.1 HAX1 knockdown inhibits oral squamous carcinoma cell migration toward LAP.

VB6 cells were transfected with control siRNA (siNTC) or HAX1 siRNA (si1-6) and Western blotting showed the decreased HAX1 expression by HAX1 siRNA (a). (b) Cell migration assays were performed across Transwell membranes whose underside was coated with 0.5% bovine serum albumin (BSA) or 0.5μg/mL LAP. Data showed knockdown of HAX1 suppressed migration by 51%. (c) To determine if HAX1 knockdown affected cell growth, the total number of cells in the well was determined by harvesting the cells from the Transwell. The total cell number was calculated as the sum from the cell number of upper chamber and lower chamber. No significant change was seen in cell growth. Data showed the mean of quadruplicate samples from four separate experiments and error bar represents one standard deviation; ***: p-value <0.001.

4.2.2 HAX1 regulates cancer cell migration in cell lines from multiple tissues

Since I confirmed that HAX1 regulated oral squamous carcinoma cells' migration toward LAP (Figure 4.1) I wished to ask whether this is a general phenomenon for cancer cells. I therefore tested a panel of cancer cells derived from other tissues including: breast epithelial cell, (MCF10 CA1a); pancreas (CFPac1 and Panc 04.03); and cervix (HeLa). Two different siRNAs (si1-6 and si192) were used to target the HAX1 isoforms to avoid potential off-target effects by using only one siRNA. Western blotting showed that siRNA (1: si1-6; 2: si192) decreased the level of endogenous HAX1 protein in all treated cells (Figure 4.2 a, b, e and f). Figure 4.2 c, d, g and h show that cell migration toward LAP was significantly ($p<0.01$) inhibited by the absence of HAX1 in all the cancer cell lines tested. Notably, β6 expression sometime was also suppressed by HAX1 knockdown (Figure 4.2, a and b), and this also probably contributes to the decreased cell migration. These data illustrate that HAX1 is a central regulator for cell migration as it is not only required for oral squamous carcinoma cell migration, but also is crucial for breast, pancreatic and cervical cancer cell migration toward LAP.

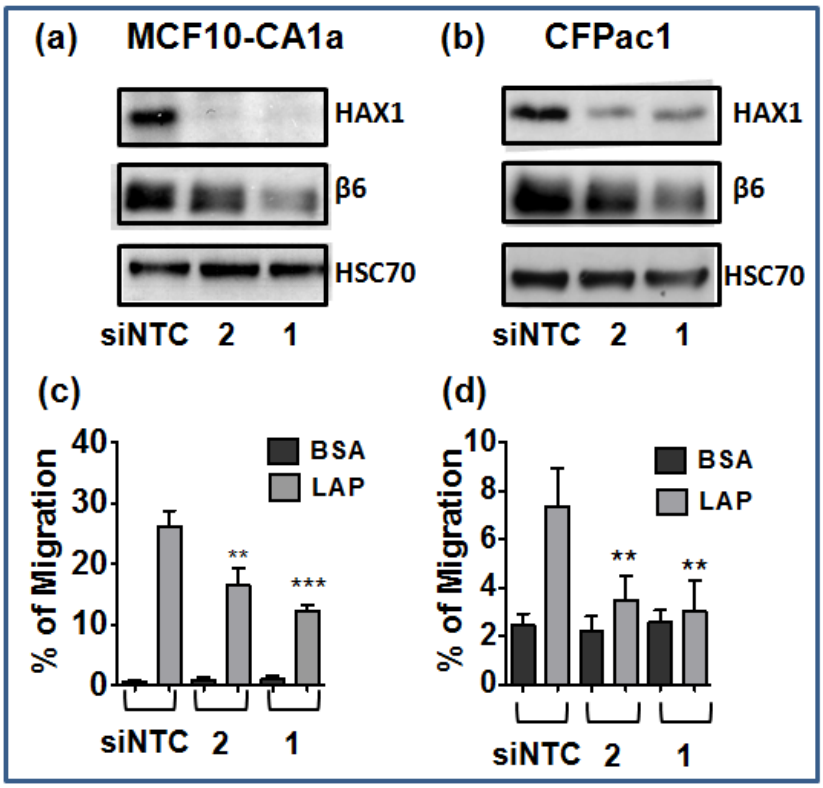
(a) MCF10-CA1a
HAX1
β6
HSC70
siNTC 2 1
(b) CFPac1
HAX1
β6
HSC70
siNTC 2 1
(c)
% of Migration
BSA
LAP
**
***
siNTC 2 1
(d)
% of Migration
BSA
LAP
**
**
siNTC 2 1

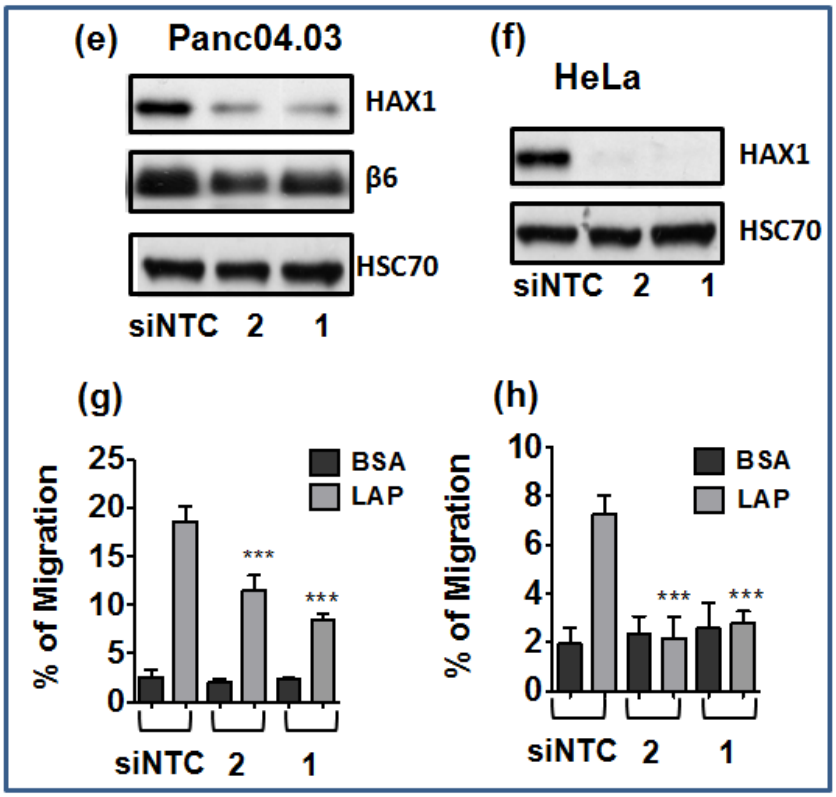
(e) Panc04.03
HAX1
β6
HSC70
siNTC 2 1
(f) HeLa
HAX1
HSC70
siNTC 2 1
(g)
% of Migration
BSA
LAP
***
***
siNTC 2 1
(h)
% of Migration
BSA
LAP
***
***
siNTC 2 1

Figure 4.2 HAX1 regulates cell migration toward LAP in breast, pancreatic, and cervical cancer cell lines.

MCF10.CA1a (breast), CFPAC1 (pancreas), Panc04.03 (pancreas) and HeLa (cervix) carcinoma cell lines were transfected with non-targeting control (siNTC) or two different HAX1 siRNAs (1: si1-6; 2: si192) and then tested in migration assays across Transwell membranes coated with 0.5% BSA or 0.5 μg/ml LAP. HAX1 expression was decreased by siRNA (a, b, e, f) and this inhibited the cell migration in all cancer cell tested by up to 60% (c, d, g, h). The % of migration was determined by the number of cells in the lower chamber relative to the total number of cells in the well. Data show the mean of quadruplicate samples from four separate experiments and error bar represents one standard deviation; **: p-value <0.01, ***: p-value <0.001.

4.2.3 HAX1 modulates αvβ6- and αvβ1–mediated cancer cell migration

Flowcytometry was performed to examine the cell-surface integrin expression profile in each of the cancer cell lines using subunit-specific antibodies. Bound antibodies were detected with Alexa-488 secondary antibodies then examined on a FACS Calibur cytometer (BD Bioscience) and analysed using Cellquest Pro software. Figure 4.3 (a-i) shows the different integrin expression patterns determined in HeLa cells as an expamle.

Figure 4.3 (j) summarises integrin expression patterns in the cell lines utilised in my studies. Thus all cell lines express the αv and β1 subunits. Using heterodimer-specific antibodies, Figure 4.3 (j) shows MCF10.CA1a expresses αvβ3 and αvβ6, CF Pac1 expresses αvβ6 and αvβ8, Panc04.03 expresses αvβ5 and αvβ6 whereas HeLa expresses αvβ5.

To determine which integrin mediates migration toward LAP, Transwell migration assays were performed with the cells treated with specific antibodies against individual integrins or their subunits. Figure 4.4 (a) shows that migration of MCF10.CA1a, CFPac1 and Panc 04.03 toward LAP was inhibited only by an antibody that blocked αvβ6. Blockage of αvβ3, αvβ5 or β1 integrin had no effect. Thus these cells lines exhibit αvβ6-dependent migration toward LAP. In contrast, blockade of αv integrins or β1 integrins inhibited migration of HeLa cells toward LAP. Since blockade of αvβ5 had no effect, and as HeLa cells lack αvβ3, αvβ6 and αvβ8, the data suggest HeLa cells express αvβ1 and that this mediates migration to

LAP. Taken together, these data show that HAX1 is required for αvβ6 and αvβ1-dependent migration.

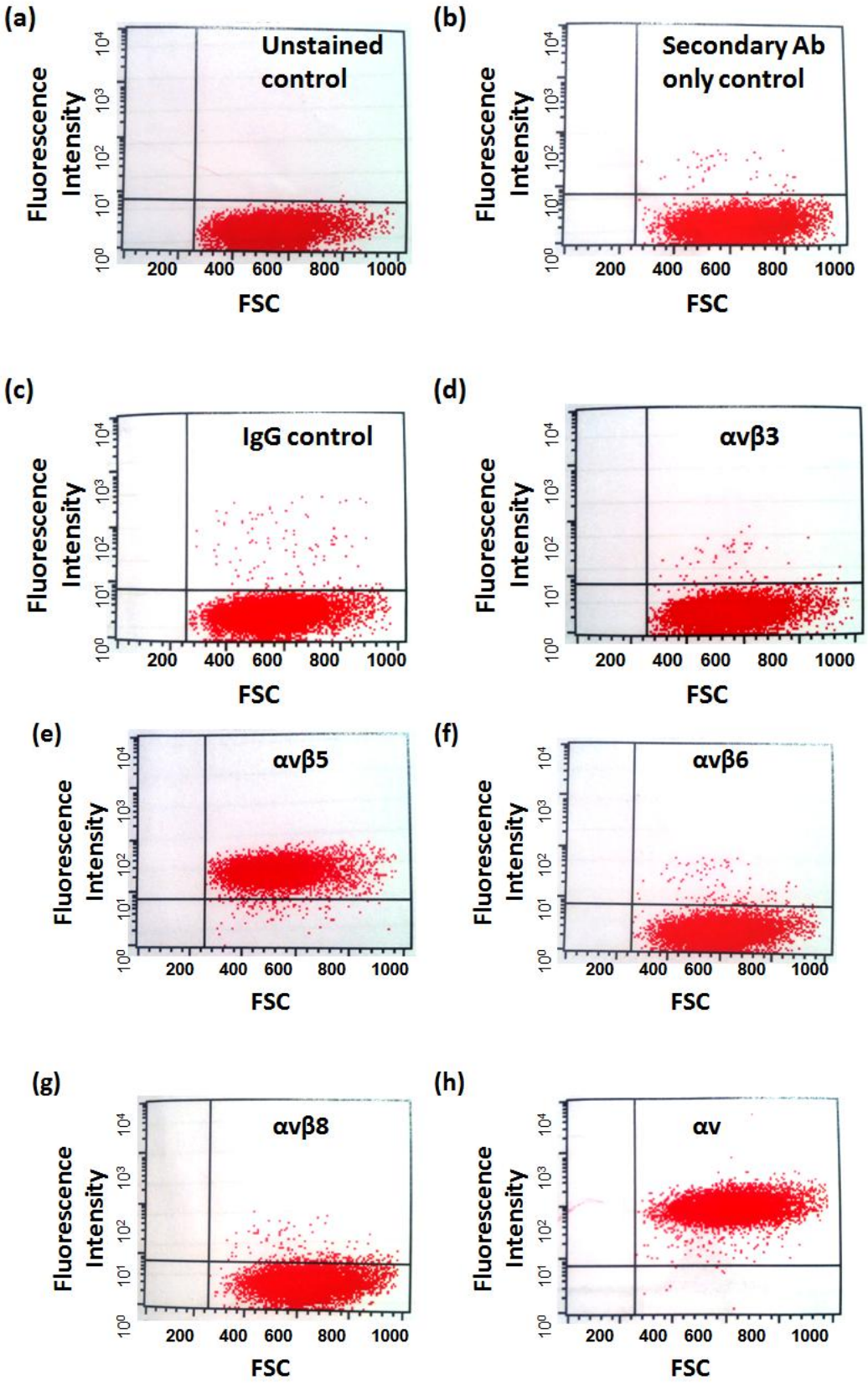
(a)
Unstained control
(b)
Secondary Ab only control
(c)
IgG control
(d)
αvβ3
(e)
αvβ5
(f)
αvβ6
(g)
αvβ8
(h)
αv
Fluorescence Intensity
FSC
200
400
600
800
1000

(i)

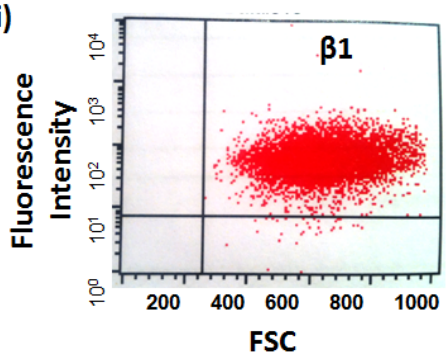

(j)

Cell line	Tissue	αvβ3	αvβ5	αvβ6	αvβ8	αv	β1
MCF10.CA1a	Breast cancer	+	-	+	-	+	+
CF Pac1	Pancreatic cancer	-	-	+	+	+	+
Panc 04.03	Pancreatic cancer	-	+	+	-	+	+
HeLa	Cervical cancer	-	+	-	-	+	+

Figure 4.3 Integrin screening by flowcytometry.

Confluent cell were harvested and incubated with specific antibodies which recognise individual integrins. Panels (a-i) show the intergrin analyse in HeLa cells. Antibodies to individual integrins were used to label cells (10µg/ml 10D5: against αvβ6 integrin, Chemicon, #MAB2077Z; 23C6: against αvβ3 integrin, Chemicon, #CBL544; P1F6: against αvβ5 integrin, Chemicon, #GEM1961; 4F1: against αvβ8 integrin, Chemicon; L230: against αv integrin, Chemicon; C4P10: against β1 integrin, Chemicon, #MAB1987;) or mouse IgG isotype control (10µg/ml, BD). Alexafluor 488 conjugated goat-anti-mouse antibody (Invitrogen, #A11001) was used as secondary antibody. Cells were analysed on a FACScalibur (Becton Dickinson) flow cytometer using Cellquest Pro software and data were generated from analysing 10,000 cells. Histograms plot forward scatter (FSC) versus mean fluorescent intensity. (j) summarises the different integrin expression profile of each cell line.

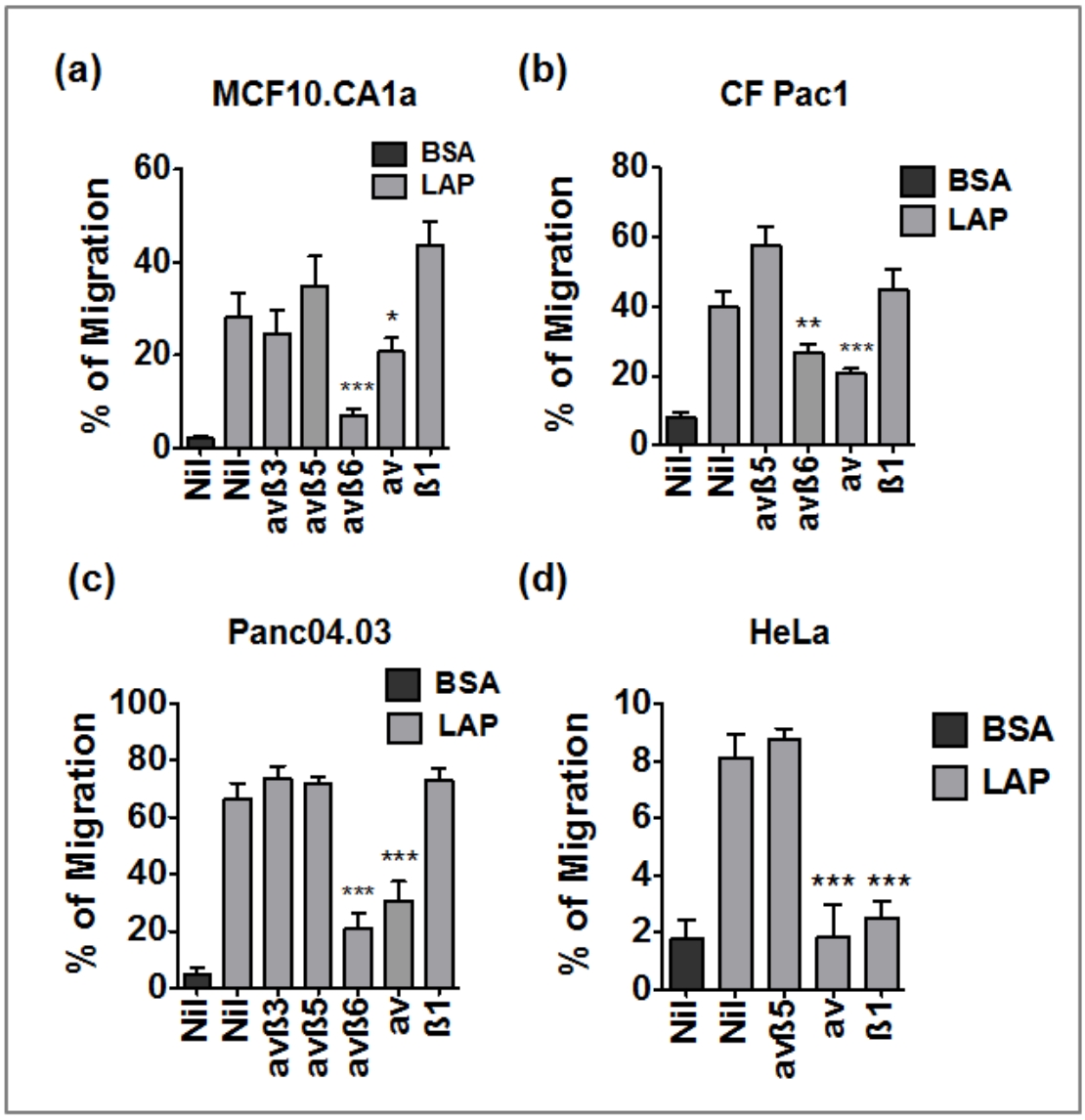

Figure 4.4 αvβ1-dependent and αvβ6-dependent migration toward LAP.

(a, b, c, d): integrin-dependent migration assay. Various antibodies specific to individual integrins were used to block integrins prior to migration assay. L230: antibody for αv, P4C10: antibody for β1, LM609: antibody for αvβ3, P1F6: antibody for αvβ5. 10D5: antibody for αvβ6. Final concentration is 10µg/ml. Data show mean+/- one standard deviation of quadruplicate samples from one experiment. *: p-value <0.05, **: p-value <0.01, ***: p-value <0.001.

4.2.4 HAX1 does not affect cell migration on collagen, fibronectin and laminin

In order to examine whether HAX1 regulates cell migration toward other ligands, migration assays were performed with HeLa and MCF10.CA1a cells toward three different matrix ligands: collagen, fibronectin and laminin. Inhibition of HAX1 expression with either of two siRNAs (si192 and si1-6) failed to affect cell migration on any of these three ligands in HeLa cells (Figure 4.5, a, c, e); in addition the growth rate overnight was not affected by the HAX1 knockdown (Figure 4.5, b, d, f). Similarly, HAX1 depletion did not affect migration on these ligands in MCF10.CA1a (Figure 4.6, a, c, e) and there was no change in cell growth (Figure 4.6, b, d, f).

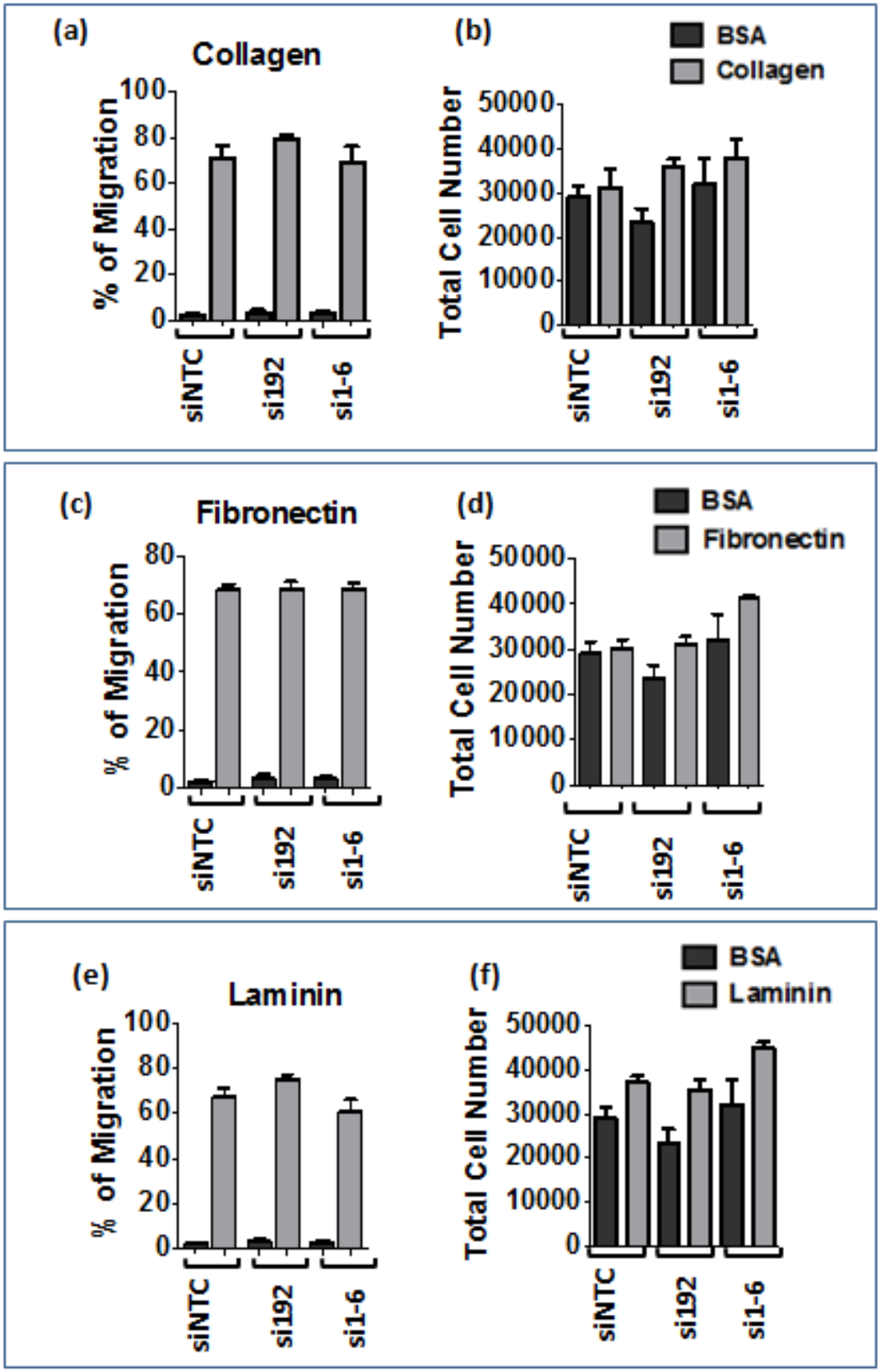
(a)
Collagen
% of Migration
100
80
60
40
20
0
siNTC
si192
si1-6
(b)
BSA
Collagen
Total Cell Number
50000
40000
30000
20000
10000
0
siNTC
si192
si1-6
(c)
Fibronectin
% of Migration
80
60
40
20
0
siNTC
si192
si1-6
(d)
BSA
Fibronectin
Total Cell Number
50000
40000
30000
20000
10000
0
siNTC
si192
si1-6
(e)
Laminin
% of Migration
100
80
60
40
20
0
siNTC
si192
si1-6
(f)
BSA
Laminin
Total Cell Number
50000
40000
30000
20000
10000
0
siNTC
si192
si1-6

Figure 4.5 HAX1 depletion does not change the cell migration toward the extracellular ligands collagen, fibronectin nor laminin in HeLa cells.

HeLa cells were treated with control siRNA (siNTC) or HAX1 siRNA (si1-6 or si192) and then were tested in migration assays across Transwell membranes whose undersides were coated with 0.5% BSA or 10 μg/ml fibronectin, type 1 collagen, laminin-1 (a, c, e). Cells were detached by trypsin and counted. (b, d, f) The total cell number was calculated as the sum from the cell number in upper chamber and lower chamber. Percentage migration was determined as the number of cells in the lower chamber relative to the total number of cells in the well. Data show mean+/- one standard deviation of quadruplicate samples from two experiments.

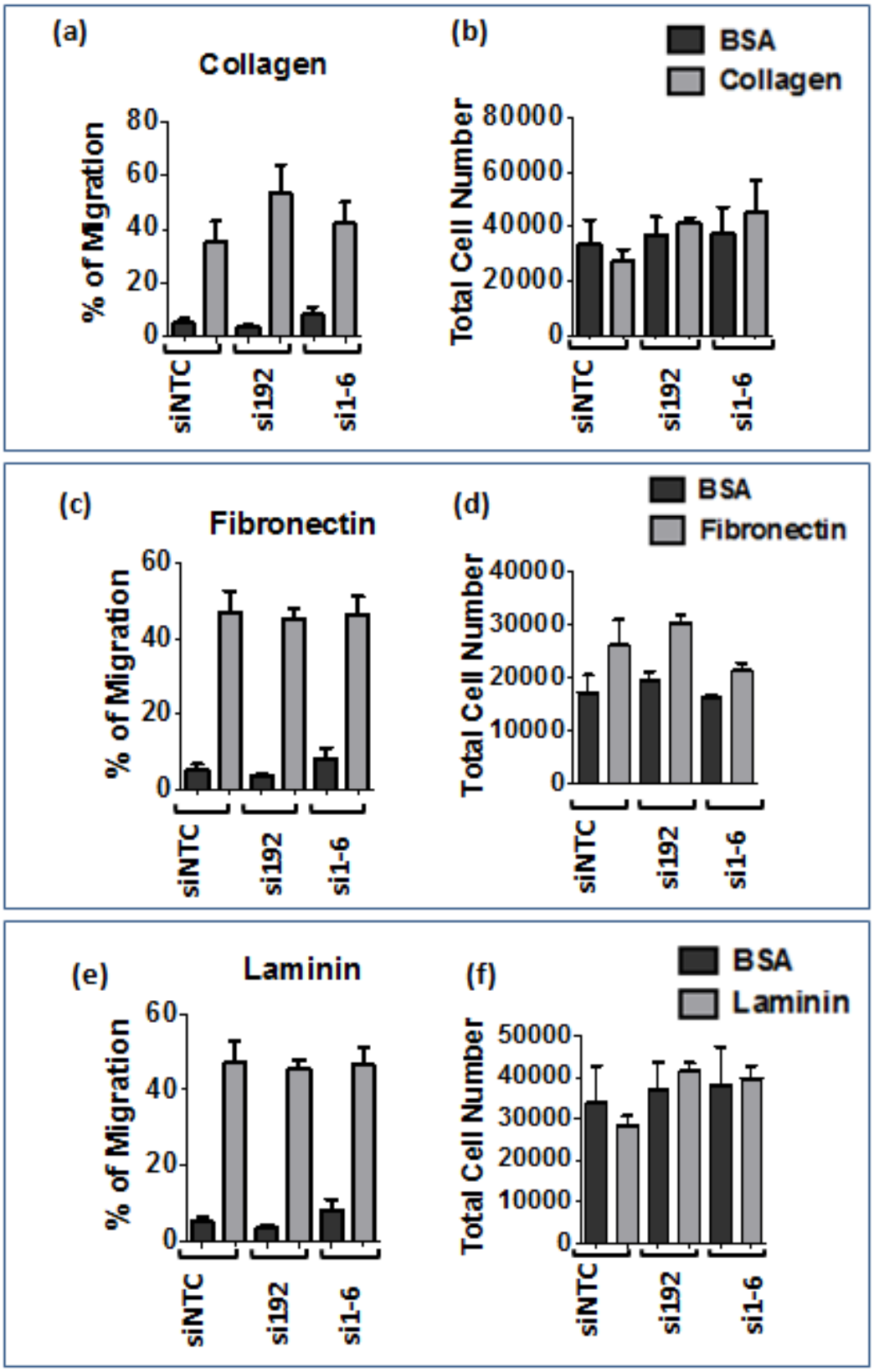
(a)
Collagen
% of Mgration
80
60
40
20
0
siNTC
si192
si1-6
(b)
BSA
Collagen
Total Cell Number
80000
60000
40000
20000
0
siNTC
si192
si1-6
(c)
Fibronectin
% of Migration
60
40
20
0
siNTC
si192
si1-6
(d)
BSA
Fibronectin
Total Cell Number
40000
30000
20000
10000
0
siNTC
si192
si1-6
(e)
Laminin
% of Migration
60
40
20
0
siNTC
si192
si1-6
(f)
BSA
Laminin
Total Cell Number
50000
40000
30000
20000
10000
0
siNTC
si192
si1-6

Figure 4.6 HAX1 depletion did not change the cell migration on the extracellular ligands collagen, fibronectin and laminin in MCF10 CA1a cells.

MCF10.CA1a cells were treated with control (siNTC) or HAX1 siRNA (si1-6 or si192) and then were tested in migration assays across Transwell membranes coated with 0.5% BSA or 10 μg/mL extracellular matrix substrate: fibronectin, type 1 collagen, laminin (a, c, e). Cells were detached by trypsin and counted. (b, d, f) The total cell number was calculated as the sum from the cell number in upper chamber and lower chamber. Percentage migration was determined as the number of cells in the lower chamber relative to the total number of cells in the well. Data show mean+/- one standard deviation of quadruplicate samples from two experiments.

4.2.5 HAX1 is not required for migration of HaCat human keratinocyte cells towards LAP

Previous sections have demonstrated that HAX1 regulates migration of various cancer cells toward LAP. To determine whether HAX1 also affects normal cells migration, I examined the immortal, but non-transformed, human keratinocyte cell line HaCat for migration toward LAP. Western blotting showed that the HAX1 knockdown was efficient with two different siRNAs to HAX1 (Figure 4.7, a, d). The Transwell migration assays however showed that the HAX1 depletion did not affect cell migration of HaCat cells when assayed at either 8 hours or 16 hours migration time point (Figure 4.7, b, e); cell growth was not affected by the HAX1 knockdown (Figure 4.7, c, f). Collectively, the data may suggest that HAX1 is an important regulator of migration toward LAP for various cancer cell types but not for the noncancerous human keratinocytes as represented by HaCat cells. Additional experiments with keratinocytes are required to confirm these observations and I would have performed such analyses had I had more time available.

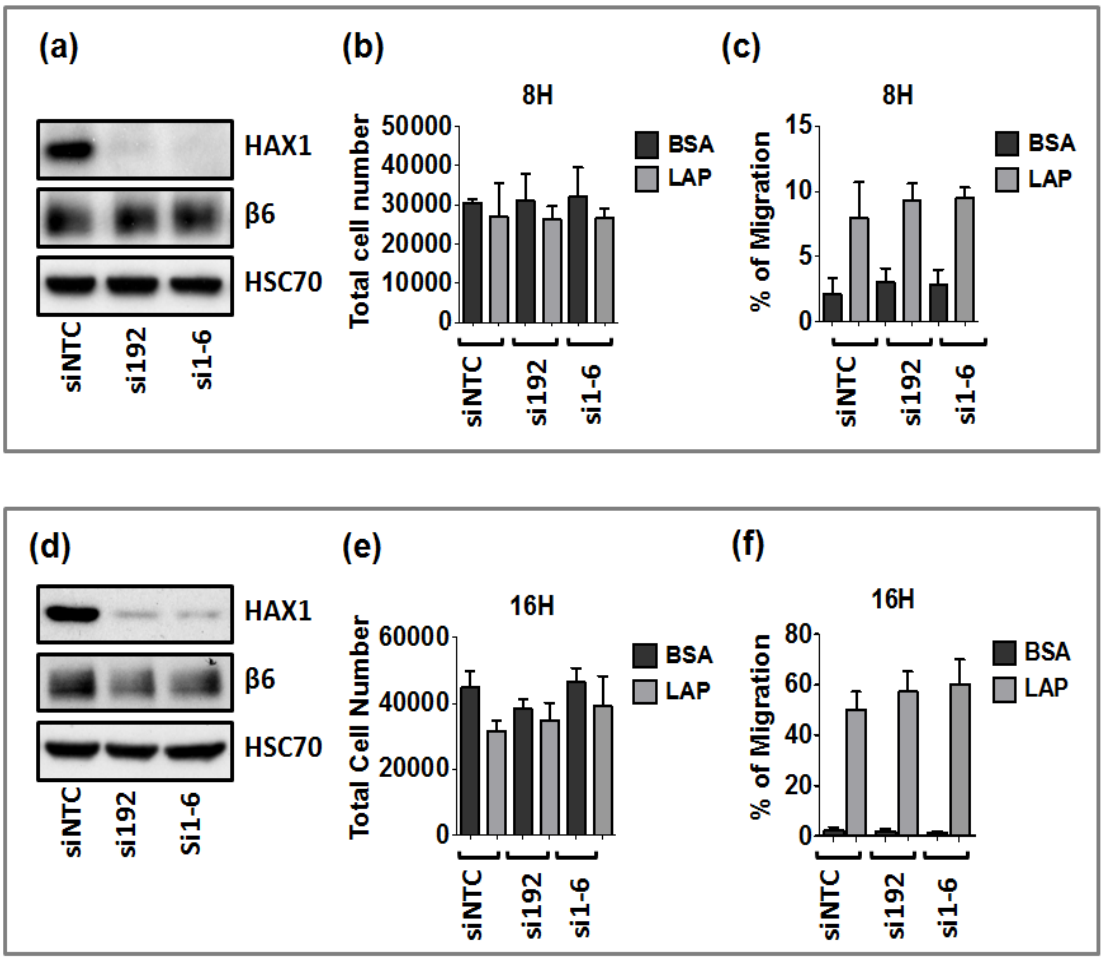

Figure 4.7 HAX1 knockdown did not affect migration toward LAP in HaCat cells.

HaCat cells were treated with control siRNA (siNTC) or HAX1 siRNA (si1-6 or si192) to knockdown HAX1 (a, d). The cells were then tested in migration assays across Transwell membranes coated with 0.5% BSA or 0.5 μg/ml LAP for 8 hours (b) or 16 hours (e). Cells were then trypsinised and the cell numbers were calculated by a CASY cell counter. Percentage of migration was determined by the number of cells in the lower chamber relative to the total number of cells in the well. Cell proliferation was also measured and shown to be unchanged (c, f). Total cell number was calculated from the numbers of cells in the upper chamber and lower chamber (c, f). The error bar represents standard deviation, done in quadruplicate from three experiments.

4.3 Discussion

Reportedly, HAX1 has been shown to regulate oral squamous carcinoma cell migration via integrin αvβ6 [1]. In the present study, I am the first to demonstrate that HAX1 is a central factor that regulates migration of various cancer cells (breast, pancreas and cervix cancer cells). Interestingly, HAX1 depletion did not affect the migration of the non-transformed keratinocyte HaCat cell line. If this were found to be repeated with primary keratinocytes, this may offer an opportunity to target cancer cells but not normal cells via approaches aimed at limiting HAX1 activity.

When I examined whether HAX1 mediated cell migration on other extracellular ligands apart from LAP, including collagen, laminin and fibronectin, the data showed that although all three ECM ligands enhanced migration of HeLa and MCF10.CA1a cells, HAX1 depletion did not affect cell migration on any of these ligands. Cancer cell migration depends on the interaction of integrin-ECM ligands, and these data suggest that HAX1 regulates cell migration mainly on LAP but not collagen, fibronectin or laminin. The reasons for these observations are not known.

LAP, latency associated peptide, is the pro-peptide of the cytokine TGF-β and its presence blocks the activation of the cytokine. TGF-β can switch from tumour suppressor in normal/ pre-malignant cells, through its ability to suppress epithelial cell growth, to tumour promoter in malignant cells, that often become refractory to its anti-proliferative effects [228]. TGF-β is secreted in a latent complex consisting of three proteins: TGF-β, LAP, and LTBP (latent TGF-β binding peptide, which anchors the complex to the ECM) [162]. LAP contains an integrin-binding site

(RGD), and the RGD-binding integrins αvβ1, αvβ3, αvβ5, αvβ6, αvβ8, αIIbβ3, α8β1 and α5β1, are all reported to bind LAP; however only integrins αvβ6 and αvβ8 are strong activators for TGF-β [162]. When integrins bind to the RGD sequence in LAP, the activation of TGF-β is triggered by a conformational change of the complex [216]. This then exposes active TGF-β and allows it bind to its receptor, probably on adjacent cells, thus initiating downstream pathways [181]. Activation by αvβ6 requires the cytoplasmic domain of integrin and a functional actin cytoskeleton, suggesting that force generated by the actin cytoskeleton and transmitted via the integrin to LAP is required for activation [162]. In contrast, αvβ8 binds to LAP and brings latent-TGF-β into close proximity of MT1-MMP which cleaves the LAP and reveals the TGF-β molecule for its receptor on an adjacent cell [162].

Adaptor proteins play an important role in regulating cell functions by interacting with regulatory molecules including integrins. As HAX1 is a binding partner for β6 [1], and my study is the first to show that HAX1 regulates multiple cancer cell lines' ability to migrate via integrin αvβ1 and αvβ6 toward LAP, these data indicate the potential role of HAX1 in activating TGF-β. Figure 4.3 shows the different integrin expression pattern to different cell lines. By blocking integrins with specific antibodies prior to migration assay, it was shown that MCF10.CA1a, CF Pac1 and Panc 04.03 depend on αvβ6 to migrate on LAP whereas HeLa cells used αvβ1 to migrate on LAP (Figure 4.4). TGF-β-integrin interaction is important for cancer progression, not only for the independent activity of the TGF-β but also as it has been shown to promote cell migration and MMP expression in carcinoma [69,181].

My results have extended our knowledge of the potential regulation of TGF-β activation. It would be very interesting to determine whether αvβ1 also can activate TGF-β and also to investigate the detailed mechanisms of how HAX1 might influence the activation of TGF-β, and therefore regulate TGFβ-dependent processes.

CHAPTER 5. DEVELOPMENT AND CHARACTERISATION OF STABLE HAX1-KNOCKDOWN

5.1 Introduction

Since HAX1 was shown to regulate migration of various cancer cell *in vitro* in the previous sections, it was necessary to generate stable HAX1 knockdown cell lines in order to test the role of HAX1 *in vivo*. In this section, I will describe the generation of stable HAX1 knockdown cell lines using four different lentiviral plasmids to HAX1 and then describe a variety of biological functions, including cell growth, apoptosis, cell migration and invasion, and how they were affected by this HAX1 depletion.

5.2 Results

5.2.1 Establishment of HAX1-stable knockdown cell lines

5.2.1.1 Bioinformatic analysis of the pGIPZ vectors targeting HAX1

To generate stable HAX1-knockdown cells, lentiviral encoding vectors were used. Four pGIPZ plasmids (p86, p87, p89, p90) were obtained from Open Biosytems, each encoding a different shRNA to HAX1. pGIPZ vectors encode both turbo-GFP and puromycin drug resistance marker allowing drug-selection of infected cells and identification of infected cells by flow cytometry or fluorescence microscopy (the detailed vector map of pGIPZ lentiviral vectors is shown in Appendix I, a and b). Empty (EMP) vector and non-targeting control (NTC) vector are also included in the

experiments as negative control. The EMP vector is the pGIPZ lentiviral vector without a shRNA insert and shRNA encoded from NTC contains no homology to known mammalian genes (information from Open Biosystem). The plasmid vectors were amplified and then purified on QIAGEN columns. The fidelity of each vector was confirmed by DNA sequencing (Figure 5.1). All the plasmids were also verified as being able to recognise the HAX1 gene by BLAST analysis. CLC Sequence 6 software (CLC Bio) was used to analyse the shRNA sequences and Figure 5.1 shows the sequences of the hairpins of shRNAs which are comprised of a 19 nucleotide (nt) loop and two 22 nucleotide sequences that form the double stranded shRNA.

Each vector was predicted to target different HAX1 variants as they targeted different regions of HAX1 as shown in Figure 5.1. By analysing the sequences via Ensembl, the results showed that shRNA produced by p86 vector binds to the 5' end of exon 3, and thus recognises HAX1.1 to HAX1.6. p87 shRNA targets the end of exon 2, recognising HAX1 variants 1 to 5. p89 vector, which generates shRNA to exon 5, recognises all isoforms except isoform 3. Targeting to exon 3, p90 shRNA binds to isoforms 1,2,4,5,6,7 and 8. All the sequences are shown in the Figure 5.2.

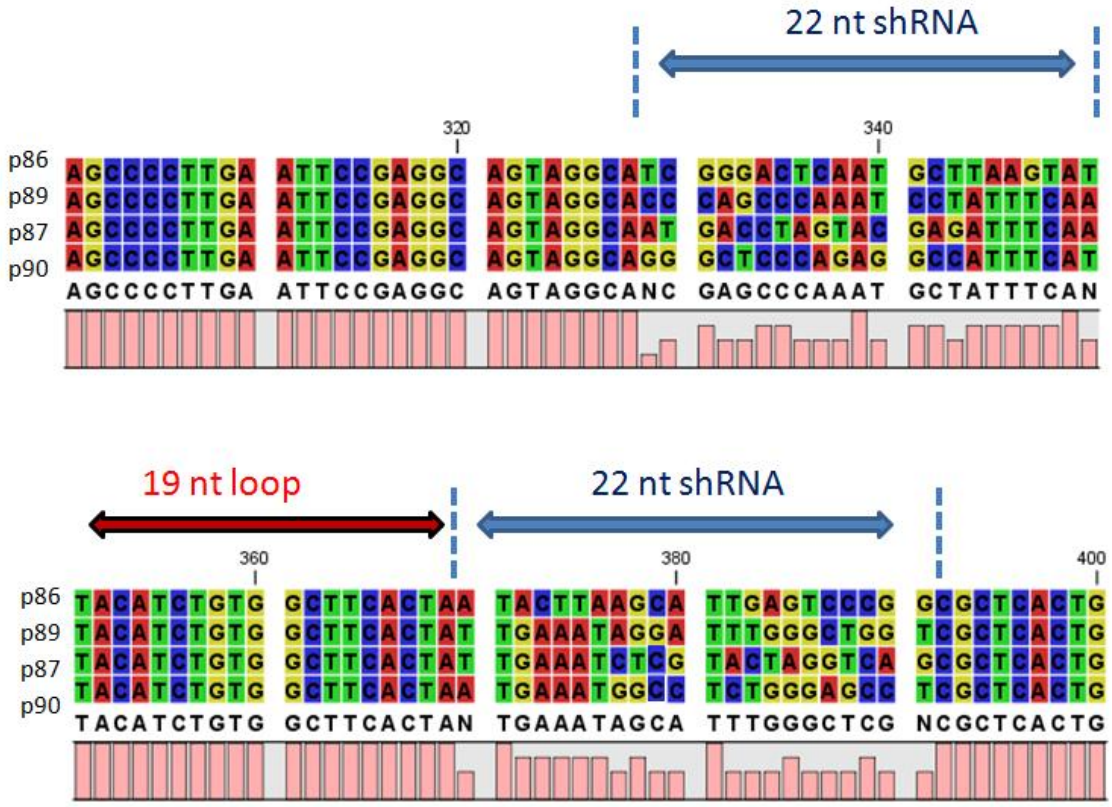

Figure 5.1 pGIPZ vector shRNA sequence analysis with CLC sequence 6 software.

Sequencing of the vectors confirmed that the vectors encoded 22 nucleotides (nt) of shRNA and a 19 nt loop. Pink bars display the level of conservation at each point in the alignment.

(a)

	Vectors	Sequences	Target	Targeted HAX1 isoforms							
				1	2	3	4	5	6	7	8
↓	86 shRNA	TCGGGACTCAATGCTTAAGTAT	Exon 3	v	v	v	v	v	v		
↓	87 shRNA	ATGACCTAGTACGAGATTTCAA	Exon 2	v	v	v	v	v			
↓	89 shRNA	CCCAGCCCAAATCCTATTTCAA	Exon 5	v	v		v	v	v	v	v
↓	90 shRNA	GGGCTCCCAGAGGCCATTTCAT	Exon 3	v	v		v	v	v	v	v

(b)

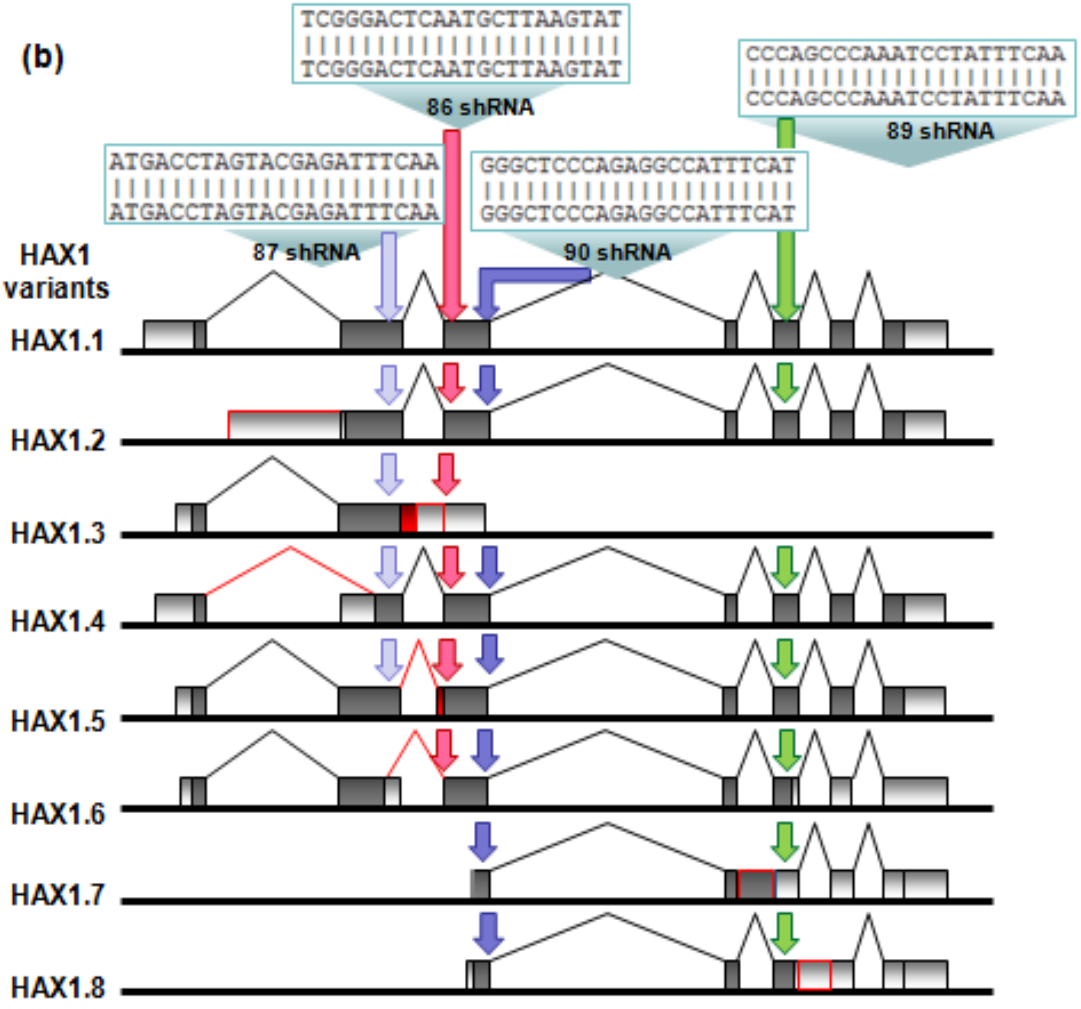

Figure 5.2 pGIPZ vectors target to different regions of HAX1 and thus target different HAX1 isoforms.

pGIPZ plasmids encode a different shRNA to different HAX1 exons. All of the vectors were checked by sequencing. Figure (a) shows the HAX1 targeting sequences of each shRNA and figure (b) shows the binding regions as coloured arrows of these shRNAs on the HAX1 genomic structure. Dark grey boxes are exons and light boxes indicate introns.

5.2.2 Stable HAX1 knockdown generated by pGIPZ-lentiviral shRNA in VB6 and H400 cells

HEK293T cells were used for the virus packaging. HEK293T cells were transfected with the lentiviral plasmids using the Fugene 6 method with the two packaging plasmids and the pGIPZ plasmid vectors (see Methods section for the experimental details). 48 hours after transfection the medium which contained released virus, was collected and HEK293T cells were analysed by flow cytometry to detect GFP for the efficiency of transfection.

Lentiviral conditioned media containing lentiviruses encoding HAX1 shRNA were then applied to VB6 and H400 oral squamous carcinoma cells. The sub-clones were named according to the shRNA (VB6-86, VB6-87, VB6-89, VB6-90, VB6-EMP and VB-NTC; H400-86, H400-87, H400-89, H400-90, H400-EMP and H400-NTC). 24 hours after HAX1 shRNA-viral infection, cells were selected with 1.25 μg/ml puromycin as the pGIPZ vectors contain this drug-resistance sequence. Cells reached confluence about 3-4 days after viral infection, and cell lysates were harvested for Western blot analysis. Results show that H400 clones have a great reduction of HAX1 protein level in infected cells (Figure 5.3, a). In contrast, Western blotting demonstrated that there was no difference in HAX1 expression after viral infection of VB6 cells (Figure 5.3, b).

To investigate this, I analysed the efficiency of viral infection in the target cells H400 and VB6, using flow cytomery to observe GFP expression (pGIPZ encodes a turbo-GFP gene). Data showed most H400 cells expressed high levels of GFP

(>90%) whereas only ~40% of VB6 showed GFP-expression. Since VB6 already is puromycin-resistant whereas H400 is puromycin-sensitive, this might explain the observed results [70]. In order to select the GFP-positive VB6 cells, I used two approaches: one was to increase puromycin concentration to ten-fold (10 µg/ml) in order to eliminate vector-free puromycin-resistant VB6 cells, and the other was to select GFP-positive cell using FACS.

In the puromycin-selection approach, cells were treated with a higher puromycin concentration (10µg/ml) for three weeks before Western blot analysis. Cell death was observed in the first week of treatment, indicating cells were sensitive to increased puromycin concentration and the theory was that only cells which express the vector-encoded gene would be able to survive from the drug-selection. However, Western blotting showed that there was no significant change in HAX1 expression in the 10µg/ml puromycin treated cells (Figure 5.4, lane5). Thus this method was abandoned.

FACS was employed to select GFP-positive VB6 sub-populations from lentiviral-infected cells. Non-infected cells were used as negative control and the top 10% GFP-expressing cells were selected from the whole population (Figure 5.5). All virally infected-VB6 cell lines, including non-targeting control (NTC), and empty vector (EMP), underwent the same selection method. These cells were expanded *in vitro* and then analysed by Western blot. Cell lysates were generated from confluent cultures of all lines and Blotted with HAX1 antibody. Figure 5.6 (a and c) shows that the level of HAX1 protein was decreased significantly by all four lentiviral vectors when compared with EMP (empty) and NTC (non-targeting control)

controls. The knockdown was analysed regularly while cells were in culture and seen to be stable even after continuous growth. Results demonstrated that HAX1 protein expression was reduced by 50-90% in both the VB6 and H400 cell lines infected with pGIPZ vectors. In H400 cells, p87 shRNA and p89 shRNA reduced HAX1 expression greatly, knocking down nearly 90% of endogenous HAX1 protein (Figure 5.6, b) whereas p86 shRNA and p90 shRNA resulted in the best knockdown in VB6 cells (Figure 5.6, d). The densitometry showed the expression of HAX1 normalised with HSC70 from >6 independent experiments each with H400 and VB6 cells.

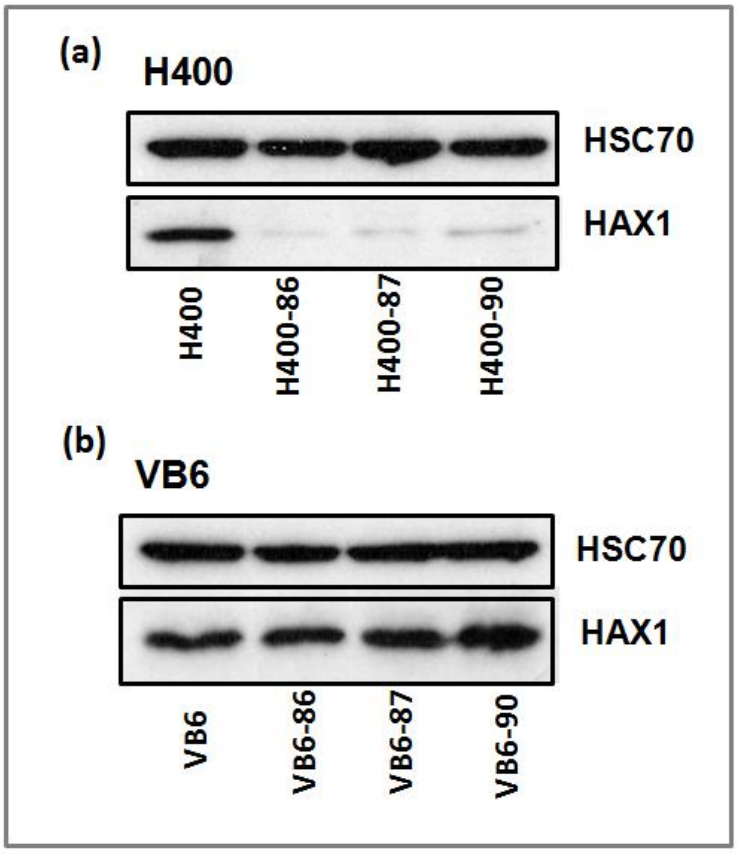

Figure 5.3 HAX1 protein expression in lentiviral–infected VB6 and H400 cells.

Cells were harvested 3-4 days after viral infection, and lysates were harvested for Western blot analysis. (a) H400 is a puromycin-sensitive cell line, and showed a great reduction of HAX1 protein level in infected cells. (b) There was no change in HAX1 protein expression levels in the lentiviral infected VB6 lines. HSC70 served as the control for equal loading.

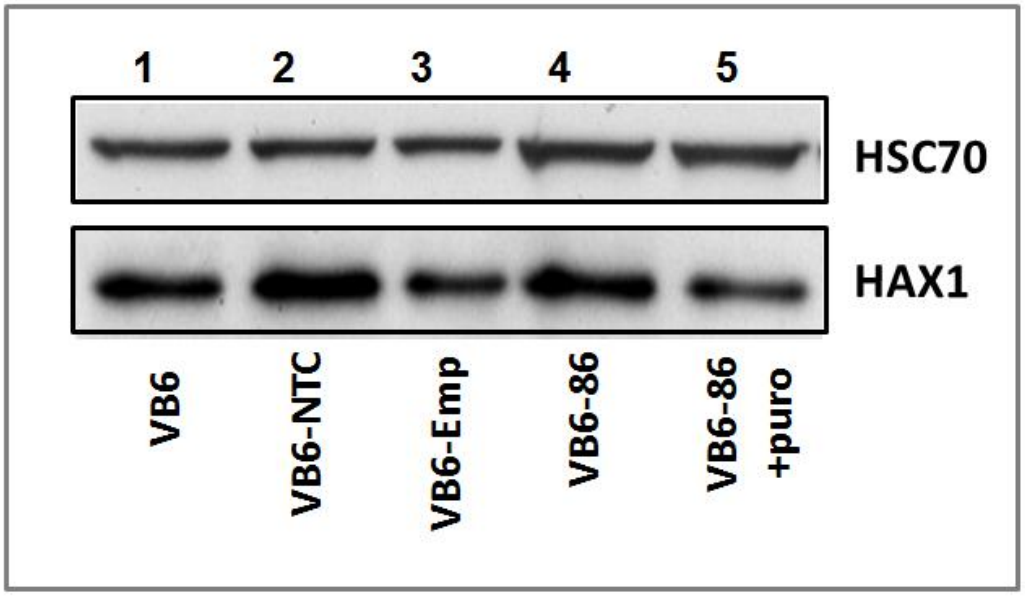

Figure 5.4 HAX1 protein expression in lentiviral-infected cells after elevated puromycin concentration treatment.

To select a HAX1-knockdown cell population, cells were treated with 10µg/ml puromycin. Resistant cells were harvested after 3 weeks in puromycin treatment. Western blot showed HAX1 expression remained relatively unchanged (lane5: VB6-86+puro).

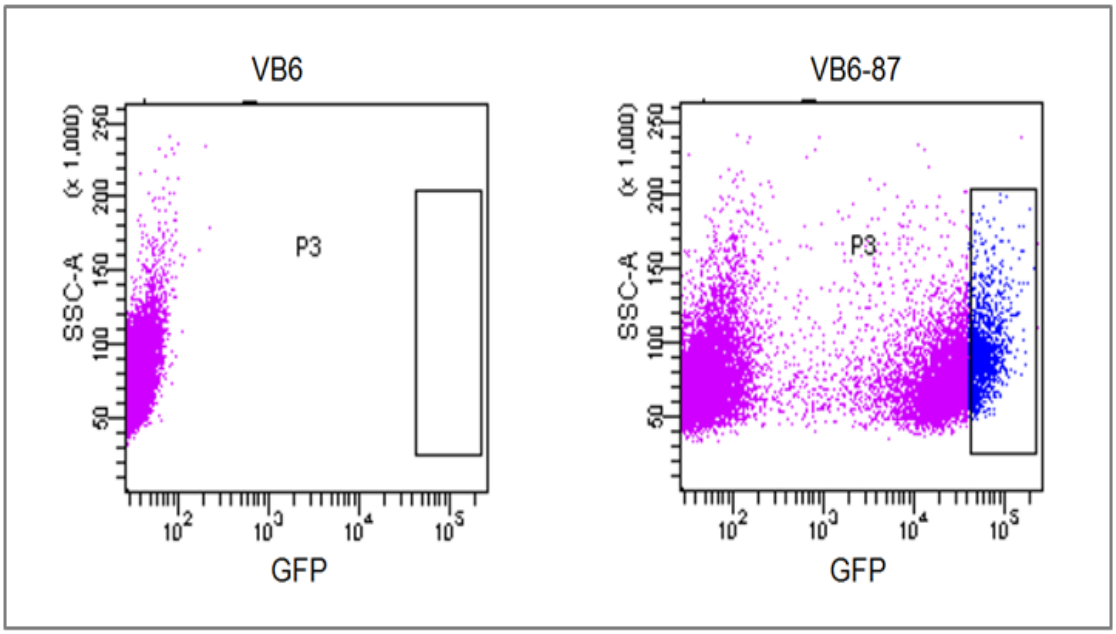

Figure 5.5 Selection of high shRNA expressing VB6 cells using FACS.

Lentiviral-infected VB6 cells (here showing an example from VB6-87) were monitored for the GFP expression and the top 10% turbo-GFP expressing cells (shown as blue events in the box) were collected.

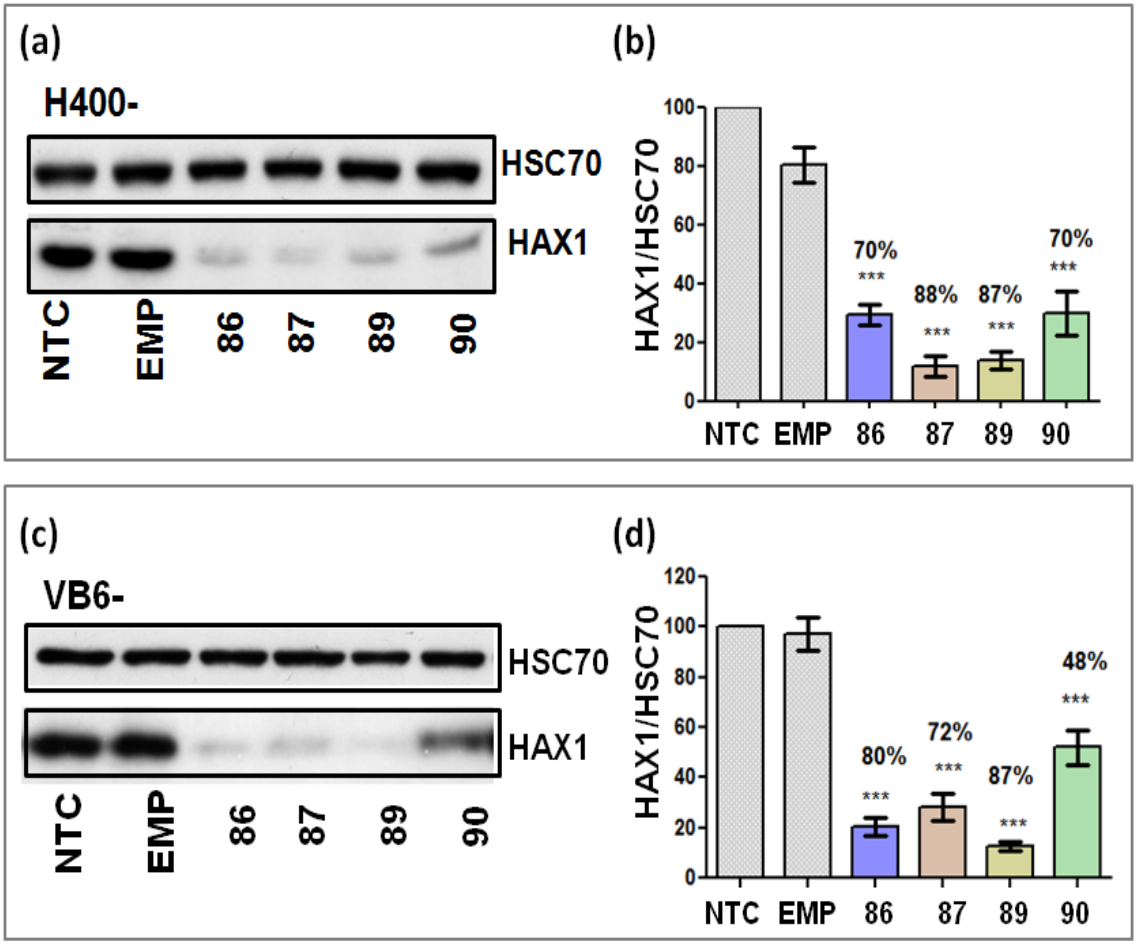

Figure 5.6 pGIPZ-lentiviral vectors knockdown HAX1 protein expression in H400 and VB6 cell lines.

H400 sub-populations were selected in puromycin, but, as VB6 already are puromycin-resistant, FACS was used to select those cells expressing the highest amount of GFP. Western blotting (a, c) shows that the four shRNA vectors all reduced HAX1 expression significantly. Samples from at least 7 separate cultures were analysed by Western blotting independently, and the degree of HAX1 reduction analysed by densitometry, compared with the non-targeting control (NTC). Data were expressed as (mean +/- 1 S.D.) and was shown in (b, d). Data show that shRNA vectors p86, p87 and p89 were the most effective in both cell lines. *** indicates P value < 0.001.

5.2.3 Individual HAX1 isoforms are reduced in pGIPZ cell lines at the mRNA level

To examine the effects of shRNA of the mRNA level, RT-PCR was performed. To monitor HAX1 isoform expression, cells were seeded into 6 well plates and total RNA was extracted with the Stratagene Absolutely RNA kit. Total RNA was quantified on the Nanodrop spectrophotometer. 1µg of RNA was reverse-transcribed and 50 ng of cDNA was amplified with specific primer pairs and these were used for the optimised, but different, PCR reactions (see Methods section). Figure 5.7 shows all HAX1 variants were reduced significantly by each of the four shRNAs (sequences were described in Figure 5.1). Using densitometry of triplicate experiments, Figure 5.8 shows the relative reduction in mRNA of each isoform. p86 and p87 shRNA achieved the best HAX1 knockdown in general, achieving up to 80% reduction, whereas p90 shRNA was the least effective. All PCR results were performed at least three times and data were expressed relative to GAPDH.

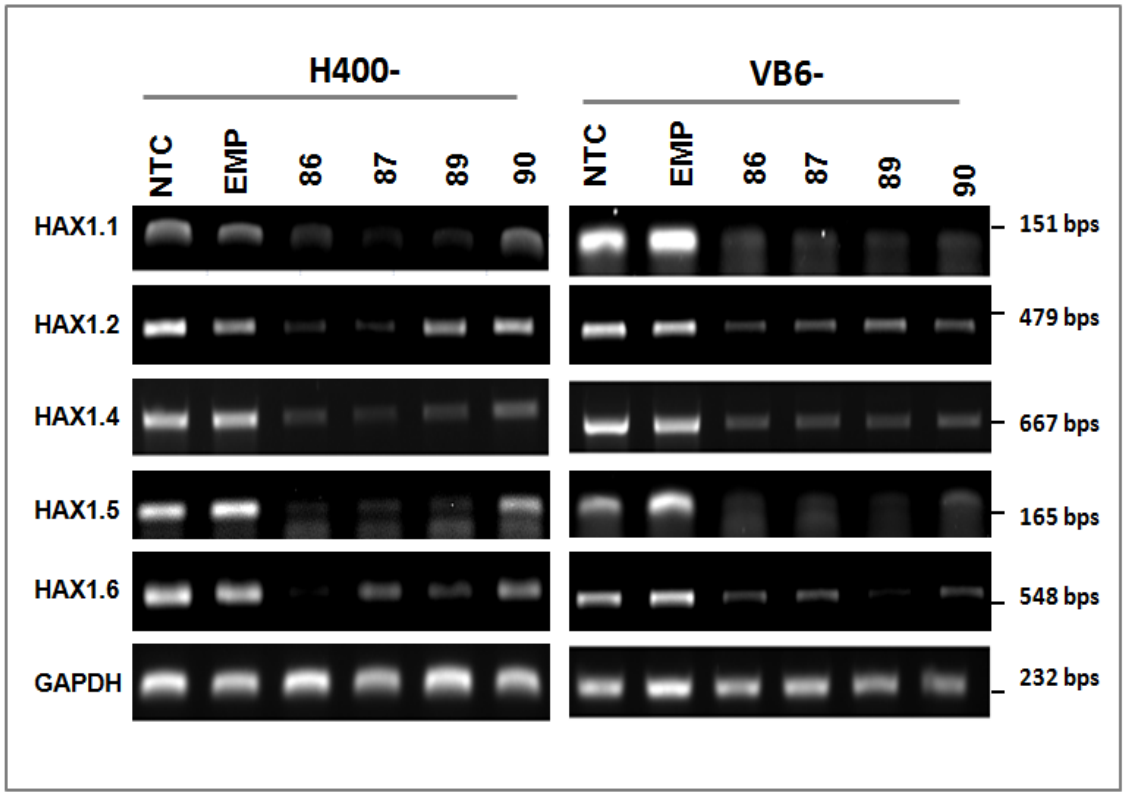

Figure 5.7 Lentiviral HAX1 shRNAs decrease expression of multiple HAX1 isoforms.

Semi-quantitative PCR was employed to analyse the mRNA level of HAX1 isoforms. Data showed all HAX1 variants were reduced by the four shRNAs. Data shown are from one of three experiments showing similar results. GAPDH was used as control.

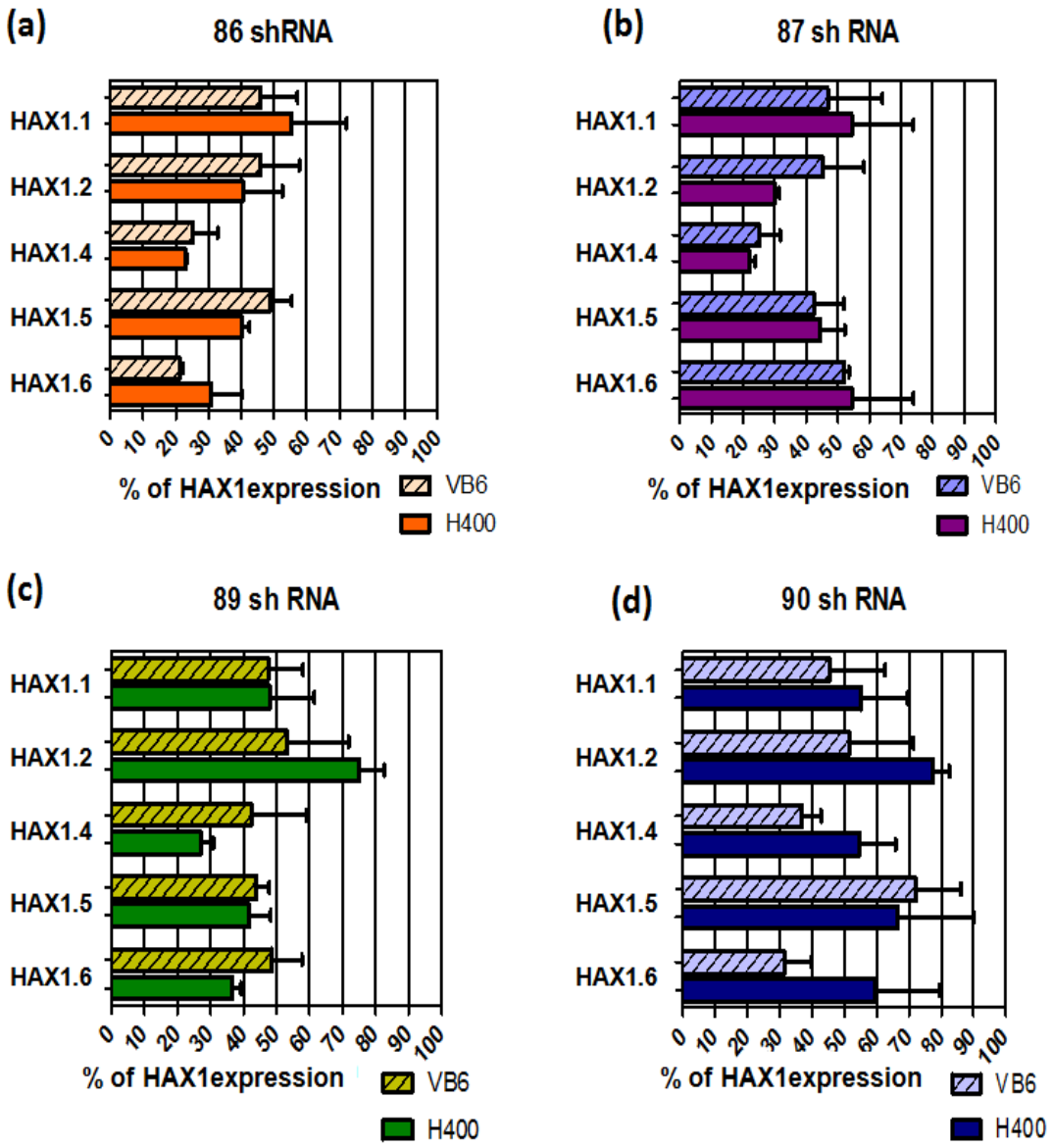

Figure 5.8 Relative reduction of mRNA for each HAX1 isoform by pGIPZ vectors.

Figures a-d show the expression of each HAX1 isoform normalised to GAPDH by densitometry and the % of HAX1 expression generated relative to non-targeting control cell lines (VB6-NTC and H400-NTC respectively). 86 and 87 shRNA performed the best HAX1 knockdown in general, achieving up to 80% reduction, whereas p90 shRNA was the least effective. All PCR analyses were performed at least three times.

5.2.4 Unchanged αvβ6 expression in HAX1 knockdown cell lines

Since HAX1 regulates integrin αvβ6 endocytosis, and this is essential for cancer cell migration [1], it is important to evaluate whether that HAX1 knockdown also affected the expression of αvβ6. Include in my earlier "transient" knockdown experiments I had shown that HAX1 depletion frequently was associated with a reduction in β6 levels. Cells were harvested from confluent density and protein concentrations were equalised. Western blot shows shRNAs reduced HAX1 expression greatly but the total β6 protein remained unchanged in all HAX1 knockdown cell lines (Figure 5.9, a and c). To determine surface αvβ6 levels, the cells were stained with antibody against β6 (10D5) and flow cytometry was used to monitor αvβ6 expression. The results demonstrated there was no obvious change in expression of β6 surface levels in any of the HAX1-reduced cells. Data are shown for p87 (Figure 5.9 b and d but similar data were seen for p86, p89 and p90 infected cells (data not shown).

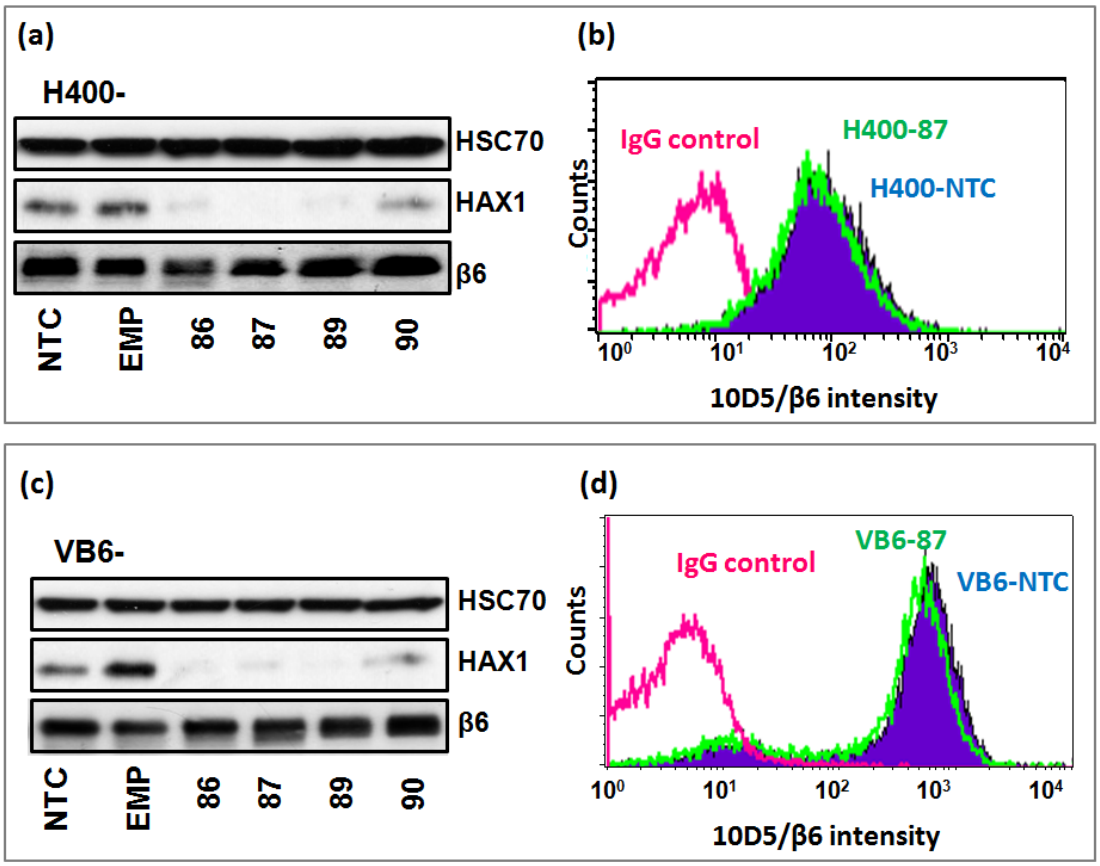

Figure 5.9. Integrin subunit β6 expression is unaffected by reduction of HAX1 expression.

Western blot showed the total β6 protein remained unchanged in HAX1 knockdown cell lines (a, b). To determine surface αvβ6 levels, cells were stained with 10D5 antibody against β6 and analysed by flow cytometry. Data showed there was no change in β6 surface protein in any of the HAX1-reduced cells. Data are shown for p87 (b and d) but similar results were seen for p86, p89, p90 and pEMP. Mouse IgG staining was set as negative control.

5.2.5 Functional assays for stable HAX1-knockdown cell lines

5.2.5.1 Stable HAX1 knockdown did not affect cell proliferation

To examine the effect of HAX1 on cell proliferation, clonogenic assays were performed with control and HAX1 stable knockdown cell lines. Cells were plated at 100 cells per well into a 6-well plates and incubated for 10 days and the colonies were stained with crystal violet (Figure 5.10, a). The colony numbers were then counted as shown in Figure 5.10 (b and c). Figure 5.10, (b and c) showed there was no difference in the colony number between control and HAX1 knockdown cells for either H400 or VB6 sub-lines.

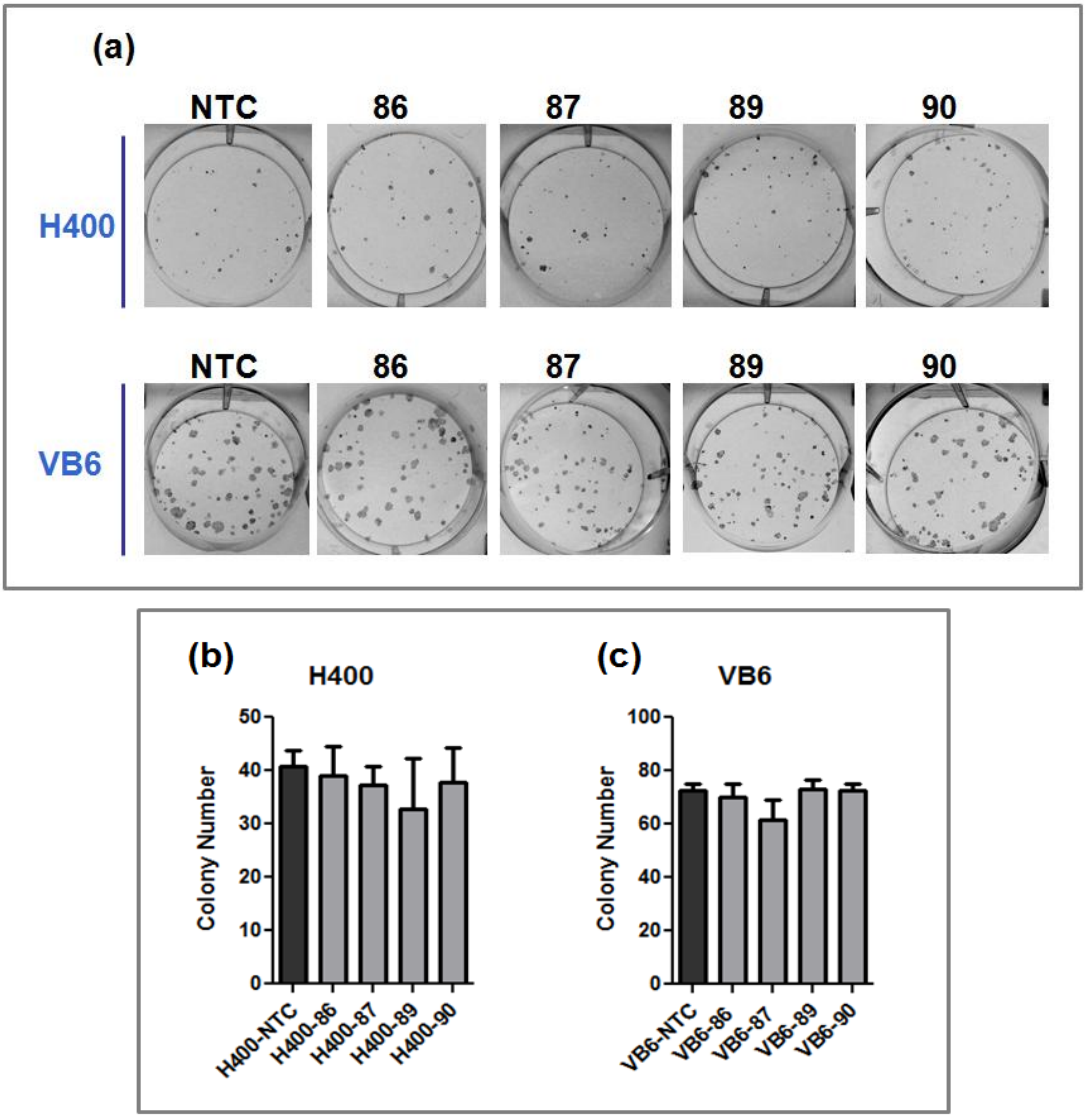

Figure 5.10 Clonogenic assay to assess the effect of stable HAX1 knockdown.

100 cells were seeded into a 6-well plate and incubated for 10 days, 0.1% crystal violet was then used to stain for colonies (a). (b, c) The number of colonies was counted with Image J software and the quantitative analysis shows surviving colonies of each cell line. Data demonstrate HAX1-knockdown cell lines did not alter clonogenicity of either H400 or VB6 cells. Columns represent mean of colonies in triplicate from one of 3 experiments showing similar results and data show mean +/- 1 S.D..

5.2.5.2Stable HAX1-knockdown did not alter cell migration on LAP

To determine the effect of HAX1 in cell migration, Transwell migration assays were performed with the two best stable HAX1-knockdown cells, VB6-86 and VB6-87. Cells were seeded on the Transwell membrane coated with BSA or LAP (for which migration of VB6 cells is mediated through αvβ6). After 16 hours incubation, cells were then trypsinised and cell numbers were counted. Western blot analysis showed the levels of HAX1 expression were reduced stably with Lentiviral shRNA. Figure 5.11 (a) shows stable HAX1 knockdown did not affect migration towards LAP compared with the control cell line (VB6-NTC). A proliferation assay run in parallel showed there was no change in cell number during the same period of incubation (Figure 5.11 c). These results which were in contrast to my findings in "transient" knockdown studies, are considered in the Discussion which follows this section of my results.

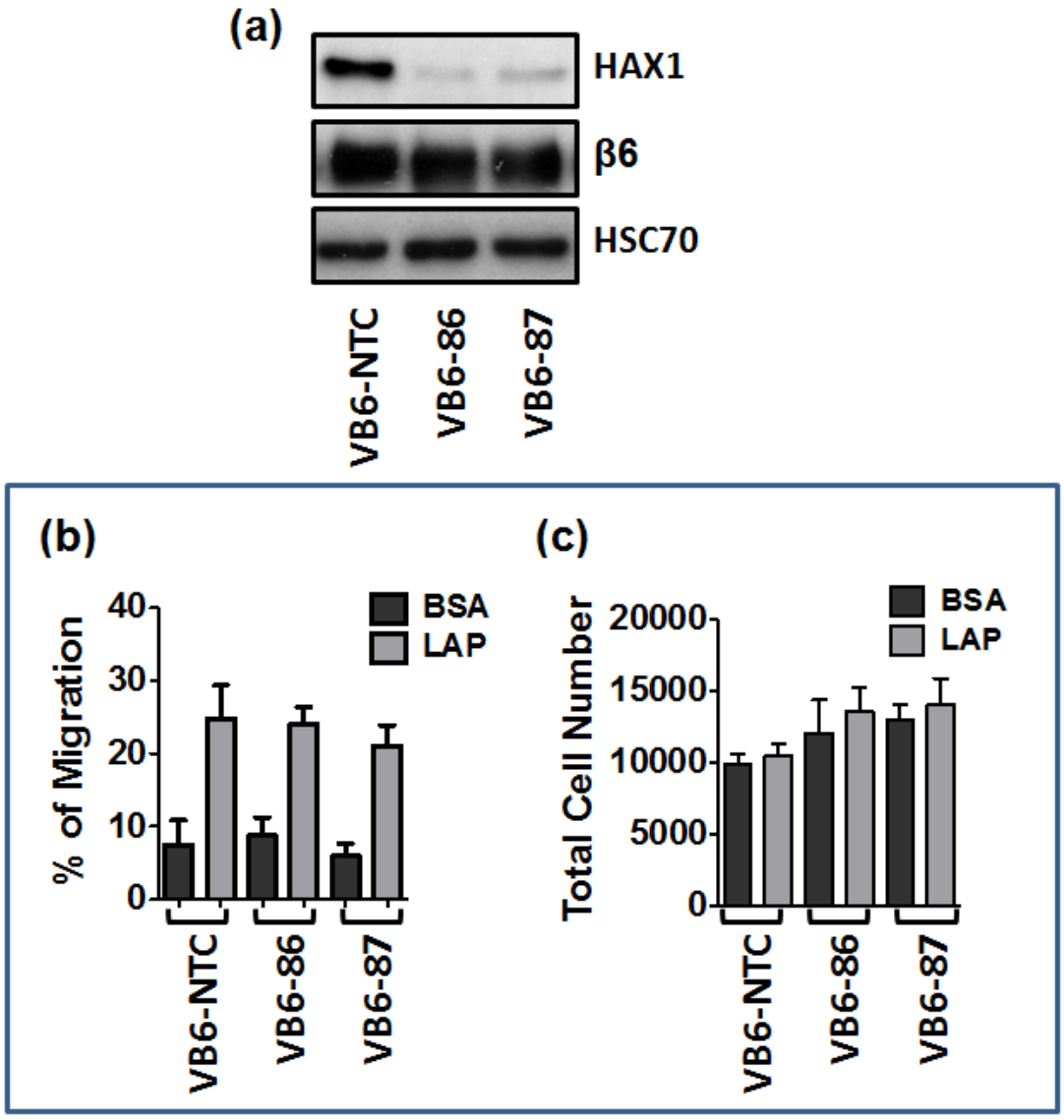

Figure 5.11 Migration of stable HAX1 knockdown cells toward LAP.

VB6 cells stably transfected with lentiviral shRNA against HAX1 (VB6-86 and VB6-87) or non-targeting control (VB6-NTC) were tested for migration across Transwell membranes whose undersides were coated with 0.5 % bovine serum albumin (BSA) or 0.5 µg/ml LAP. Percentage of migration was calculated by the number of cells in the lower chamber divided by total cell number. Western blot analysis confirmed that HAX1 expression was suppressed and the β6 levels were unchanged (b). The cell migration of the stable HAX1-knockdown cell lines showed no significant difference to that of the control cell line (VB6-NTC) (a). Data are presented as mean +/- 1 SD from one of three experiments which were performed in quadruplicate.

5.2.5.3Stable HAX1-knockdowns did not affect invadopodia formation ability

Invadopodia are actin-rich membrane protrusions found in cancer cells which are responsible for degrading the underlying substrate during invasion [229,230]. Interestingly, cortactin is one of the few cytoskeleton proteins required for the assembly of invadopodia in carcinoma cells [231] and it also forms a complex with HAX1 [49]. Therefore to determine whether HAX1 affects invadopodia formation and ECM degradation, cells were seeded onto coverslips pre-coated with rhodamine-gelatin and incubated for 2, 3 and 4 hours. Invadopodia activity was observed by the black degradation in the red background (rhodamine in Figure 5.12, a) and the cell nucleus was stained with DAPI, whereas GFP represents shRNA-positive cells. Figure 5.12 (a) shows the 4 hours incubation on a thin (approximately 1 µm) layer of fluorescently conjugated gelatin. The cells formed focal areas of digested matrix that appear as dark spots or 'holes', denoting invadopodia activity. GFP-positive staining showed the cells expressing lentiviral vectors, and the analysis was conducted only with GFP-positive cells. Data showed there was no significant change in the number of invadopodia positive cells or the number of Invadopodia-positive cells per GFP-positive cell (Figure 5.12, b and c).

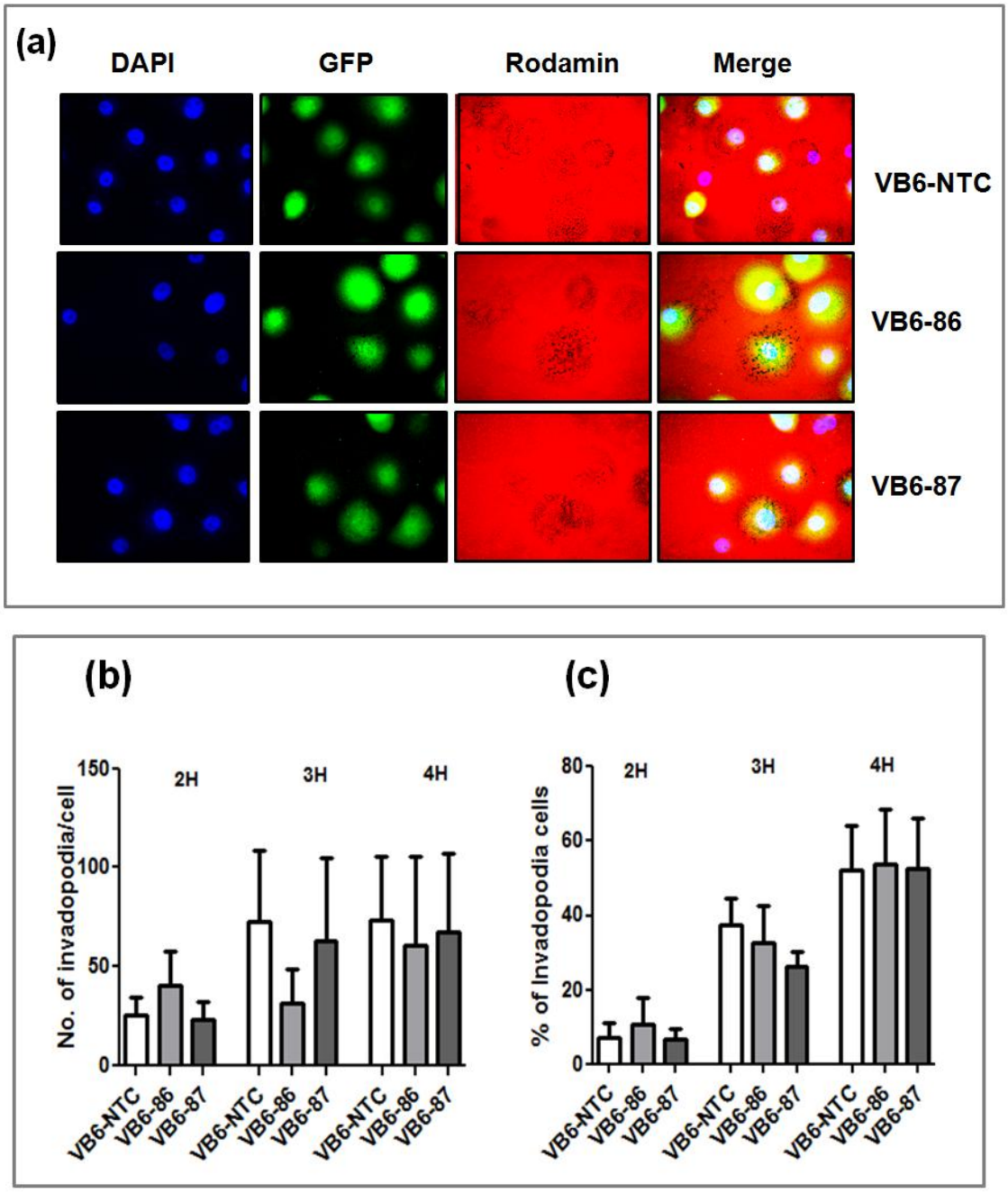

Figure 5.12 Invadopodia formation assay.

(a) shows 4 hours culture on a thin layer of fluorescently conjugated gelatin, cells form focal areas of digested matrix that appear as dark spots or 'holes'.(b) shows the number of invadopodia degraded "holes" per cells at 2 , 3 and 4 hours time points. Figure (c) shows the percentage of invadopodia positive cells. All the cells analysed were GFP-positive (shRNA-expressing cells).

5.2.5.4No significant effect of stable HAX1 knockdown on cancer cell invasion

Previous studies from my lab had shown that endogenous HAX1 was required both for integrin αvβ6-dependent migration and carcinoma invasion in a transient knockdown model with siRNA [1]. In Chaptor 4 I showed that I was able to replicate these results, and indeed I was able to extend the observation to additional cell lines, with regard to migration toward an αvβ6 liand, LAP. Because my stable knockdown lines had no such reduction in migratory capacity I next sought to examine whether their invasive activity was affected. Matrigel invasion assays were performed to examine the effects of stable HAX1 knockdown on invasive ability comparing with control cell line (NTC) and HAX1 knockdown cell lines (86, 87, 89 and 90). Invasion assays were performed over 72 hours, and the cells invaded through to the lower chamber were trypsinised and counted. Transwell invasion assay experiments were repeated three times, with sextuplicate wells for each treatment. Data showed there was no significant change between HAX1 knockdown cells and control cells derived from either H400 or VB6 (Figure 5.13, a, b). I also examined invasion using a quantitative three-dimensional organotypic gel assay, which is designed to reflect more closely the *in vivo* tumour environment than the Matrigel invasion assays [220]. Thus cells were cultured on three-dimensional gels composed of Matrigel and type 1 collagen embedded with fibroblasts and grown for 14 days. The gels were then fixed, bisected, and processed to paraffin. Figure 5.13 (c-f and h-k) shows bright field images of H&E stained sections. H400-86 cells demonstrated a significant reduction compared with NTC control, however this decrease was not meaningful in comparison with another control cell line VB6-EMP (Figure 5.13, g).

A similar trend was also observed in VB6 cell lines where no significant difference was seen (Figure 5.13, i). The invasion index was calculated using the product of the average depth of invasion, the number of invading particles, and the area of the invading particles.

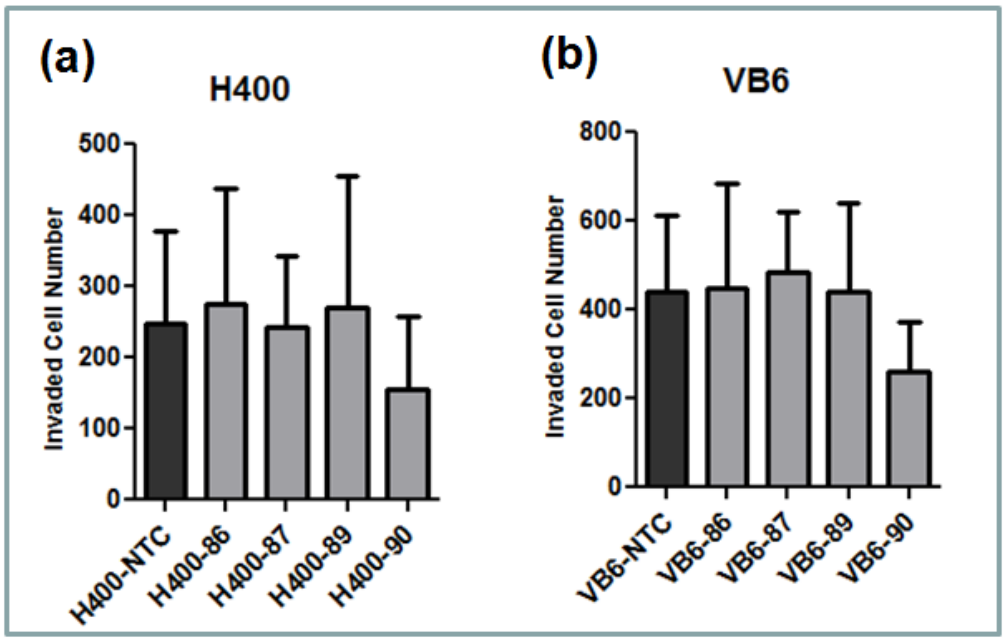
(a)
H400
Invaded Cell Number
500
400
300
200
100
0
H400-NTC
H400-86
H400-87
H400-89
H400-90
(b)
VB6
Invaded Cell Number
800
600
400
200
0
VB6-NTC
VB6-86
VB6-87
VB6-89
VB6-90

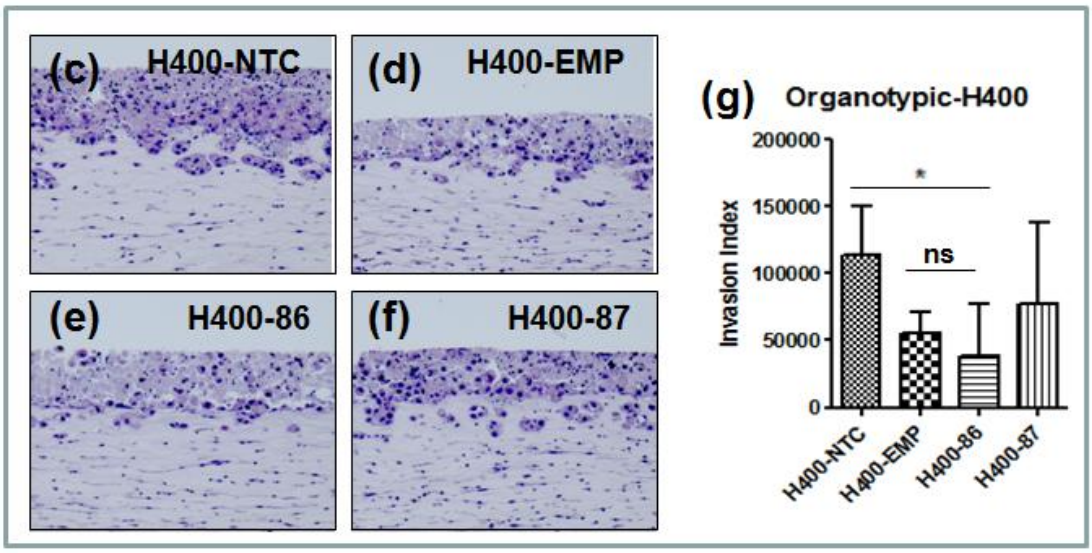
(c) H400-NTC
(d) H400-EMP
(e) H400-86
(f) H400-87
(g) Organotypic-H400
Invasion Index
200000
150000
100000
50000
0
*
ns
H400-NTC
H400-EMP
H400-86
H400-87

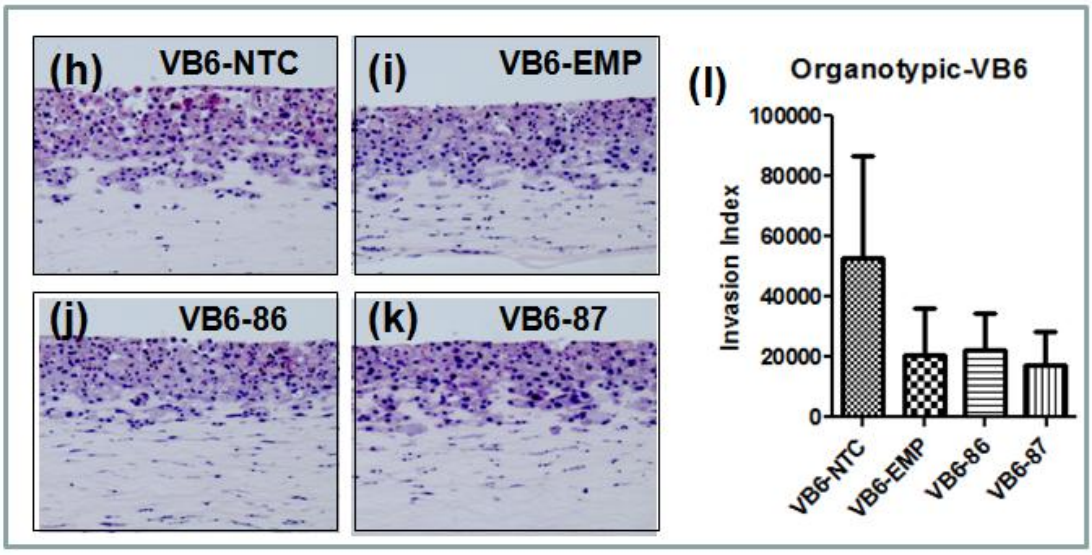
(h) VB6-NTC
(i) VB6-EMP
(j) VB6-86
(k) VB6-87
(l) Organotypic-VB6
Invasion Index
100000
80000
60000
40000
20000
0
VB6-NTC
VB6-EMP
VB6-86
VB6-87

Figure 5.13 Effect of stable HAX1 knockdown on invasive propensity.

Invasion assays were performed with stable HAX1-knockdown H400 (a) and VB6 cell lines (b). Data showed there was no significant change in control and HAX1-knockdown cells. Transwell invasion assay experiments show one from three similar experiments, with sextuplicate wells for each treatment. (c-l) Three-dimensional organotypic tumour cell invasion assays were performed and assays terminated after 14 days. (c-f and h-k) show bright field images of H&E stained sections and (g and l) show the invasion index that compares 86 and 87 cells with control cell lines NTC and EMP. Invasion index was calculated as previously described and plotted as a bar chart. Data show results for three individual organotypic gels and represent mean +/- SD, *: p-value <0.05

5.2.5.5 Stable HAX1 knockdown did not affect the susceptibility to drug-induced apoptosis

Overexpression of HAX1 is found in lesional psoriasis patients where it is linked to increased epidermal proliferation and reduced apoptosis of keratinocytes [23]. On the other hand, HAX1 deletion caused neuronal cell apoptosis in mice [135]. Moreover, HAX1 was shown to protect cells from apoptosis induced by Bax [12], hydroxia/rexygenation [21], etopside [123] and 5-FU [109] treatments. To determine the effect of HAX1 on susceptibility to apoptosis, a cytotoxic assay was performed with three cytotoxic drugs: Cisplatin, Taxol and 5-FU, all known to induce cytotoxity by causing apoptosis [115,232,233]. Different doses of the drugs (10^{-8}, 10^{-7}, 10^{-6}, 10^{-5}, 10^{-4}, 10^{-3}, 10^{-2}, 10^{-1}, 10^{0}, 10^{1}μM) were used to induce cell death in HAX1 knockdown cell lines (VB6-86 and VB6-87; H400-86 and H400-87 were chosen as they exhibited the best HAX1 knockdown among four shRNAs) in comparison with control cells (VB6-NTC; H400-NTC). The cells were exposed to different concentrations of drugs for 72 hours and the cell viability was determined by the MTT assay. Data showed HAX1 knockdown did not affect susceptibility to cytotoxic drugs in VB6 and H400 HAX1-knochdown cell lines (Figure 5.14 and Figure 5.15). This result was observed to be repeatable (n=3).

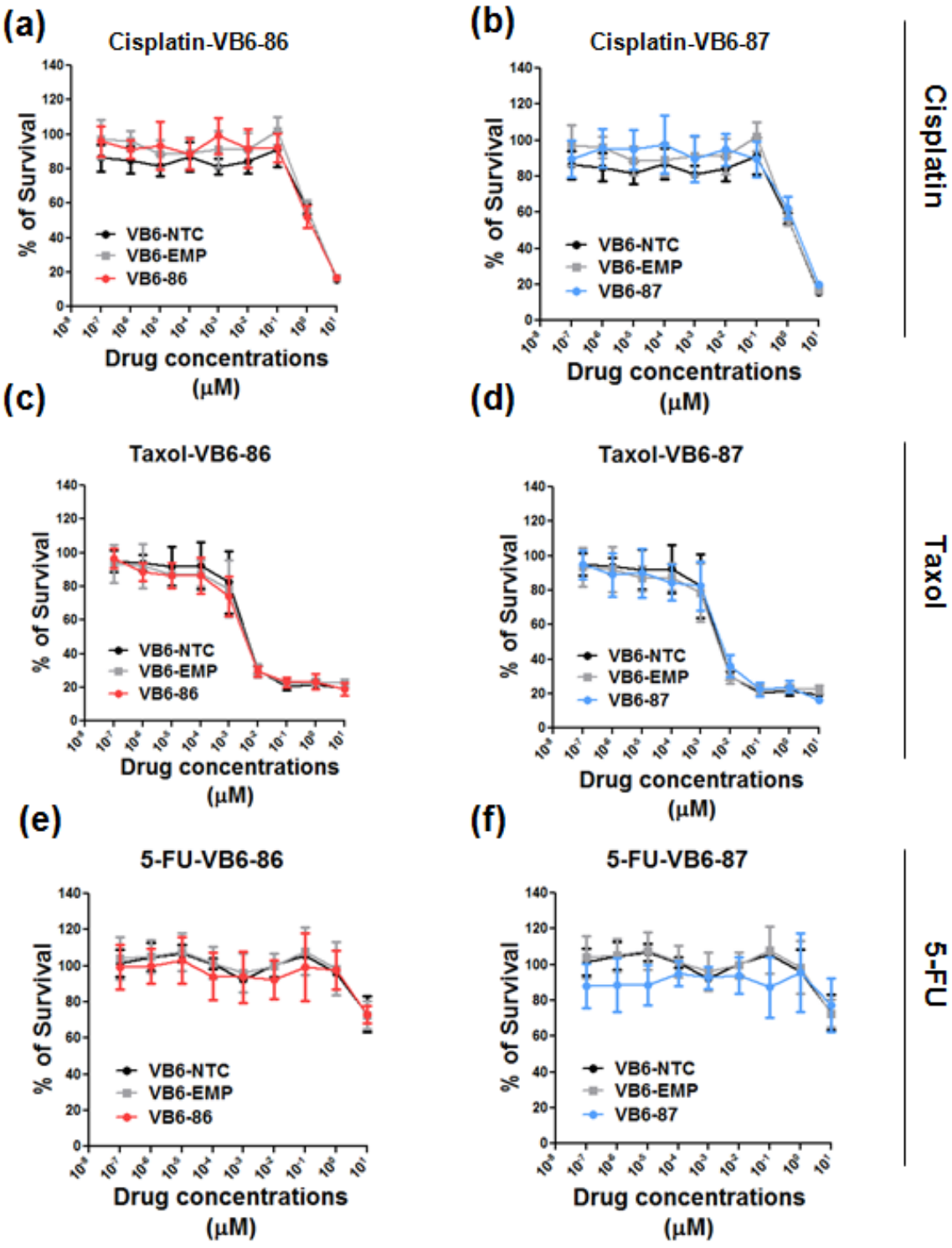
(a)
Cisplatin-VB6-86
% of Survival
VB6-NTC
VB6-EMP
VB6-86
Drug concentrations (μM)
(b)
Cisplatin-VB6-87
% of Survival
VB6-NTC
VB6-EMP
VB6-87
Drug concentrations (μM)
Cisplatin
(c)
Taxol-VB6-86
% of Survival
VB6-NTC
VB6-EMP
VB6-86
Drug concentrations (μM)
(d)
Taxol-VB6-87
% of Survival
VB6-NTC
VB6-EMP
VB6-87
Drug concentrations (μM)
Taxol
(e)
5-FU-VB6-86
% of Survival
VB6-NTC
VB6-EMP
VB6-86
Drug concentrations (μM)
(f)
5-FU-VB6-87
% of Survival
VB6-NTC
VB6-EMP
VB6-87
Drug concentrations (μM)
5-FU

Figure 5.14 Stable HAX1-knockdown in VB6 cell line showed no change in sensitivity to cytotoxic drugs.

HAX1-knockdown VB6 lines were treated with the drugs Taxol, Cisplatin and 5-FU at different doses for 72 hours (10^{-8}, 10^{-7}, 10^{-6}, 10^{-5}, 10^{-4}, 10^{-3}, 10^{-2}, 10^{-1}, 10^{0}, 10^{1}μM). Cell viability after drug treatment was measured by the MTT assay. Data showed that the susceptibility to the cytotoxic drugs was similar in the VB6-86 cell line (red) and the VB6-87 cell line (blue) in comparison with two control cell lines VB6-NTC and VB6-EMP. Data are presented as mean +/- one S.D of optical density (OD) readings of four replicate samples. Figure shows one of three independent experiments.

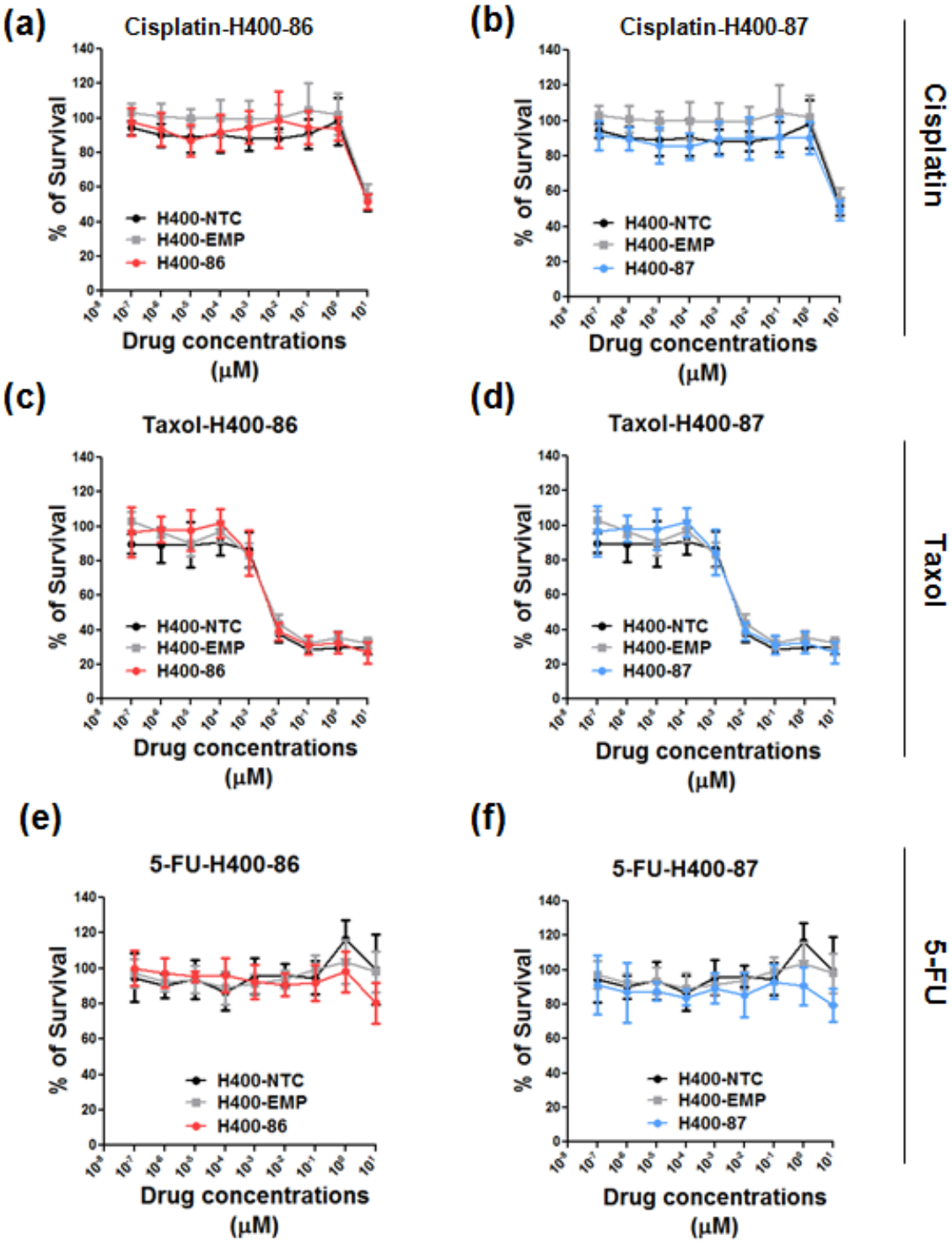
(a)
Cisplatin-H400-86
% of Survival
Drug concentrations (μM)
H400-NTC
H400-EMP
H400-86
(b)
Cisplatin-H400-87
H400-87
Cisplatin
(c)
Taxol-H400-86
(d)
Taxol-H400-87
Taxol
(e)
5-FU-H400-86
(f)
5-FU-H400-87
5-FU

Figure 5.15 Stable HAX1-knockdown in H400 cell line showed no change in sensitivity to cytotoxic drugs.

HAX1-knockdown H400 lines were treated with the drugs Taxol, Cisplatin and 5-FU at different doses for 72 hours (10^{-8}, 10^{-7}, 10^{-6}, 10^{-5}, 10^{-4}, 10^{-3}, 10^{-2}, 10^{-1}, 10^{0}, 10^{1}µM). Cell viability after drug treatment was measured by the MTT assay. Data showed that the susceptibility to the cytotoxic drugs was similar in the H400-86 cell line (red) and the H400-87 cell line (blue) in comparison with two control cell lines H400-NTC and H400-EMP. Data are presented as mean +/- 1 S.D of optical density (OD) readings of four replicate samples. Figure shows one of three independent experiments.

5.3 Discussion

Following on from my findings in Chapter 4, when I showed a marked impact of HAX1 depletion on cell function in transient experiments, I thought it would be important to establish stable HAX1 depleted cell lines.

To establish stable HAX1 knockdown cell lines, I used four lentiviral vectors from OpenBio systems to achieve the goal. The pGIPZ lentiviral system is a powerful RNAi tool in most cell types as the replication incompetent lentivirus is able to infect both dividing and non-dividing target cells efficiently [234]. Also, the vector integrates into the genome of the target cell enabling long-term expression of the genetic cargo.

RNA interference (RNAi) was first discovered in plants, the mechanism showing that double-stranded RNA (dsRNA) targets homologous mRNA for degradation [235,236]. Since then this specific gene silencing has been used widely. RNAi can be induced by synthetic small-interfering RNAs (siRNAs) or by intracellular generation of siRNA from short-hairpin RNAs (shRNAs) delivered as part of a plasmid. siRNAs are about 20-24 nucleotides long regulatory RNAs that provide the protection against exogenous nucleic acids, such as from viruses [237], and have been transfected into cells for gene silencing. However, the gene suppression is only for a transient period as siRNA is diluted and degraded with cell division [238,239] Therefore, delivery of shRNA encoding vectors has been investigated for RNAi, as the effects are long lasting because they are continually produced in the cells [240].

Using the pGIPZ vectors I was able to generate four HAX1 stable knockdown cell lines in both VB6 and H400 cells with p86, p87, p89 and p90 vectors. Western blot showed HAX1 protein expression was reduced by 50-90% in both VB6 and H400 cell lines. At the mRNA level, quantitative RT-PCR was used to examine HAX1 isoform expression by specific primers of the four plasmids. It was shown that p86 and p87 shRNA achieved the best HAX1 knockdown, in general, achieving up to 80% reduction, whereas p90 shRNA was the least effective. All the shRNAs showed a reduction of HAX1 isoforms.

Disappointingly, none of the stable HAX1-knockdown cell lines exhibited any biological functions that differed from the controls. I observed in VB6 cells, where HAX1 transiently was knocked down with siRNA, the ability to migrate to LAP was suppressed significantly (Figure 4.1). However repeated attempts showed no change in migration toward LAP of any of the stable knockdowns. This lack of difference compared with empty and non-targeting controls also was observed in cell growth assays (Clonogenic assay), sensitivity to cytotoxic agents, and invasive activity. Clonogenic assays evaluate the ability of individual cells to undergo sufficient proliferation so as to form a macroscopically visible colony [241]. Caution should be used in such experiments so as to make sure that the environment of the clonogenic assay remains undisturbed throughout the assay. However, in the protocol that I have used, I have changed the growth media which may have affected the final results and must be considered in interpreting these data.

I also tested the behaviour of HAX1-modified cells in the organotypic gel assay, which is designed to reflect more closely the *in vivo* tumour environment. The effect

of stable HAX1 knockdown cells were evaluated by invasion index which was calculated by using the product of the average depth of invasion, the number of invading particles (ie groups of cells), and the area of the invading particles, assessed from image analysis of sections cut from the gels. These data showed no significant difference between the cells analysed. However I did not plot the size of the invading particles and the area of the invading particles separately, and these measurements would have provided different aspects to the analysis and may have shown differences overall.

It was disappointing, given the effort I had put into establishing the stable lines, to find that there was no apparent impact of HAX1 depletion on the monitored cellular characteristics. At this time I am unable to account for the differences, repeatable differences, between the stable and the transient experiments (though the apparent reduction in β6 levels in the transient versus the stable lines might be an avenue worth pursuing). Given that transient knockdown experiments appear to "work", it may be that HAX1 is so important to cell homeostasis, at stable HAX1 knockdown cells re-programme to address the loss of HAX1. It must be considered that it could also be potential "off-target" effects explain the inability of stable knockdown cells to replicate transient knockdown phenotypes. There is also the possibility that the clones I chose to analyse were peculiar in some way. Whatever the reasons behind these disappointing results I resolved not to use the stable cell lines further. Thus for the later part of my thesis I choose to use transient knockdown methods to study HAX1 biology.

CHAPTER 6. RESTORATION OF INDIVIDUAL HAX1 ISOFORMS IN TRANSIENTLY HAX1-DEFICIENT CELLS

6.1 Introduction

In order to study the biological functions of individual HAX1 isoforms, a specific siRNA, (si86) which targets to isoforms 1-6, was used to knockdown all major isoforms of HAX1. Then, individual HAX1 isoforms, which were mutated so as to be resistant to si86-siRNA degradation, were transfected into these transiently HAX1-null cells. This model enabled me to study the roles of individual HAX1 isoforms in cell migration, apoptosis and autophagy. In this section I will firstly describe the characterisation of the RNAi-resistant isoforms then describe their subcellular distributions in VB6 and HeLa cells. Secondly, I will demonstrate the role of individual HAX1 isoforms in cell migration, apoptosis and autophagy.

6.2 Results

6.2.1 Mutated HAX1 isoforms are protected from siRNA degradation

6.2.1.1 Design of HAX1 siRNA (si86) and si86-resistant HAX1 isoforms

To achieve the HAX1 knockdown, si86 siRNA was designed to knockdown endogenous HAX1. Blast and CLC analysis showed si86 recognises the beginning of exon 3 and this targets to HAX1.1-HAX1.6, as shown in the schematic illustration in

Figure 6.1 (a). In order to study the biological functions of individual HAX1 isoforms, mutated HAX1 isoforms were generated that would resist siRNA degradation (designed and generated by Dr. Delphine Lees, Barts Cancer Institute). Even though a single nucleotide mismatch should be sufficient to abolish the activity of an siRNA [242], three bases were mutated to ensure the RNAi-resistance in these HAX1 isoforms. Site-directed mutagenesis was used to insert three silent mutations (T390C.G393A.T396C) into exon 3 of FLAG-tagged HAX1 isoform constructs (Figure 6.1, a). As the altered codons still encoded the original amino acids (Leu, Lys and Tyr) the biological activity of mutant isoforms should be similar to the wild-type versions (Figure 6.1, b). Mutated isofoms were generated for isoforms 1, 2, 4 and 5 as they all contain the αvβ6 binding site (see Introduction).

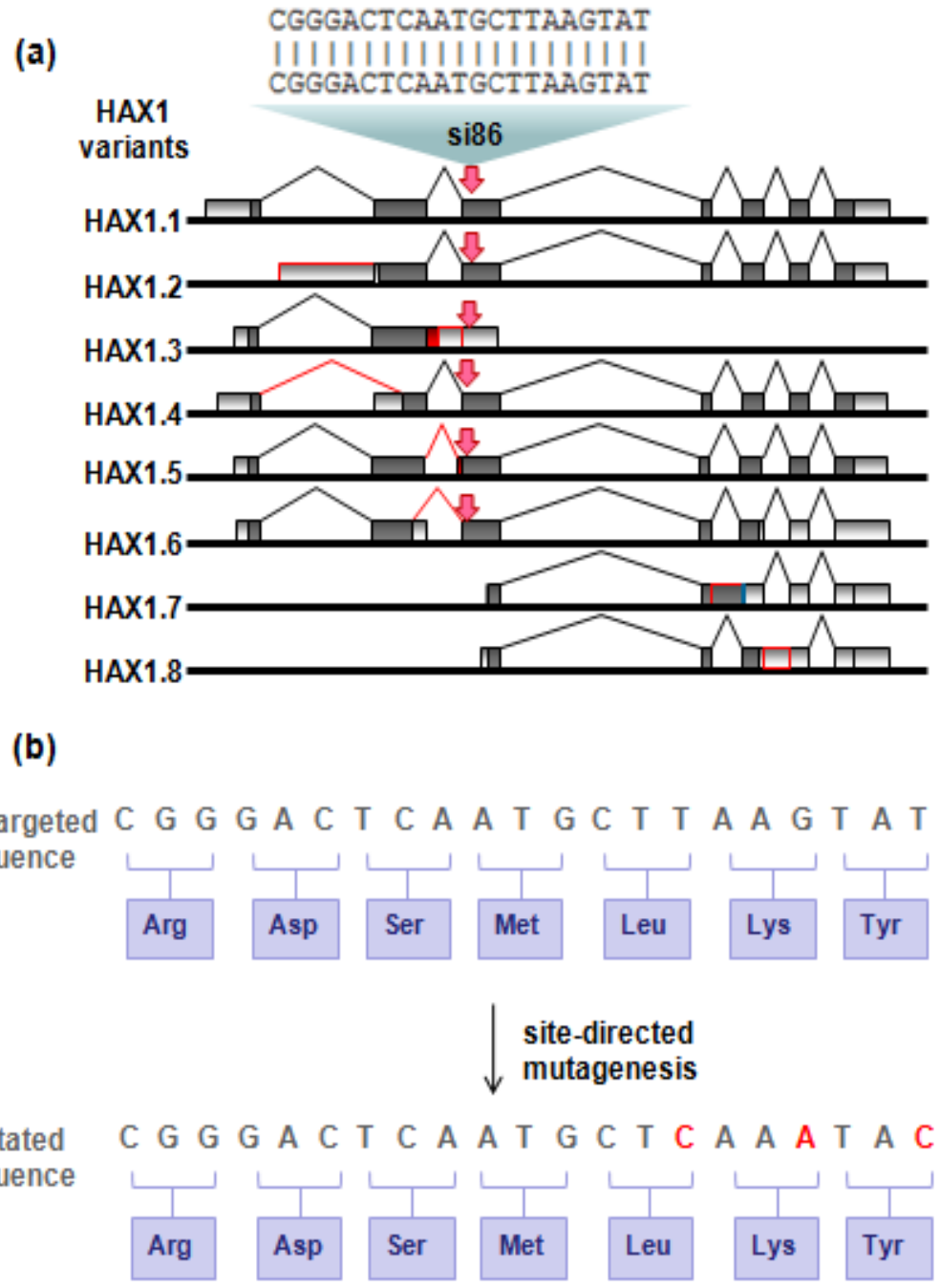
(a)
CGGGACTCAATGCTTAAGTAT
CGGGACTCAATGCTTAAGTAT
HAX1 variants
si86
HAX1.1
HAX1.2
HAX1.3
HAX1.4
HAX1.5
HAX1.6
HAX1.7
HAX1.8
(b)
si86 targeted sequence
C G G G A C T C A A T G C T T A A G T A T
Arg
Asp
Ser
Met
Leu
Lys
Tyr
site-directed mutagenesis
mutated sequence
C G G G A C T C A A T G C T C A A A T A C
Arg
Asp
Ser
Met
Leu
Lys
Tyr

Figure 6.1 Creation of FLAG-tagged isoforms 1,2,4,5 by site-directed mutagenesis.

(a) si86 siRNA recognises the 5'end of exon 3 and targets to HAX1.1-HAX1.6 as shown by pink arrows. Dark boxes indicate exons and light boxes represent introns, the red lines show the alternative splicing. (b) The mutated sequence was marked from si86 targeted sequence by site-directed mutagenesis. The mutated bases are replaced by point mutations (shown as red: T➔C; G➔A; T➔C) and the sequence codes for the same amino acids (Leu, Lys and Tyr).

6.2.1.2Mutant HAX1 isoforms are protected from si86-induced RNAi

To examine the efficiency of si86 siRNA, VB6 cells were transfected and the cell lysates harvested after 48 hours. Western blot analysis showed si86 efficiently knocked down the expression of endogenous HAX1 compared with control siRNA (siNTC) in Figure 6.2 (a). To examine expression of the mutated HAX1 isoforms, the mutated isoforms were transfected into VB6 cells 24 hours after si86 siRNA transfection and the cell lysates were harvested after two days incubation. Western blotting showed that the mutant HAX1 isoforms were successfully expressed in the siRNA-treated VB6 cells (Figure 6.2, b). The HAX1 expression was validated by both anti-HAX1 (RD) and anti-FLAG antibodies, and the Blot displayed different molecular weights for the individual isoforms (HAX1.1 is about 31 kDa, HAX1.2 is about 28 kDa, HAX1.4 is about 26 kDa and HAX1.5 is about 32 kDa). The HAX1 Blot demonstrated multiple bands for each isoform, indicating that overexpression of isoforms may result in degradation in the cell (Figure 6.2, b). Vec indicates control cells which were treated with control vector after si86 knockdown.

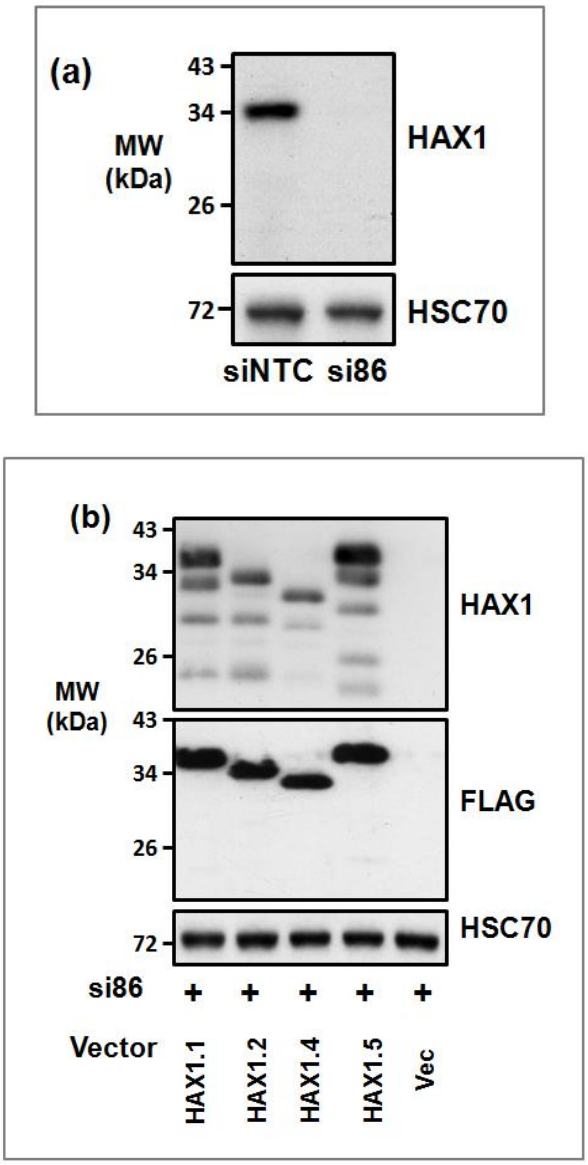

Figure 6.2 HAX1 isoforms are protected from siRNA-degradation.

(a) VB6 cells were treated with si86 siRNA or control siRNA (NTC) for 48 hours, and the lysates were subjected to Western blot. Data showed si86 efficiently knocks down the endogenous HAX1. (b) Mutant isoforms (HAX1.1-5) or empty vector (vec) were transfected into HAX1 siRNA (si86) treated VB6 cells. Cell lysates were harvested two days after isoform restoration and antibodies to HAX1 (RD) and FLAG were employed to Blot the molecules. HSC70 served as a loading control. The mutant isoforms were successfully expressed in si86-treated cells and displayed different molecular weights (HAX1.1 is approximately 31 kDa, HAX1.2 is approximately 28 kDa, HAX1.4 is approximately 26 kDa and HAX1.5 is approximately 32 kDa). Vec: control vector.

6.2.2 Subcellular distribution of HAX1

6.2.2.1 HAX1 isoforms 1, 4 and 5 predominantly associate with mitochondria whereas isoform 2 exhibits a cytoplasmic expression pattern

The literature has reported that HAX1 is expressed in multiple subcellular localisations in different cell types and is associated with different binding partners (see Introduction-1.1.3.2: Subcellular localisation of HAX1). In order to gain a better understanding of the subcellular expression of HAX1 isoforms, immunofluorescent staining was performed to investigate the subcellular distribution of individual HAX1 isoforms. HAX1 isoforms were transfected into si86-treated VB6 and HeLa cells and the immunofluorescent staining was performed 48 hours after transfection. Mitotracker was incubated with the cells for 30 minutes to label mitochondria prior to harvesting. Cells were labelled with the anti-HAX1 antibody (RD) or anti-FLAG to stain the restored HAX1 isoforms after fixation and permeabilisation. Confocal microscopy revealed that HAX1.1, HAX1.4 and HAX1.5 are localised mostly to mitochondria (Figure 6.3 and Figure 6.4 for VB6 cells, Figure 6.5 and Figure 6.6 for HeLa cells). In contrast, HAX1.2 exhibited a predominantly cytoplasmic localisation with a small amount of membrane localisation (Figure 6.3 for VB6 and Figure 6.5 for HeLa). Negative control cells (si86 transfection without any isoform restoration) did not show any staining by anti-HAX1 and anti-FLAG antibodies (indicates as si86, Figure 6.3 and Figure 6.5)

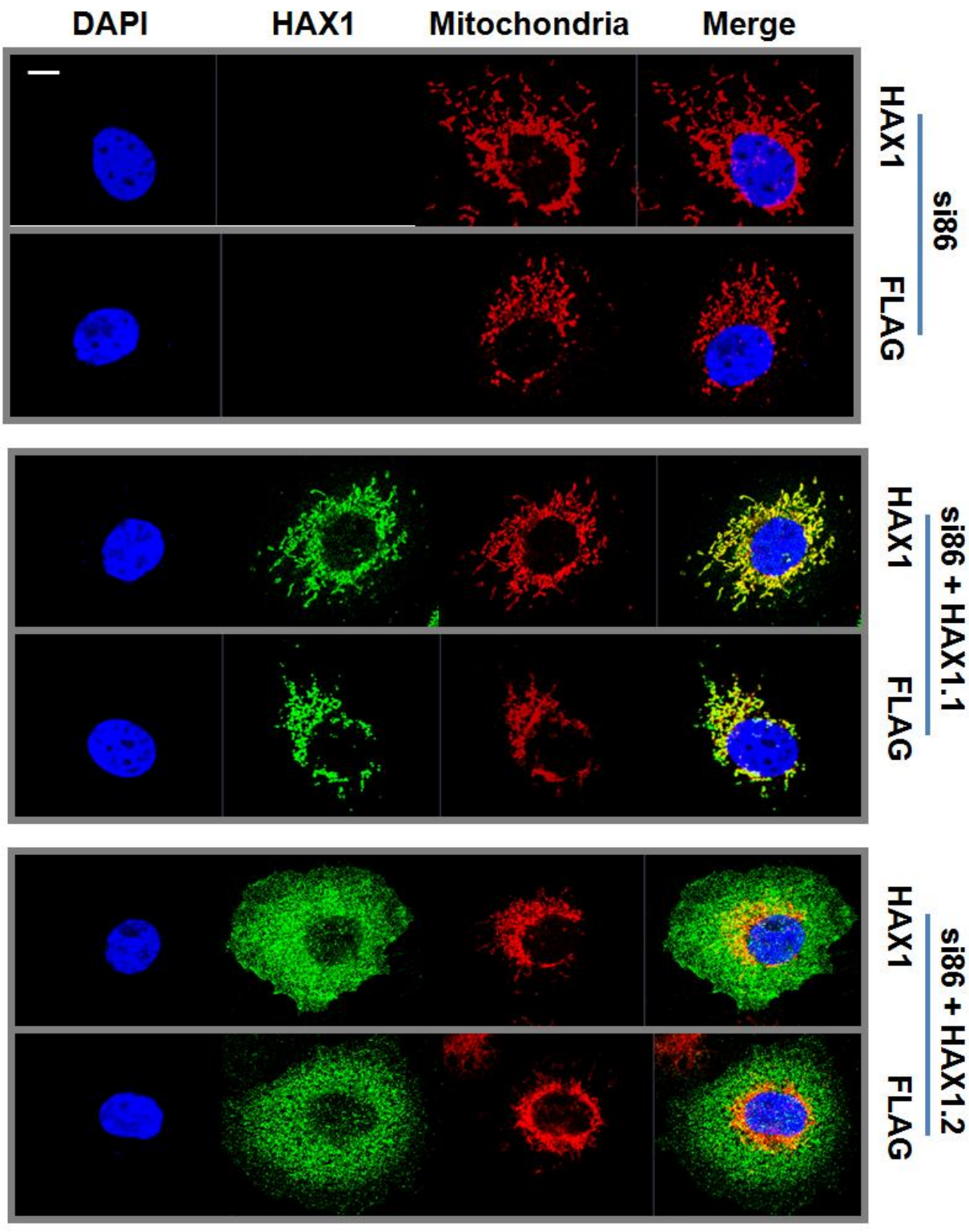
DAPI
HAX1
Mitochondria
Merge
si86
HAX1
FLAG
si86 + HAX1.1
HAX1
FLAG
si86 + HAX1.2
HAX1
FLAG

Figure 6.3 The subcellular distribution of HAX1 isoforms 1 and 2 in VB6 cells.

si86 siRNA treated VB6 cells were transfected with mutant HAX1 isoforms and mitotracker was incubated with the cells for 30 minutes prior to harvesting. Cells were labelled with the anti-HAX1 antibody (RD) and anti-FLAG to stain the restored HAX1 isoforms after fixation and permeabilisation. Cell nuclei were stained with DAPI. Confocal microscopy revealed that HAX1.1 localised mostly to mitochondria as the two colours (green for HAX1 and red for mitochondria) from different fluorochromes merged (as yellow) whereas si86 only transfected cells did not show any staining pattern. HAX1.2 revealed a very unique expression pattern in cytoplasm. The staining from both anti-HAX1 and anti-FLAG antibodies demonstrated similar patterns of HAX1 expression for each isoforms. Scale bar indicates 10μm.

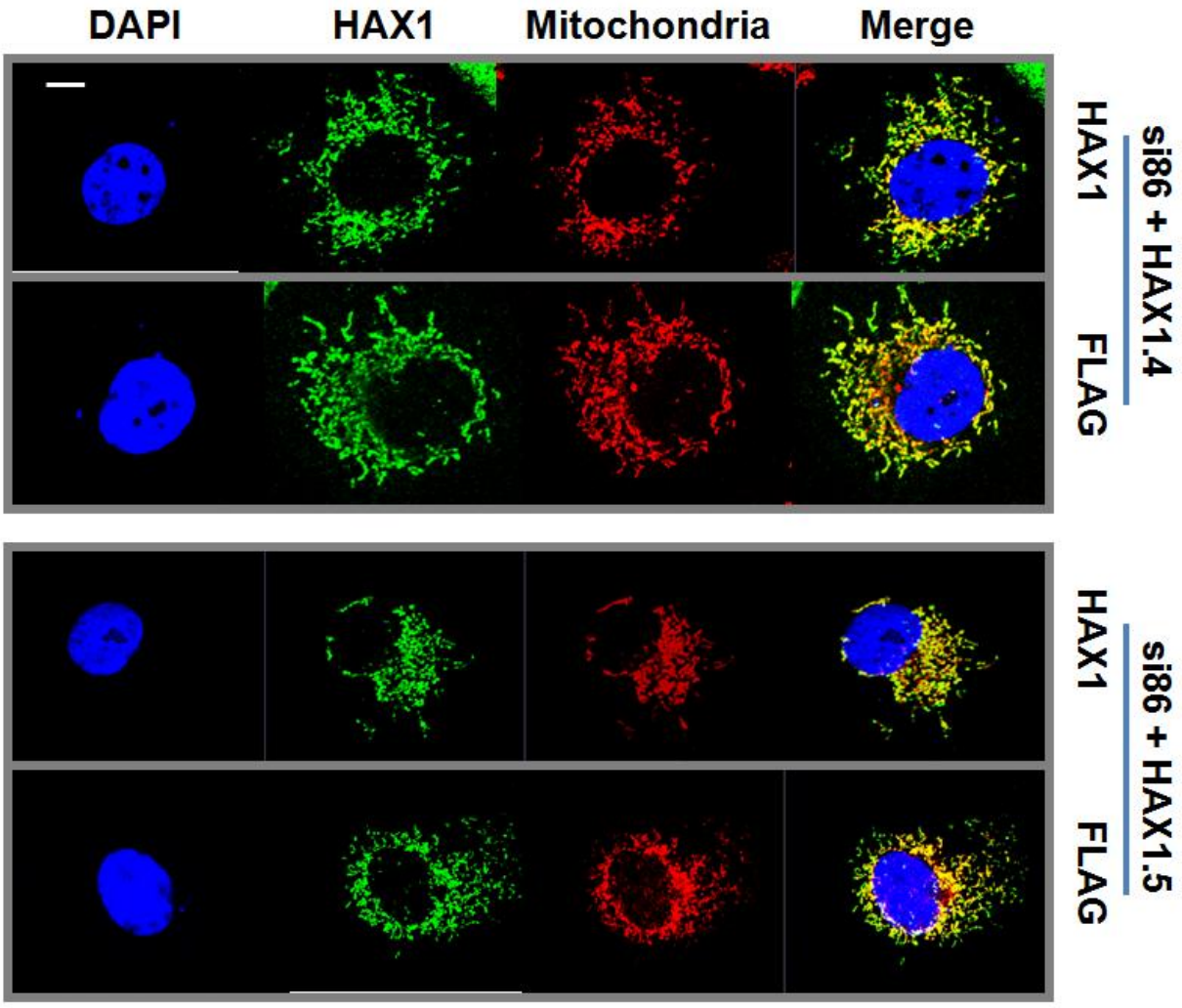

Figure 6.4 The subcellular distribution of HAX1 isoforms 4 and 5 in VB6 cells.

si86 siRNA treated VB6 cells were transfected with mutant HAX1 isoforms and mitotracker was incubated with the cells for 30 minutes prior to harvesting. Cells were labelled with the anti-HAX1 antibody (RD) and anti-FLAG to stain the restored HAX1 isoforms after fixation and permeabilisation. Cell nuclei were stained with DAPI. Confocal microscopy revealed that HAX1.4 and HAX1.5 localised mostly to mitochondria as the two colours (green for HAX1 and red for mitochondria) from different fluorochromes merged (as yellow). The staining from both anti-HAX1 and anti-FLAG antibodies demonstrated similar patterns of HAX1 expression for each isoform. Scale bar indicates 10µm.

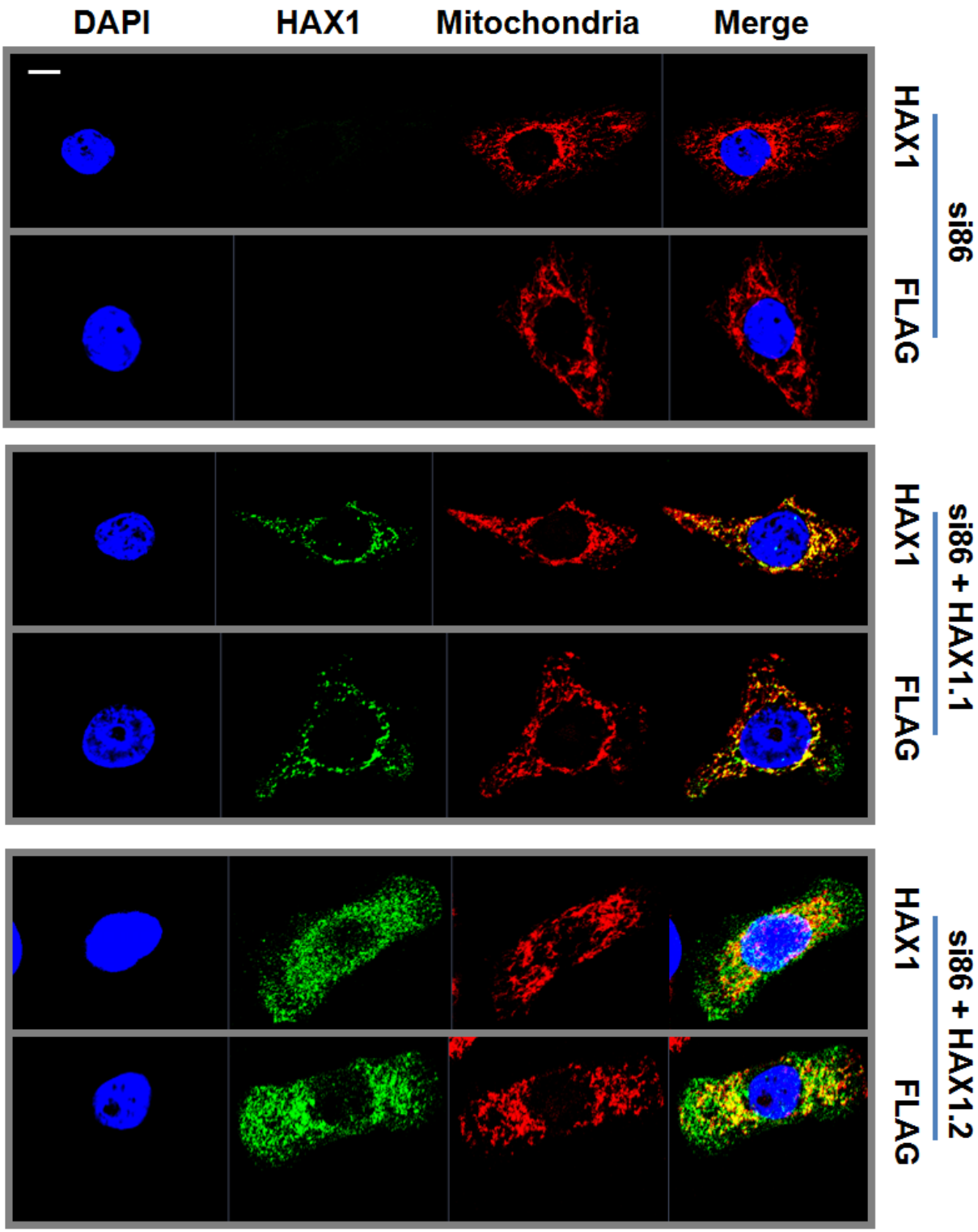
DAPI
HAX1
Mitochondria
Merge
HAX1
FLAG
si86
HAX1
FLAG
si86 + HAX1.1
HAX1
FLAG
si86 + HAX1.2

Figure 6.5 The subcellular distribution of HAX1 isoforms 1 and 2 in HeLa cells.

si86 siRNA treated HeLa cells were transfected with mutant HAX1 isoforms and mitotracker was incubated with the cells for 30 minutes prior to harvesting. Cells were labelled with the anti-HAX1 antibody (RD) and anti-FLAG to stain the restored HAX1 isoforms after fixation and permeabilisation. Cell nuclei were stained with DAPI. Confocal microscopy revealed that HAX1.1 localised mostly to mitochondria as the two colours (green for HAX1 and red for mitochondria) from different fluorochromes merged (as yellow) whereas si86 only transfected cells did not show any staining pattern. HAX1.2 revealed a very unique expression pattern in cytoplasm. The staining from both anti-HAX1 and anti-FLAG antibodies demonstrated similar patterns of HAX1 expression for each isoform. Scale bar indicates 10μm.

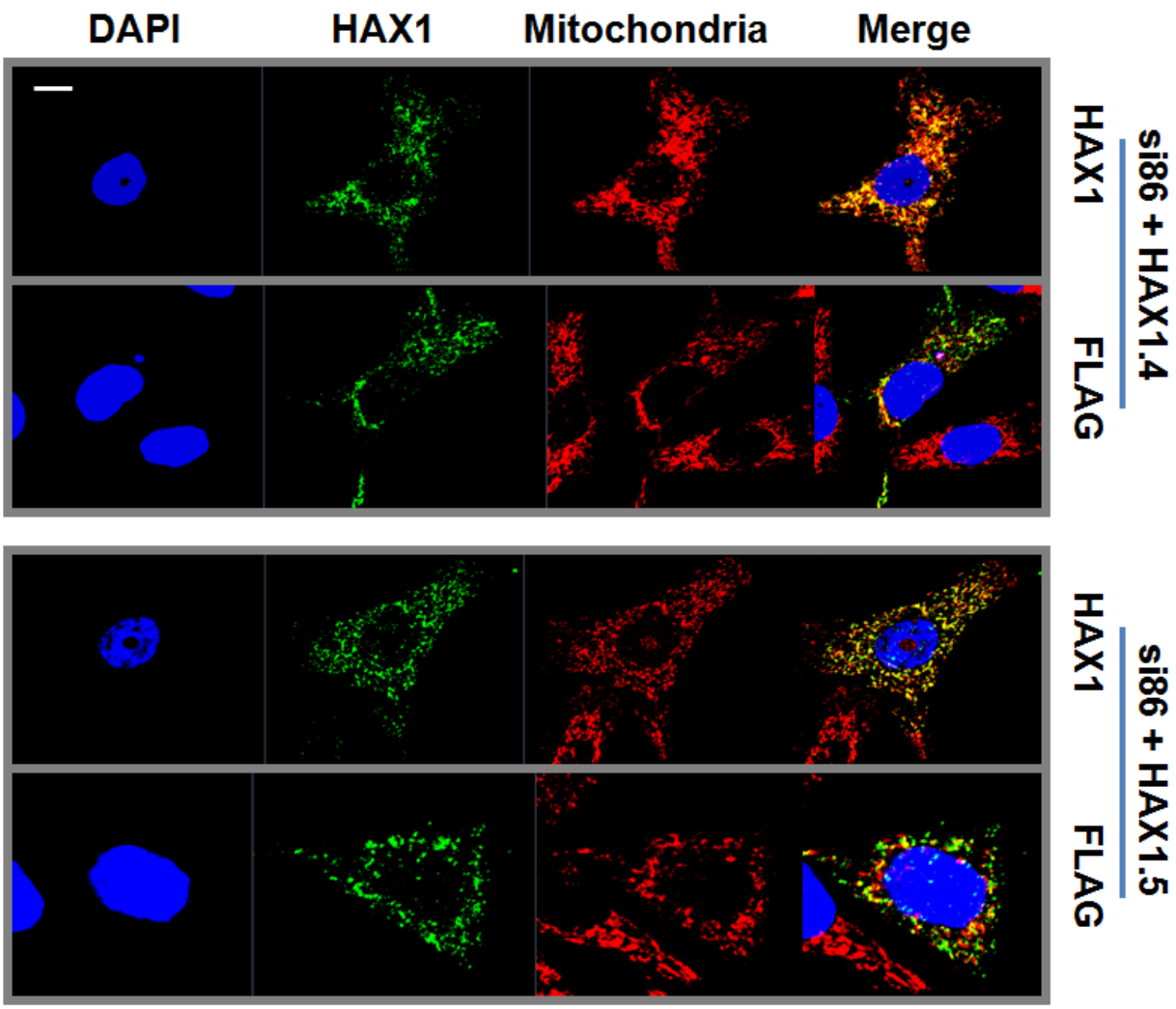

Figure 6.6 The subcellular distribution of HAX1 isoforms 4 and 5 in HeLa cells.

si86 siRNA treated HeLa cells were transfected with mutant HAX1 isoforms and mitotracker was incubated with the cells for 30 minutes prior to harvesting. Cells were labelled with the anti-HAX1 antibody (RD) and anti-FLAG to stain the restored HAX1 isoforms after fixation and permeabilisation. Cell nuclei were stained with DAPI. Confocal microscopy revealed that HAX1.4 and HAX1.5 localised mostly to mitochondria as the two colours (green for HAX1 and red for mitochondria) from different fluorochromes merged (as yellow). The staining from both anti-HAX1 and anti-FLAG antibodies demonstrated similar patterns of HAX1 expression for each isoform. Scale bar indicates 10µm.

6.2.2.2Wound healing experiments showed HAX1 isoforms did not change their subcellular localisation in migrating cells

HAX1 has been reported to regulate cell migration in both some normal and certain cancer cells (see Introduction: 1.1.4.3: HAX1 regulates cell migration). A recent study also demonstrated that HAX1 appeared in the leading edge and at the rear uropod localisation of migrating neutrophils [20]. In order to investigate the localisation of HAX1 isoforms in motile cells, scratch wound healing assays were performed on the HAX1-knockdown si86-treated VB6 cells in which the mutant HAX1 isoforms had been restored. Once the transfected cells had reached confluency, the wound scratches were then generated and the cells were allowed to migrate for approximately 16 hours. Cells were subsequently fixed and stained for HAX1 (RD antibody), mitochondria (Mitotracker) and nucleus (DAPI). Confocal microscopy showed representative cells that had migrated into the scratch (Figure 6.7, a, c, e, g); several cells in the leading front to the wound were examined at high power and were representative of the migrating cells (Figure 6.7, b, d, f, h). All the isoforms displayed their subcellular distributions observed in non-migrating cells. Thus HAX1.1, HAX1.4 and HAX1.5 remained localised to mitochondria (Figure 6.7, a, b, e, f, g, h) whereas HAX1.2 remained distributed in the cytoplasm and sometimes also was observed in cell membrane (Figure 6.7, c and d).

HAX1.1
a
b
HAX1.2
c
d
HAX1.4
e
f
HAX1.5
g
h

Figure 6.7 Distribution of HAX1 isoforms in migrating cells.

HAX1.1, HAX1.2, HAX1.4 and HAX1.5 were transfected into VB6 cells whose endogenous HAX1 was knocked down with siRNA si86. A scratch wound was made in confluent monolayers and cells were allowed to incubate at 37 °C for 16 hours. Mitochondria (red) were labelled 30 minutes before cells were fixed and HAX1 isoforms were labelled with anti-FLAG antibodies (green) and the nuclei were labelled with DAPI (blue). Cells at the leading edge were examined closely. Figures show low power image (10x magnification objective lens) and a high power image (63x magnification objective lens) of a representative cell from the image. Data showed HAX1.1 (a, b), HAX1.4 (e, f) and HAX1.5 (g, h) were distributed in a mitochondrial pattern in migrated cells. HAX1.2 (c, d) again located to the cytoplasm and plasma membrane. The images were scanned and collected using a Zeiss confocal microscope (Zeiss LSM 710).

6.2.3 Overexpression of individual HAX1 isoforms did not affect cell growth

6.2.3.1 Knockdown of endogenous HAX1 does not affect growth of HeLa cells

To examine the effect of HAX1 on cell growth (ie the sum of cell proliferation and cell death), HeLa cells were transfected with the HAX1 siRNA (si86) or control siRNA (siNTC). The cells were then seeded into 96-well plates for various times (1, 2, 4, 6, 8 days) and the proliferation was measured by labelling nuclei with DNA-binding fluorescent dye PicoGreen (Invitrogen). The relative fluorescence was quantitatively measured using a 96-well plate fluorospectrophotometer. Western blot analysis showed the HAX1 knockdown by siRNA si86 was effective for up to 8 days into the proliferation assay (Figure 6.8, a). Picogreen staining showed that HAX1-knockdown did not affect cell growth of the HeLa cells (Figure 6.8, b).

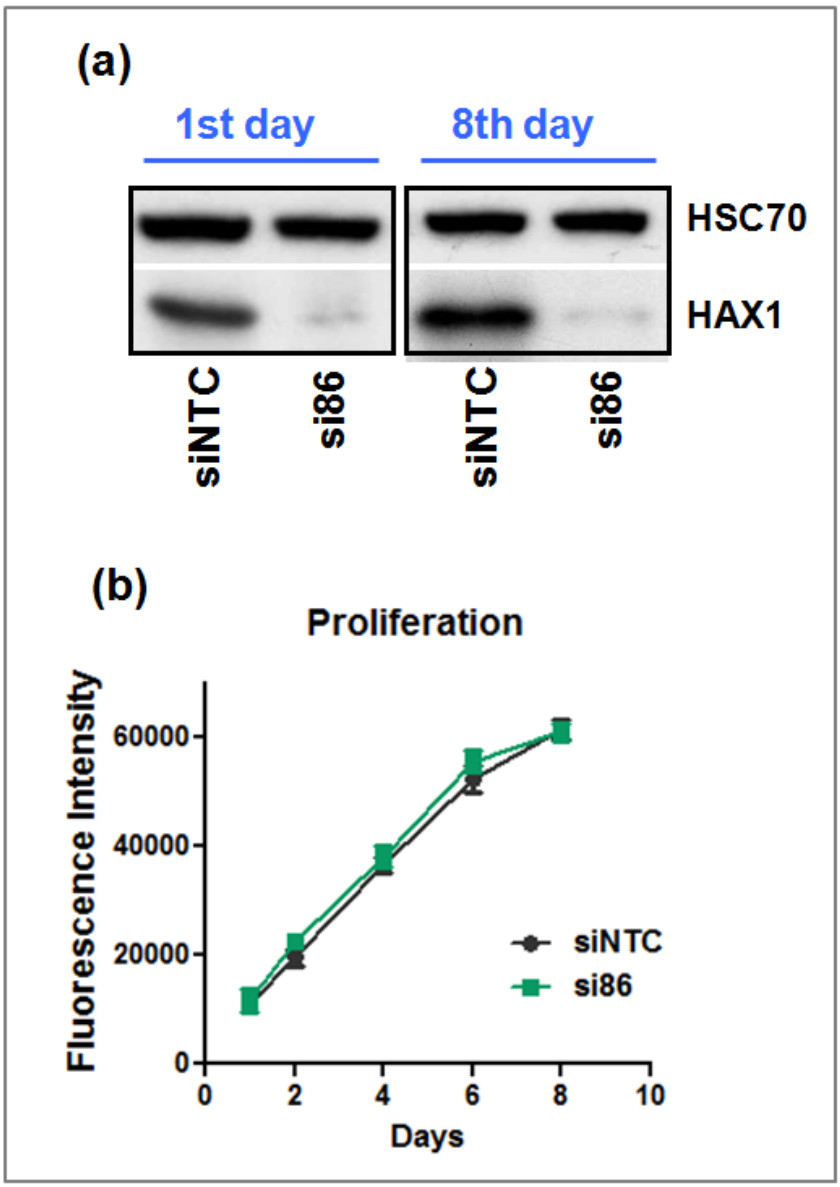

Figure 6.8 HAX1 knockdown did not affect HeLa cell growth.

HeLa cells were transfected with control siRNA (siNTC) or HAX1 siRNA (si86) and then were cultured in a 96-well plate for 1, 2, 4, 6 and 8 days. (a) HAX1 protein levels were determined by Western blotting at day1 and day8. HAX1 expression was suppressed by siRNA (si86). HSC70 was used as control. (b) Picogreen growth assay demonstrated no difference in the HAX1-depleted cells (si86) compared with control cells (siNTC). The data represent triplicate samples from one of two independent experiments and are expressed as mean +/- 1 SD.

6.2.3.2HAX1 isoforms did not alter cell growth

To examine the effect of individual HAX1 isoforms on cell growth, HeLa cells were trasfected with HAX1 siRNA (si86) and then restored with HAX1.1, HAX1.2, HAX1.4 and HAX1.5. The cells were then seeded into 96-well plates for various times (1, 2, 4, 6, 8 days) and the proliferation was measured by Picogreen staining. Figure 6.9 (a) shows that HAX1.1, HAX1.2 and HAX1.5 were successfully expressed over the 8 days period of the proliferation experiment. However the expression of HAX1.4 was very poor and thus it was not possible to draw conclusions. Picogreen staining showed there was no difference in cell growth caused by any of the transfected isoforms compared with control cells (vec: control vector only treatment) (Figure 6.9, b, c, d, e).

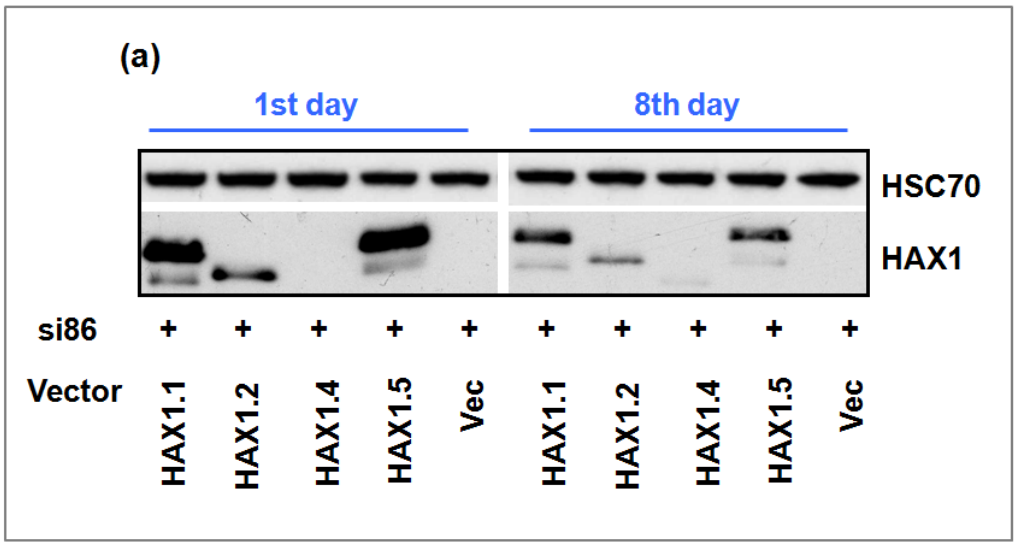
(a)
1st day
8th day
HSC70
HAX1
si86 + + + + + + + + + +
Vector
HAX1.1
HAX1.2
HAX1.4
HAX1.5
Vec
HAX1.1
HAX1.2
HAX1.4
HAX1.5
Vec

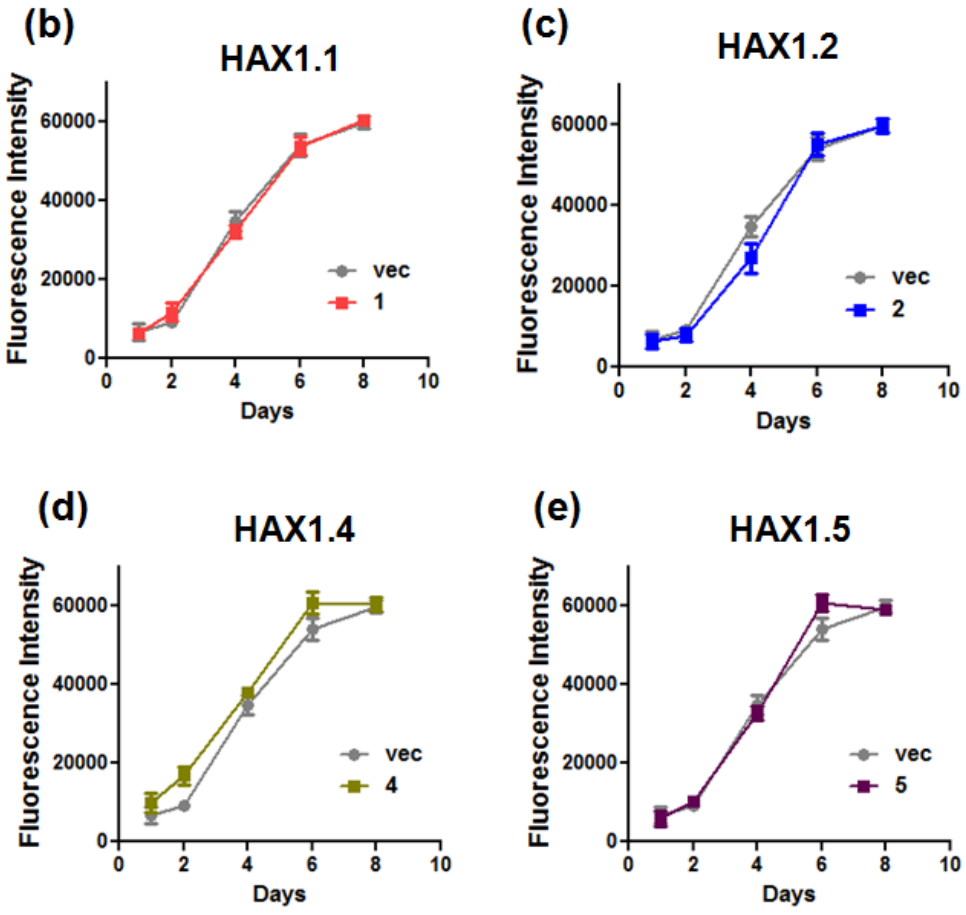
(b)
HAX1.1
Fluorescence Intensity
60000
40000
20000
0
0 2 4 6 8 10
Days
vec
1
(c)
HAX1.2
Fluorescence Intensity
60000
40000
20000
0
0 2 4 6 8 10
Days
vec
2
(d)
HAX1.4
Fluorescence Intensity
60000
40000
20000
0
0 2 4 6 8 10
Days
vec
4
(e)
HAX1.5
Fluorescence Intensity
60000
40000
20000
0
0 2 4 6 8 10
Days
vec
5

Figure 6.9 Individual HAX1 isoforms do not alter cell growth.

Individual HAX1 isoforms were transfected with HAX1 siRNA (si86) and then were cultured in a 96-well plate for 1, 2, 4, 6, 8 days. The fluorescent dye Picogreen was employed to measure total DNA and it is correlated with the relative number of cells. (a) Western blot analysis showed that the HAX1 isoforms were expressed from the first day through to the eighth day. Growth assays were performed with cells expressing HAX1 isoforms versus vector (vec) and showed no difference (b-e). Note that HAX1.4 expression was relatively poor and only seen after longer exposure time of the blot (data not shown) therefore was not possible to draw conclusions. The data represent triplicate samples from two independent experiments and are expressed as mean +/- 1 SD.

6.2.4 HAX1.2 negatively regulates cell migration

To examine the effect of HAX1 isoforms on cell migration, migration assays were performed with HAX1-knockdown cells reconstituted with different individual isoforms. Thus VB6 cells were transfected with HAX1 siRNA (si86) to knockdown all HAX1 isoforms and the FLAG-tagged isoforms (HAX1.1, HAX1.2, HAX1.4 or HAX1.5; or vector only: vec) were restored 24 hours later. Western blotting confirmed that the mutant isoforms were protected from the siRNA degradation (Figure 6.10, a). A parallel proliferation assay showed no significant difference in total cell numbers during the same period of time caused by any of the treatments (Figure 6.10, c). Cell migration was examined toward BSA or TGF-β latency associated peptide (LAP) coated-Transwells. Results showed expression of HAX1.2 significantly decreased cell migration compared with control cells (vec) (Figure 6.10, b). These result was observed repeatedly (n=5). To confirm this effect I also used an siRNA that specificanlly knocks down HAX1.2 (si1p2, see Methods). RT-PCR showed that si1p2 efficiently suppresses HAX1.2 but did not affect cell growth (Figure 6.10, d and f). In contrast to the results obtained with isoform transfection, knockdown of HAX1.2 was sufficient to increase cell migration toward LAP compared with the non-targeting control siRNA treated cells (Figure 6.10, e). Together, these findings indicate HAX1.2 exhibits a distinct role from the other isoforms as it appears negatively regulates αvβ6-dependent cell migration in VB6 cells.

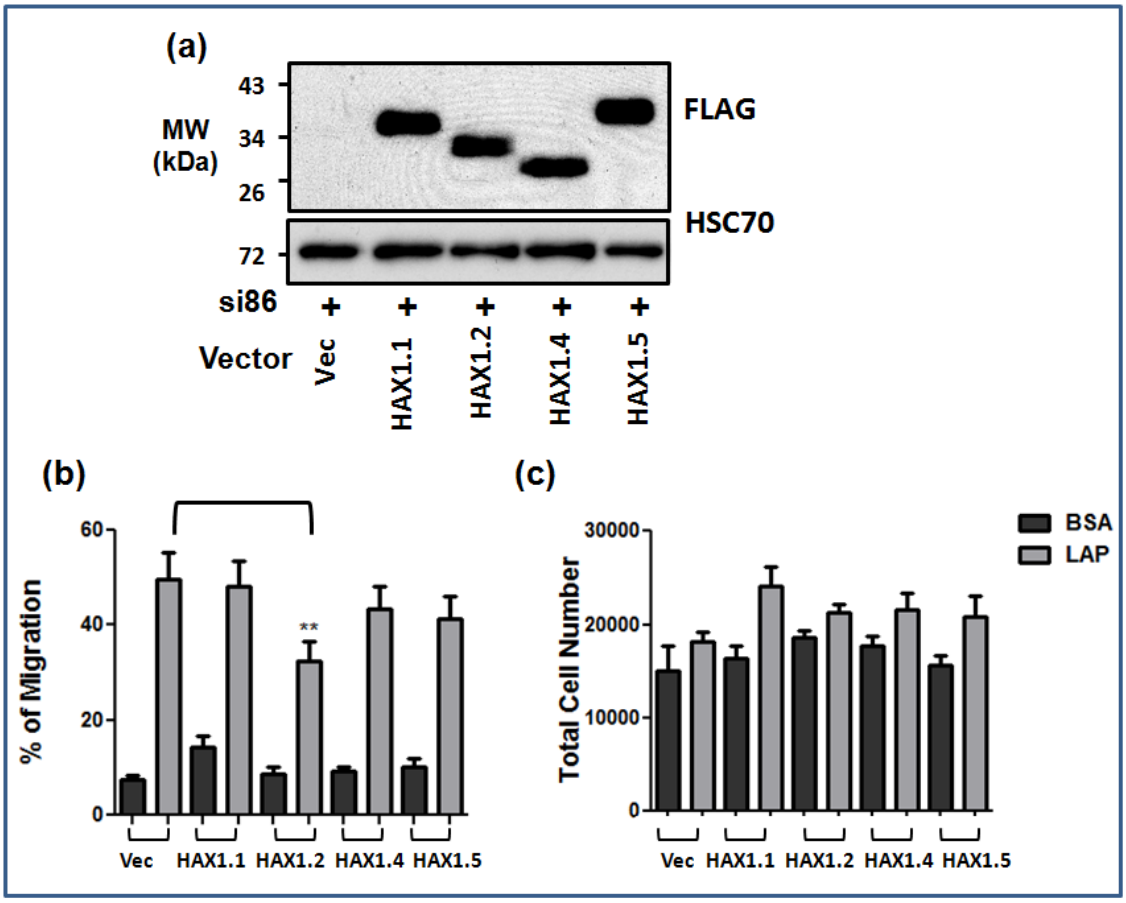
(a)
MW (kDa)
43
34
26
72
FLAG
HSC70
si86 + + + + +
Vector Vec HAX1.1 HAX1.2 HAX1.4 HAX1.5
(b)
% of Migration
60
40
20
0
**
Vec HAX1.1 HAX1.2 HAX1.4 HAX1.5
(c)
Total Cell Number
30000
20000
10000
0
BSA
LAP
Vec HAX1.1 HAX1.2 HAX1.4 HAX1.5

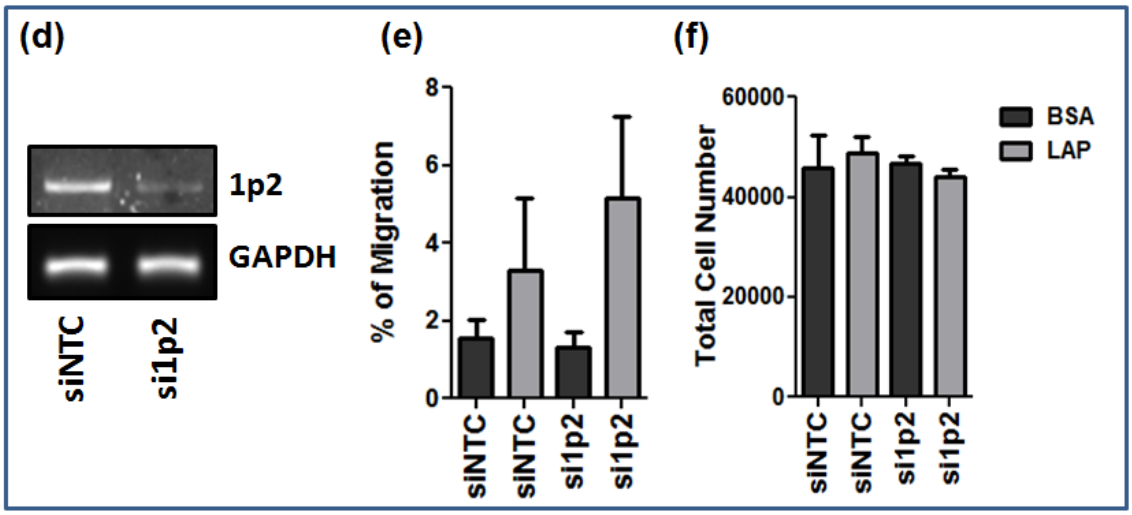
(d)
1p2
GAPDH
siNTC
si1p2
(e)
% of Migration
8
6
4
2
0
siNTC siNTC si1p2 si1p2
(f)
Total Cell Number
60000
40000
20000
0
BSA
LAP
siNTC siNTC si1p2 si1p2

Figure 6.10 HAX1.2 negatively regulates migration.

VB6 cells migration toward TGF-β latency associated peptide (LAP) is αvβ6-dependent [181]. To test the role of different HAX1 isoforms in this process, VB6 cells were initially transfected with HAX1 siRNA (si86) to knockdown endogenous HAX1. The individual HAX1 isoforms (HAX1.1, HAX1.2, HAX1.4 and HAX1.5) were restored into these HAX1 depleted cells. Western blotting showed the isoforms were protected from siRNA degradation (a). (b) Cell migration assays were performed across Transwell membranes coated with 0.5% bovine serum albumin (BSA) or 0.5μg/mL LAP. HAX1.2 exhibited significantly ($p<0.01$) decreased cell migration while the proliferation did not show difference as a consequence of these treatments (c). The data represent one of five independent experiments. In reverse experiments, VB6 cells were transfected with non-targeting siRNA (siNTC) or si1p2 that targets only HAX1.2 (see Methods). RT-PCR studies confirmed that HAX1.2 was knocked down by si1p2 (d). GAPDH served as control. (d) Transwell migration assays were performed with these siRNA treated VB6 cells. The HAX1.2 depletion elevated the cell mobility on LAP compared with the control cells (e). The data represent one of four independent experiments showing similar results. (f) A parallel proliferation study did not show a significant difference between treatments.

6.3 Discussion

HAX1 is a family of proteins generated by alternative splicing, comprised of generally similar proteins with different molecular weights. I expressed individual HAX1 isoforms, which are mutated to protect the coding sequence from siRNA degradation, in cells transiently rendered HAX1-null by siRNA; successful expression of HAX1 isoforms was confirmed by blotting both HAX1 and FLAG. Different segments of HAX1 isoforms were observed by probing with an anti-HAX1 antibody, indicating some degradation might occur in these overexpressing cells. Several intracellular molecules have been reported to target to HAX1. HAX1 may be degraded by Omi in cells treated with various apoptotic stimuli (H_2O_2, Etoposide, cisplatin) [30]. Caspase-3 interacts with HAX1 and this is reported to cleave HAX1 in apoptotic cells [118]. A recent study also showed that Granzyme B cleaves HAX1 into two major fragments: an N-terminal fragment that localises to mitochondria and a C-terminal fragment that localises to the cytosol [243]. Thus excessive expression of HAX1 could be degraded by different pathways.

Immunofluorescent staining revealed the different subcellular distributions of HAX1 isoforms. HAX1.1, HAX1.4 and HAX1.5 showed a “classic” HAX1-mitochondrial pattern whereas HAX1.2 demonstrated a diffuse expression pattern in cells. Structurally, HAX1.2 lacks the first exon, and uses an alternative start codon 27 bases inside exon 2 (of HAX1.1). This produces a protein that lacks the first 26 a.a. of HAX1.1, starting just 3 a.a. before the acid box, with a predicted molecular mass of 28.64 kDa [2]. Interestingly, the N-terminus of HAX1 (a.a. 1-59) was reported as a required sequence for entry into mitochondria [130]. The lack of these N-terminal

amino acids may account for the lack of mitochondrial-specific localisation shown by HAX1.2 and also refine the specific sequence required for mitochondrial localisation.

HAX1 has been reported to regulate cytoskeleton proteins as well as integrins to mediate cell migration. To investigate individual isoforms in migration, assays were performed with the cells expressing different HAX1 isoforms. Results from Transwell migration assays showed that expression of HAX1.2 significantly down regulated cell migration on LAP by 40 % (compared with vector control). In the loss of function experiments, knocking down isoform 2 only by specific siRNA showed the opposite effect increasing migration. Together these data show a very unique role for HAX1.2 which is expressed in every cell type analysed thus far where it could exert its biological activity of negatively regulating cell migration.

The results from cell proliferation assays showed there was no difference in HAX1 isoform expression cells compared with vector control treated cells. However, the level of HAX1.4 was very poor and thus was not possible to conclude the role of this isoform in cell proliferation.

CHAPTER 7. THE ROLE OF HAX1 IN AUTOPHAGY

7.1 Introduction

HAX1 has been implicated as having a substantial role in regulation of autophagy. It has been reported that HAX1 is a substrate for Omi/HtrA2 [30], a protease responsible for degradation of caspases [244], and which also is a positive regulator of autophagy [245]. Moreover, HAX1 is a substrate for caspase-3, a protease that can cleave Beclin-1 to inhibit autophagy during the terminal stages of apoptosis [246]. A recent study also demonstrated a direct link between HAX1 and autophagy. Li *et al* showed that HAX1 inhibits autophagy by binding to Beclin-1 and the authors suggested that Omi/HtrA2 activates autophagy through interactions with, or cleavage, of HAX1 [87]. Taken together, HAX1 has been indicated to regulate autophagy, which is an important process for tumourigenesis. Thus I investigated further the role of the different HAX1 isoforms in autophagy in this section.

7.2 Results

7.2.1 Chloroquine (CQ) induces autophagosome accumulation in VB6 cells.

To investigate the association of HAX1 and autophagy, chloroquine (CQ) was used to regulate autophagy via autophagosome formation [81,85]. CQ inhibits autophagy by raising the lysosomal pH, which in turn, leads to inhibition of the fusion of the autophagosomes with lysosomes and consequently lysosomal enzyme-dependent

protein degradation is inhibited (Figure 7.1, a) [81]. The microtubule associated protein light chain 3b-II (LC3b-II) was used as a marker for the induction of autophagy since, during autophagy, cytosolic LC3b-I is processed to its lipidated form, LC3b-II [81]. The LC3b-II associates with newly formed autophagophores and subsequently participates in both membrane elongation and cargo recognition, and its presence continues on mature autophagosomes ([81] and Figure 7.1 [a]). Thus, accumulation of a punctate LC3b pattern in cells represents the formation of autophagosomes and evidence of the process of autophagy (Figure 7.1, a) [81,247-249].

To determine whether CQ causes an accumulation of autophagic vesicles in VB6 cells, the levels of LC3b were monitored in cells treated with CQ. The cell lysates were collected from VB6 cells treated with 50 µM CQ for 24 hours and subjected to Western blot analysis using an LC3b antibody that recognises both cytosolic LC3b-I and the autophagy-specific LC3b-II. Figure 7.1 (b) shows there was a significant increase in the level of LC3b-II expressed in the CQ-treated cells compared with the basal endogenous expression of LC3b in the untreated cells, as determined by Western blotting. To confirm that autophagosomes form in VB6 cells, the cells also were examined by confocal microscopy. Immunofluorescent staining showed the presence of LC3b positive vesicles in the cytoplasm of cells treated with CQ (Figure 7.1, c). In contrast, no such vesicles were detected in control cells (Figure 7.1, c).

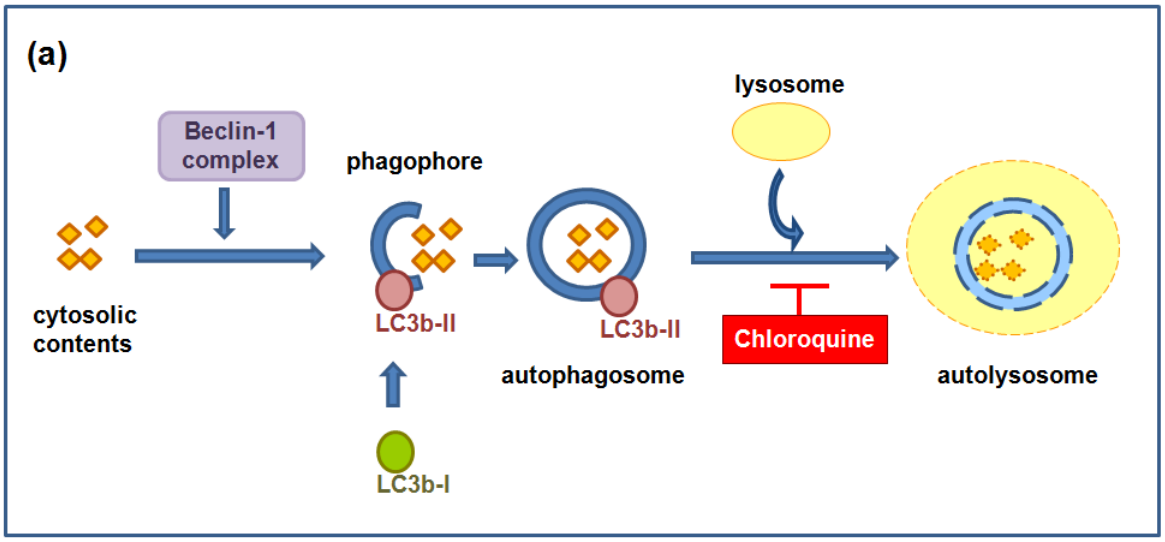
(a)
Beclin-1 complex
phagophore
lysosome
cytosolic contents
LC3b-II
LC3b-II
Chloroquine
autophagosome
autolysosome
LC3b-I

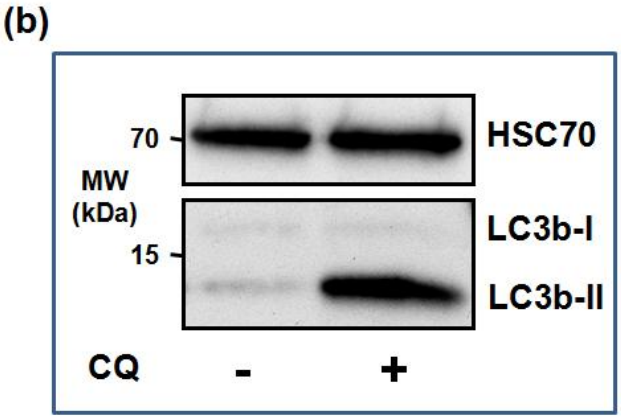
(b)
70
HSC70
MW (kDa)
LC3b-I
15
LC3b-II
CQ
-
+

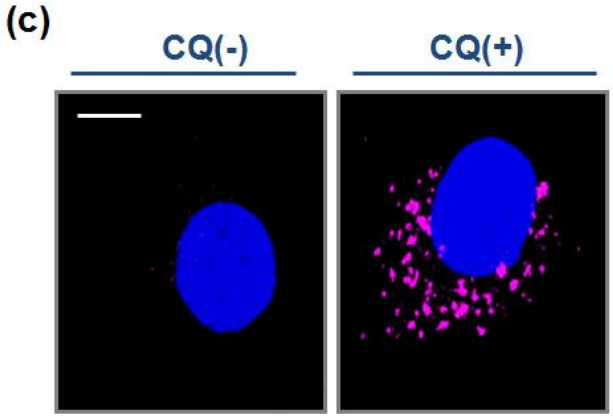
(c)
CQ(-)
CQ(+)

Figure 7.1 Chloroquine (CQ) induces autophagosome accumulation in VB6 cells.

(a) Schematic diagram of autophagy. Autophagy is a catabolic process that results in the degradation of the cytosolic contents including abnormal protein aggregates and excess or damaged organelles. The general process of autophagy involves sequestration of cytosol contents into a double-membrane vesicle, termed the autophagosome, which then fuses with lysosomes to become autolysosomes where the cargo is degraded by acidic lysosomal enzymes. The Beclin-1 complex is essential for initiation of the formation of the phagophore. Cytosolic LC3b-I is then conjugated to phosphatidylethanolamine (PE) as the autophagy specific form LC3b-II which attaches to the autophagosome membrane. CQ is an inhibitor of autophagy by blocking lysosome–autophagosome fusion and the subsequent lysosomal protein degradation. (b) Western blot analysis of VB6 whole cell lysates collected at 24 hours after 50 µM CQ treatment. Western blotting showed an increased level of autophagy specific LC3b-II expression in CQ-treated cells (CQ[+]). HSC70 served as loading control. (c) VB6 cells plated on coverslips were treated with 50 µM CQ for 24 hours and then LC3b was detected by fluorescence immunochemistry (LC3b Ab; Cell Signalling). The confocal microscopy images demonstrated the accumulation of punctate LC3b immunoreactivity (magenta) in CQ-treated cells [CQ(+)] whereas the untreated cells [CQ(-)] did not display any LC3b staining. Cell nuclei were counterstained with DAPI (blue). Scale bar= 10µm

7.2.2 Endogenous HAX1 is not colocalised with autophagic vesicles

To investigate whether HAX1 physically localised to the autophagosome, confocal microscopy was used to examine the subcellular localisation of HAX1 in CQ-treated cells. VB6 cells were exposed to 50 μM CQ for 24 hours to induce the accumulation of autophagosomes and both HAX1 and LC3b antibodies were used in double immunofluorescence staining experiments. Confocal images showed that the endogenous HAX1 was localised in its typical mitochondrial-like pattern (green) whereas anti-LC3b antibody identified cytoplasmic vesicles (red) (Figure 7.2). Thus there is no colocalisation observed for endogenous HAX1 and LC3b (Figure 7.2) in VB6 cells.

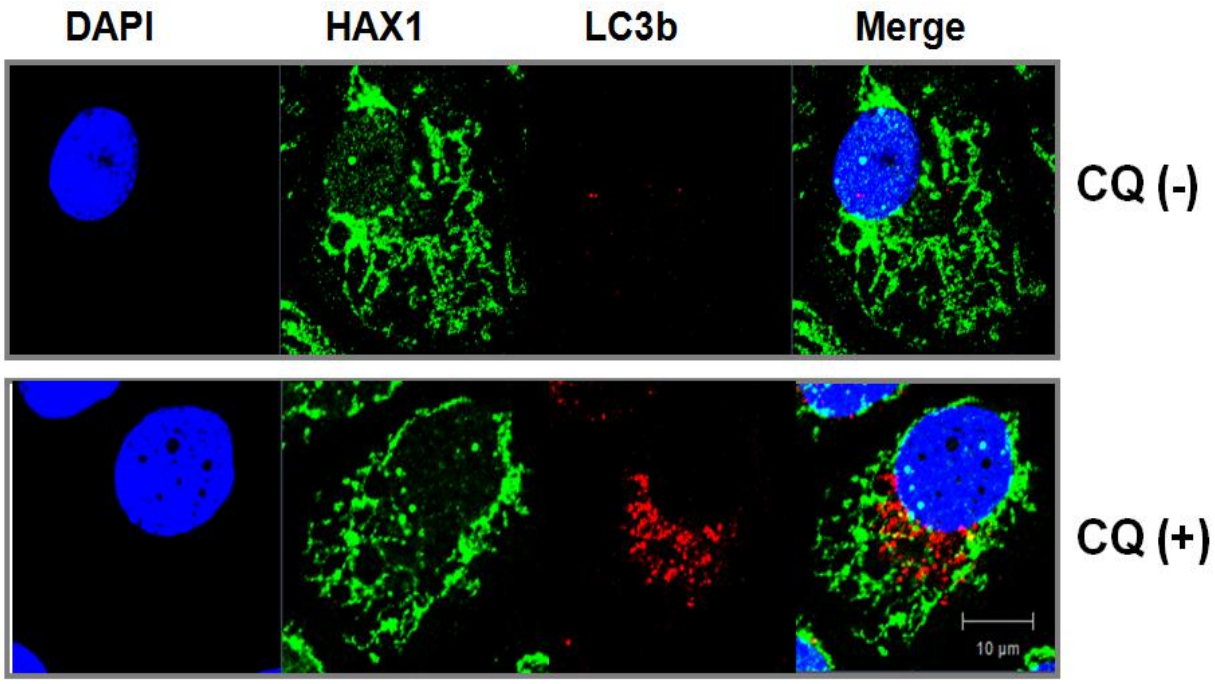

Figure 7.2 HAX1 does not colocalise to autophagosomes.

VB6 cells were treated with 50 µM Chloroquine (CQ) for 24 hours and then the cells were fixed and permeabilised before labelling for HAX1 (RD, green) and autophagosomes (LC3b; Cell Signalling, red), and nuclei (DAPI, blue). Confocal microscopy images demonstrated the accumulation of LC3b immunoreactivity in CQ-treated cells compared with the absence of LC3b staining in CQ(-) cells, confirming CQ induction of autophagosomes. HAX1 expression pattern did not colocalise with the LC3b staining and remained in a mitochondrial-like pattern. Scale bar indicates 10µm.

7.2.3 Autophagy is activated by both serum starvation and rapamycin treatment in VB6 cells

Although there appeared to be no physical colocalisation of HAX1 and autophagosomes, the study from Li *et al* still suggested HAX1 regulates autophagy by repressing Beclin-1 [87]. In order to investigate the role of HAX1 in autophagy, I first examined whether autophagy is activated in response to different stimuli in VB6 cells. It was reported that rapamycin or amino acid deprivation induced autophagic flux [250,251], but the sensitivity to these stimuli depended on the cell type [78]. Therefore I cultured VB6 cells in nutrient-rich growth media or incubated them for 0.5, 2, 4, 6, 24 and 48 hours in serum-deficient media under what represent starvation conditions. Western blotting showed that maximum expression of LC3b-II and Beclin-1 increased at 6 hours and decreased after 24 hours (Figure 7.3, a).

To test rapamycin-induced autophagy, the VB6 cells were treated with 1, 10, 20 μM of rapamycin for 24 or 48 hours in growth media. Wetsern Blot analysis showed an increase in expression of LC3b-II and Beclin-1 in response to all concentrations of rapamycin used (Figure 7.3, b). Thus at 24 hours there was a 1.8 fold increase in LC3b-II at 1μM, 1.6 fold at 10 μM and 1.3 fold at 20 μM. Beclin-1 was increased 1.5, 1.6 and 2-fold for all 3 concentrations. At 48 hours the increase in LC3b-II was slightly reduced (maximum 1.2 fold at 1 μM) whereas Beclin-1 showed maximum expression at 10 μM (3.5 fold). However, it should be noted that at 48 hours rapamycin treatment, the cells clearly exhibited cytotoxicity (data not shown). Taking the data together, 6 hours of serum starvation and 1μM rapamycin treatment

for 24 hours were established as the parameters to be used for autophagy induction in my study.

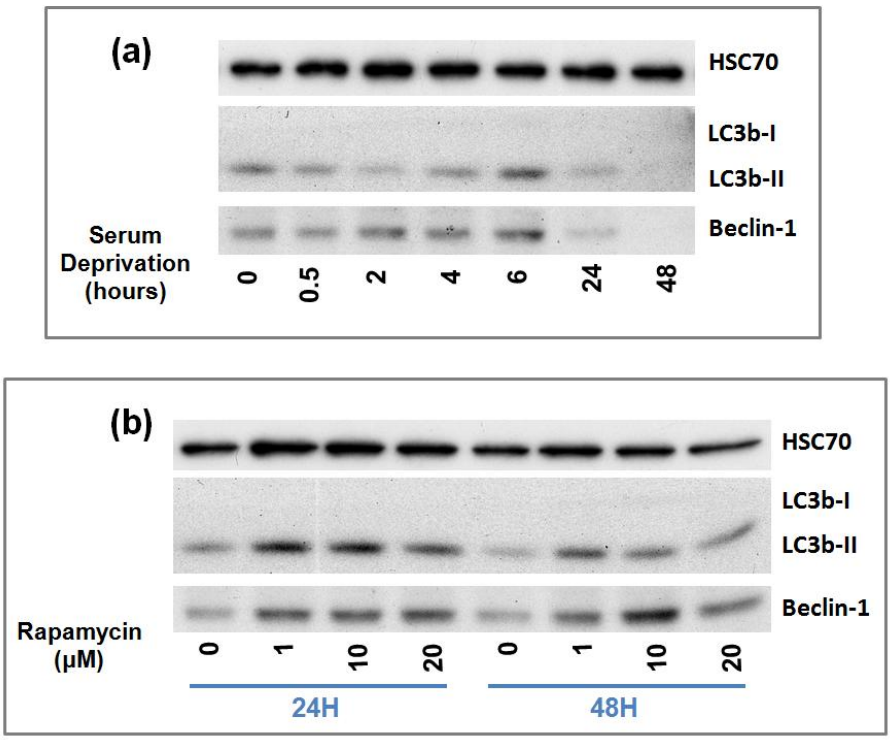

Figure 7.3 Induction of autophagy in VB6 cells by serum starvation and rapamycin treatment.

(a) VB6 cells were cultured in nutrient-rich growth media or incubated for 0.5, 2, 4, 6, 24, 48 hours under serum starvation conditions. Cells were then lysed and the proteins resolved by SDS-PAGE. Western blotting showed increased levels of the autophagy-specific protein LC3b-II in response to serum deprivation for up to 6 hours, a similar response was seen for Beclin-1 expression. By 24 hours the level of LC3b-II and Beclin-1 had diminished dramatically. (b) For the rapamycin-induced autophagy, the VB6 cells were treated with 1, 10 or 20 μM of rapamycin for 24 or 48 hours. Western blot was employed to detect endogenous LC3b-I, LC3b-II and Beclin-1. Data showed that, relative to the untreated cells (0 μM), the LC3b-II and Beclin-1 protein levels were increased in all rapamycin treatments (1, 10, 20 μM) at both the first 24 hours and 48 hours treatments.

7.2.4 Endogenous HAX1 negatively regulates autophagy

To investigate the role of endogenous HAX1 in autophagy, VB6 cells were treated with control siRNA (siNTC) or HAX1 siRNA (si86) and cultured for 24 hours in growth media as control (Figure 7.4, a, lane 1 and 2) or 1μM rapamycin for 24 hours (Figure 7.4, a, lane 3 and 4), or serum starvation for 6 hours (Figure 7.4, a, lane 5, 6) to induce autophagy. Western blots showed that, in the control siRNA (siNTC) treated cells, the amount of Beclin-1 and LC3b-II increased after rapamycin and serum deprivation treatments, indicating increased autophagy flux (Figure 7.4, a, lane 3 and 5 compared with 1, densitometry shown in b and c). Western blotting showed that the HAX1 expression level was sufficiently inhibited by the si86 siRNA (Figure 7.4, a, lane 2, 4, 6) and HAX1 depletion increased levels of both LC3b-II and Beclin-1 (Figure 7.4, a, 4 and 6) compared with control cells (Figure 7.4, a, 3 and 5) in response to both rapamycin and serum starvation. These observations of the elevated levels of Beclin-1 and LC3b-II in HAX1 depleted cells suggest that endogenous HAX1 negatively regulates autophagy.

An accumulation of autophagosomes (as indicated LC3b-II on a Western blot), could reflect either increased autophagosome formation, due to increases in autophagic activity, or reduced turnover of autophagosomes (by blockade the fusion of autophagosome and lysosome) [78]. The latter can occur when there are defects in fusion between the autophagosome and the lysosome, thus a block in autophagy results in autophagosome accumulation and this needs to be differentiated from fully functional autophagy [55]. To evaluate whether the increase of LC3b-II in the HAX1 depleted cells is due to increased autophagy or reduced turnover of autophagosomes,

the autophagy inhibitor chloroquine (CQ) was employed in this experiment. CQ is a molecule that blocks the autophagosome-lysosome fusion by raising intralysosomal pH of lysosomes [78]. The level of LC3b-II would increase in the normal autophagy flux after treating cells with CQ and this allows one to distinguish from the blockage of autophagosome degradation [78,85]. Western blotting showed the LC3b-II level was increased after the inhibition of autophagosome-lysosome fusion by the CQ treatment (Figure 7.5, a and b, lane 3) as compared with the CQ untreated cells (lane 1), indicating that the increased autophagy is due to increased autophagic flux and not to blockage of autophagosome turnover. Compared with the CQ-untreated HAX1 knockdown cells (Figure 7.5, a and b, lane 2), the CQ treatment (lane 4) also showed increased LC3b-II levels indicating there was competent autophagy flux. Densitometry was used to analyse the change from three independent Western blot analysis (Figure 7.5, b). Taken together, the data showed HAX1 depletion increased the induction of autophagy flux but did not affect the turnover of autophagosomes; these data therefore suggested that endogenous HAX1 is a negative regulator for autophagy.

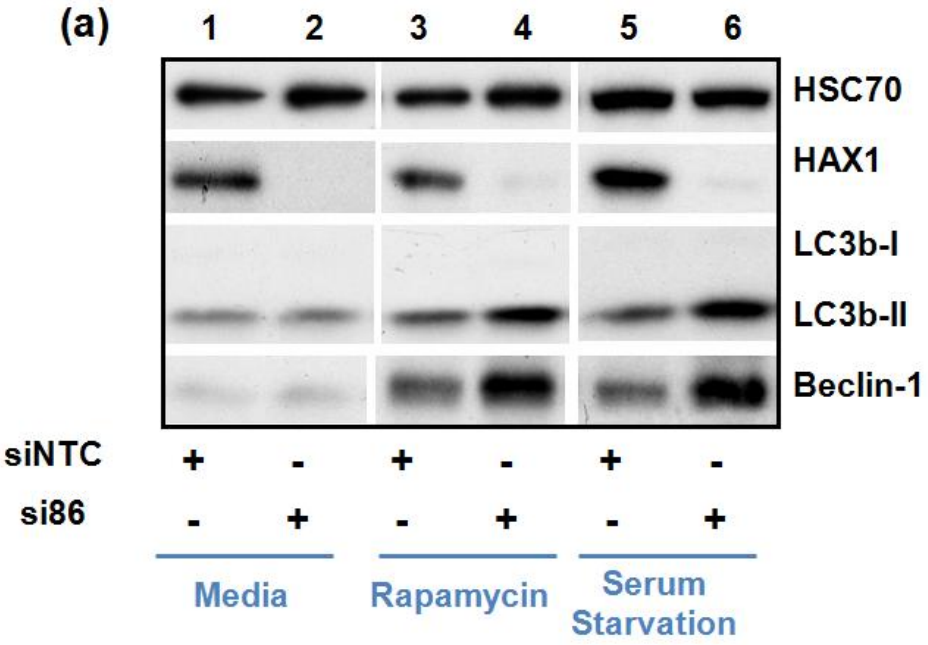
(a)
1
2
3
4
5
6
HSC70
HAX1
LC3b-I
LC3b-II
Beclin-1
siNTC
si86
Media
Rapamycin
Serum Starvation

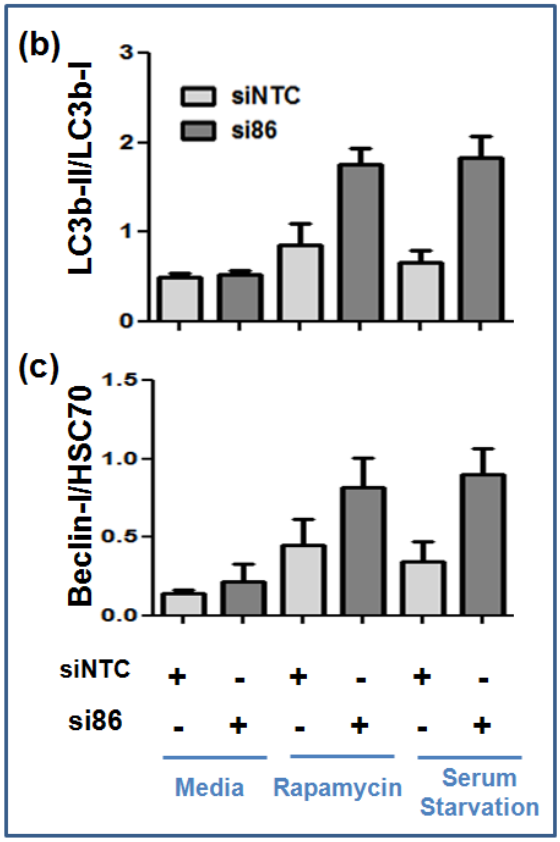
(b)
LC3b-II/LC3b-I
siNTC
si86
(c)
Beclin-I/HSC70
siNTC
si86
Media
Rapamycin
Serum Starvation

Figure 7.4 Endogenous HAX1 suppresses autophagy.

(a) VB6 cells were transfected with HAX1 siRNA (si86) or control siRNA (siNTC). After 24 hours incubation, the cells were then cultured in nutrient-rich growth media (lane 1, 2) or in 1μM rapamycin treatment for 24 hours (lane 3, 4) or incubated in starvation conditions for 6 hours (lane 5, 6) Lane 2, 4, 6 showed the efficient HAX1 protein knockdown by HAX1 siRNA (si86). Induction of autophagy with either Rapamycin (lane 3 and 4) or serum starvation (lane 5 and 6) resulted in an increased expression of both LC3b-II and Beclin-1. Moreover, in the absence of endogenous HAX1 (lane 4 and 6), this increase was enhanced further. Thus HAX1 inhibits autophagy induced by these methods. The densitometry data represent three independent experiments and are expressed as mean +/- 1 SD.

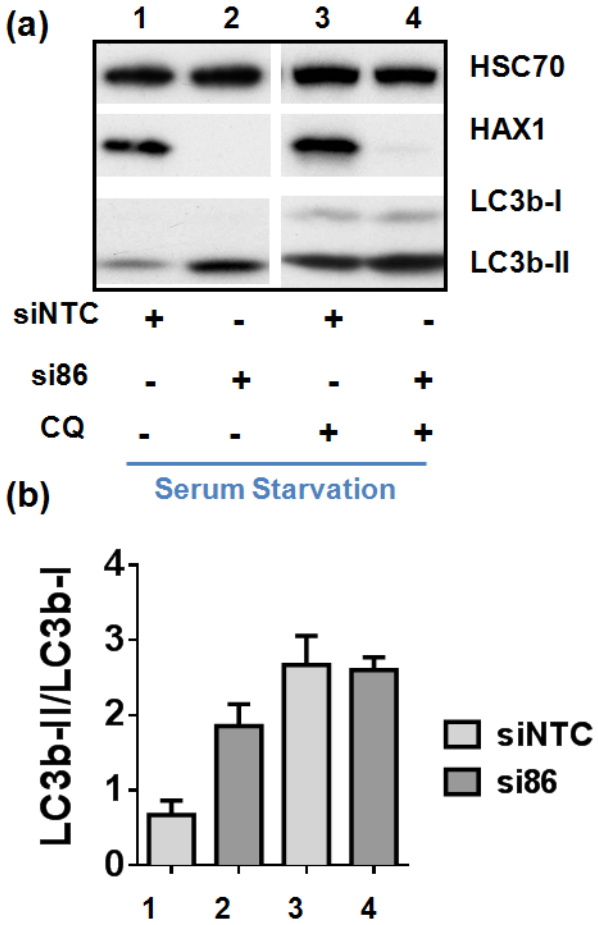

Figure 7.5 HAX1 does not affect autophagosome turnover.

VB6 cells were treated with HAX1 siRNA (si86) or control siRNA (siNTC) for 24 hours. Media was then replaced with serum-free media or serum free-media with 50M CQ for 6 hours. The cell lysates were harvested and subjected to Western blot. HAX1 Blot showed the efficient HAX1 knockdown in the siRNA treated cells (lane 2 and 4). LC3b and Beclin-1 showed the increase of autophagy flux after serum starvation in HAX1 depleted cells (lane 2) compared with control cells (lane 1). CQ treatment showed increased LC3b-II in both control cells (lane 3) and HAX1 depleted cells (lane 4) compared with CQ-non-treated cells (lane 1 and 2 respectively), indicating the existence competent autophagy flux. (b) Densitometry was used to analyse the change from Western blot and it represents three independent experiments and are expressed as mean +/- 1 SD.

7.2.5 HAX1.1, HAX1. 2 and HAX1.5 increase autophagy

To investigate the roles of individual HAX1 isoforms in autophagy, HeLa cells were employed as the model for this study (as this model was that used in the study from Li *et al* [87]). Individual HAX1 isoforms were restored into the HAX1 siRNA-treated HeLa cells (si86) and then cultured in growth media or serum-free media. Western blotting for HAX1 showed the mutant isoforms were protected from the siRNA degradation (Figure 7.6, a and d), again it was apparent that each isoform has a different molecular weight (Figure 7.6, a and d). Serum starvation triggered autophagy as shown in the increased levels of LC3b-II in all cell lines with restored HAX1 isoforms and control (Figure 7.6, a and d, and densitometry showed in e compared with b) and the increased level of Beclin-1 (Figure 7.6, a and b, and the densitometry showed in f compared with c). Note HAX1.4 expression was poor, both LC3b and Becin-1 levels were similar to basal level of vector control (Figure 7.6, d, e and f). In serum starvation treatment (Figure 7.6, d), the expression of LC3b-II (Figure 7.6, e) and Beclin-1 levels (Figure 7.6, f) showed that HAX1.1, 1.2 and 1.5 increased the autophagy flux compared with the control vector (vec) whereas HAX1.4 exhibited weak expressing level therefore is unable to draw conclusion (Figure 7.6, d). These data suggested HAX1.1, HAX1.2 and HAX1.5 induce autophagy by increasing Beclin-1 and LC3b-II levels.

To evaluate the role of HAX1 isoforms in the turnover of autophagosomes, CQ treatments were also included in the experiments. If the autophagy flux is competent (no blockage in the autophagosome-lysosome fusion) in the cell, an increased LC3B-II level should be observed after CQ treatment. Western blotting showed that the

LC3b-II level increased in vector control cells after CQ treatment (Figure 7.6, h) compared with non-CQ treatment (Figure 7.6, e), indicating the presence of a competent autophagy flux. Thus, it was concluded that the increased LC3b-II and Beclin-1 levels were due to the increased induction of autophagy in control cells. On the other hand, LC3b-II did not increase in HAX1.1, HAX1.2, HAX1.4 (with poor expression) and HAX1.5 expressing cells after the inhibition of autophagosome-lysosome fusion by CQ (Figure 7.6, h compared with e), indicating the autophagosome-lysosome degradation blockage had occurred in these isoform expressing cells. Taken together, the data appear to indicate that HAX1.1, HAX1.2 and HAX1.5 positively regulate autophagy by increasing the activation of autophagy (increased Beclin-1 level in serum-starvation) and also by blocking the lysosome-dependent degradation (unchanged LC3b-II in CQ treatment).

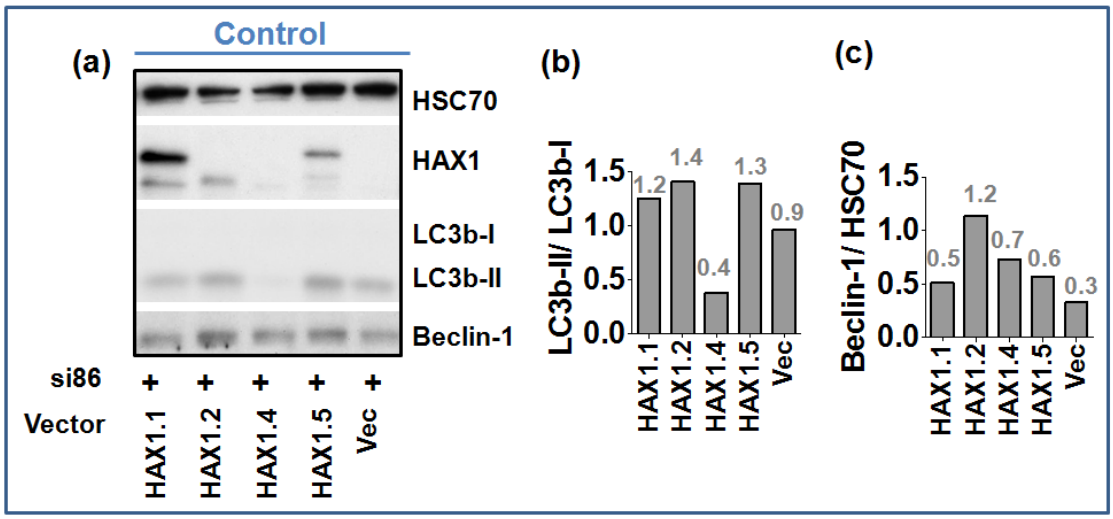
Control
(a)
HSC70
HAX1
LC3b-I
LC3b-II
Beclin-1
si86 + + + + +
Vector HAX1.1 HAX1.2 HAX1.4 HAX1.5 Vec
(b)
LC3b-II/ LC3b-I
1.2 1.4 0.4 1.3 0.9
HAX1.1 HAX1.2 HAX1.4 HAX1.5 Vec
(c)
Beclin-1/ HSC70
0.5 1.2 0.7 0.6 0.3
HAX1.1 HAX1.2 HAX1.4 HAX1.5 Vec

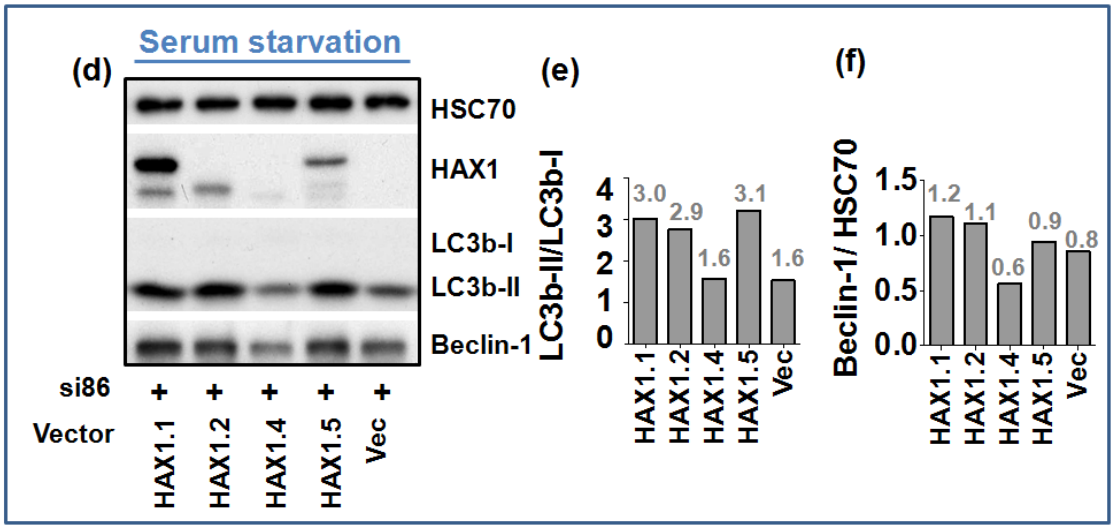
Serum starvation
(d)
HSC70
HAX1
LC3b-I
LC3b-II
Beclin-1
si86 + + + + +
Vector HAX1.1 HAX1.2 HAX1.4 HAX1.5 Vec
(e)
LC3b-II/LC3b-I
3.0 2.9 1.6 3.1 1.6
HAX1.1 HAX1.2 HAX1.4 HAX1.5 Vec
(f)
Beclin-1/ HSC70
1.2 1.1 0.6 0.9 0.8
HAX1.1 HAX1.2 HAX1.4 HAX1.5 Vec

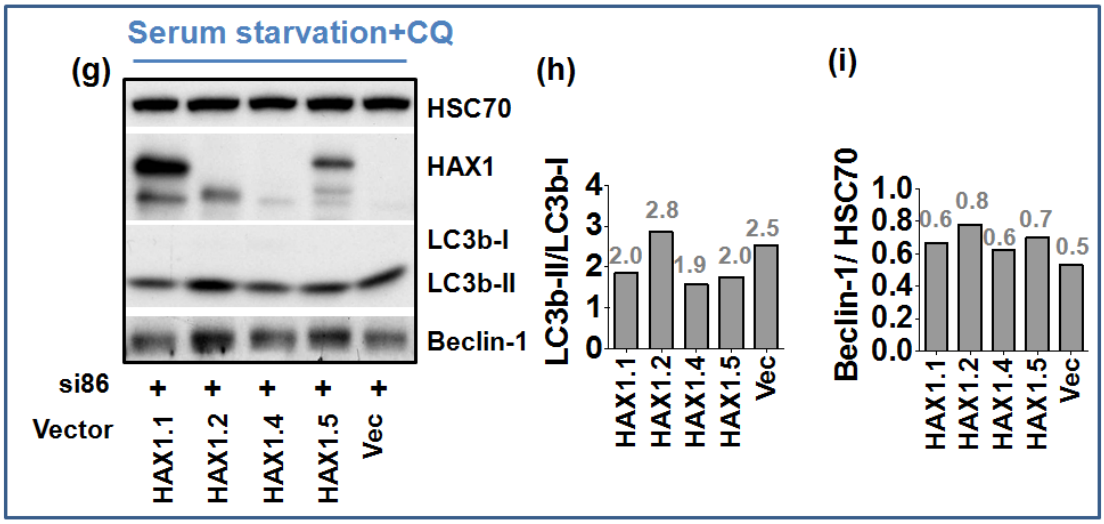
Serum starvation+CQ
(g)
HSC70
HAX1
LC3b-I
LC3b-II
Beclin-1
si86 + + + + +
Vector HAX1.1 HAX1.2 HAX1.4 HAX1.5 Vec
(h)
LC3b-II/LC3b-I
2.0 2.8 1.9 2.0 2.5
HAX1.1 HAX1.2 HAX1.4 HAX1.5 Vec
(i)
Beclin-1/ HSC70
0.6 0.8 0.6 0.7 0.5
HAX1.1 HAX1.2 HAX1.4 HAX1.5 Vec

Figure 7.6 The role of HAX1 isoforms in modulating autophagy.

HAX1 isoforms, or empty vectors, were transfected into HAX1-depleted (si86-treated) HeLa cells. Cells were then cultured in growth media or under conditions of serum starvation for 6 hours and the cell lysate subjected to Western blot. (a, d and g) Blot for HAX1 show the HAX1 isoforms were protected from RNAi degradation (HAX1.4 displayed a weak expression). (d, e and f) shows the general increased LC3b-II and Beclin-1 levels in serum starvation treatment compared with non-treated cells (a, b and c). HAX1.1, HAX1.2 and HAX1.5 showed the more pronounced increase in both LC3b-II and Beclin-1 compared with the control vector (e and f). CQ treatment showed the increased LC3b-II level in control cells (vec; h compared with e) whereas the HAX1 isoforms did not show the same change. The densitometry data represent two independent experiments with similar results.

7.3 Discussion

It is suggested that cancer cells alter autophagy in order to meet the requirement for increased metabolism [252]. Currently, there are nearly 20 clinical trials registered with the USA National Cancer Institute (http://www.cancer.gov/clinicaltrials) exploring anti-autophagy strategies in a variety of human cancers, indicating this is a potential novel approach to target cancer cells [252].

Omi/HtrA2 and caspase-3, the reported binding partners of HAX1, are involved in the regulation of autophagy [245,246]. HAX1 also was reported to associate with autophagy [87]. To examine the role of HAX1 in the autophagy process, I first attempted immunofluorescent staining for HAX1 and LC3b. LC3b proteins play a key role in the maturation of the autophagosome [78]. LC3b precursors are proteolytically processed to form cytosolic LC3b-I [78]. Upon initiation of autophagy, the C-terminal glycine is modified by addition of phosphatidylethanolamine (PE) to form LC3b-II, which translocates to autophagosomes in a punctate distribution which is a pattern that can be observed under microscopic examination [78]. Immunofluorescent staining showed there was no co-localisation or interaction of endogenous HAX1 and autophagosomes (detected as punctate LC3b staining).

Although there was no interaction between HAX1 and LC3b, the study from Li *et al* reported that HAX1 inhibited autophagy by binding to Beclin-1 and it was suggested that Omi/HtrA2 activates autophagy through interactions with, or cleavage of, HAX1 [87]. Thus I performed experiments to examine the association between HAX1 and

the autophagy molecules Beclin-1 and downstream LC3b-II. Western blot showed that HAX1 depletion by siRNA increased the levels of Beclin-1 and LC3b-II in both rapamycin- and serum starvation- induced autophagy. CQ is a molecule which blocks autophagosome-lysosome fusion by raising intralysosomal pH of lysosomes, therefore it can be used to distinguish the increased autophagy flux from the blockage of autophagosome degradation [78]. CQ treatment increased the level of LC3b-II in si86-treated cells, suggesting the increased autophagy (LC3b-II and Beclin-1) is due to increased autophagic flux. Thses data suggest the inhibitory role of endogenous HAX1 in regulating autophagy and the observation is in line with other study [87].

To evaluate the role of individual isoforms, the mutated isoforms were transfected into the si86-treated cells. Western blot showed HAX1.1, 1.2 and 1.5 increased the LC3b-II and Beclin-1 levels compared with the control vector, whereas HAX1.4 expression was very poor, I cannot confidently conclude anything definite about its likely role in these experiments. Moreover, the levels of LC3b-II were not affected by CQ treatment in HAX1.1, HAX1.2 and HAX1.5 expressing cells, indicating the autophagosome-lysosome degradation blockage had occurred in these isoform expressing cells. Taken together, the data suggest HAX1.1, HAX1.2 and HAX1.5 positively regulate autophagy both by increasing the activation of autophagic flux (increased Beclin-1 level in serum-starvation) and also by blocking the lysosome-dependent degradation (unchanged LC3b-II in CQ treatment). The fact thet endogenous HAX1 and isoforms are conflicting to each other in autophagy regulation is confusing, however these are the results I obtained and the repeatable data indicate the reliability in these experiments. It raises the question that whether

HAX1 isoforms infeluence each other or there are external molecules that control the functions of HAX1, certainly, more investigation is needed.

CHAPTER 8. THE ROLE OF HAX1 IN CELL DEATH

8.1 Introduction

Apoptosis is a complex biological process that kills unrequired cells during animal development, normal homeostasis and the immune response [253]. Apoptosis is mediated by a family of aspartate specific cysteine proteases known as caspases [99]. Among the caspase family, caspase-3, an effector caspase, plays a crucial role in the execution of apoptosis [99]. Caspase-3 is activated by an initiator caspase, such as caspase-9, through cleavage at a specific internal aspartate residue [92]. Activated caspase-3 cleaves downstream substrates such as PARP [poly(ADP-ribose) polymerase], lamin, fodrin, and also Bcl-2, leading to the characteristic morphological changes in apoptotic cells [92,97-99]. Caspase activation is also under delicate and balanced regulation. IAP (inhibitor of apoptosis protein) proteins inhibit caspase activity, whereas Smac/Diablo antagonises IAP [122,254]. XIAP, a ubiquitous IAP, can inhibit both caspase-9, the initiator caspase of the mitochondrial apoptotic pathway, and the downstream effector caspases, caspase-3 and caspase-7 [122,254].

Studies have indicated that HAX1 is involved in apoptosis regulation. HAX1 is a substrate for caspase-3 but overexpression of HAX1 also inhibits caspase-3 catalytic activity and blocks the initiation of apoptosis [117,118]. Other studies also showed HAX1 represses post-mitochondrial caspase-9 activation and cell death during hypoxia-reoxygenation and this protects cardiac myocytes from cell death [21,119]. Moreover, a HAX1/XIAP complex is reported to inhibit apoptosis by enhancing the

stability of XIAP against proteosomal degradation [123]. Additionally, several point mutations and frame shift mutations within the HAX1 gene are associated with neutrophil depletion by causing increased sensitivity to apoptosis and this is linked to the human disease SCN [16,24]. Thus in this chapter I will investigate the role of several HAX1 isoforms in apoptosis.

8.2 Results

8.2.1 Endogenous HAX1 exhibits a diffuse expression pattern in apoptotic cells

HAX1 has been reported to interact with caspase-3 by acting as a substrate for this enzyme [118]. To investigate the subcellular distribution of HAX1 and caspase-3 in apoptosis, 100 μM 5-FU was added to culture for 72 hours to induce cell death in VB6 cells. Indirect four-colour immunofluorescence staining was employed to analyse simultaneously for HAX1, caspase-3, mitochondria and the cell nucleus. Activated caspase-3 was used as the indicator for the apoptotic cells and the staining appeared in the cell nucleus, as reported previously [255,256]. Confocal images showed the activated caspase-3 was observed in the 5-FU treated VB6 cells, indicating that apoptosis had occurred (Figure 8.1, a). Endogenous HAX1 was predominantly concentrated in mitochondria in the cells cultured in growth media whereas in apoptotic cells (caspase-3 staining positive cells) HAX1 appeared in a more diffuse pattern with localisations in nucleus, mitochondria and also cytoplasm (Figure 8.1, a). The images also demonstrated the negative caspase-3 staining under normal conditions (no 5-FU treatment) whereas in the apoptosis conditions, HAX1

was expressed in the cell nucleus where caspase-3 also appeared (Figure 8.1, a). Mitochondrial remodelling and fragmentation have been described in connection with many modes of apoptosis [257], and it was also observed in some apoptotic cells (activated caspase-3 positive cells) after 5-FU treatment (Figure 8.1, b, arrow). Again, Figure 8.1, (b) shows that HAX1 presents a typical mitochondrial staining in the caspase-3 negative cells (Figure 8.1, b, arrow head) whereas it displayed a more diffused pattern in the apoptotic cells (Figure 8.1**,** b , arrow).

In order to confirm the changes of the subcellular localisation of HAX1 which were observed by confocal microscopy, cell fractionation was performed with VB6 cells treated with/without the 100 μM of 5FU. Equivalent amounts of protein extracted from the different cellular fractions were subjected to Western blot. To ensure the purity of each fraction, the appropriate markers were also blotted for indicator proteins (actin for cytosolic marker; β6 interin subunit for heavy membrane marker; lamin for nucleus marker). The data showed HAX1 is expressed abundantly in the heavy membrane fraction and a small amount in the cell nucleus fractions (Figure 8.1**,** c, lane 3, 4, 5, 6). Consistent with the immunofluorescence images, cell fractionation showed the expression level of cytosolic HAX1 is increased by 5-FU treatment (Figure 8.1, c, lane 1 compares with lane 2), a slight increase of HAX1 in the nucleus and heavy membrane fractions was also observed in the 5-FU treatment (Figure 8.1, c, lane 3 compared with lane 4; lane 5 compared with lane 6). Thus endogenous HAX1 relocates/ increases its expression in the cytosol of apoptotic cells.

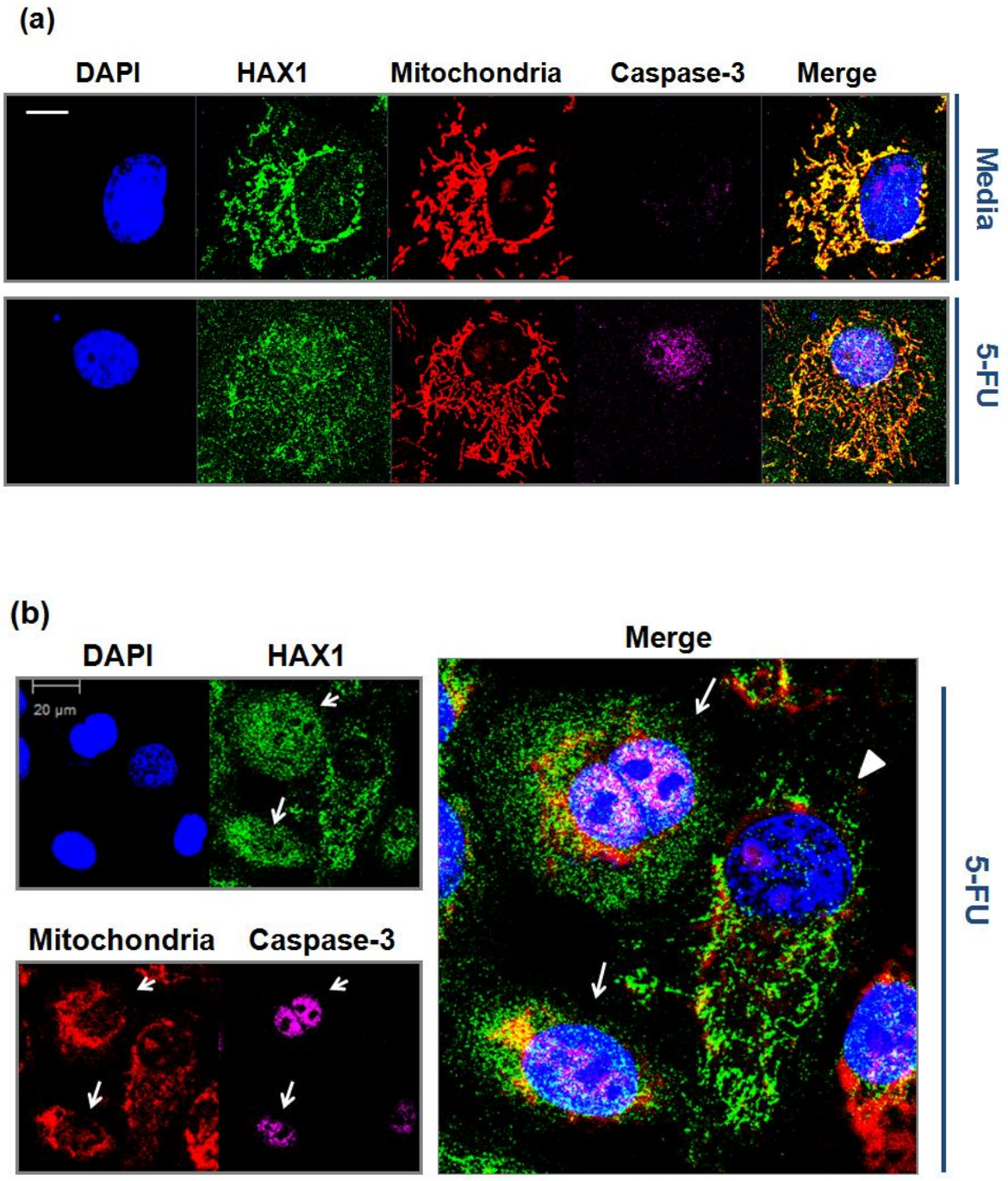
(a)
DAPI
HAX1
Mitochondria
Caspase-3
Merge
Media
5-FU
(b)
DAPI
HAX1
Merge
20 μm
Mitochondria
Caspase-3
5-FU

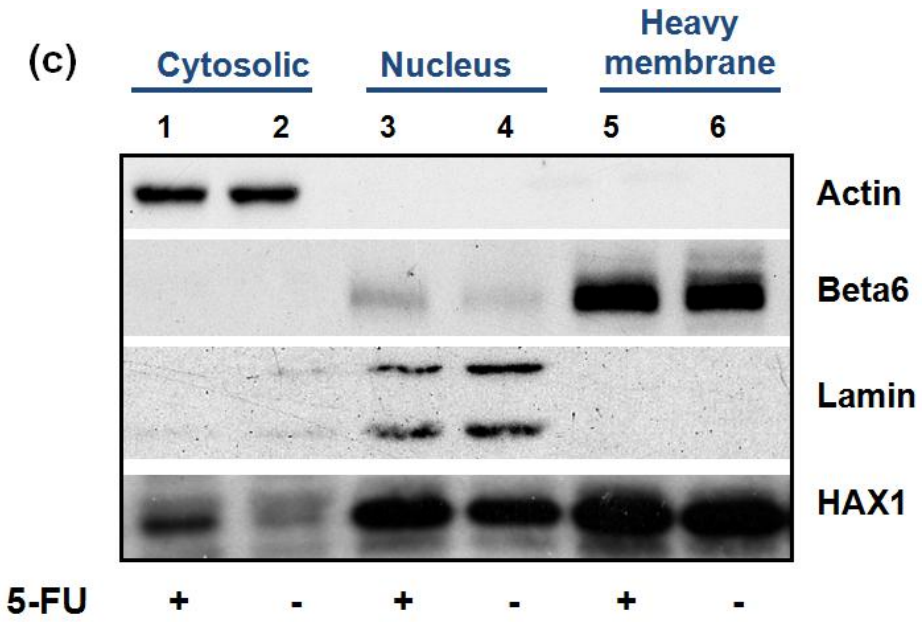

Figure 8.1 HAX1 changes localisation during cell apoptosis

(a) VB6 cells were treated with 100 µM of 5-FU or growth media for 72 hours and the cells were then labelled for HAX1 (RD), nucleus (DAPI; blue), mitochondria (Mitotracker; red) and caspase-3 (Cell signalling; magenta). HAX1 is concentrated in the mitochondria in the cells grown in media whereas a rather diffuse expression pattern, showing nuclear and cytosolic expression, of HAX1 was evident in cells under 5-FU treatment. Caspase-3 was used as an indicator of cell apoptosis. Scale bar =10 µm. (b) Apoptotic cells and non-apoptotic cells in the same field. Arrows indicated the apoptotic cells with positive caspase-3 staining and deformed mitochondria as well as a diffuse HAX1 expression pattern; arrowhead indicates a caspase-3-negative cell with normal mitochondria and mitochondrial HAX1 expression. (c) Equivalent amount of protein extract from cellular fractions showed that HAX1 is dominantly present in heavy membrane and nuclear fractions (lane 3, 4, 5, 6). The cytosolic expression of HAX1 is elevated in the 5-FU treatment (lane 1 compare to lane 2). To ensure the purity of each fraction, the appropriate markers were also Blotted (actin for cytosolic marker; beta6 for heavy membrane marker; lamin for nucleus marker). Note there is weak β6 in the nuclear fraction that may suggest some contamination with the heavy membrane fraction.

8.2.2 Endogenous HAX1 promotes cell apoptosis

Studies have shown that HAX1 regulates HeLa cell apoptosis induced by etopiside [30,118]. Etoposide is a cytotoxic drug that induces cell apoptosis by inhibiting topoisomerase and inducing double-strand breaks in the DNA [258,259]. To investigate further the role of endogenous HAX1 in apoptosis, Etoposide-induced cell death was used as a model in this experiment. HeLa cells were transfected with HAX1 siRNA (si86) or control siRNA (siNTC) and apoptosis was induced with 1μM Etoposide for 24 hours. Western blotting was employed to blot for the apoptotic molecules: cleaved (activated) caspase-3 and the downstream cleaved PARP. Activated caspase-3 is an effector caspase that cleaves the downstream target proteins, such as PARP, and that consequently induce cell apoptosis [98]. Figure 8.2 (a) shows that Etoposide treatment induced cleaved caspase-3 and cleaved PARP confirming cell apoptosis was induced in the control siRNA (siNTC) treated cells. Western blotting showed the efficient knockdown of HAX1 by si86, and this significantly decreased the amount of cleaved caspase-3 and cleaved PARP induced by Etoposide treatment compared with control cells (Figure 8.2, a). To quantify this change, densitometry analysis was performed for cleaved caspase-3 and cleaved PARP from three independent experiments and this is plotted is in Figure 8.2, b and c. These data showed >50% reduction in the levels of cleaved caspase-3 and cleaved PARP in HAX1-depleted cells.

To verify the changes observed from Western blotting, cytotoxic assays were performed with three different cytotoxic drugs: Taxol, Etoposide and 5-FU, each of which exert different mechanisms to induce apoptosis [30,109,259]. Taxol binds to

the microtubules and leads to the cell mitosis arrest [260]; Etoposide acts as a topoisomerase inhibitor to induce DNA strand breaks [258]; and 5-FU irreversibly inhibits thymidylate synthase [261]. HeLa cells were transfected with control siRNA (siNTC) or HAX1 siRNA (si86) and exposed to different concentrations of the cytotoxic agents. The cell viability was measured by the MTT assay after 72 hours. Compared with the control cells, HAX1 knockdown cells (si86) displayed a small, but significant, increased cell survival in Taxol treatments (Figure 8.2, d and e): HAX1 siRNA significantly increased the cell survival in general ($p<0.05$), especially in the low concentration range treatment (from 0.001-0.1 nM, $p<0.01$). Apexdix III shows three independent Taxol-induced cell death experiments and all three experiments demonstrated the increased cell survival by HAX1 knockdown. In contrast HAX1 knockdown had no consistent effect on cyctotoxicity induced by either etoposide or 5-FU (Appendix IV and Appendix V). Experiments were performed in quadruplicate and repeated three times. In consultation with statistician Adam Brentnall (Barts Cancer Institute), the Mann-Whitney U test was used to analyse the significance of the change in the survival fraction between control cells and HAX1 knockdown cells using the combined data (Figure 8.2, f, g, h). These observations indicate a possible pro-apoptotic function for endogenous HAX1 in Taxol-induced cell death. However, since there was no consistent effect on cell death caused by etoposide or 5-FU, and as these three drugs induce cell death by three different mechanisms, this may indicate that the involvement of HAX1 is determined by the mechanism of activation of the cell-death process.

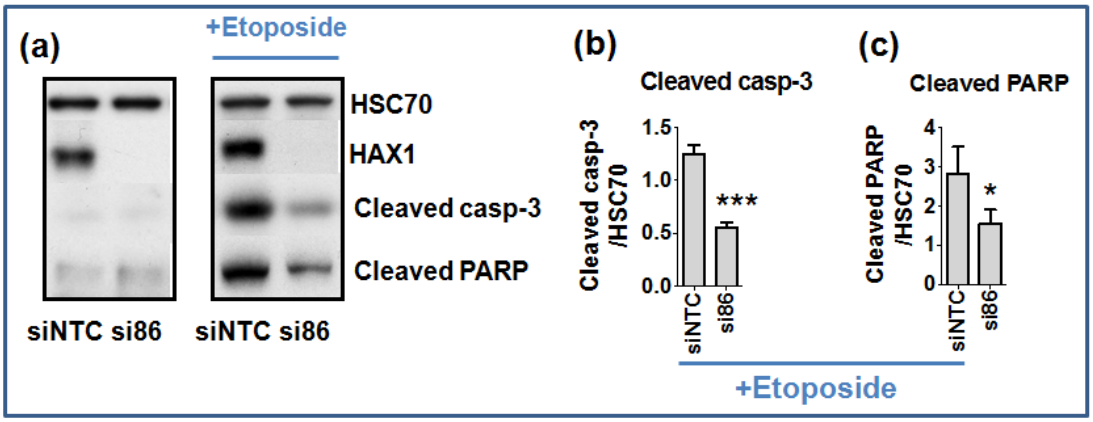
(a)
+Etoposide
HSC70
HAX1
Cleaved casp-3
Cleaved PARP
siNTC si86
siNTC si86
(b)
Cleaved casp-3
Cleaved casp-3 /HSC70
1.5
1.0
0.5
0.0
***
siNTC
si86
(c)
Cleaved PARP
Cleaved PARP /HSC70
4
3
2
1
0
*
siNTC
si86
+Etoposide

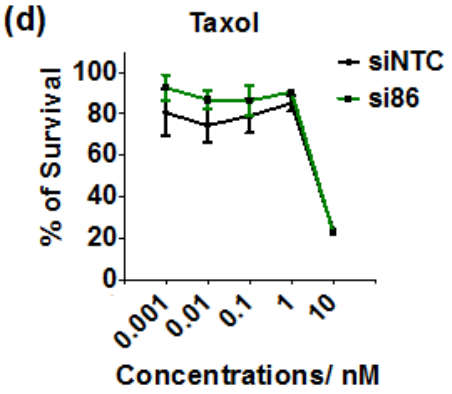
(d)
Taxol
siNTC
si86
% of Survival
100
80
60
40
20
0
0.001
0.01
0.1
1
10
Concentrations/ nM

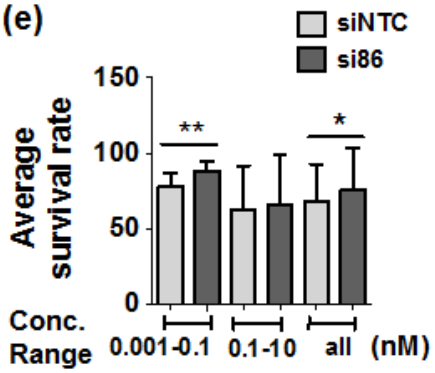
(e)
siNTC
si86
Average survival rate
150
100
50
0
**
*
Conc. Range
0.001-0.1
0.1-10
all
(nM)

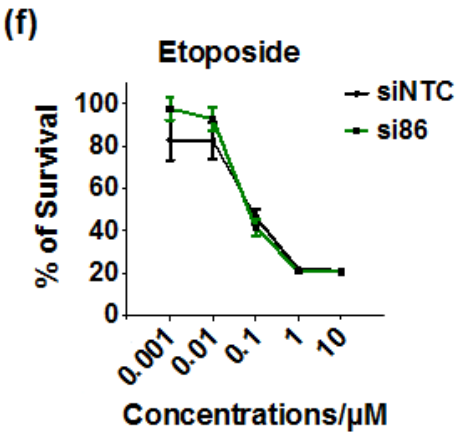
(f)
Etoposide
siNTC
si86
% of Survival
100
80
60
40
20
0
0.001
0.01
0.1
1
10
Concentrations/μM

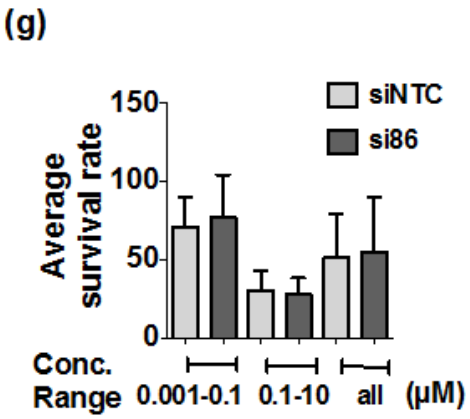
(g)
siNTC
si86
Average survival rate
150
100
50
0
Conc. Range
0.001-0.1
0.1-10
all
(μM)

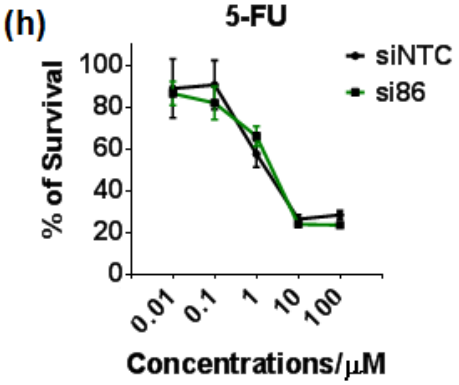
(h)
5-FU
siNTC
si86
% of Survival
100
80
60
40
20
0
0.01
0.1
1
10
100
Concentrations/μM

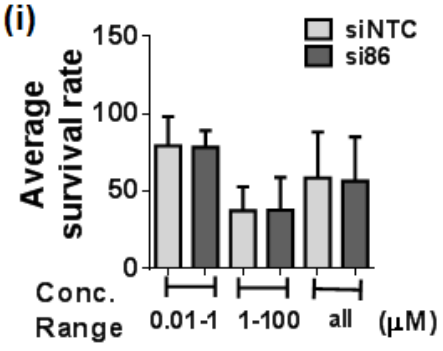
(i)
siNTC
si86
Average survival rate
150
100
50
0
Conc. Range
0.01-1
1-100
all
(μM)

Figure 8.2 The role of endogenous HAX1 in response to cytotoxic drug-induced cell apoptosis and cell death.

(a) Apoptosis was induced by exposure to 1 μM Etoposide for 24 hours. Elevated levels of cleaved caspase-3 and cleaved PARP indicated apoptosis was induced. Western blotting showed the Etoposide-induced increase in cleaved caspase-3 and cleaved PARP were reduced by siRNA knockdown of HAX1. (b, c) Densitometry showed an average >50% reduction in cleaved caspase-3 and cleaved PARP from three independent experiments. (d, f, h) MTT assays were performed with cells treated with various concentrations of Taxol (d), Etoposide (f) and 5-FU (h) for 72 hours. HAX1 knockdown (si86) cells displayed increased cell viability compared with control cells (siNTC) in treatments with Taxol. Data are presented as percentage of survival which base on the optical density (OD) readings of quadruplicates. The data show one of three indenedent experiment and are presented as mean +/- 1 S.D. (e, g, i). The results from all three experiments are shown in Appendix III, IV and V. Mann-Whitney U test was employed to determine statistical significance. *, $P < 0.05$, **, $P < 0.01$.

8.2.3 HAX1.1 increases the levels of cleaved caspase-3 and cleaved PARP

To investigate the roles of individual isoforms in cell apoptosis, HAX1.1 was transfected into the HAX1 transiently knocked-down cells (by si86) and then exposed to 1μM Etoposide for 24 hours. Cell lysates were prepared and subjected to Western blotting analysis. Figure 8.3 (a) shows that the HAX1.1 was protected from the siRNA degradation. The levels of cleaved caspase-3 and downstream cleaved PARP were significantly increased by the presence of HAX1.1 during the Etoposide-induced cell apoptosis (Figure 8.3, a, b). Again, cytotoxic assays were performed with three different cytotoxic drugs: Taxol, Etoposide and 5-FU. The cells were exposed to different concentrations of drugs for 72 hours and the cell viability was determined by MTT assay. Data show HAX1.1 expressing cells did not affect cell viability in all treatments (Figure 8.3, d, e, f, g, h and i; Appendix VI, VII and VIII). Althought one of three independent experiments showed a significant decreased cell survival caused by HAX1.1 in low concentration (0.001-0.1 μM) of Etoposide treatment (Appendix VII, c and d), there was no significant changes observed in the other two experiments (Appendix VII, a, d, e and f). Thus HAX1.1 increases cleaved caspase-3 and cleaved PARP, but does not alter the cell survival after Taxol and 5-FU treatment. It is difficult to draw conclusion in the effect of this isofom in Etoposide-induced cell death due to the inconsistent results.

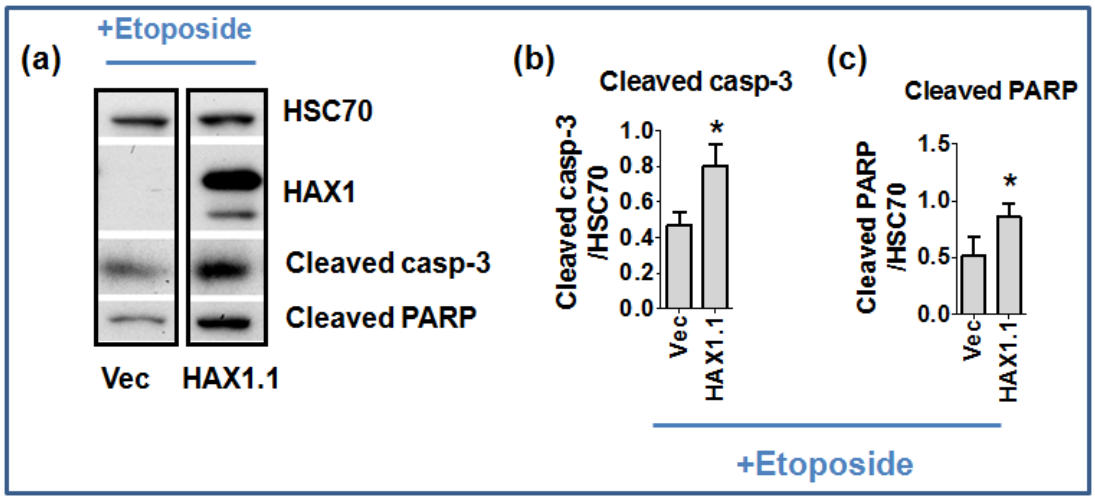
(a)
+Etoposide
HSC70
HAX1
Cleaved casp-3
Cleaved PARP
Vec
HAX1.1
(b)
Cleaved casp-3
Cleaved casp-3 /HSC70
1.0
0.8
0.6
0.4
0.2
0.0
*
Vec
HAX1.1
(c)
Cleaved PARP
Cleaved PARP /HSC70
1.5
1.0
0.5
0.0
*
Vec
HAX1.1
+Etoposide

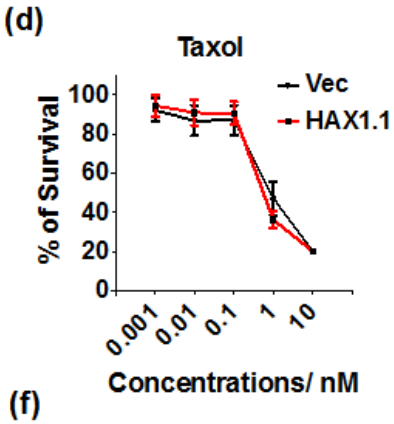
(d)
Taxol
Vec
HAX1.1
% of Survival
100
80
60
40
20
0
0.001
0.01
0.1
1
10
Concentrations/ nM

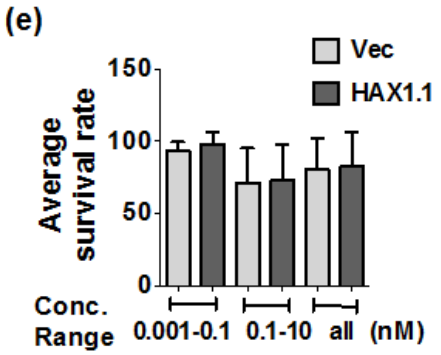
(e)
Vec
HAX1.1
Average survival rate
150
100
50
0
Conc. Range
0.001-0.1
0.1-10
all
(nM)

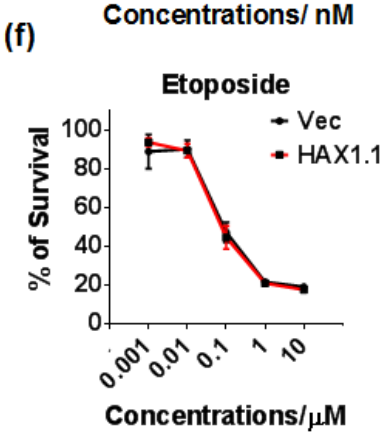
(f)
Etoposide
Vec
HAX1.1
% of Survival
100
80
60
40
20
0
0.001
0.01
0.1
1
10
Concentrations/μM

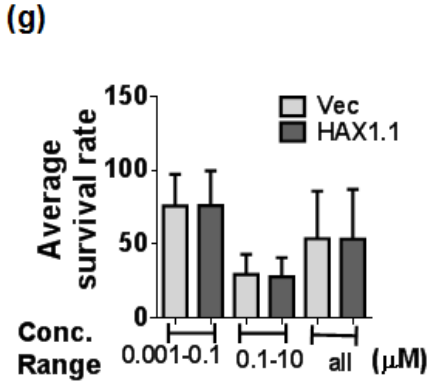
(g)
Vec
HAX1.1
Average survival rate
150
100
50
0
Conc. Range
0.001-0.1
0.1-10
all
(μM)

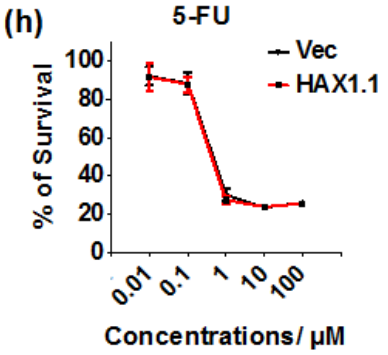
(h)
5-FU
Vec
HAX1.1
% of Survival
100
80
60
40
20
0
0.01
0.1
1
10
100
Concentrations/ μM

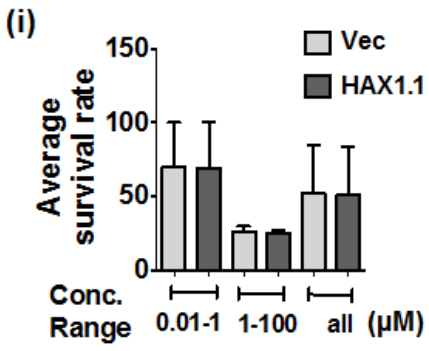
(i)
Vec
HAX1.1
Average survival rate
150
100
50
0
Conc. Range
0.01-1
1-100
all
(μM)

Figure 8.3 The role of HAX1.1 in cytotoxic drug-induced cell death.

(a) HeLa cells were transfected with si86 to knockdown endogenous HAX1 and then restored with HAX1.1. Apoptosis was induced by exposure to 1 μM Etoposide for 24 hours. Western blotting showed that the presence of HAX1.1 increased the amount of cleaved caspase-3 and cleaved PARP compared with vector control (vec: empty vector control). Densitometry from three independent experiments showed an increase in cleaved caspase-3 and cleaved PARP (b and c). (d, f, h) MTT assays were performed with HAX1.1 expressing cells treated with Taxol (d), Etoposide (f) and 5-FU (h) for 72 hours. HAX1.1 expression did not cause changes in cell viability in all drug treatments (d, e, f, g, h and i). Data are presented as percentage of survival which base on the optical density (OD) readings of quadruplicates. The data show one of three indenedent experiment and are presented as mean +/- 1 S.D. (e, g, i). The results from all three experiments are shown in Appendix VI, VII and VIII. Mann-Whitney U test was employed to determine statistical significance.

8.2.4 HAX1.2 promotes cell survival from Etoposide and 5-FU induced cell death

To evaluate the role of HAX1.2 in cell apoptosis, HAX1.2 was transfected into the HAX1 transiently-deficient cells (by si86) which then were exposed to 1μM Etoposide for 24 hours. Cell lysates were then prepared and subjected to Western blotting analysis. Figure 8.4 (a) shows that the mutant HAX1.2 was protected from the siRNA degradation. Western blot demonstrated that there was no significant change in the levels of cleaved caspase-3 and downstream cleaved PARP as a result of the presence of HAX1.2 from three independent experiments (Figure 8.4, a, b, c). Cytotoxic assays were performed with three different cytotoxic drugs. The cells were exposed to different concentrations of drugs for 72 hours and the cell viability was determined by MTT assay. Data showed cell viability was increased with HAX1.2 in the one of three Taxol treatment (Figure 8.4, d and e, Appendix IX). The cell survival also was small but significantly, increased by HAX1.2 in two of three (Figure 8.4, h and i, Appendix XI) 5-FU treatment and in all three independent experiment in Etoposide treatments (Figure 8.4, f and g, Appendix X). The sizes of these changes were not dramatic but the trend was repetable, and thus these observations suggest HAX1.2 protects cells from Etoposide and 5-FU-indiced cell death, possibly, through a caspase-3-independent pathway.

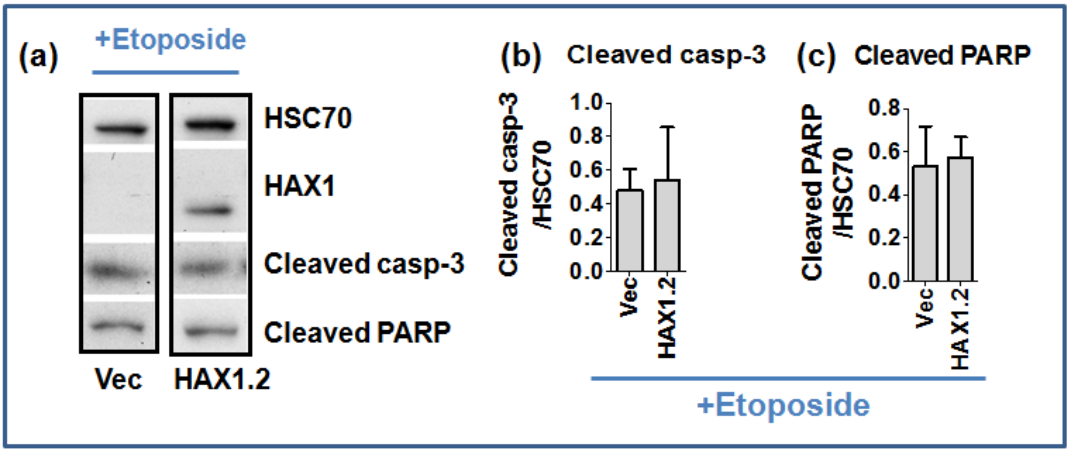
(a)
+Etoposide
HSC70
HAX1
Cleaved casp-3
Cleaved PARP
Vec
HAX1.2
(b) Cleaved casp-3
Cleaved casp-3 /HSC70
1.0
0.8
0.6
0.4
0.2
0.0
Vec
HAX1.2
(c) Cleaved PARP
Cleaved PARP /HSC70
0.8
0.6
0.4
0.2
0.0
Vec
HAX1.2
+Etoposide

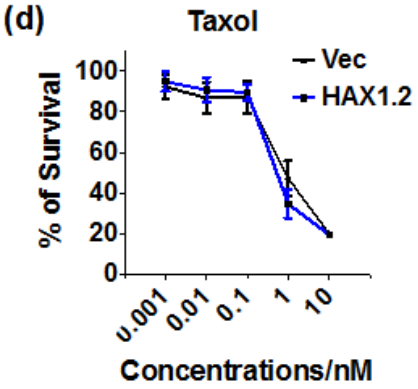
(d)
Taxol
Vec
HAX1.2
% of Survival
100
80
60
40
20
0
0.001
0.01
0.1
1
10
Concentrations/nM

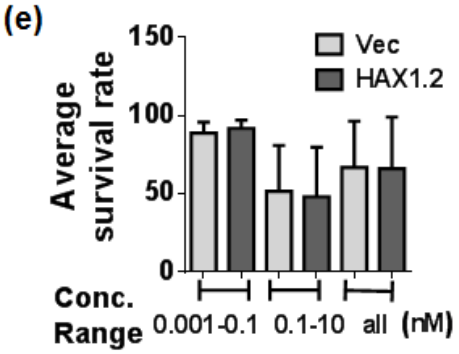
(e)
Vec
HAX1.2
Average survival rate
150
100
50
0
Conc. Range
0.001-0.1
0.1-10
all
(nM)

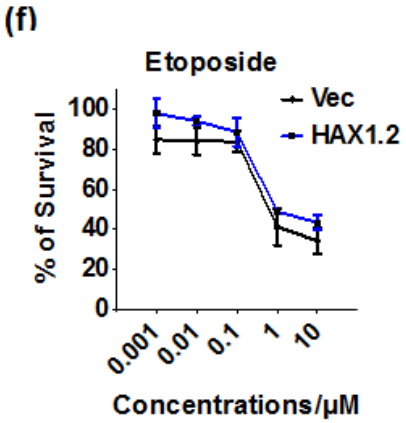
(f)
Etoposide
Vec
HAX1.2
% of Survival
100
80
60
40
20
0
0.001
0.01
0.1
1
10
Concentrations/μM

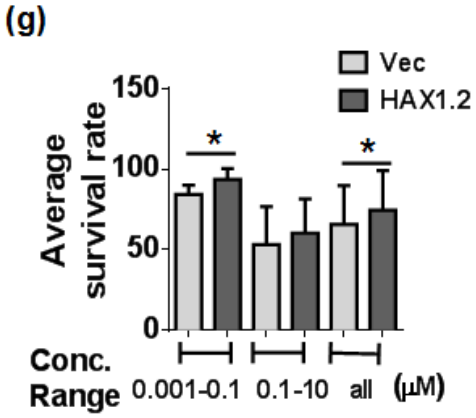
(g)
Vec
HAX1.2
Average survival rate
150
100
50
0
*
*
Conc. Range
0.001-0.1
0.1-10
all
(μM)

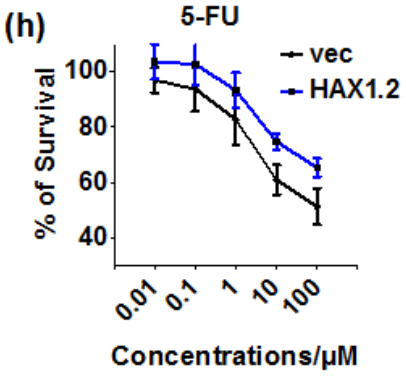
(h)
5-FU
vec
HAX1.2
% of Survival
100
80
60
40
0.01
0.1
1
10
100
Concentrations/μM

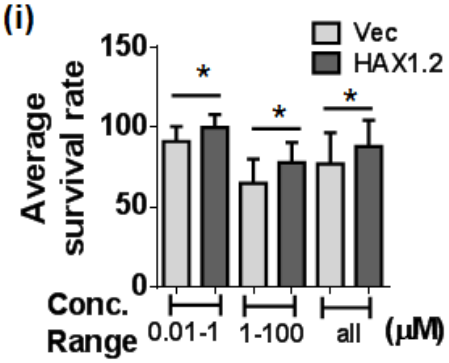
(i)
Vec
HAX1.2
Average survival rate
150
100
50
0
*
*
*
Conc. Range
0.01-1
1-100
all
(μM)

Figure 8.4 HAX1.2 exhibits anti-apoptotic function.

Apoptosis was induced by exposure HeLa cells to 1 μM Etoposide for 24 hours. Western blotting showed no difference in the levels of cleaved caspase-3 and cleaved PARP in cells expressing HAX1.2 induced by Etoposide compared with the control (vec: empty vector control) (a, b, c). MTT assays were performed with cells treated with three different cytotoxic drugs: Taxol (d), Etoposide (f) and 5-FU (h) for 72 hours. Cell expressing HAX1.2 displayed increased cell viability compared with control cells (vec) in Etoposide and 5-FU treatments (f, g, h and i). Data are presented as percentage of survival which base on the optical density (OD) readings of quadruplicates. The data show one of three indenedent experiment and are presented as mean +/- 1 S.D. (e, g, i). The results from all three experiments are shown in Appendix IX, X and XI. Mann-Whitney U test was employed to determine statistical significance. *, $P < 0.05$.

8.2.5 HAX1.5 did not alter cell survival in response to cytotoxic drugs

To evaluate the role of HAX1.5 in cell apoptosis, HAX1.5 was transfected into the HAX1 transiently-knockdown HeLa cells (si86) and such cells then were exposed to 1μM Etoposide for 24 hours. Cell lysates were then prepared and subjected to Western blotting analysis. Figure 8.5 (a) shows that HAX1.5 was protected from the siRNA degradation, it also demonstrated that there was no change in the levels of cleaved caspase-3 or the downstream cleaved PARP in the presence of HAX1.5 (Figure 8.5, a, b and c). Cytotoxic assays were performed with three different cytotoxic drugs. The cells were exposed to different concentrations of drugs for 72 hours and the cell viability was determined by MTT assay. The results show that there was no change in cell survival in HAX1.5 expressing cells compared with control cells in overall drug treatments (Figure 8.5, d, e, f, g, h and i). Significant increased cell survival was also observed in HAX1.5 expressing cells in one of each three independent experiments (Appendix XII-XIV). The changes were very small and not repeatable. It is difficult to draw a conclusion in this isoform as the data were not consistent.

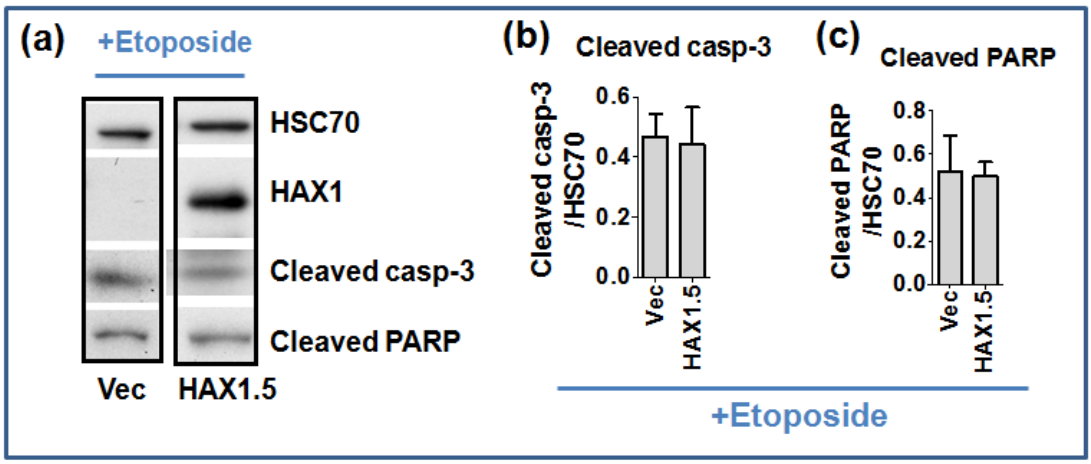
(a)
+Etoposide
HSC70
HAX1
Cleaved casp-3
Cleaved PARP
Vec
HAX1.5
(b)
Cleaved casp-3
Cleaved casp-3 /HSC70
0.6
0.4
0.2
0.0
Vec
HAX1.5
(c)
Cleaved PARP
Cleaved PARP /HSC70
0.8
0.6
0.4
0.2
0.0
Vec
HAX1.5
+Etoposide

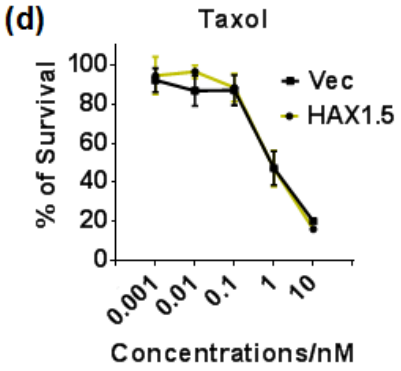
(d)
Taxol
% of Survival
100
80
60
40
20
0
Vec
HAX1.5
0.001
0.01
0.1
1
10
Concentrations/nM

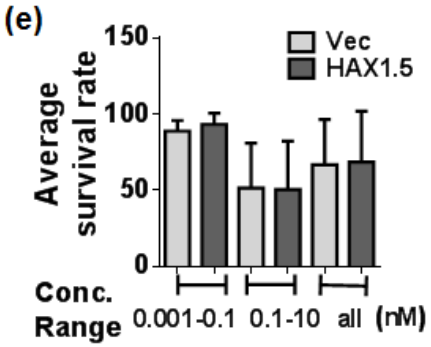
(e)
Average survival rate
150
100
50
0
Vec
HAX1.5
Conc. Range
0.001-0.1
0.1-10
all
(nM)

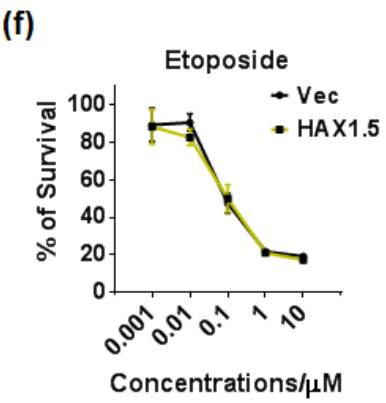
(f)
Etoposide
% of Survival
100
80
60
40
20
0
Vec
HAX1.5
0.001
0.01
0.1
1
10
Concentrations/μM

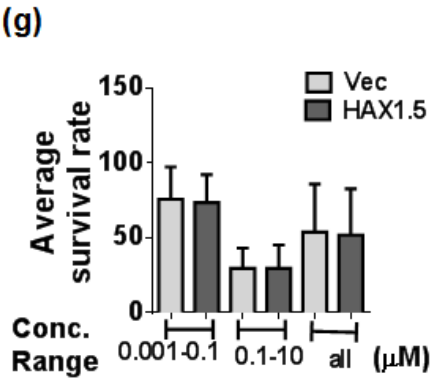
(g)
Average survival rate
150
100
50
0
Vec
HAX1.5
Conc. Range
0.001-0.1
0.1-10
all
(μM)

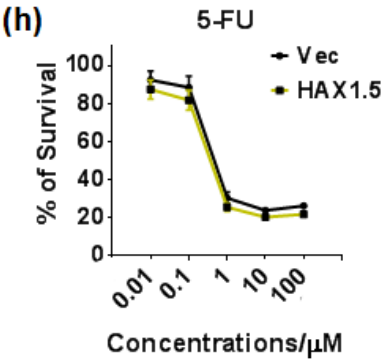
(h)
5-FU
% of Survival
100
80
60
40
20
0
Vec
HAX1.5
0.01
0.1
1
10
100
Concentrations/μM

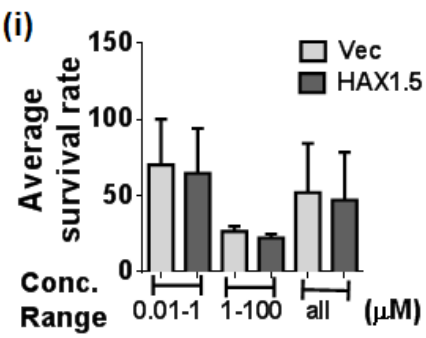
(i)
Average survival rate
150
100
50
0
Vec
HAX1.5
Conc. Range
0.01-1
1-100
all
(μM)

Figure 8.5 HAX1.5 and cell death.

(a, b, c) Apoptosis was induced by exposure of HeLa cells to 1 μM Etoposide for 24 hours. Western blotting showed no difference in the levels of cleaved caspase-3 and cleaved PARP in cells expressing HAX1.5 compared with the control (vec: empty vector). MTT assays were performed with cells treated with three different cytotoxic agents: Taxol (d), Etoposide (f) and 5-FU (h) for 72 hours. Mann-Whitney U test was employed to determine statistical significance (e, g, i). Overall, HAX1.5 did not alter the cell survival (d, e, f, g, h and i). But small and significant increases were observed in one of three independent experiments of all three drugs (Appendix XII-XIV). Data are presented as percentage of survival which base on the optical density (OD) readings of quadruplicates. The data show one of three indenedent experiment and are presented as mean +/- 1 S.D.

HAX1 isoforms	Significant changes of drug induced cell death								
	Taxol			Etoposide			5-FU		
	Results from three independent experiments								
si86 (HAX1-null)	↑	↑	↑	-	-	-	↑	-	-
HAX1.1	-	-	-	↓	-	-	-	-	-
HAX1.2	↑	-	-	↑	↑	↑	↑	↑	-
HAX1.5	↑	-	-	↑	-	-	↑	-	-

Table 8.1 Summary of the effect of the HAX1 isoforms in drug induced cell death.

This table summarises the significant changes by HAX1 knockdown (si86) and HAX1 isoform restoration in cell death from three independent experiments, which showed in three columns under each drug trestments. Mann-Whitney U test was used to analyse the significant changes. "-" indicates there is no significant change and the arrow show the significant increase or decrease in cell death upon different drug treatments. The experiments were performed in quadruplicate and the detailed results were shown in Appendix III- XIV.

8.2.6 HAX1 isoforms are degraded during cell death

It is reported that HAX1 is degraded by caspase-3 and Omi/HtrA2 during cell apoptosis [30,118]. To investigate the role of isoforms in this process, individual HAX1 isoforms were restored into the HAX1 siRNA-treated (si86) HeLa cells and the cells were then treated with/without 1 μM Etoposide for 24 hours. Cell lysates were harvested and subjected to Western blot. Cleaved caspase-3 was used as an indicator for the induction of cell apoptosis (Figure 8.6, a), Western blot showed the increased cleaved caspase-3 levels in all cell lysates following Etoposide treatments (Figure 8.6, a). To quantify these changes, densitometry of the FLAG Blot from three independent experiments is shown in Figure 8.6, b .The Blot for HAX1 and the FLAG-tag showed the decreased levels of isoforms from the cells treated with Etoposide, suggesting that these HAX1 isoforms are regulated, and possibly degraded, during cell apoptosis. Again the HAX1.4 was observed to have very poor, or possibly, unstable expression by the end of my study. I was unable to express HAX1.4 reliably even after I attempted several times to re-extract the plasmids to improve their purity and therefore I excluded HAX1.4 from this experiment.

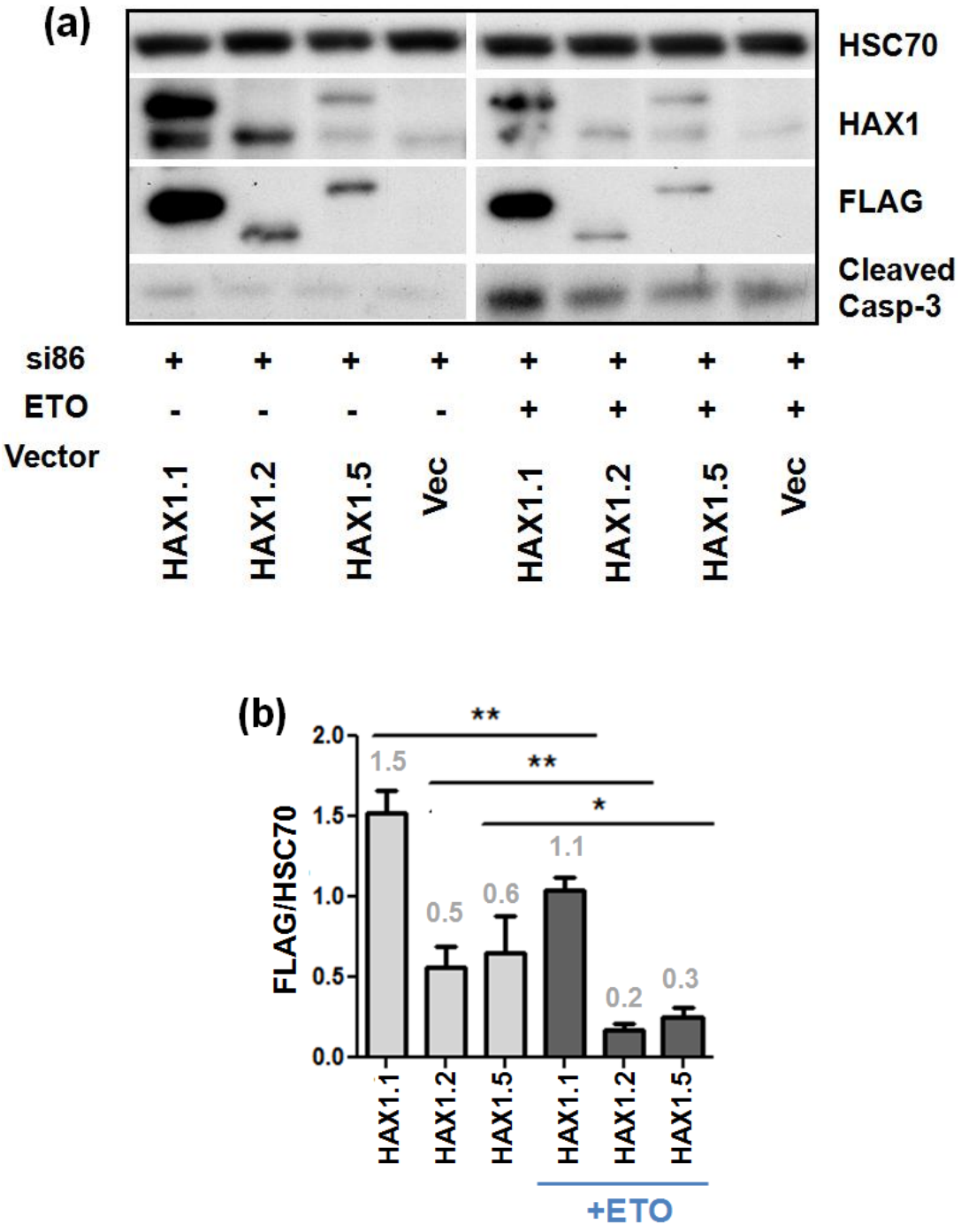
(a)
HSC70
HAX1
FLAG
Cleaved Casp-3
si86 + + + + + + + +
ETO - - - - + + + +
Vector
HAX1.1
HAX1.2
HAX1.5
Vec
HAX1.1
HAX1.2
HAX1.5
Vec
(b)
FLAG/HSC70
2.0
1.5
1.0
0.5
0.0
**
**
*
1.5
0.5
0.6
1.1
0.2
0.3
HAX1.1
HAX1.2
HAX1.5
HAX1.1
HAX1.2
HAX1.5
+ETO

Figure 8.6 Levels of HAX1 isoforms are reduced following Etoposide treatment.

Individual HAX1 isoforms were transfected into the HAX1 knockdown HeLa cells (si86) and the total cell lysates were prepared after 1μM Etoposide treatment for 24 hours. The first four lanes show the lysates from cells incubated in the growth media. The HAX1 isoform level was decreased in the cells treated with Etoposide. Thus HAX1.1, HAX1.2 and HAX1.5 were reduced by 26.6%, 60% and 50% respectively. HSC70 was used to verify equal protein loading. Vec represents the control vector only treatment. Data are presented as mean +/- 1 S.D from three independent experiments. *, $P < 0.05$, **, $P < 0.01$.

8.3 Discussion

Several reports have found that HAX1 changes its subcellular localisations and this can affect its interaction with certain binding partners and have an impact on biological functions. For example, HAX1 interacts with PLN and this association was found to cause a subcellular redistribution of HAX1 from mitochondria to the ER and this change was associated with a response which enhanced the protective effects of HAX1 on cell survival [28,130]. Caspase-3 is a central regulator for apoptosis and it is reported to interact with HAX1 and cleave HAX1 [118]. Therefore immunofluorescent staining was employed to examine the interaction of these two molecules and also to examine the localisation of HAX1 in apoptotic cells. Confocal images reveal that, although endogenous HAX1 is not colocalised with activated caspase-3, the pattern of HAX1 was altered in apoptotic cells from its mitochondrial staining to a more diffuse pattern. The cell fractionation and Western blotting studies confirmed the change of subcellular localisation of HAX1 since the expression was increased in the cytosolic and nuclear portions after 5-FU treatment. Mitochondria play a critical role in cell death via regulating the release of pro-apoptotic proteins including cytochrome c and AIF (apoptosis-inducing factor), into the cytosol [262]. The released cytochrome c activates caspase-9, in concert with the cytosolic factor dATP (or ATP) and apoptotic protease-activating factor-1, and subsequently activates caspase-3 via proteolytic processing [262]. Thus when mitochondrial membrane permeabilisation is induced by death signals, mitochondrially localised HAX1 may be released by the loss of the barrier function of the outer mitochondrial membrane.

Chemotherapy has been shown to be an effective therapy for many tumours and drugs such as Etoposide, 5-FU and Taxol are considered as the typical chemotherapeutics. These agents work by inducing apoptosis, via different mechanisms, in treated cells. To date, this present study is the first to report the correlation between individual HAX1 isoforms and cell death following exposure to the three agents. I performed both gain and loss of function experiments to demonstrate the different roles of different isoforms in cell death.

Knockdown endogenous HAX1 by siRNA (si86) significantly increase the cell survival in Taxol-induced cell apoptosis and this is correlated with decreased levels of cleaved caspase-3 and cleaved PARP which observed by Westen blotting. Data show there was no significant change in cell survival in Etoposide treatment despite the decreased levels of cleaved caspase-3 and cleaved PARP after Etoposide treatment. The difference may be caused by the different incubation times between these two experiments: 24 hours incubation time for the Western blotting versus 72 hours incubation time for the cytotoxic assays. More investigation is needed to understand the underlying mechanisms. These data suggest that endogenous HAX1 may play a pro-apoptotic role in cell death. Although this finding is conflicting with the majority of studies, my results are repeatable with the same trend, indicating there maight be a new role of HAX1 in regulating cell apoptosis.

In line with the finding of HAX1-knockdown decreased the levels of cleaved caspase-3 and cleaved PARP, the restoration of HAX1.1 showed increased cleaved caspase-3 and cleaved PARP after 24 hours Etoposide treatment. However, there was no significant change in cell survival that observed in this isoform, this may

indicate HAX1.1 exhibits pro-apoptotic role in the early time point (24 hours) rather than 72 hours drug-induced cytotoxic assays. In contrast, HAX1.2 did not cause any significant change in cleaved caspase-3 and cleaved PARP levels by Western blot after Etoposide treatment, but increased cell survival over 72 hours cytotoxic assay. The results showed that HAX1.2 decreased sensitivity of HeLa cells to Etoposide and 5-FU, suggesting that this isoforms may enhance the chemoresistance by protecting cell death from cytotoxic effects induced by these two drugs. The unchanged level of cleaved caspase-3 indicates that the possible mechanism may not involve the caspase-3 pathway. Although these observations were highly repeatable, it is clear that I have no mechanistic explaination for these changes and that more investigation is needed to reveal the processes behind these observations. On the other hand, HAX1.5 had no effect on levels of cleaved caspase-3 or cleaved PARP compared with control cells, and also showed unchanged (inconsistent) results in cell survival in overall cytotoxic experimrnts; thus this isoform did not show a consistent effect on cell viability.

Reportedly, HAX1 degradation occurs due to the cleavage by different molecules such as Omi/HtrA2, caspase-3 and Granzyme B [30,118,243]. Lee *et al* showed that HAX1 was cleaved by caspase-3 in HeLa cells after Etoposide treatment. In my study I also showed the decreased expression of HAX1 isoforms (by both anti-HAX1 and anti-FLAG Blot) after Etoposide treatment. This is the first to show HAX1 isoforms are associated with degredation during apoptosis.

CHAPTER 9. FINAL DISCUSSION

Throughout this study I have tried to make clear that, to date, most previous studies that have examined the biology of HAX1, have considered HAX1 as a single molecule, whereas our laboratory proved that it is in fact a family of splice variant molecules. This probably explains why so many subcellular localisations and so many different functions have been attributed to HAX1. Thus I began with the hypothesis:

The multiple functions and subcellular localisation attributed to HAX1 are due to the presence of multiple isoforms whose individual functions and subcellular localisation may differ from each other.

I believe that in large part I have confirmed that my hypothesis was correct, but also it is clear that there is still so much more to do to determine the precise role of these various isoforms in different cellular behaviours.

The nature of the HAX1 family of proteins is such that they share significant sequence homology between each isoform and this close relationship undoubtedly increased the complexity of this study. Thus it was not possible to design siRNA that would target each individual HAX1 isoform (except HAX1.2) and there are no HAX1 isoform specific antibodies available. Therefore I was forced to use siRNA-protected isoforms with a limited panel of antibodies; technically demanding approaches which often provided indirect, rather than direct, evidence.

The first task was to check antibody specificity and efficiency for HAX1. The data in Figure 3.1, Figure 3.2, Figure 3.3 and Figure 3.4 show that only the goat anti-HAX1 antibody (RD) and mouse anti-HAX1 antibody (BD) recognised endogenous HAX1 in Western blot and by immunochemistry; siRNA to HAX1 confirming antigen specificity. As a result of my early studies, the Santa Cruz antibodies were no longer used but it does call to question the results others have achieved using these reagents. I was also fortunate that, prior to my arrival, a postdoctoral research fellow, Dr. Delphine Lees, had generated FLAG-tagged HAX1 isoform constructs and siRNAs that could be used for my studies. The main study could now commence.

9.1 HAX1 expression is cell density dependent

Integrin αvβ6 has been reported to be expressed in a density-dependent manner which increases MMP-9 secretion as cells reach confluence [223]. This is indicated to facilitate ECM degradation, which helps overcome crowding and restores cell proliferation as well as cell invasion [223]. In the present study, in my initial experiments, I observed variation in HAX1 expression levels with different cell cultures and thus I was encouraged to investigate whether HAX1 also is influenced by cell density. This revealed that endogenous HAX1 levels, like integrin αvβ6, are cell-density dependent; in addition the house keeping proteins (HSC70, tubulin and actin) also need at least 48 hours to stabilise their expression levels after seeding and this finding has had an impact on how other investigators in the laboratory conduct their investigations.

Many proteins are synthesised in a cell density-dependent manner (eg. TGF-β, αvβ6) [223,263] and this can regulate protein synthesis and therefore the functions of these proteins under different circumstances. For example, at high cell density of vascular smooth muscle cells, TGF-β promotes cell proliferation but also promotes synthesis of perlecan and biglycan [263]. This is suggested to be involved in the regulation of endothelial cell functions by growth factors and cytokines and, with the increased accumulation of extracellular matrix, during the repair of vascular injury [263]. As cell density regulates the expression of HAX1 this also may modulate biological behaviour of cells. Thus these observations may be very important for the study of cellular functions of HAX1. While I chose to analyse HAX1 biology using cells that were confluent, thereby ensuring highest expression, it is possible that low HAX1 expression may cause cells to behave differently.

9.2 HAX1 subcellular localisation

9.2.1 Subcellular localisation of endogenous HAX1

HAX1 has been reported to localise in multiple cellular compartments (mitochondria, ER, cell nucleus) [3,19,27]. In the present study, using monoclonal and goat polyclonal anti-HAX1 antibodies, endogenous HAX1 was localised predominantly to mitochondria; a pattern which was observed by using immunofluorescence staining and a cell fractionation technique. This is not a surprise finding as HAX1 is reported to interact with several mitochondrial molecules (Omi/HtrA2, PARL, GrB) [30,135,140,243]. By residing in the

mitochondria; HAX1 is reported to execute pro-apoptotic functions by maintaining mitochondrial membrane potentials [30,135,140]. Apart from the abundant expression in mitochondria, cell fractionation experiments also demonstrated endogenous HAX1 appeared in the cell nuclear fractions (consistent with reports of interactions with nuclear binding partners such as vimentin, mRNA, DNA polymerase β mRNA, EBNA5 [27,32,224]) and minimal expression in the cell cytoplasm (enabling binding to molecules such as uPAR, XIAP, Gα13, PELO and αvβ6 [1,49,56,64,123]).

I examined the subcellular localisation of each individual isoform for the using HAX1.1, HAX1.2, HAX1.4 and HAX1.5 overexpressed in VB6 and HeLa cells. The confocal images revealed HAX1.1, HAX1.4 and HAX1.5 showed a "classic" HAX1-mitochondrial pattern whereas HAX1.2 demonstrated a strikingly diffus expression pattern in VB6 and HeLa cells. Borgese *et al* have shown that the mitochondrial targeting signals are contained either within the N-terminal or the C-terminal regions of members of the Bcl-2 family, and these sequences are recognised by importing proteins of the outer and inner mitochondrial membranes [118,119]. In a recent study, Yap *et al* reported that the N-terminus of HAX1 (a.a. 1-59) is responsible for targeting to mitochondria [19]. The HAX1.2 variant produces a protein that lacks the first N-terminal 26 a.a. (compared with HAX1.1) by alternative splicing [2], possibly accounting for the mitochondrial non-specific localisation which was shown by this isoform. The confirmation that HAX1 isoforms existed in different subcellular localisations confirmed an important aspect of the central hypothesis of this thesis: it seems logical to suggest that if they are in different places then they probably are doing different things.

9.2.2 Different endogenous HAX1 expression patterns in apoptosis and confluent cultures

Several studies have noted that HAX1 proteins can change in their subcellular localisation. I showed that the mitochondrial HAX1 proteins appeared to change their distribution to a more punctuate, cytoplasmic localisation when cells were highly confluent (Figure 3.8) or when exposed to cytotoxic drugs (Figure 8.1). Thus while HAX1.2 is predominantly cytoplasmic, this does not exclude that the others, mitochondrial HAX1 isoforms may also occasionally function in non-mitochondrial localisations. Thus when mitochondrial membrane permeabilisation is induced e.g. by death signals, mitochondrial HAX1 may be released by the loss of the barrier function of the outer mitochondrial membrane leading to variations in its localisation pattern.

9.3 HAX1 and cancer cell migration

In the present study, I have demonstrated that HAX1 is a central factor that regulates migration of multiple different cancer cells (breast, pancreas and cervix cancer cells). Intriguingly, HAX1 seemed to regulate migration only on LAP, a ligand that is predominantly recognised by αv-integrins. Why HAX1 should regulate only LAP-dependent migration is unknown but might suggest HAX1 regulates functions related to interaction with TGF-β, since this cytokine is secreted in the latent form bound covalently to LAP. Integrin regulation of TGF-β activation is critical for wound repair [69] and, when it is over active, this cytokine can cause fibrosis [216].

Thus it would be interesting to look more closely at HAX1 regulation of TGF-β signalling, a pathway which could have a substantial impact on tumour progression.

To investigate the individual isoforms in cell migration, different HAX1 isoforms were examined. Results from Transwell migration assays showed that HAX1.2 when overexpressed on itsown significantly down regulated cell migration on LAP by 40 % compared with the vector control. HAX1.2 knockdown, by specific siRNA, resulted in increased migration of targeted cells. Together these data suggest an unique role for HAX1.2 in cell migration resulting in diminished cell motility. It remains puzzling why I was unable to show similar effects on migration in stable HAX1-null cell lines and points the need for further investigation in the area.

9.4 HAX1 in autophagy

In this report I show conflicting data about the regulation of autophagy by HAX1. Thus total HAX1 depletion by siRNA increased the level of Beclin-1 and LC3b-II, suggesting endogenous HAX1 plays a role in repressing autophagy and this is in line with observations in a recent study [87].

In contrast, Western blot showed expression of HAX1.1, 1.2 and 1.5 increased autophagy (LC3b-II and Beclin-1 levels were increased) in transiently HAX1-deficient cells. One possibility is that the global knockdown of HAX1 isoforms regulate a key isoform, or isoforms, that is required to suppress autophagy. It is clear

from my studies that the role of HAX1 isoforms in autophagy also requires additional investigation.

9.5 HAX1 and apoptosis

Overexpression of HAX1 has been reported to protect cells from cell death under Fas treatment, γ-irradiation and serum deprivation [3], Bax-induced apoptosis [12] and HAX1 antisense mRNA increased ultraviolet-induced apoptosis [23]. These data suggest that HAX1 is involved in both death receptor (extrinsic) and non-death receptor (intrinsic) mitochondrial-mediated apoptosis pathways. In this study, I repeatedly showed that, by comparing with HAX1 knockdown, the endogenous HAX1 sensitised cells to increased susceptibility to cytotoxic drug treatments correlating with increased levels of cleaved caspase-3 and of the downstream cleaved PARP. These data indicate that endogenous HAX1 activates caspase-dependent cell apoptosis. In contrast, HAX1.2 decreased sensitivity to cytotoxic drug induced cell death with no change in the level of cleaved caspase-3 or cleaved PARP, indicating HAX1.2 may link to cell death via a caspase-3-independent pathway. Caspase-independent cell death pathways are an important safeguard mechanism to protect the organism against unwanted and potential harmful cells when caspase-mediated routes fail; they can also be triggered in response to cytotoxic agents or other death stimuli [264]. For example, Omi/HtrA2, a binding partner of HAX1, plays a role in caspase-dependent cell death, but it can also act as an effector protein in necrosis-like programmed cell death [88,265]. There is a possibility that HAX1 could affect cell death by cooperating with its binding partners. To date, my study is the first to report a correlation between individual

HAX1 isoforms and different outcomes in relation to cell death. Thus, endogenous HAX1 induces a caspase-3 dependent cell apoptosis whereas HAX1.2 is sufficient to protect cells from caspase-independent cell death. HAX1.1 increased the level of cleaved caspase-3 and cleaved PARP whiout significant change in cell survival and HAX1.5 was not observed to alter cell viability. Again, different isoforms appear to perform different functions and this helps to explain why the literature, with regard to HAX1 and apoptosis, is so complex.

9.6 Autophagy and apoptosis

Autophagy and apoptosis are connected both positively and negatively, and extensive crosstalk exists between the two processes [253]. The functional relationship between apoptosis and autophagy is complex in the sense that, in several scenarios, autophagy constitutes a stress adaptation that avoids cell death (and *de facto* suppresses apoptosis), whereas in other cellular settings, autophagy constitutes an alternative pathway to cellular demise that is called autophagic cell death (or type II cell death) [253]. In general terms, it appears that similar stimuli can induce either apoptosis or autophagy depending on the circumstances and molecular pathways dictate the choice between autophagy and apoptosis [253]. BAX and BAK are two members of the BCL2 family that are required for mitochondrial outer membrane permeabilisation [266]. Mouse embryonic fibroblasts (MEFs) from double-knockout $Bax^{-/-}$ $Bak^{-/-}$ mice were shown to be resistant to a range of apoptosis inducers. When treated with DNA damaging agents, such as Etoposide, $Bax^{-/-}$ $Bak^{-/-}$ MEFs failed to undergo apoptosis and instead manifested massive autophagy followed by delayed

cell death [266]. HAX1.2 may use a similar route to regulate cell apoptosis and autophagy as it promoted autophagy but also showed the protection of cell death from various cytotoxic drugs.

9.7 The distinct role of HAX1.2

HAX1.2 displays a unique role in some biological functions: it shows a distinct expression in cytoplasm, inhibits cell migration, promotes autophagy and represses cell death induced by various cytotoxic agents. As a result of alternative splicing, HAX1.2 lacks the first exon, starting 27 bases inside exon 2, producing a protein that lacks the first 26 a.a. [2]. Interestingly, Grzybowska *et al* found a 26 a.a. sequence within the prototypical rat HAX1 isoform1 that may function in mitochondrial localisation [267], another report from Yap *et al* also showed that the N-ternimal of HAX1 1-59 a.a. is required for the mitochondrial localisation [19]. These studies explain the non-mitochondrial-specific licalisation that observed to HAX1.2 in this study. N-terminal sequence of full-length HAX1 also found for other functions: 1-113 a.a. is responsible for neutrophil adhesion [20] and 1-261 a.a. associates with anti-apoptosis [21], the fact that many functions assigned to N-termical sequence may give the explaination for the dynamic roles that HAX1.2 has involved in. Nevertheless, a recent report showed that HAX1.2 was up-regulated in breast cancer tissues compared with matching normal tissues [149]. My data also indicate the anti-cell death and inhibition of cancer cell migration, suggesting possible roles that HAX1.2 may involve in cancer progression.

9.8 Future plans

The fact that the HAX1 family of isoforms share such high sequence homology significantly increased the complexity of this study. The commercial antibodies available for HAX1 bind epitopes that detect most isoforms of HAX1. By Western blotting, my data show that all these antibodies recognise the major HAX1 band at around 34 kDa, a molecular weight corresponding to HAX1.1 and HAX1.5. Smaller bands were observed in blots but their identification is complicated by the unknown proportions of endogenous expression levels of different individual isoforms, and possible differences in their degradation, both of which would cause changes in observed levels of these smaller HAX1-related proteins. Recently, two antibodies from Sigma became available that claimed to detect specifically isoform HAX1.1 (Sigma, #PRS4711) and isoform HAX1.4 (Sigma, PRS4715). I tested these antibodies on cells where I had over-expressed these single isoforms, separately. Western blot (data not shown) revealed that the antibody for HAX1.1 also recognised HAX1.5 whereas the antibody for HAX1.4 failed to detect anything. For similar reasons, the genetic homology of the HAX1 isoforms also clearly causes a difficulty for designing a siRNA to target only one single HAX1 isoform. Thus it is extremely difficult to study the biological functions of the individual endogenous HAX1 isoforms.

In the early stage of my study, I aimed to examine the individual HAX1 isoforms by using a lentiviral stable knockdown approach, followed by re-expression of individual isoforms. To generate the stable lines was time-consuming as was establishing the characterisation of these HAX1-null cells lines. All the biological

functions examined (proliferation, migration, invadopodia formation, Traswell invasion, organotypic invasion and apoptosis) using the stable HAX1 knockdown cell lines did not show the significance of HAX1 in any of these previously reported HAX1-associated biological activities. We suspect that HAX1 has important, but as yet unidentified, roles in biology that required cells to reprogram themselves in order to overcome the permanent absence of HAX1. It was a serious setback but by using a transient-knockdown method, I successfully investigated the functions of the individual HAX1 isoforms in the later stages of my project. There were a number of experiments that I was not able to perform due to the time constraints and these could have enhanced the value of this study; these include the following:

- The C-terminal of HAX1 (a.a 271-279) interacts with the β subunit of integrin αvβ6, and regulates αvβ6 endocytosis, which is required for cancer cell migration and invasion [1]. Truncated HAX1 isoforms (isoforms that lack of the β6 binding site) have been generated by my colleague Dr Delphine Lees and are ready to use. This would allow the investigation of the impact of the interaction between individual HAX1 isoforms and αvβ6 in many biological aspects such as cell migration, invasion, apoptosis, autophagy as well as their subcellular distribution.
- The crosstalk between autophagy and apoptosis play important roles in regulating cancer cell survival. In some settings, autophagy constitutes a stress adaptation that avoids cell death by suppressing apoptosis, and in others, it can lead to death itself, either in collaboration with apoptosis or as a back-up mechanism when the former is defective [253]. The molecular regulators of both pathways are inter-connected and both pathways share

several genes that are critical for their respective execution [253]. Thus it would be interesting to examine the impact of HAX1 isoforms in autophagy and apoptosis pathways, in the same cells. Thus some molecules are implicated in both pathways; for example both Omi/HtrA2 and caspase-9 are reported to be involved in autophagy and apoptosis and both are binding partners to HAX1 [87,253].

- The urokinase-type plasminogen activator (uPA) receptor (uPAR) has been implicated in cell migration and invasion [268]. Active uPA proteolytically converts the inactive zymogen, plasminogen, to the active enzyme, plasmin, which can then break down ECM components, including the ability to cleave LAP and activate TGFβ [63,268]. It is reported that HAX1 interacts with uPAR and that HAX1 overexpression augments cell proliferation and migration in uPAR-stimulated cells [64,65] thus it would be interesting to examine the functions of specific HAX1 isoforms in the link between uPAR, TGF-β and migration.

9.9 Summary

In summary, the central hypothesis of this thesis has been established. That is HAX1 isoforms do exist in different subcellular localisations and do perform different functions. It must also be acknowledged that, when comparing global knockdown of HAX1 with restoration of individual HAX1 isoforms, for certain experiments the results appeared to be conflicting. This may suggest that the experiments were not directly comparable as in the si86 knockdown experiments multiple HAX1 isoforms were removed that may have been co-operating to exert their biological behaviours. In Figure 9.1 I have attempted to combine my data into a model of how HAX1 isoforms might influence diverse cell behaviours. This should not be considered absolute but rather a model still in development. However, given how many biological processes HAX1 is involved in, further analysis of this highly complex and complicated family of proteins is to be encouraged as an area of investigation.

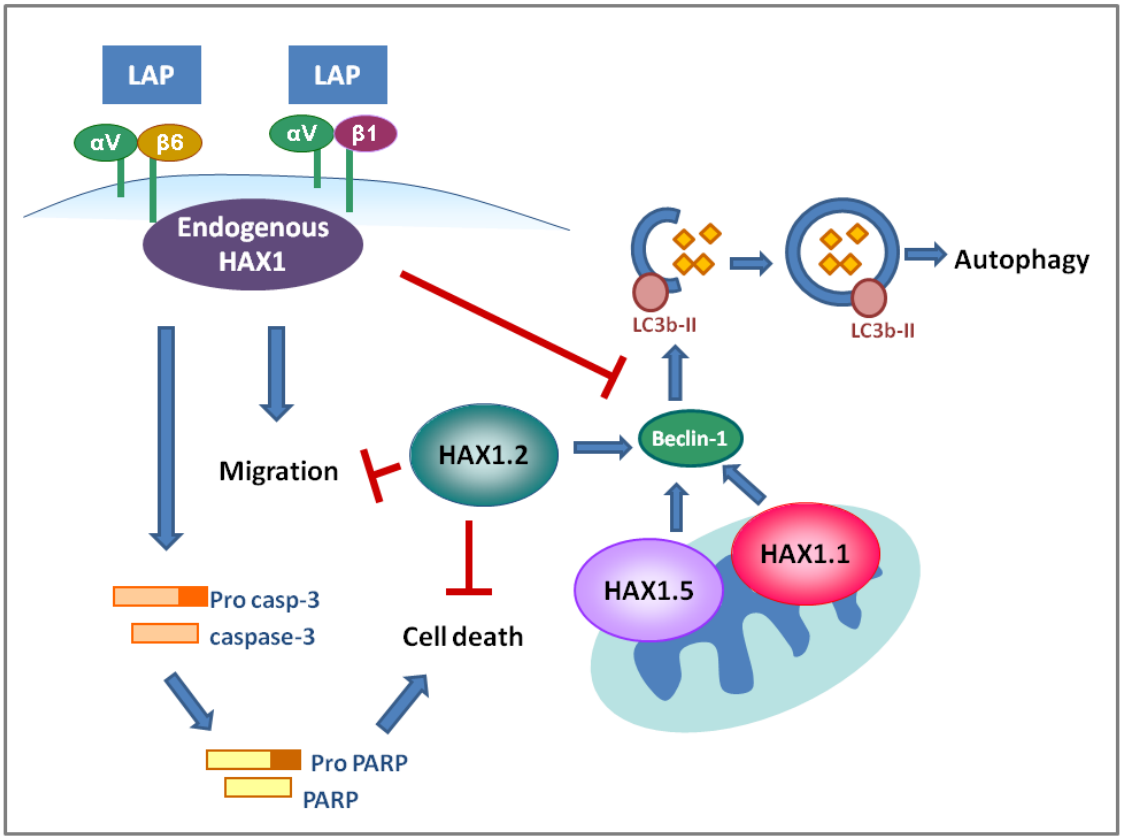

Figure 9.1 Schematic illustration of possible subcellular functions of HAX1 isoforms.

Endogenous HAX1 is required for migration of various cancer cells (oral, breast, pancreas and cervix) toward LAP via integrin αvβ6 and αvβ1. It also promotes cell apoptosis by increasing the levels of cleaved capsase-3 and downstream cleaved PARP. Moreover, in the autophagy process, endogenous HAX1 plays a inhibitory role by inhibiting the levels of Beclin-1 and LC3b. HAX1.2 is an unique isoform that is expressed in the cytoplasm whereas the other isoforms reside predoninantely in mitochondria. HAX1.2 also regulates cell migration by diminishing the cell motility toward LAP. HAX1.2 promotes cell survival possibly via caspase-3 independent pathway whereas HAX1.1 enhance the levels of cleaved capsae-3 and cleaved PARP without any observed changes in cell viability. HAX1.1, HAX1.2 and HAX1.5 also promote autophagy by increasing the levels of Brclin-1 and LC3b-II.

APPENDIX I- (a)

Features of the pGIPZ vector

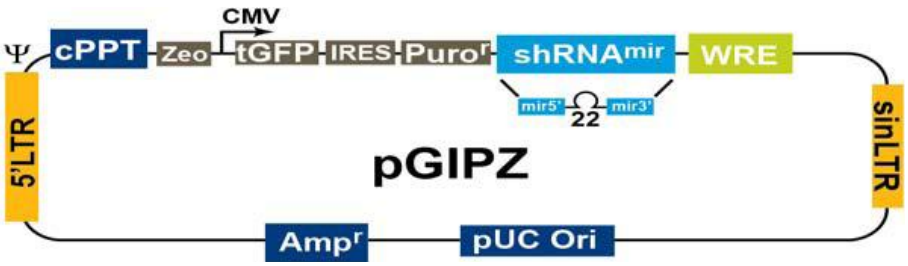

Vector Element	Utility
CMV Promoter	RNA Polymerase II promoter
cPPT	Central Polypurine tract helps translocation into the nucleus of non-dividing cells
WRE	Enhances the stability and translation of transcripts
TurboGFP	Marker to track shRNAmir expression
IRES-puro resistance	Mammalian selectable marker
Amp resistance	Ampicillin (carbenicillin) bacterial selectable marker
5'LTR	5' long terminal repeat
pUC ori	High copy replication and maintenance of plasmid in *E. coli*
SIN-LTR	3' Self inactivating long terminal repeat (Shimada, et al. 1995)
RRE	Rev response element
Zeo resistance	Bacterial selectable marker

APPENDIX I- (b)

Detailed vector map of pGIPZ™ lentiviral vector

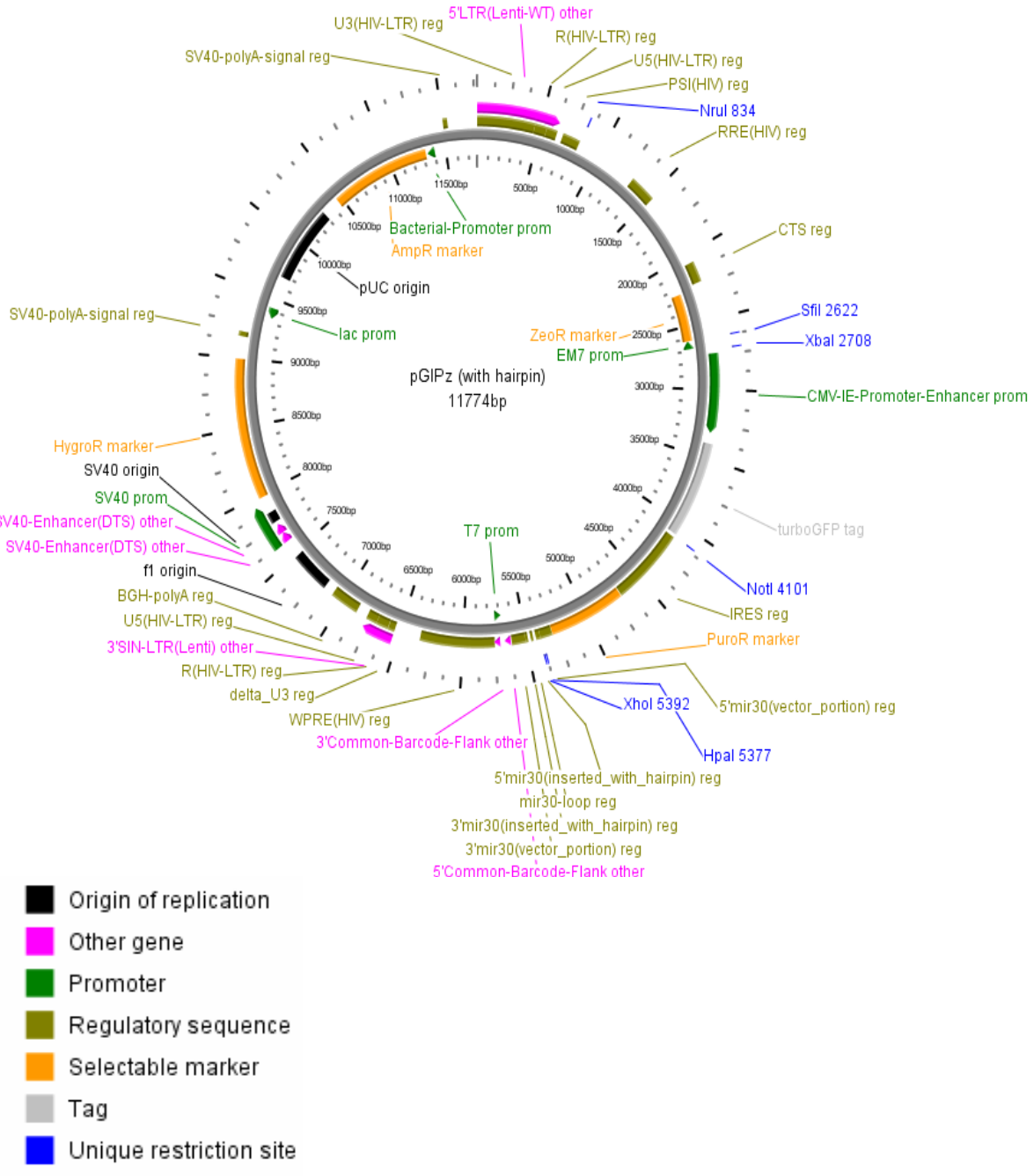

APPENDIX II

Detailed vector map of pFLAG-CMV2 vector

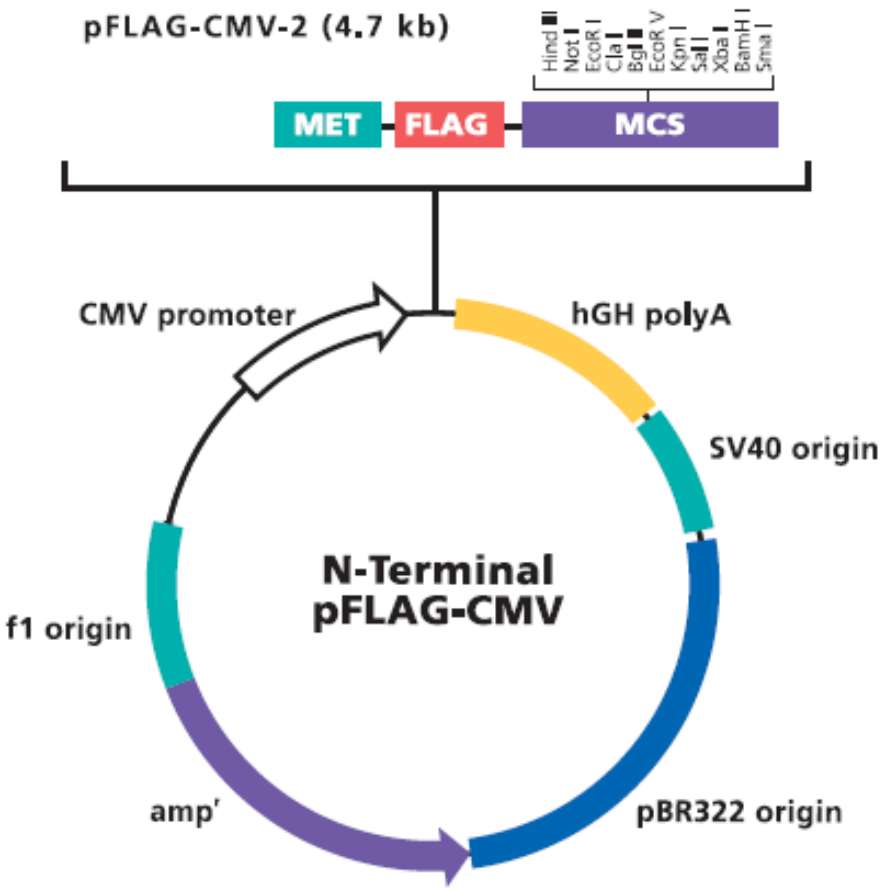

APPENDIX III

The effect of Taxol induced cell death in HAX1-null (si86 treated) HeLa cells.

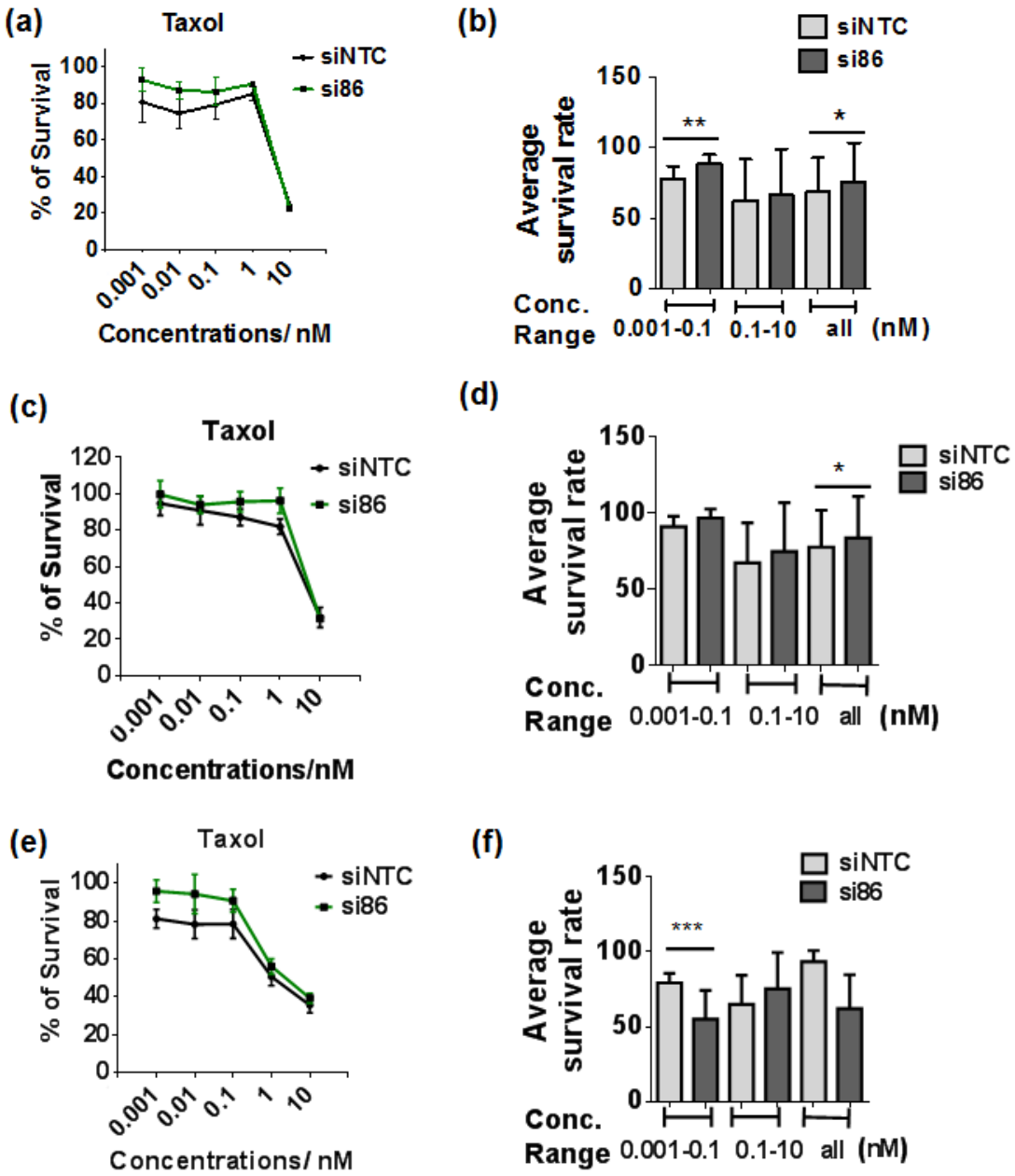

APPENDIX IV

The effect of Etoposide induced cell death in HAX1-null (si86 treated) HeLa cells.

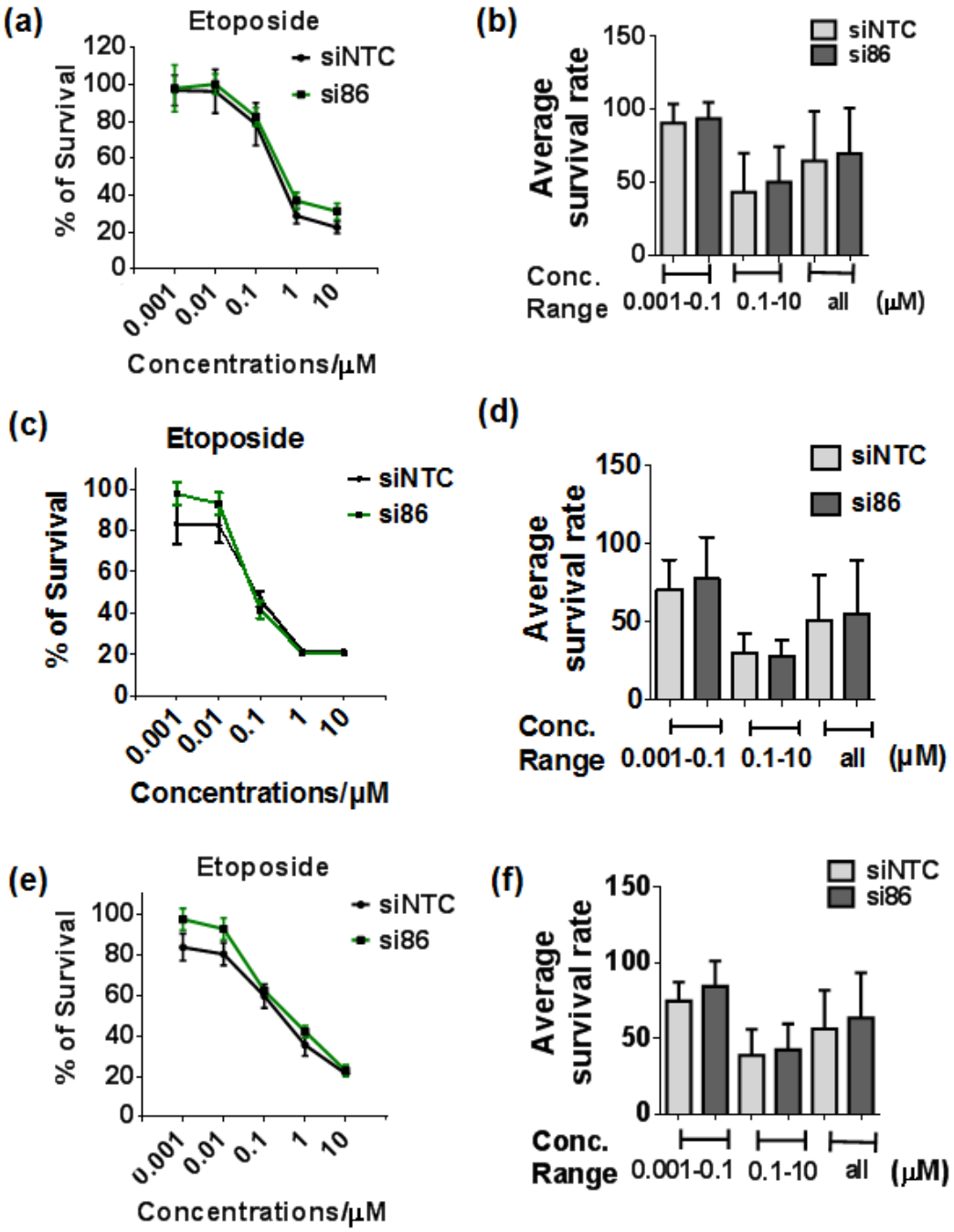

APPENDIX V

The effect of 5-FU induced cell death in HAX1-null (si86 treated) HeLa cells.

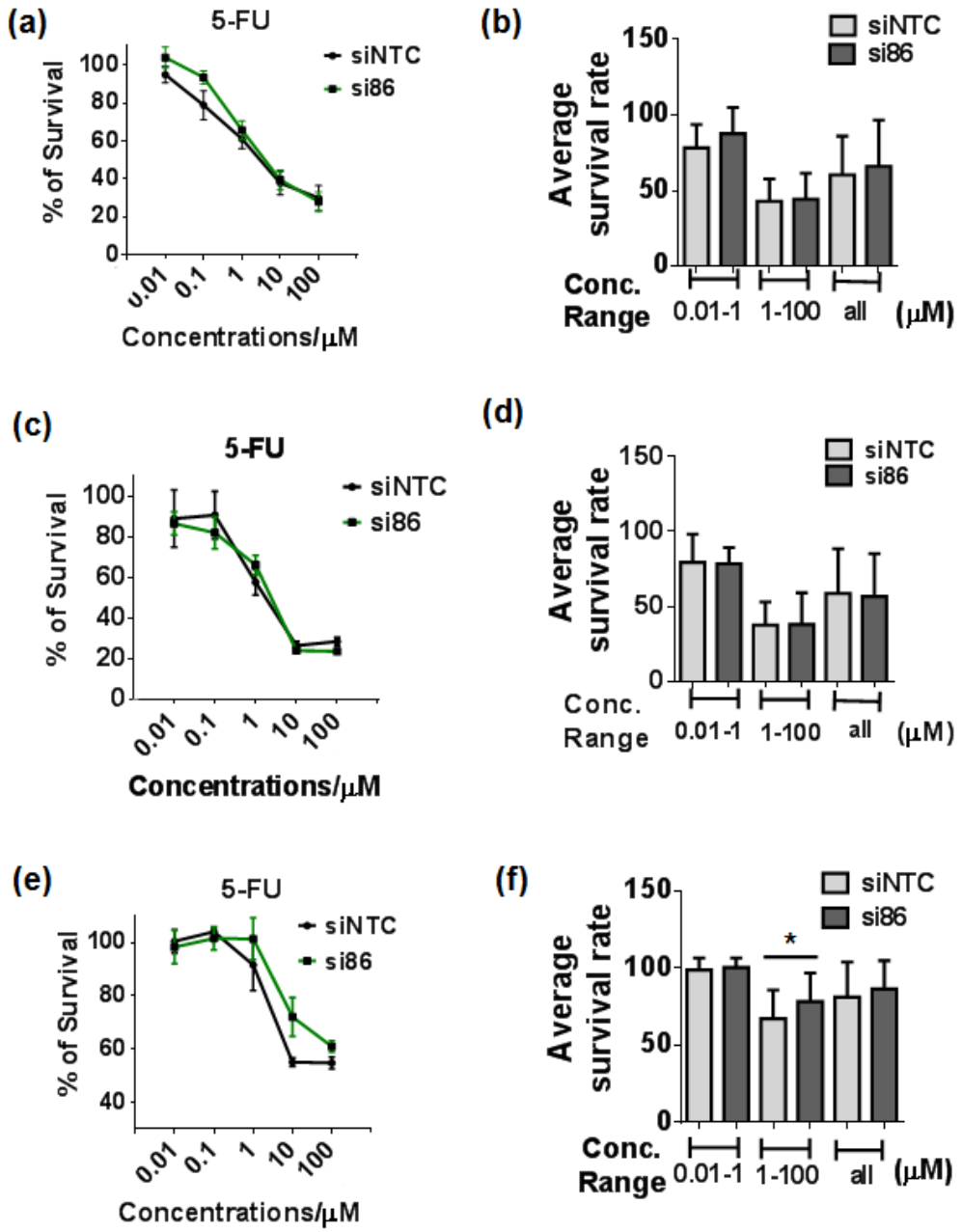

APPENDIX VI

The effect of Taxol induced cell death in HeLa cells expressing HAX1.1.

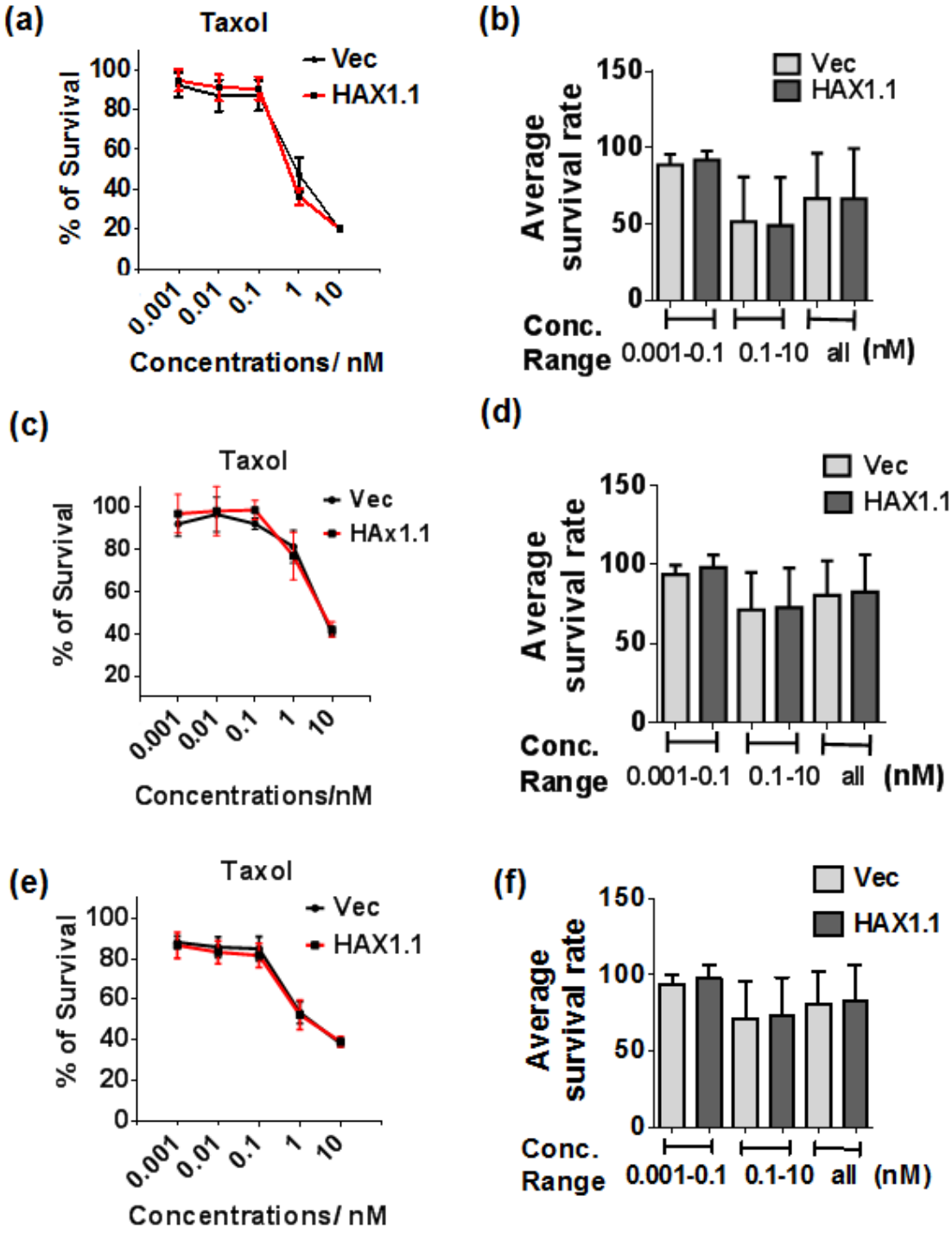

APPENDIX VII

The effect of Etoposide induced cell death in HeLa cells expressing HAX1.1.

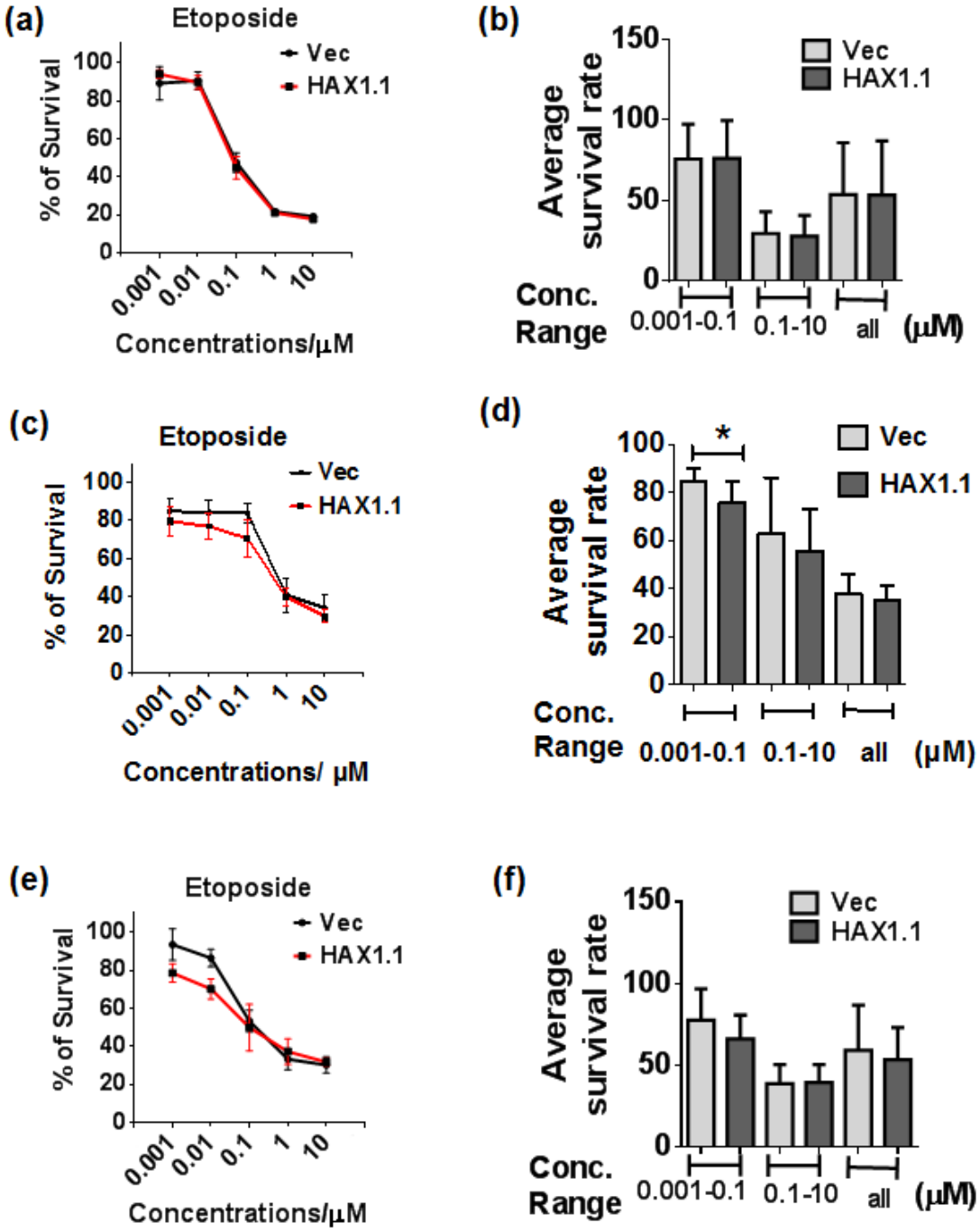

APPENDIX VIII

The effect of 5-FU induced cell death in HeLa cells expressing HAX1.1.

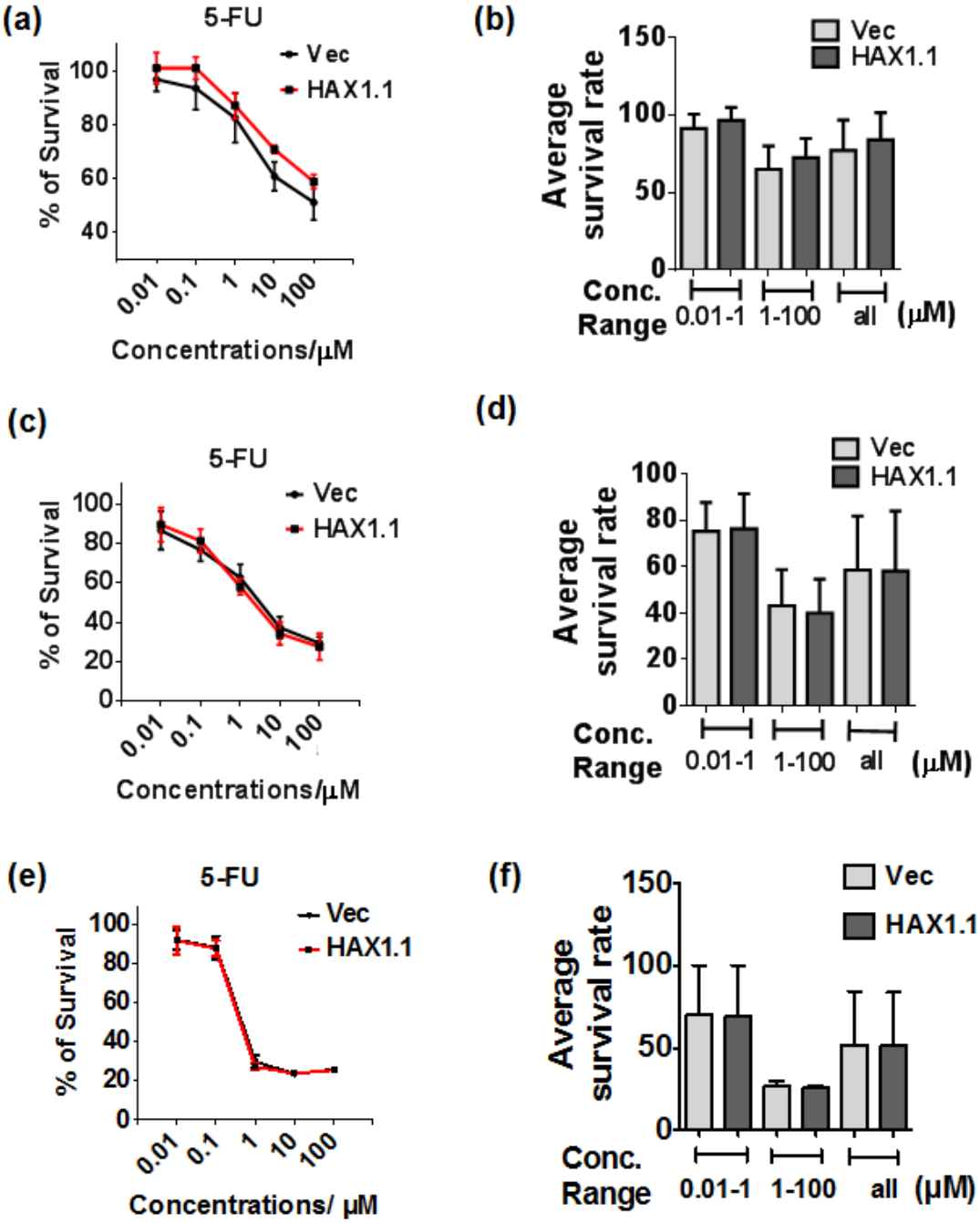

APPENDIX IX

The effect of Taxol induced cell death in HeLa cells expressing HAX1.2.

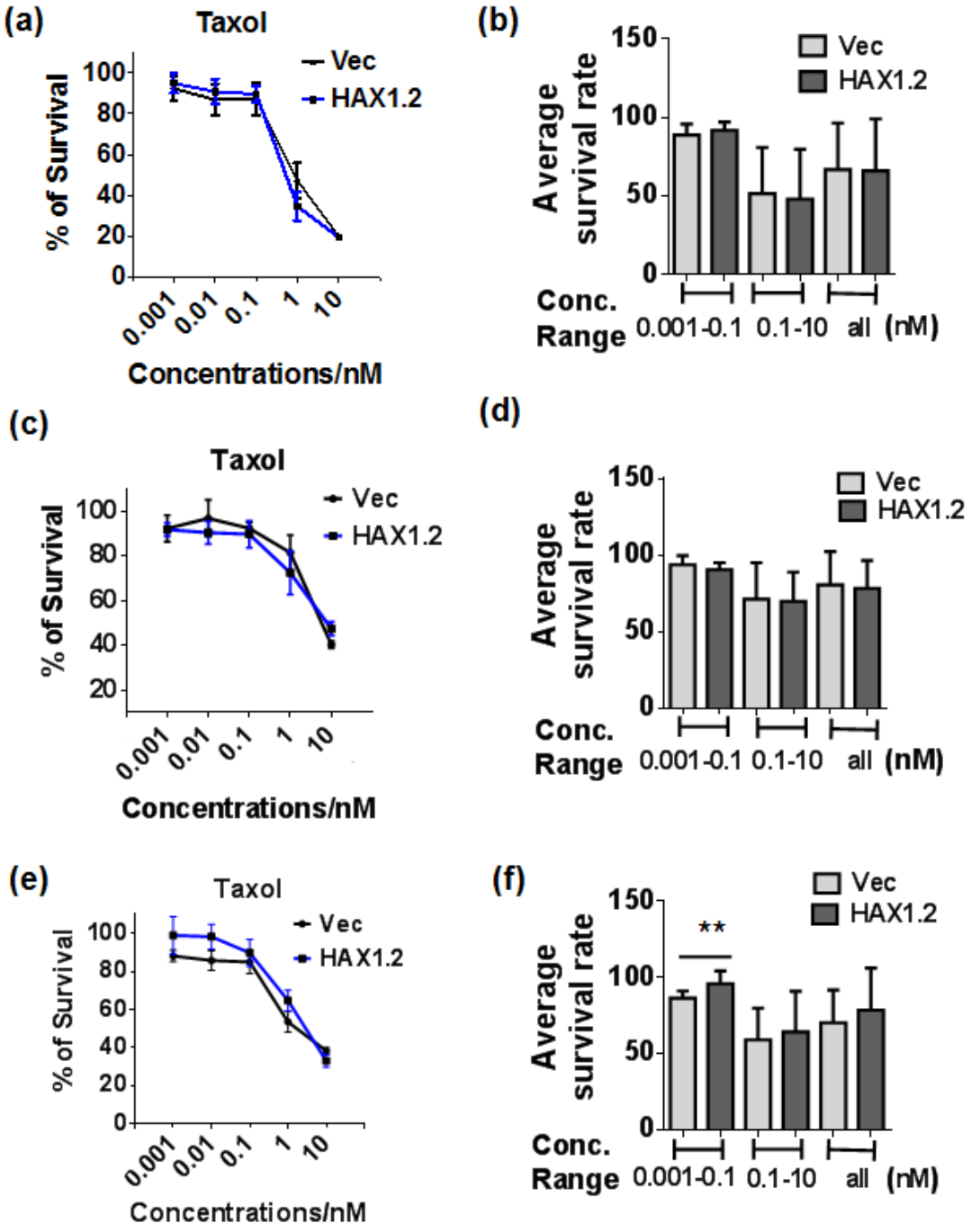

APPENDIX X

The effect of Etoposide induced cell death in HeLa cells expressing HAX1.2.

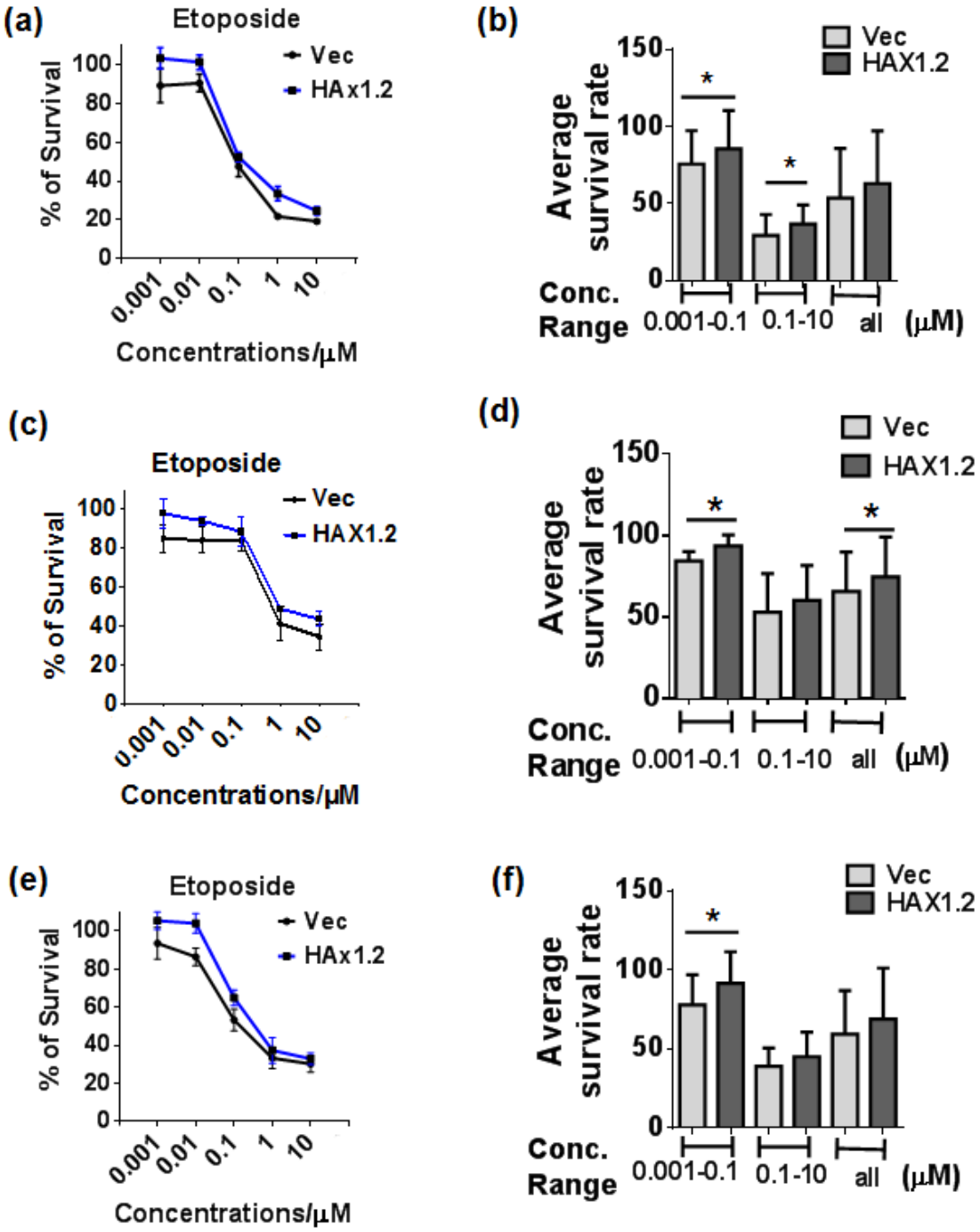

APPENDIX XI

The effect of 5-FU induced cell death in HeLa cells expressing HAX1.2.

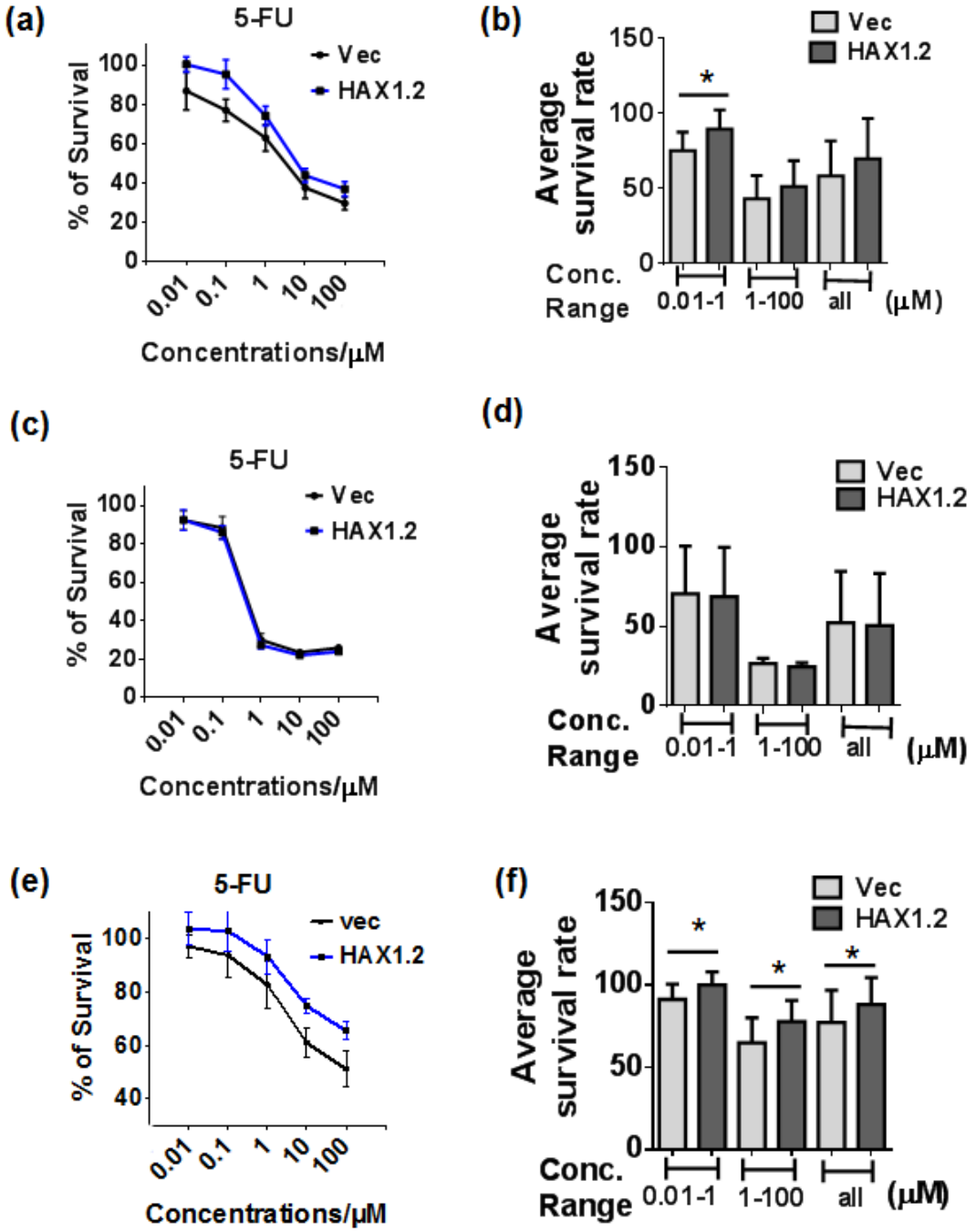

APPENDIX XII

The effect of Taxol induced cell death in HeLa cells expressing HAX1.5.

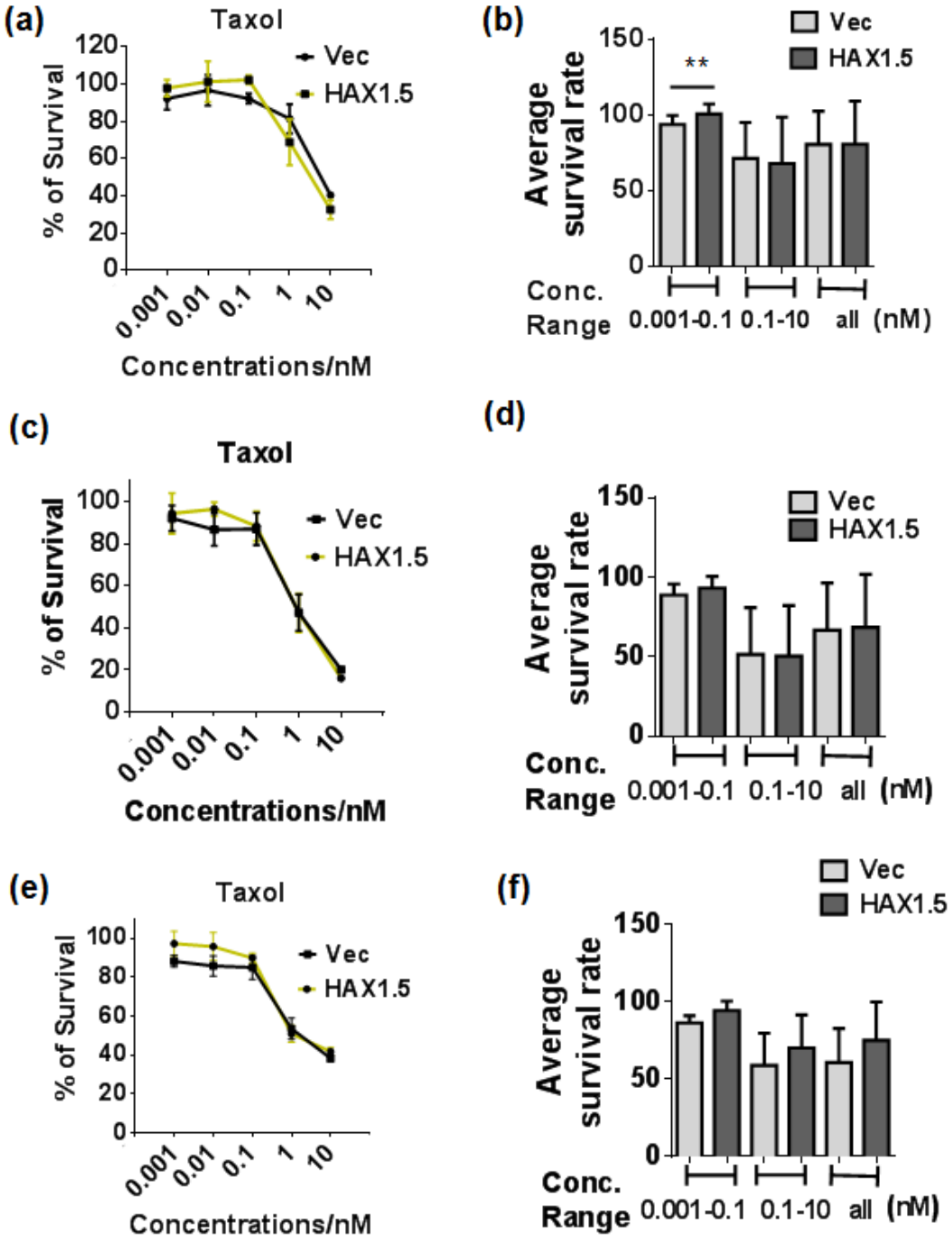

APPENDIX XIII

The effect of Etoposide induced cell death in HeLa cells expressing HAX1.5.

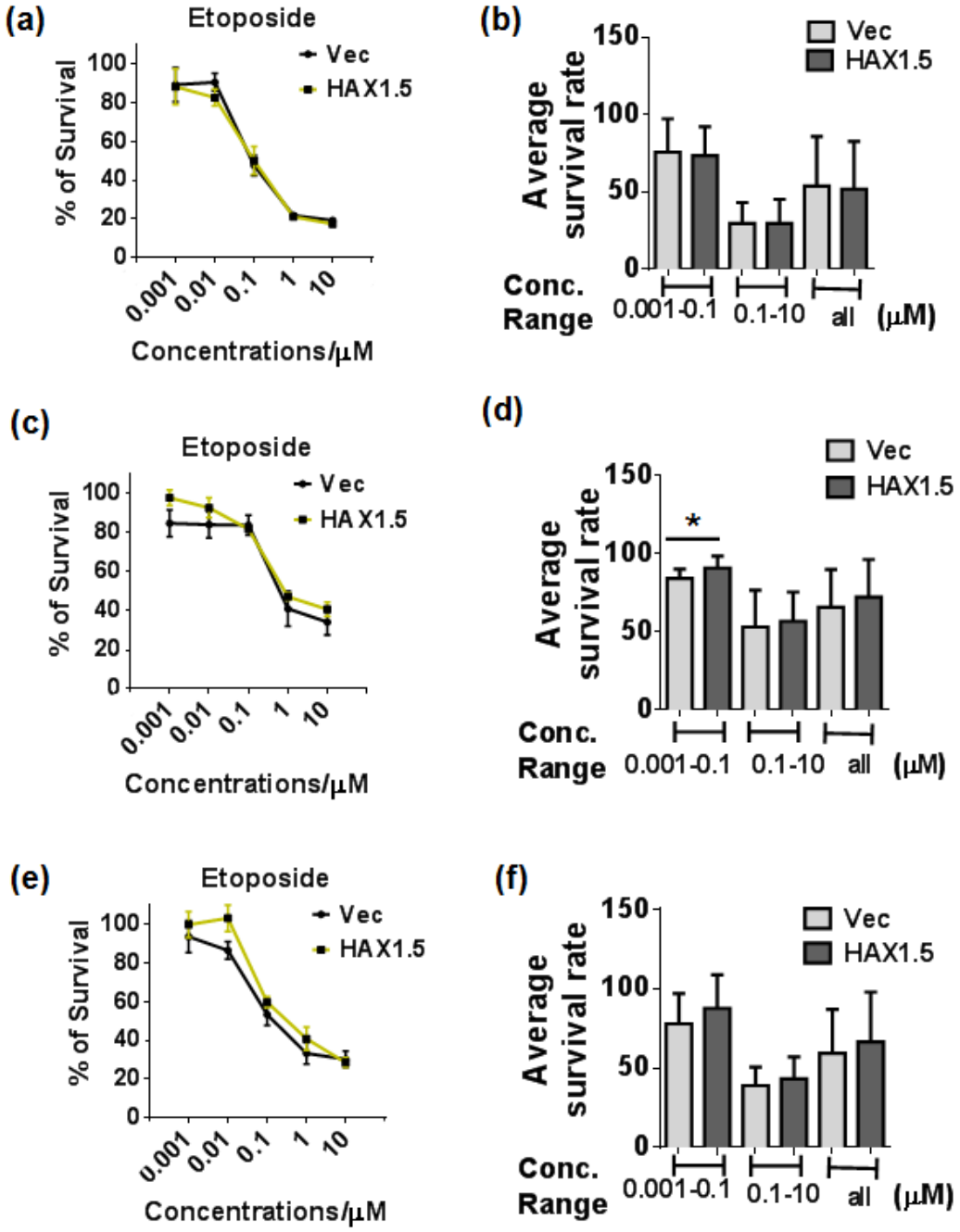

APPENDIX XIV

The effect of 5-FU induced cell death in HeLa cells expressing HAX1.5.

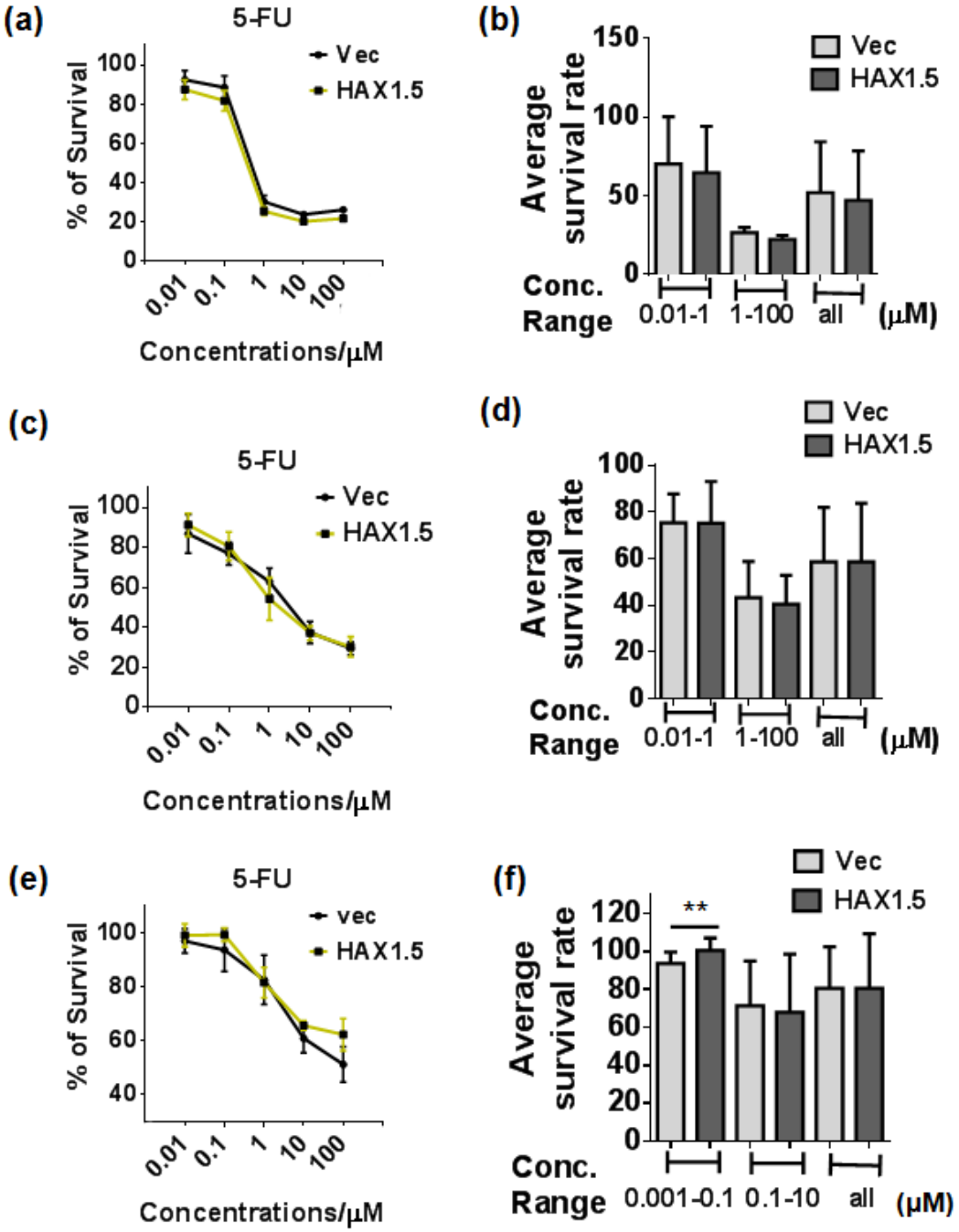

CHAPTER 10. REFERENCES

1. Ramsay AG, Keppler MD, Jazayeri M, et al. HS1-associated protein X-1 regulates carcinoma cell migration and invasion via clathrin-mediated endocytosis of integrin alphavbeta6. Cancer Res 2007;67:5275-5284

2. Lees DM, Hart IR, Marshall JF. Existence of multiple isoforms of HS1-associated protein X-1 in murine and human tissues. J Mol Biol 2008;379:645-655

3. Suzuki Y, Demoliere C, Kitamura D, et al. HAX-1, a novel intracellular protein, localized on mitochondria, directly associates with HS1, a substrate of Src family tyrosine kinases. J Immunol 1997;158:2736-2744

4. Yamanashi Y, Fukuda T, Nishizumi H, et al. Role of tyrosine phosphorylation of HS1 in B cell antigen receptor-mediated apoptosis. J Exp Med 1997;185:1387-1392

5. Brunati AM, Donella-Deana A, James P, et al. Molecular features underlying the sequential phosphorylation of HS1 protein and its association with c-Fgr protein-tyrosine kinase. J Biol Chem 1999;274:7557-7564

6. Taniuchi I, Kitamura D, Maekawa Y, et al. Antigen-receptor induced clonal expansion and deletion of lymphocytes are impaired in mice lacking HS1 protein, a substrate of the antigen-receptor-coupled tyrosine kinases. EMBO J 1995;14:3664-3678

7. Kahner BN, Dorsam RT, Mada SR, et al. Hematopoietic lineage cell specific protein 1 (HS1) is a functionally important signaling molecule in platelet activation. Blood 2007;110:2449-2456

8. Gallagher AR, Cedzich A, Gretz N, Somlo S, Witzgall R. The polycystic kidney disease protein PKD2 interacts with Hax-1, a protein associated with the actin cytoskeleton. Proc Natl Acad Sci U S A 2000;97:4017-4022

9. Foggensteiner L, Bevan AP, Thomas R, et al. Cellular and subcellular distribution of polycystin-2, the protein product of the PKD2 gene. J Am Soc Nephrol 2000;11:814-827

10. Scheffers MS, Le H, van der Bent P, et al. Distinct subcellular expression of endogenous polycystin-2 in the plasma membrane and Golgi apparatus of MDCK cells. Hum Mol Genet 2002;11:59-67

11. Yin H, Morioka H, Towle CA, et al. Evidence that HAX-1 is an interleukin-1 alpha N-terminal binding protein. Cytokine 2001;15:122-137

12. Sharp TV, Wang HW, Koumi A, et al. K15 protein of Kaposi's sarcoma-associated herpesvirus is latently expressed and binds to HAX-1, a protein with antiapoptotic function. J Virol 2002;76:802-816

13. Klein C. Congenital neutropenia. Hematology Am Soc Hematol Educ Program 2009:344-350

14. Boztug K, Klein C. Novel genetic etiologies of severe congenital neutropenia. Curr Opin Immunol 2009;21:472-480

15. Skokowa J, Fobiwe JP, Dan L, Thakur BK, Welte K. Neutrophil elastase is severely down-regulated in severe congenital neutropenia independent of ELA2 or HAX1 mutations but dependent on LEF-1. Blood 2009;114:3044-3051

16. Klein C, Grudzien M, Appaswamy G, et al. HAX1 deficiency causes autosomal recessive severe congenital neutropenia (Kostmann disease). Nat Genet 2007;39:86-92

17. Shimizu A, Tada K, Shukunami C, et al. A novel alternatively spliced fibroblast growth factor receptor 3 isoform lacking the acid box domain is expressed during chondrogenic differentiation of ATDC5 cells. J Biol Chem 2001;276:11031-11040

18. Rechsteiner M, Rogers SW. PEST sequences and regulation by proteolysis. Trends Biochem Sci 1996;21:267-271

19. Yap SV, Vafiadaki E, Strong J, Kontrogianni-Konstantopoulos A. HAX-1: a multifaceted antiapoptotic protein localizing in the mitochondria and the sarcoplasmic reticulum of striated muscle cells. J Mol Cell Cardiol 2010;48:1266-1279

20. Cavnar PJ, Berthier E, Beebe DJ, Huttenlocher A. Hax1 regulates neutrophil adhesion and motility through RhoA. J Cell Biol 2011;193:465-473

21. Han Y, Chen YS, Liu Z, et al. Overexpression of HAX-1 protects cardiac myocytes from apoptosis through caspase-9 inhibition. Circ Res 2006;99:415-423

22. Yap SV, Vafiadaki E, Strong J, Kontrogianni-Konstantopoulos A. HAX-1: a multifaceted antiapoptotic protein localizing in the mitochondria and the

sarcoplasmic reticulum of striated muscle cells. J Mol Cell Cardiol;48:1266-1279

23. Mirmohammadsadegh A, Tartler U, Michel G, et al. HAX-1, identified by differential display reverse transcription polymerase chain reaction, is overexpressed in lesional psoriasis. J Invest Dermatol 2003;120:1045-1051

24. Carlsson G, van't Hooft I, Melin M, et al. Central nervous system involvement in severe congenital neutropenia: neurological and neuropsychological abnormalities associated with specific HAX1 mutations. J Intern Med 2008;264:388-400

25. Yap SV, Koontz JM, Kontrogianni-Konstantopoulos A. HAX-1: a family of apoptotic regulators in health and disease. J Cell Physiol 2011;226:2752-2761

26. Yedavalli VS, Shih HM, Chiang YP, et al. Human immunodeficiency virus type 1 Vpr interacts with antiapoptotic mitochondrial protein HAX-1. J Virol 2005;79:13735-13746

27. Dufva M, Olsson M, Rymo L. Epstein-Barr virus nuclear antigen 5 interacts with HAX-1, a possible component of the B-cell receptor signalling pathway. J Gen Virol 2001;82:1581-1587

28. Vafiadaki E, Sanoudou D, Arvanitis DA, et al. Phospholamban interacts with HAX-1, a mitochondrial protein with anti-apoptotic function. J Mol Biol 2007;367:65-79

29. Kawaguchi Y, Nakajima K, Igarashi M, et al. Interaction of Epstein-Barr virus nuclear antigen leader protein (EBNA-LP) with HS1-associated protein X-1: implication of cytoplasmic function of EBNA-LP. J Virol 2000;74:10104-10111

30. Cilenti L, Soundarapandian MM, Kyriazis GA, et al. Regulation of HAX-1 anti-apoptotic protein by Omi/HtrA2 protease during cell death. J Biol Chem 2004;279:50295-50301

31. Ortiz DF, Moseley J, Calderon G, et al. Identification of HAX-1 as a protein that binds bile salt export protein and regulates its abundance in the apical membrane of Madin-Darby canine kidney cells. J Biol Chem 2004;279:32761-32770

32. Sarnowska E, Grzybowska EA, Sobczak K, et al. Hairpin structure within the 3'UTR of DNA polymerase beta mRNA acts as a post-transcriptional regulatory element and interacts with Hax-1. Nucleic Acids Res 2007;35:5499-5510

33. Caswell PT, Vadrevu S, Norman JC. Integrins: masters and slaves of endocytic transport. Nat Rev Mol Cell Biol 2009;10:843-853

34. Oberndorfer I, Schmid D, Geisberger R, et al. HS1-associated protein X-1 interacts with membrane-bound IgE: impact on receptor-mediated internalization. J Immunol 2006;177:1139-1145

35. Al-Maghrebi M, Brule H, Padkina M, et al. The 3' untranslated region of human vimentin mRNA interacts with protein complexes containing eEF-1gamma and HAX-1. Nucleic Acids Res 2002;30:5017-5028

36. Nury D, Chabanon H, Levadoux-Martin M, Hesketh J. An eleven nucleotide section of the 3'-untranslated region is required for perinuclear localization of rat metallothionein-1 mRNA. Biochem J 2005;387:419-428

37. Morris EJ, Evason K, Wiand C, L'Ecuyer TJ, Fulton AB. Misdirected vimentin messenger RNA alters cell morphology and motility. J Cell Sci 2000;113 (Pt 13):2433-2443

38. Modem S, Reddy TR. An anti-apoptotic protein, Hax-1, inhibits the HIV-1 rev function by altering its sub-cellular localization. J Cell Physiol 2008;214:14-19

39. Frankel AD, Young JA. HIV-1: fifteen proteins and an RNA. Annu Rev Biochem 1998;67:1-25

40. Rottner K, Stradal TE. Actin dynamics and turnover in cell motility. Curr Opin Cell Biol 2011;23:569-578

41. Pollard TD, Borisy GG. Cellular motility driven by assembly and disassembly of actin filaments. Cell 2003;112:453-465

42. Parsons JT, Horwitz AR, Schwartz MA. Cell adhesion: integrating cytoskeletal dynamics and cellular tension. Nat Rev Mol Cell Biol 2010;11:633-643

43. Kurokawa K, Nakamura T, Aoki K, Matsuda M. Mechanism and role of localized activation of Rho-family GTPases in growth factor-stimulated fibroblasts and neuronal cells. Biochem Soc Trans 2005;33:631-634

44. Insall RH, Machesky LM. Actin dynamics at the leading edge: from simple machinery to complex networks. Dev Cell 2009;17:310-322

45. Narumiya S, Tanji M, Ishizaki T. Rho signaling, ROCK and mDia1, in transformation, metastasis and invasion. Cancer Metastasis Rev 2009;28:65-76

46. Kirkbride KC, Sung BH, Sinha S, Weaver AM. Cortactin: a multifunctional regulator of cellular invasiveness. Cell Adh Migr 2011;5:187-198

47. Gong H, Shen B, Flevaris P, et al. G protein subunit Galpha13 binds to integrin alphaIIbbeta3 and mediates integrin "outside-in" signaling. Science 2010;327:340-343

48. Riobo NA, Manning DR. Receptors coupled to heterotrimeric G proteins of the G12 family. Trends Pharmacol Sci 2005;26:146-154

49. Radhika V, Onesime D, Ha JH, Dhanasekaran N. Galpha13 stimulates cell migration through cortactin-interacting protein Hax-1. J Biol Chem 2004;279:49406-49413

50. Burnicka-Turek O, Kata A, Buyandelger B, et al. Pelota interacts with HAX1, EIF3G and SRPX and the resulting protein complexes are associated with the actin cytoskeleton. BMC Cell Biol;11:28

51. Margolis B, Silvennoinen O, Comoglio F, et al. High-efficiency expression/cloning of epidermal growth factor-receptor-binding proteins with Src homology 2 domains. Proc Natl Acad Sci U S A 1992;89:8894-8898

52. Chu PY, Huang LY, Hsu CH, et al. Tyrosine phosphorylation of growth factor receptor-bound protein-7 by focal adhesion kinase in the regulation of cell migration, proliferation, and tumorigenesis. J Biol Chem 2009;284:20215-20226

53. Siamakpour-Reihani S, Peterson TA, Bradford AM, et al. Grb7 binds to Hax-1 and undergoes an intramolecular domain association that offers a model for Grb7 regulation. J Mol Recognit 2010;24:314-321

54. Xi R, Doan C, Liu D, Xie T. Pelota controls self-renewal of germline stem cells by repressing a Bam-independent differentiation pathway. Development 2005;132:5365-5374

55. Passos DO, Doma MK, Shoemaker CJ, et al. Analysis of Dom34 and its function in no-go decay. Mol Biol Cell 2009;20:3025-3032

56. Burnicka-Turek O, Kata A, Buyandelger B, et al. Pelota interacts with HAX1, EIF3G and SRPX and the resulting protein complexes are associated with the actin cytoskeleton. BMC Cell Biol 2010;11:28

57. Kim JT, Kim KD, Song EY, et al. Apoptosis-inducing factor (AIF) inhibits protein synthesis by interacting with the eukaryotic translation initiation factor 3 subunit p44 (eIF3g). FEBS Lett 2006;580:6375-6383

58. Inoue H, Pan J, Hakura A. Suppression of v-src transformation by the drs gene. J Virol 1998;72:2532-2537

59. Tambe Y, Yoshioka-Yamashita A, Mukaisho K, et al. Tumor prone phenotype of mice deficient in a novel apoptosis-inducing gene, drs. Carcinogenesis 2007;28:777-784

60. Hu CD, Chinenov Y, Kerppola TK. Visualization of interactions among bZIP and Rel family proteins in living cells using bimolecular fluorescence complementation. Mol Cell 2002;9:789-798

61. Smith TC, Fang Z, Luna EJ. Novel interactors and a role for supervillin in early cytokinesis. Cytoskeleton (Hoboken) 2010;67:346-364

62. Crowley JL, Smith TC, Fang Z, Takizawa N, Luna EJ. Supervillin reorganizes the actin cytoskeleton and increases invadopodial efficiency. Mol Biol Cell 2009;20:948-962

63. Smith HW, Marshall CJ. Regulation of cell signalling by uPAR. Nat Rev Mol Cell Biol 2010;11:23-36

64. Mekkawy AH, De Bock CE, Lin Z, et al. Novel protein interactors of urokinase-type plasminogen activator receptor. Biochem Biophys Res Commun 2010;399:738-743

65. Mekkawy AH, Morris DL, Pourgholami MH. HAX1 Augments Cell Proliferation, Migration, Adhesion, and Invasion Induced by Urokinase-Type Plasminogen Activator Receptor. J Oncol 2012;2012:950749

66. Ahmed N, Riley C, Rice GE, Quinn MA, Baker MS. Alpha(v)beta(6) integrin-A marker for the malignant potential of epithelial ovarian cancer. J Histochem Cytochem 2002;50:1371-1380

67. Huang XZ, Wu JF, Cass D, et al. Inactivation of the integrin beta 6 subunit gene reveals a role of epithelial integrins in regulating inflammation in the lung and skin. J Cell Biol 1996;133:921-928

68. Janes SM, Watt FM. Switch from alphavbeta5 to alphavbeta6 integrin expression protects squamous cell carcinomas from anoikis. J Cell Biol 2004;166:419-431

69. Thomas GJ, Nystrom ML, Marshall JF. Alphavbeta6 integrin in wound healing and cancer of the oral cavity. J Oral Pathol Med 2006;35:1-10

70. Thomas GJ, Lewis MP, Whawell SA, et al. Expression of the alphavbeta6 integrin promotes migration and invasion in squamous carcinoma cells. J Invest Dermatol 2001;117:67-73

71. Matsubara K, Imai K, Okada S, et al. Severe developmental delay and epilepsy in a Japanese patient with severe congenital neutropenia due to HAX1 deficiency. Haematologica 2007;92:e123-125

72. Yoshinaga-Ohara N, Takahashi A, Uchiyama T, Sasada M. Spatiotemporal regulation of moesin phosphorylation and rear release by Rho and serine/threonine phosphatase during neutrophil migration. Exp Cell Res 2002;278:112-122

73. Peckl-Schmid D, Wolkerstorfer S, Konigsberger S, et al. HAX1 deficiency: impact on lymphopoiesis and B-cell development. Eur J Immunol 2010;40:3161-3172

74. Sridhar S, Botbol Y, Macian F, Cuervo AM. Autophagy and disease: always two sides to a problem. J Pathol 2012;226:255-273

75. Levine B, Mizushima N, Virgin HW. Autophagy in immunity and inflammation. Nature 2011;469:323-335

76. Luo S, Rubinsztein DC. Apoptosis blocks Beclin 1-dependent autophagosome synthesis: an effect rescued by Bcl-xL. Cell Death Differ 2010;17:268-277

77. Hansen TE, Johansen T. Following autophagy step by step. BMC Biol 2011;9:39

78. Klionsky DJ, Abeliovich H, Agostinis P, et al. Guidelines for the use and interpretation of assays for monitoring autophagy in higher eukaryotes. Autophagy 2008;4:151-175

79. Reggiori F, Klionsky DJ. Autophagosomes: biogenesis from scratch? Curr Opin Cell Biol 2005;17:415-422

80. Mizushima N, Yoshimori T, Ohsumi Y. The role of Atg proteins in autophagosome formation. Annu Rev Cell Dev Biol 2011;27:107-132

81. Klionsky DJ, Emr SD. Autophagy as a regulated pathway of cellular degradation. Science 2000;290:1717-1721

82. Geng J, Klionsky DJ. The Atg8 and Atg12 ubiquitin-like conjugation systems in macroautophagy. 'Protein modifications: beyond the usual suspects' review series. EMBO Rep 2008;9:859-864

83. Baehrecke EH. Autophagy: dual roles in life and death? Nat Rev Mol Cell Biol 2005;6:505-510

84. Pankiv S, Clausen TH, Lamark T, et al. p62/SQSTM1 binds directly to Atg8/LC3 to facilitate degradation of ubiquitinated protein aggregates by autophagy. J Biol Chem 2007;282:24131-24145

85. Mizushima N, Yoshimori T. How to interpret LC3 immunoblotting. Autophagy 2007;3:542-545

86. http://www.cellsignal.com/reference/pathway/Autophagy.html.

87. Li B, Hu Q, Wang H, et al. Omi/HtrA2 is a positive regulator of autophagy that facilitates the degradation of mutant proteins involved in neurodegenerative diseases. Cell Death Differ 2010;17:1773-1784

88. Suzuki Y, Imai Y, Nakayama H, et al. A serine protease, HtrA2, is released from the mitochondria and interacts with XIAP, inducing cell death. Mol Cell 2001;8:613-621

89. Vande Walle L, Lamkanfi M, Vandenabeele P. The mitochondrial serine protease HtrA2/Omi: an overview. Cell Death Differ 2008;15:453-460

90. Jeyaraju DV, Cisbani G, De Brito OM, Koonin EV, Pellegrini L. Hax1 lacks BH modules and is peripherally associated to heavy membranes: implications for Omi/HtrA2 and PARL activity in the regulation of mitochondrial stress and apoptosis. Cell Death Differ 2009;16:1622-1629

91. Galluzzi L, Joza N, Tasdemir E, et al. No death without life: vital functions of apoptotic effectors. Cell Death Differ 2008;15:1113-1123

92. Raff M. Cell suicide for beginners. Nature 1998;396:119-122

93. Kroemer G, Galluzzi L, Vandenabeele P, et al. Classification of cell death: recommendations of the Nomenclature Committee on Cell Death 2009. Cell Death Differ 2009;16:3-11

94. Tait SW, Green DR. Mitochondria and cell death: outer membrane permeabilization and beyond. Nat Rev Mol Cell Biol 2010;11:621-632

95. Li J, Yuan J. Caspases in apoptosis and beyond. Oncogene 2008;27:6194-6206

96. Degterev A, Yuan J. Expansion and evolution of cell death programmes. Nat Rev Mol Cell Biol 2008;9:378-390

97. Chang HY, Yang X. Proteases for cell suicide: functions and regulation of caspases. Microbiol Mol Biol Rev 2000;64:821-846

98. Kurokawa M, Kornbluth S. Caspases and kinases in a death grip. Cell 2009;138:838-854

99. Riedl SJ, Salvesen GS. The apoptosome: signalling platform of cell death. Nat Rev Mol Cell Biol 2007;8:405-413

100. Chipuk JE, Bouchier-Hayes L, Green DR. Mitochondrial outer membrane permeabilization during apoptosis: the innocent bystander scenario. Cell Death Differ 2006;13:1396-1402

101. Best SM. Viral subversion of apoptotic enzymes: escape from death row. Annu Rev Microbiol 2008;62:171-192

102. Kim HE, Du F, Fang M, Wang X. Formation of apoptosome is initiated by cytochrome c-induced dATP hydrolysis and subsequent nucleotide exchange on Apaf-1. Proc Natl Acad Sci U S A 2005;102:17545-17550

103. Du C, Fang M, Li Y, Li L, Wang X. Smac, a mitochondrial protein that promotes cytochrome c-dependent caspase activation by eliminating IAP inhibition. Cell 2000;102:33-42

104. Verhagen AM, Ekert PG, Pakusch M, et al. Identification of DIABLO, a mammalian protein that promotes apoptosis by binding to and antagonizing IAP proteins. Cell 2000;102:43-53

105. Scaffidi C, Fulda S, Srinivasan A, et al. Two CD95 (APO-1/Fas) signaling pathways. EMBO J 1998;17:1675-1687

106. Chowdhury D, Lieberman J. Death by a thousand cuts: granzyme pathways of programmed cell death. Annu Rev Immunol 2008;26:389-420

107. Wang L, Du F, Wang X. TNF-alpha induces two distinct caspase-8 activation pathways. Cell 2008;133:693-703

108. Wilson NS, Dixit V, Ashkenazi A. Death receptor signal transducers: nodes of coordination in immune signaling networks. Nat Immunol 2009;10:348-355

109. Banerjee A, Saito K, Meyer K, et al. Hepatitis C virus core protein and cellular protein HAX-1 promote 5-fluorouracil-mediated hepatocyte growth inhibition. J Virol 2009;83:9663-9671

110. Johns HL, Doceul V, Everett H, et al. The classical swine fever virus N-terminal protease N(pro) binds to cellular HAX-1. J Gen Virol 2010;91:2677-2686

111. Galluzzi L, Brenner C, Morselli E, Touat Z, Kroemer G. Viral control of mitochondrial apoptosis. PLoS Pathog 2008;4:e1000018

112. Anderton E, Yee J, Smith P, et al. Two Epstein-Barr virus (EBV) oncoproteins cooperate to repress expression of the proapoptotic tumour-suppressor Bim: clues to the pathogenesis of Burkitt's lymphoma. Oncogene 2008;27:421-433

113. Gorlich D, Mattaj IW. Nucleocytoplasmic transport. Science 1996;271:1513-1518

114. Longley DB, Harkin DP, Johnston PG. 5-fluorouracil: mechanisms of action and clinical strategies. Nat Rev Cancer 2003;3:330-338

115. Osaki M, Tatebe S, Goto A, et al. 5-Fluorouracil (5-FU) induced apoptosis in gastric cancer cell lines: role of the p53 gene. Apoptosis 1997;2:221-226

116. Jourdain A, Martinou JC. Mitochondrial outer-membrane permeabilization and remodelling in apoptosis. Int J Biochem Cell Biol 2009;41:1884-1889

117. Li WB, Feng J, Geng SM, et al. Induction of apoptosis by Hax-1 siRNA in melanoma cells. Cell Biol Int 2009;33:548-554

118. Lee AY, Lee Y, Park YK, et al. HS 1-associated protein X-1 is cleaved by caspase-3 during apoptosis. Mol Cells 2008;25:86-90

119. Shaw J, Kirshenbaum LA. HAX-1 represses postmitochondrial caspase-9 activation and cell death during hypoxia-reoxygenation. Circ Res 2006;99:336-338

120. Li P, Nijhawan D, Budihardjo I, et al. Cytochrome c and dATP-dependent formation of Apaf-1/caspase-9 complex initiates an apoptotic protease cascade. Cell 1997;91:479-489

121. Zou H, Li Y, Liu X, Wang X. An APAF-1.cytochrome c multimeric complex is a functional apoptosome that activates procaspase-9. J Biol Chem 1999;274:11549-11556

122. Srinivasula SM, Hegde R, Saleh A, et al. A conserved XIAP-interaction motif in caspase-9 and Smac/DIABLO regulates caspase activity and apoptosis. Nature 2001;410:112-116

123. Kang YJ, Jang M, Park YK, et al. Molecular interaction between HAX-1 and XIAP inhibits apoptosis. Biochem Biophys Res Commun 2010;393:794-799

124. Lindemann JP, Jones LR, Hathaway DR, Henry BG, Watanabe AM. beta-Adrenergic stimulation of phospholamban phosphorylation and Ca2+-ATPase activity in guinea pig ventricles. J Biol Chem 1983;258:464-471

125. MacLennan DH, Kranias EG. Phospholamban: a crucial regulator of cardiac contractility. Nat Rev Mol Cell Biol 2003;4:566-577

126. Denmeade SR, Isaacs JT. The SERCA pump as a therapeutic target: making a "smart bomb" for prostate cancer. Cancer Biol Ther 2005;4:14-22

127. Mattiazzi A, Mundina-Weilenmann C, Guoxiang C, Vittone L, Kranias E. Role of phospholamban phosphorylation on Thr17 in cardiac physiological and pathological conditions. Cardiovasc Res 2005;68:366-375

128. Haghighi K, Schmidt AG, Hoit BD, et al. Superinhibition of sarcoplasmic reticulum function by phospholamban induces cardiac contractile failure. J Biol Chem 2001;276:24145-24152

129. Hagemann D, Kuschel M, Kuramochi T, et al. Frequency-encoding Thr17 phospholamban phosphorylation is independent of Ser16 phosphorylation in cardiac myocytes. J Biol Chem 2000;275:22532-22536

130. Vafiadaki E, Arvanitis DA, Pagakis SN, et al. The anti-apoptotic protein HAX-1 interacts with SERCA2 and regulates its protein levels to promote cell survival. Mol Biol Cell 2009;20:306-318

131. Palmer AE, Jin C, Reed JC, Tsien RY. Bcl-2-mediated alterations in endoplasmic reticulum Ca2+ analyzed with an improved genetically encoded fluorescent sensor. Proc Natl Acad Sci U S A 2004;101:17404-17409

132. Pinton P, Ferrari D, Magalhaes P, et al. Reduced loading of intracellular Ca(2+) stores and downregulation of capacitative Ca(2+) influx in Bcl-2-overexpressing cells. J Cell Biol 2000;148:857-862

133. Nutt LK, Pataer A, Pahler J, et al. Bax and Bak promote apoptosis by modulating endoplasmic reticular and mitochondrial Ca2+ stores. J Biol Chem 2002;277:9219-9225

134. Kadomatsu T, Mori M, Terada K. Mitochondrial import of Omi: the definitive role of the putative transmembrane region and multiple processing sites in the amino-terminal segment. Biochem Biophys Res Commun 2007;361:516-521

135. Chao JR, Parganas E, Boyd K, et al. Hax1-mediated processing of HtrA2 by Parl allows survival of lymphocytes and neurons. Nature 2008;452:98-102

136. Li W, Srinivasula SM, Chai J, et al. Structural insights into the pro-apoptotic function of mitochondrial serine protease HtrA2/Omi. Nat Struct Biol 2002;9:436-441

137. Artal-Sanz M, Tavernarakis N. Prohibitin and mitochondrial biology. Trends Endocrinol Metab 2009;20:394-401

138. Nijtmans LG, de Jong L, Artal Sanz M, et al. Prohibitins act as a membrane-bound chaperone for the stabilization of mitochondrial proteins. EMBO J 2000;19:2444-2451

139. McClung JK, Danner DB, Stewart DA, et al. Isolation of a cDNA that hybrid selects antiproliferative mRNA from rat liver. Biochem Biophys Res Commun 1989;164:1316-1322

140. Kasashima K, Ohta E, Kagawa Y, Endo H. Mitochondrial functions and estrogen receptor-dependent nuclear translocation of pleiotropic human prohibitin 2. J Biol Chem 2006;281:36401-36410

141. Nijtmans LG, Artal SM, Grivell LA, Coates PJ. The mitochondrial PHB complex: roles in mitochondrial respiratory complex assembly, ageing and degenerative disease. Cell Mol Life Sci 2002;59:143-155

142. Stojanovski D, Muller JM, Milenkovic D, et al. The MIA system for protein import into the mitochondrial intermembrane space. Biochim Biophys Acta 2008;1783:610-617

143. Kang YJ, Jang M, Park YK, et al. Molecular interaction between HAX-1 and XIAP inhibits apoptosis. Biochem Biophys Res Commun;393:794-799

144. Germeshausen M, Grudzien M, Zeidler C, et al. Novel HAX1 mutations in patients with severe congenital neutropenia reveal isoform-dependent genotype-phenotype associations. Blood 2008;111:4954-4957

145. Smith BN, Ancliff PJ, Pizzey A, et al. Homozygous HAX1 mutations in severe congenital neutropenia patients with sporadic disease: a novel mutation in two unrelated British kindreds. Br J Haematol 2009;144:762-770

146. Zeidler C, Germeshausen M, Klein C, Welte K. Clinical implications of ELA2-, HAX1-, and G-CSF-receptor (CSF3R) mutations in severe congenital neutropenia. Br J Haematol 2009;144:459-467

147. Ishikawa N, Okada S, Miki M, et al. Neurodevelopmental abnormalities associated with severe congenital neutropenia due to the R86X mutation in the HAX1 gene. J Med Genet 2008;45:802-807

148. Carlsson G, Elinder G, Malmgren H, et al. Compound heterozygous HAX1 mutations in a Swedish patient with severe congenital neutropenia and no neurodevelopmental abnormalities. Pediatr Blood Cancer 2009;53:1143-1146

149. Trebinska A, Rembiszewska A, Ciosek K, et al. HAX-1 overexpression, splicing and cellular localization in tumors. BMC Cancer 2010;10:76

150. Fadeel B, Grzybowska E. HAX-1: a multifunctional protein with emerging roles in human disease. Biochim Biophys Acta 2009;1790:1139-1148

151. Jiang Y, Zhang W, Kondo K, et al. Gene expression profiling in a renal cell carcinoma cell line: dissecting VHL and hypoxia-dependent pathways. Mol Cancer Res 2003;1:453-462

152. Hynes RO. Integrins: bidirectional, allosteric signaling machines. Cell 2002;110:673-687

153. Takada Y, Ye X, Simon S. The integrins. Genome Biol 2007;8:215

154. Lynam E, Sklar LA, Taylor AD, et al. Beta2-integrins mediate stable adhesion in collisional interactions between neutrophils and ICAM-1-expressing cells. J Leukoc Biol 1998;64:622-630

155. Rathinam R, Alahari SK. Important role of integrins in the cancer biology. Cancer Metastasis Rev;29:223-237

156. Xiong JP, Goodman SL, Arnaout MA. Purification, analysis, and crystal structure of integrins. Methods Enzymol 2007;426:307-336

157. Xu Z, Shen MX, Ma DZ, Wang LY, Zha XL. TGF-beta1-promoted epithelial-to-mesenchymal transformation and cell adhesion contribute to TGF-beta1-enhanced cell migration in SMMC-7721 cells. Cell Res 2003;13:343-350

158. Guo W, Giancotti FG. Integrin signalling during tumour progression. Nat Rev Mol Cell Biol 2004;5:816-826

159. Berrier AL, Yamada KM. Cell-matrix adhesion. J Cell Physiol 2007;213:565-573

160. Ruoslahti E, Pierschbacher MD. Arg-Gly-Asp: a versatile cell recognition signal. Cell 1986;44:517-518

161. Desgrosellier JS, Cheresh DA. Integrins in cancer: biological implications and therapeutic opportunities. Nat Rev Cancer;10:9-22

162. DiCara D, Rapisarda C, Sutcliffe JL, et al. Structure-function analysis of Arg-Gly-Asp helix motifs in alpha v beta 6 integrin ligands. J Biol Chem 2007;282:9657-9665

163. Ginsberg MH, Partridge A, Shattil SJ. Integrin regulation. Curr Opin Cell Biol 2005;17:509-516

164. Roberts GC, Critchley DR. Structural and biophysical properties of the integrin-associated cytoskeletal protein talin. Biophys Rev 2009;1:61-69

165. Liddington RC, Ginsberg MH. Integrin activation takes shape. J Cell Biol 2002;158:833-839

166. Lowell CA, Mayadas TN. Overview: studying integrins in vivo. Methods Mol Biol 2012;757:369-397

167. Podolnikova NP, Yermolenko IS, Fuhrmann A, et al. Control of integrin alphaIIb beta3 outside-in signaling and platelet adhesion by sensing the physical properties of fibrin(ogen) substrates. Biochemistry;49:68-77

168. Carragher NO, Frame MC. Focal adhesion and actin dynamics: a place where kinases and proteases meet to promote invasion. Trends Cell Biol 2004;14:241-249

169. Li S, Guan JL, Chien S. Biochemistry and biomechanics of cell motility. Annu Rev Biomed Eng 2005;7:105-150

170. Gilmore AP. Anoikis. Cell Death Differ 2005;12 Suppl 2:1473-1477

171. Chiarugi P, Giannoni E. Anoikis: a necessary death program for anchorage-dependent cells. Biochem Pharmacol 2008;76:1352-1364

172. Varner JA, Cheresh DA. Integrins and cancer. Curr Opin Cell Biol 1996;8:724-730

173. Hanahan D, Folkman J. Patterns and emerging mechanisms of the angiogenic switch during tumorigenesis. Cell 1996;86:353-364

174. Weaver VM, Lelievre S, Lakins JN, et al. beta4 integrin-dependent formation of polarized three-dimensional architecture confers resistance to apoptosis in normal and malignant mammary epithelium. Cancer Cell 2002;2:205-216

175. Adams JC, Watt FM. Changes in keratinocyte adhesion during terminal differentiation: reduction in fibronectin binding precedes alpha 5 beta 1 integrin loss from the cell surface. Cell 1990;63:425-435

176. Montgomery AM, Reisfeld RA, Cheresh DA. Integrin alpha v beta 3 rescues melanoma cells from apoptosis in three-dimensional dermal collagen. Proc Natl Acad Sci U S A 1994;91:8856-8860

177. Simpson CD, Anyiwe K, Schimmer AD. Anoikis resistance and tumor metastasis. Cancer Lett 2008;272:177-185

178. Cohen LA, Guan JL. Mechanisms of focal adhesion kinase regulation. Curr Cancer Drug Targets 2005;5:629-643

179. Lu Q, Rounds S. Focal adhesion kinase and endothelial cell apoptosis. Microvasc Res 2012;83:56-63

180. Fletcher DA, Mullins RD. Cell mechanics and the cytoskeleton. Nature;463:485-492

181. Thomas GJ, Hart IR, Speight PM, Marshall JF. Binding of TGF-beta1 latency-associated peptide (LAP) to alpha(v)beta6 integrin modulates behaviour of squamous carcinoma cells. Br J Cancer 2002;87:859-867

182. Thomas GJ, Lewis MP, Hart IR, Marshall JF, Speight PM. AlphaVbeta6 integrin promotes invasion of squamous carcinoma cells through up-regulation of matrix metalloproteinase-9. Int J Cancer 2001;92:641-650

183. Friedl P, Wolf K. Tumour-cell invasion and migration: diversity and escape mechanisms. Nat Rev Cancer 2003;3:362-374

184. Friedl P, Wolf K. Tube travel: the role of proteases in individual and collective cancer cell invasion. Cancer Res 2008;68:7247-7249

185. Poincloux R, Lizarraga F, Chavrier P. Matrix invasion by tumour cells: a focus on MT1-MMP trafficking to invadopodia. J Cell Sci 2009;122:3015-3024

186. Deryugina EI, Quigley JP. Matrix metalloproteinases and tumor metastasis. Cancer Metastasis Rev 2006;25:9-34

187. Hofmann UB, Westphal JR, Waas ET, et al. Coexpression of integrin alpha(v)beta3 and matrix metalloproteinase-2 (MMP-2) coincides with MMP-2 activation: correlation with melanoma progression. J Invest Dermatol 2000;115:625-632

188. Ebrahimnejad A, Streichert T, Nollau P, et al. CEACAM1 enhances invasion and migration of melanocytic and melanoma cells. Am J Pathol 2004;165:1781-1787

189. Ramos DM, Dang D, Sadler S. The role of the integrin alpha v beta6 in regulating the epithelial to mesenchymal transition in oral cancer. Anticancer Res 2009;29:125-130

190. Niu J, Dorahy DJ, Gu X, et al. Integrin expression in colon cancer cells is regulated by the cytoplasmic domain of the beta6 integrin subunit. Int J Cancer 2002;99:529-537

191. Morgan K, Stevens EB, Shah B, et al. beta 3: an additional auxiliary subunit of the voltage-sensitive sodium channel that modulates channel gating with distinct kinetics. Proc Natl Acad Sci U S A 2000;97:2308-2313

192. Tang CH, Wei Y. The urokinase receptor and integrins in cancer progression. Cell Mol Life Sci 2008;65:1916-1932

193. Ghosh AK, Vaughan DE. PAI-1 in tissue fibrosis. J Cell Physiol 2011;227:493-507

194. Degryse B, Neels JG, Czekay RP, et al. The low density lipoprotein receptor-related protein is a motogenic receptor for plasminogen activator inhibitor-1. J Biol Chem 2004;279:22595-22604

195. Chapman HA, Wei Y. Protease crosstalk with integrins: the urokinase receptor paradigm. Thromb Haemost 2001;86:124-129

196. Nip J, Rabbani SA, Shibata HR, Brodt P. Coordinated expression of the vitronectin receptor and the urokinase-type plasminogen activator receptor in metastatic melanoma cells. J Clin Invest 1995;95:2096-2103

197. Dalvi N, Thomas GJ, Marshall JF, et al. Modulation of the urokinase-type plasminogen activator receptor by the beta6 integrin subunit. Biochem Biophys Res Commun 2004;317:92-99

198. Stefansson S, Lawrence DA. The serpin PAI-1 inhibits cell migration by blocking integrin alpha V beta 3 binding to vitronectin. Nature 1996;383:441-443

199. Deng G, Curriden SA, Hu G, Czekay RP, Loskutoff DJ. Plasminogen activator inhibitor-1 regulates cell adhesion by binding to the somatomedin B domain of vitronectin. J Cell Physiol 2001;189:23-33

200. Guo W, Pylayeva Y, Pepe A, et al. Beta 4 integrin amplifies ErbB2 signaling to promote mammary tumorigenesis. Cell 2006;126:489-502

201. Trusolino L, Bertotti A, Comoglio PM. A signaling adapter function for alpha6beta4 integrin in the control of HGF-dependent invasive growth. Cell 2001;107:643-654

202. Nishimura T, Kaibuchi K. Numb controls integrin endocytosis for directional cell migration with aPKC and PAR-3. Dev Cell 2007;13:15-28

203. Kumari S, Mg S, Mayor S. Endocytosis unplugged: multiple ways to enter the cell. Cell Res 2010;20:256-275

204. Ezratty EJ, Bertaux C, Marcantonio EE, Gundersen GG. Clathrin mediates integrin endocytosis for focal adhesion disassembly in migrating cells. J Cell Biol 2009;187:733-747

205. Sandvig K, Pust S, Skotland T, van Deurs B. Clathrin-independent endocytosis: mechanisms and function. Curr Opin Cell Biol 2011;23:413-420

206. Yang JT, Bader BL, Kreidberg JA, et al. Overlapping and independent functions of fibronectin receptor integrins in early mesodermal development. Dev Biol 1999;215:264-277

207. Bates RC. The alphaVbeta6 integrin as a novel molecular target for colorectal cancer. Future Oncol 2005;1:821-828

208. Marsh D, Dickinson S, Neill GW, et al. alpha vbeta 6 Integrin promotes the invasion of morphoeic basal cell carcinoma through stromal modulation. Cancer Res 2008;68:3295-3303

209. Sipos B, Hahn D, Carceller A, et al. Immunohistochemical screening for beta6-integrin subunit expression in adenocarcinomas using a novel

monoclonal antibody reveals strong up-regulation in pancreatic ductal adenocarcinomas in vivo and in vitro. Histopathology 2004;45:226-236

210. Breuss JM, Gallo J, DeLisser HM, et al. Expression of the beta 6 integrin subunit in development, neoplasia and tissue repair suggests a role in epithelial remodeling. J Cell Sci 1995;108 (Pt 6):2241-2251

211. Eslami A, Gallant-Behm CL, Hart DA, et al. Expression of integrin alphavbeta6 and TGF-beta in scarless vs scar-forming wound healing. J Histochem Cytochem 2009;57:543-557

212. Yang GY, Xu KS, Pan ZQ, et al. Integrin alpha v beta 6 mediates the potential for colon cancer cells to colonize in and metastasize to the liver. Cancer Sci 2008;99:879-887

213. Zhang ZY, Xu KS, Wang JS, et al. Integrin alphanvbeta6 acts as a prognostic indicator in gastric carcinoma. Clin Oncol (R Coll Radiol) 2008;20:61-66

214. Hazelbag S, Kenter GG, Gorter A, et al. Overexpression of the alpha v beta 6 integrin in cervical squamous cell carcinoma is a prognostic factor for decreased survival. J Pathol 2007;212:316-324

215. Elayadi AN, Samli KN, Prudkin L, et al. A peptide selected by biopanning identifies the integrin alphavbeta6 as a prognostic biomarker for nonsmall cell lung cancer. Cancer Res 2007;67:5889-5895

216. Margadant C, Sonnenberg A. Integrin-TGF-beta crosstalk in fibrosis, cancer and wound healing. EMBO Rep 2010;11:97-105

217. Wipff PJ, Hinz B. Integrins and the activation of latent transforming growth factor beta1 - an intimate relationship. Eur J Cell Biol 2008;87:601-615

218. Grimm D. Small silencing RNAs: state-of-the-art. Adv Drug Deliv Rev 2009;61:672-703

219. Shain KH, Landowski TH, Dalton WS. Adhesion-mediated intracellular redistribution of c-Fas-associated death domain-like IL-1-converting enzyme-like inhibitory protein-long confers resistance to CD95-induced apoptosis in hematopoietic cancer cell lines. J Immunol 2002;168:2544-2553

220. Nystrom ML, Thomas GJ, Stone M, et al. Development of a quantitative method to analyse tumour cell invasion in organotypic culture. J Pathol 2005;205:468-475

221. Yee KS, Wilkinson S, James J, Ryan KM, Vousden KH. PUMA- and Bax-induced autophagy contributes to apoptosis. Cell Death Differ 2009;16:1135-1145

222. Kwiecinska A, Ottosson-Wadlund A, Ceder R, et al. HAX-1 expression in human B lymphoma. Leukemia 2011;25:868-872

223. Niu J, Gu X, Ahmed N, et al. The alphaVbeta6 integrin regulates its own expression with cell crowding: implications for tumour progression. Int J Cancer 2001;92:40-48

224. Corbi N, Batassa EM, Pisani C, et al. The eEF1gamma subunit contacts RNA polymerase II and binds vimentin promoter region. PLoS One 2010;5:e14481

225. Gradl G, Faust D, Oesch F, Wieser RJ. Density-dependent regulation of cell growth by contactinhibin and the contactinhibin receptor. Curr Biol 1995;5:526-535

226. Levine EM, Becker Y, Boone CW, Eagle H. CONTACT INHIBITION, MACROMOLECULAR SYNTHESIS, AND POLYRIBOSOMES IN CULTURED HUMAN DIPLOID FIBROBLASTS. Proc Natl Acad Sci U S A 1965;53:350-356

227. Hanahan D, Weinberg RA. The hallmarks of cancer. Cell 2000;100:57-70

228. Bierie B, Moses HL. Tumour microenvironment: TGFbeta: the molecular Jekyll and Hyde of cancer. Nat Rev Cancer 2006;6:506-520

229. Buccione R, Caldieri G, Ayala I. Invadopodia: specialized tumor cell structures for the focal degradation of the extracellular matrix. Cancer Metastasis Rev 2009;28:137-149

230. Gimona M, Buccione R, Courtneidge SA, Linder S. Assembly and biological role of podosomes and invadopodia. Curr Opin Cell Biol 2008;20:235-241

231. Artym VV, Zhang Y, Seillier-Moiseiwitsch F, Yamada KM, Mueller SC. Dynamic interactions of cortactin and membrane type 1 matrix metalloproteinase at invadopodia: defining the stages of invadopodia formation and function. Cancer Res 2006;66:3034-3043

232. Henkels KM, Turchi JJ. Cisplatin-induced apoptosis proceeds by caspase-3-dependent and -independent pathways in cisplatin-resistant and -sensitive human ovarian cancer cell lines. Cancer Res 1999;59:3077-3083

233. Bacus SS, Gudkov AV, Lowe M, et al. Taxol-induced apoptosis depends on MAP kinase pathways (ERK and p38) and is independent of p53. Oncogene 2001;20:147-155

234. Map-pGIPZ V, Resistance A, Protocol I, et al. Expression Arrest™ GIPZ lentiviral shRNAmir.

235. Montgomery MK, Xu S, Fire A. RNA as a target of double-stranded RNA-mediated genetic interference in Caenorhabditis elegans. Proc Natl Acad Sci U S A 1998;95:15502-15507

236. Fire A, Xu S, Montgomery MK, et al. Potent and specific genetic interference by double-stranded RNA in Caenorhabditis elegans. Nature 1998;391:806-811

237. Voinnet O. RNA silencing as a plant immune system against viruses. Trends Genet 2001;17:449-459

238. Elbashir SM, Harborth J, Lendeckel W, et al. Duplexes of 21-nucleotide RNAs mediate RNA interference in cultured mammalian cells. Nature 2001;411:494-498

239. Hamilton A, Voinnet O, Chappell L, Baulcombe D. Two classes of short interfering RNA in RNA silencing. EMBO J 2002;21:4671-4679

240. Grimm D, Pandey K, Kay MA. Adeno-associated virus vectors for short hairpin RNA expression. Methods Enzymol 2005;392:381-405

241. Woolston C, Martin S. Analysis of tumor and endothelial cell viability and survival using sulforhodamine B and clonogenic assays. Methods Mol Biol 2011;740:45-56

242. Elbashir SM, Martinez J, Patkaniowska A, Lendeckel W, Tuschl T. Functional anatomy of siRNAs for mediating efficient RNAi in Drosophila melanogaster embryo lysate. EMBO J 2001;20:6877-6888

243. Han J, Goldstein LA, Hou W, et al. Deregulation of mitochondrial membrane potential by mitochondrial insertion of granzyme B and direct Hax-1 cleavage. J Biol Chem 2010;285:22461-22472

244. Bhuiyan MS, Fukunaga K. Activation of HtrA2, a mitochondrial serine protease mediates apoptosis: current knowledge on HtrA2 mediated myocardial ischemia/reperfusion injury. Cardiovasc Ther 2008;26:224-232

245. Li B, Hu Q, Wang H, et al. Omi/HtrA2 is a positive regulator of autophagy that facilitates the degradation of mutant proteins involved in neurodegenerative diseases. Cell Death Differ

246. Rohn TT, Wirawan E, Brown RJ, et al. Depletion of Beclin-1 due to proteolytic cleavage by caspases in the Alzheimer's disease brain. Neurobiol Dis 2011;43:68-78

247. Lee JA, Gao FB. Regulation of Abeta pathology by beclin 1: a protective role for autophagy? J Clin Invest 2008;118:2015-2018

248. Klionsky DJ. Autophagy: from phenomenology to molecular understanding in less than a decade. Nat Rev Mol Cell Biol 2007;8:931-937

249. Manjithaya R, Subramani S. Autophagy: a broad role in unconventional protein secretion? Trends Cell Biol;21:67-73

250. Wu YT, Tan HL, Huang Q, et al. Autophagy plays a protective role during zVAD-induced necrotic cell death. Autophagy 2008;4:457-466

251. Bhutia SK, Dash R, Das SK, et al. Mechanism of autophagy to apoptosis switch triggered in prostate cancer cells by antitumor cytokine melanoma differentiation-associated gene 7/interleukin-24. Cancer Res 2010;70:3667-3676

252. Kimmelman AC. The dynamic nature of autophagy in cancer. Genes Dev 2011;25:1999-2010

253. Maiuri MC, Zalckvar E, Kimchi A, Kroemer G. Self-eating and self-killing: crosstalk between autophagy and apoptosis. Nat Rev Mol Cell Biol 2007;8:741-752

254. Gao Z, Tian Y, Wang J, et al. A dimeric Smac/diablo peptide directly relieves caspase-3 inhibition by XIAP. Dynamic and cooperative regulation of XIAP by Smac/Diablo. J Biol Chem 2007;282:30718-30727

255. Pasinelli P, Houseweart MK, Brown RH, Jr., Cleveland DW. Caspase-1 and -3 are sequentially activated in motor neuron death in Cu,Zn superoxide dismutase-mediated familial amyotrophic lateral sclerosis. Proc Natl Acad Sci U S A 2000;97:13901-13906

256. Kamada S, Kikkawa U, Tsujimoto Y, Hunter T. Nuclear translocation of caspase-3 is dependent on its proteolytic activation and recognition of a substrate-like protein(s). J Biol Chem 2005;280:857-860

257. Karbowski M, Youle RJ. Dynamics of mitochondrial morphology in healthy cells and during apoptosis. Cell Death Differ 2003;10:870-880

258. Hande KR. Etoposide: four decades of development of a topoisomerase II inhibitor. Eur J Cancer 1998;34:1514-1521

259. Bava SV, Puliappadamba VT, Deepti A, et al. Sensitization of taxol-induced apoptosis by curcumin involves down-regulation of nuclear factor-kappaB and the serine/threonine kinase Akt and is independent of tubulin polymerization. J Biol Chem 2005;280:6301-6308

260. Kumar N. Taxol-induced polymerization of purified tubulin. Mechanism of action. J Biol Chem 1981;256:10435-10441

261. Schuetz JD, Wallace HJ, Diasio RB. 5-Fluorouracil incorporation into DNA of CF-1 mouse bone marrow cells as a possible mechanism of toxicity. Cancer Res 1984;44:1358-1363

262. Martinou JC, Green DR. Breaking the mitochondrial barrier. Nat Rev Mol Cell Biol 2001;2:63-67

263. Kaji T, Yamada A, Miyajima S, et al. Cell density-dependent regulation of proteoglycan synthesis by transforming growth factor-beta(1) in cultured bovine aortic endothelial cells. J Biol Chem 2000;275:1463-1470

264. Broker LE, Kruyt FA, Giaccone G. Cell death independent of caspases: a review. Clin Cancer Res 2005;11:3155-3162

265. Okada M, Adachi S, Imai T, et al. A novel mechanism for imatinib mesylate-induced cell death of BCR-ABL-positive human leukemic cells: caspase-independent, necrosis-like programmed cell death mediated by serine protease activity. Blood 2004;103:2299-2307

266. Shimizu S, Kanaseki T, Mizushima N, et al. Role of Bcl-2 family proteins in a non-apoptotic programmed cell death dependent on autophagy genes. Nat Cell Biol 2004;6:1221-1228

267. Grzybowska EA, Sarnowska E, Konopinski R, et al. Identification and expression analysis of alternative splice variants of the rat Hax-1 gene. Gene 2006;371:84-92

268. Blasi F, Carmeliet P. uPAR: a versatile signalling orchestrator. Nat Rev Mol Cell Biol 2002;3:932-943

269. Ahmed N, Pansino F, Clyde R, et al. Overexpression of alpha(v)beta6 integrin in serous epithelial ovarian cancer regulates extracellular matrix degradation via the plasminogen activation cascade. Carcinogenesis 2002;23:237-244